

Department of Biology
University of Fribourg
(Switzerland)

**Coordination of growth and cell division
by the TORC1 nutrient signaling pathway
in *Saccharomyces cerevisiae***

THESIS

presented to the Faculty of Science of the University of Fribourg (Switzerland)
in consideration for the award of the academic grade of *Doctor rerum naturalium*

by

Marta Moreno Torres

from

Valencia (Spain)

Thesis No: 1973

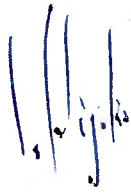
UniPrint

2016

Accepted by the Faculty of Science of the University of Fribourg (Switzerland) upon the recommendation of Prof. Sergio Moreno and Prof. Jürg Bähler. President of the Jury: Prof. Simon Sprecher.

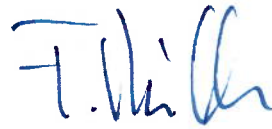
Fribourg, the 28th of June 2016

Thesis supervisor(s)

A handwritten signature in blue ink, appearing to read 'C. De Virgilio'.

Prof. Claudio De Virgilio

Dean

A handwritten signature in blue ink, appearing to read 'F. Müller'.

Prof. Fritz Müller

***Por su cariño, su apoyo y su orgullo de abuelo incondicional.
Ya es nuestra yayo!***

Summary	9
Résumé	11
Introduction	13
1. The cell cycle	15
2. <i>Saccharomyces cerevisiae</i> as a model organism	15
3. Cell cycle regulation in <i>Saccharomyces cerevisiae</i>	17
4. Cyclin dependent kinases: master regulators of the cell cycle	19
4.1 Cyclins: key determinants of Cdk activity	20
4.1.1. G1-Cyclins	21
4.1.2. B-type cyclins	23
4.2. Control of Cdk1 activity by phosphorylation.....	24
4.2.1. Cdk1-activating phosphorylation by the Cdk-activating kinase	24
4.2.2. Cdk1 inhibitory phosphorylation	25
4.3 Cdk1 inhibition by cyclin dependent kinase inhibitors	26
4.3.1. <i>FAR1</i>	27
4.3.2. <i>PHO81</i>	28
4.3.3. <i>SIC1</i>	28
4.3.3.1. Molecular mechanism of Sic1 inhibition of Clb-Cdk1 complexes	31
4.3.3.2. Sic1 regulation at the M/G1 transition	32
4.3.3.3. Sic1 regulation at the G1/S transition.....	33
4.3.3.4. Sic1 regulation by kinases and phosphatases	34
4.4. Cdk1 kinase subunits: Cks.....	36
5. Cell cycle transcriptional regulation.....	39
5.1. The Start checkpoint cluster	39
5.2. The S/G2 cluster.....	40
5.3. The M to early-G1 cluster	41
6. Cell cycle proteolytic regulation	42
6.1. Proteolysis at Start.....	43
6.2. Proteolysis at anaphase	44
7. Cell cycle regulation in quiescent cells.....	45
8. Nutrient signaling pathways control the decision between proliferation and entry	
into quiescence	47
8.1. TORC1	49
8.2. PKA.....	53
8.3. Pho85	54

9. Rim15 regulates transcription factors	55
10. Rim15 coordinates transcription with posttranscriptional mRNA protection	56
11. Yeast endosulfines Igo1/2 inhibit protein phosphatase 2A	57
12. The Gwl-Ensa/Arpp19-PP2A-B55δ pathway controls mitosis	58
Aim and outline	62
Aim and outline.....	64
CHAPTER I:.....	66
TORC1 controls G1-S cell cycle transition in yeast via Mpk1 and the greatwall kinase pathway.....	66
CHAPTER II:	92
Regulatory mechanisms of Sic1 stabilization by Thr¹⁷³ phosphorylation	92
2.1 Introduction	94
2.2 Results	95
2.2.1. Sic1 Thr ¹⁷³ phosphorylation promotes binding to Cks1.....	95
2.2.2. Sic1-Thr ¹⁷³ phosphorylation prevents Cln/Clb-Cdk1-dependent multiphosphorylation of Sic1	100
2.3 Discussion	105
CHAPTER III:.....	110
TORC1 controls G1 cyclins via the greatwall kinase pathway.....	110
3.1. Introduction	112
3.2 Results	115
3.2.1. The greatwall kinase pathway regulates <i>XBP1</i> mRNA and Xbp1 protein levels.....	115
3.2.2. The greatwall kinase pathway regulates Msa1, but not Msa2, protein levels.....	121
3.2.3. The greatwall kinase pathway is not involved in the regulation of Whi5 protein levels	123
3.2.4. Loss of Rim15-Igo1/2 changes the Stb1 migration pattern independently of Cdc55	124
3.2.5. Loss of Rim15-Igo1/2 alters Nmr1 protein levels in rapamycin-treated cells.....	125
3.2.6. A combined role for Xbp1, Msa1/2 and Sic1 in rapamycin-induced G1 arrest.....	126
3.3. Discussion	128
CHAPTER IV:	130
Genetic screen for suppressors of the defect in exit from the rapamycin-induced G0 arrest	130
4.1. Introduction	132
4.2. Results	133

4.2.1. JK9-3D cells are defective in the exit from rapamycin-induced growth arrest.....	133
4.2.2. Hyperactive <i>TOR1</i> alleles suppress the <i>EGO</i> phenotype in JK9-3D cells	134
4.2.3. Genetic selection for suppressors of the JK9-3D <i>EGO</i> phenotype	135
4.3. Discussion	140
General Discussion.....	144
Concluding remarks	146
Open questions regarding the TORC1 regulatory mechanisms in cell cycle control... ..	148
Significance in human diseases.....	151
Materials and Methods	154
Growth conditions	156
Standard conditions	156
Rapamycin treatments.....	156
Nutrient starvation	157
Fluorescence-activated cell sorting and budding index analyses	157
Preparation of mRNAs for Northern blot and quantitative Real-Time PCR.....	158
NaOH extraction of proteins for immunoblot analysis	158
Co-immunoprecipitation	159
Recombinant protein purification	160
Mpk1 protein kinase assays	160
PP2A^{Cdc55} protein phosphatase assay	161
Microscopic analyses	161
Mass Spectrometry	162
Genomic DNA preparation	162
Analysis of Next Generation Sequencing data	163
References.....	170
Appendix.....	204

List of abbreviations:

APC: Anaphase-Promoting Complex
BI: Budding Index
CAK: Cdk Activating Kinase
CKI: Cyclin dependent Kinase Inhibitor
CKS: Cdk1 Kinase Subunit
ECB: Early Cell cycle Box
EGOC: Exit from rapamycin-induced GrOwth arrest Complex
FBP: F-Box Protein
FKBP12: FK506 Binding Protein 12
FRB: FKB12-Rapamycin-Binding
FACS: Fluorescence-Activated Cell Sorting
GDP: Guanosine DiPhosphate
GTP: Guanosine TriPhosphate
GTPase: Guanosine TriPhosphatase
HECT: Homologous to the EG-AP Carboxyl Terminus
HPLC: High Performance Liquid Chromatography
MAP: Mitogen Activated Protein
MBF: Mlu1 cell cycle box Binding Factor
MCB: Mlu1 Cell cycle Box
NEBD: Nuclear Envelope BreakDown
NLS: Nuclear Localization Signal
ORF: Open Reading Frame
Pi: Inorganic Phosphate
PI3K: Phosphatidyl Inositol 3' Kinase
PPase: Protein Phosphatase
pRB: Retinoblastoma protein
pre-RC: pre-Replicative Complex
PDS: Post-Diauxic Shift
PKA: Protein Kinase A
PP2A: Protein Phosphatase 2A
RNA: RiboNucleic Acid
mRNA: messenger RNA
mTORC1: mammalian TORC1
SAC: Spindle Assembly Checkpoint
SAPK: Stress Activated Protein Kinase
SBF: Swi4 cell cycle box Binding Factor
SCB: Swi4 Cell cycle Box
SCF: Skp/Cullin/F-box
STRES: Stress Response Elements
TCA: TriChloroacetic Acid
TOR: Target Of Rapamycin
TORC1: Target Of Rapamycin Complex I
uORF: upstream Open Reading Frame
UTR: Untranslated Region

Summary

Living organisms coordinate cell growth with cell division in response to the availability of essential nutrients. Upon nutrient deprivation, cells arrest cell cycle progression in late G1 and enter into a reversible non-dividing but metabolically active state known as quiescence or G0. Under unfavorable conditions, failure to entry appropriately into this quiescent state may result in DNA replication and chromosome segregation errors and therefore loss of viability. In multicellular organisms, improper control of entry into and exit from quiescence may lead to uncontrolled proliferation and ultimately to tumor development.

In the yeast *Saccharomyces cerevisiae* several nutrient signaling pathways coordinate cell growth and division in response to nutrient availability. The work presented in this manuscript is focused on the master regulator of cell growth the Target Of Rapamycin Complex 1 (TORC1). Following starvation, inactivation of TORC1 results in the activation of the protein kinase Rim15, which orchestrates most aspects of the G0 program including proper G1 arrest. Rim15 controls most of its downstream readouts by inhibiting (indirectly via the yeast endosulfines Igo1/2) the protein phosphatase PP2A^{Cdc55}. Although many efforts have been made in deciphering the molecular mechanisms by which TORC1 regulates cell proliferation, many questions still need to be addressed. The aim of this thesis is to understand whether the TORC1-Rim15-Igo1/2-PP2A^{Cdc55} signaling pathway impinges on G1 cell cycle events and if positive, to elucidate the underlying molecular mechanisms.

Based on the previous observations that *rim15Δ* mutant cells exhibit a defect in G1 cell cycle arrest after rapamycin treatment, we show in the first chapter that TORC1 downregulation following rapamycin treatment or nutrient deprivation results in G1 cyclins clearance and accumulation of the Cdk1 inhibitor Sic1 in a Rim15-Igo1/2-dependent manner. Here, we demonstrate that Sic1 accumulation upon TORC1 inactivation requires a stabilizing phosphorylation event specifically at residue Thr¹⁷³ that is mediated by the mitogen-activated protein kinase Mpk1. This phosphorylation is counterbalanced by PP2A^{Cdc55} that is inhibited under TORC1 inactivating conditions by the greatwall kinase-activated endosulfines. By this dual mechanism, TORC1 coordinates the START checkpoint with nutrient availability.

In the second chapter we investigate the molecular mechanisms by which Thr¹⁷³ promotes Sic1 stability. We undertook co-immunoprecipitation analysis followed by mass-spectrometry of the co-precipitating partners of Sic1 and Sic1^{T173A} that were pulled-down

from rapamycin-treated cells. This approach allowed us to conclude that phosphorylation of Thr¹⁷³ in Sic1 promotes binding of Sic1 to the cyclin-dependent protein kinase regulatory subunit and adaptor Cks1, thereby preventing Cdk1-dependent phosphorylation of the N-terminal domain of Sic1. Although details of this control mechanism remain to be deciphered, it is apparent that this mode of control ultimately prevents Sic1 ubiquitination by the SCF^{Cdc4} complex and subsequent degradation.

In the third chapter we investigate the mechanisms by which Rim15-Igo1/2 contribute to the control of G1 cyclins downregulation upon TORC1 inactivation. Here we show that the greatwall pathway controls G1 cyclins transcription and/or mRNA stability, probably by regulating transcription factors such as Xbp1 and Msa1 that play a role in G1 cyclins transcription control. The results presented in this chapter confirm the importance of Rim15 and Igo1/2 in the control of the G1 cell cycle machinery. Nevertheless, their precise role regarding G1 cyclins control remains to be elucidated.

Finally, in the fourth chapter we perform a genetic screen in which we try to identify suppressors of the defect of JK9-3D wild-type cells in exiting quiescence following rapamycin treatment. By the identification of the mutations responsible of the latter suppressor phenotype we aim to identify potential new regulators and/or targets of TORC1 which may allow us to gain further insight into the mechanisms controlling exit from quiescence.

In the final chapter we discuss our results from chapter I, II, III and IV in the context of the current literature and provide an outline of the most important experiments that may follow up on the discoveries resulting from this study.

Résumé

Les organismes vivants coordonnent la croissance des cellules avec la division cellulaire, en réponse à la disponibilité des éléments nutritifs essentiels. En absence de nutriments, les cellules arrêtent la progression du cycle cellulaire en phase G1 tardive et elles rentrent dans un état réversible dans le quel elles ne se divisent pas, mais elles sont métaboliquement actives, connu comme quiescence ou G0. En conditions pas favorables, l'échec de rentrer correctement dans cet état de quiescence peut se résoudre en fautes pendant la réplication de l'ADN et erreurs de ségrégation des chromosomes et, par conséquent, la perte de viabilité. Dans les organismes multicellulaires, un mauvais contrôle d'entrée et de sortie de la quiescence, peut conduire à une prolifération incontrôlée et finalement au développement tumoral.

Chez la levure *Saccharomyces cerevisiae*, plusieurs voies de signalisation des nutriments coordonnent la croissance des cellules et la division en réponse à la disponibilité des nutriments. Le travail présenté dans ce manuscrit se concentre sur le maître régulateur de la croissance cellulaire: le Target Of Rapamycin Complex 1 (TORC1). Après la privation des nutriments, l'inactivation de TORC1 se traduit dans l'activation de la protéine kinase Rim15 qui orchestre la majorités des aspects du programme G0, inclus le correct arrêt en G1. Rim15 contrôle la plus part des protéines qui se trouvent dans sa voie de signalisation, en inhibent (indirectement à travers les endosulfines de levure Igo1/2) la protéine phosphatase PP2A^{Cdc55}. Même si beaucoup d'efforts ont été faits pour déchiffrer les mécanismes moléculaires à travers les quels TORC1 règle la prolifération cellulaire, on cherche encore la réponse à nombreuse questions. Le but de cette thèse est celui de comprendre si la voie de signalisation TORC1-Rim15-Igo1/2-PP2A^{Cdc55} affecte les événements de la phase G1 du cycle cellulaire et, si oui, éclairer les mécanismes moléculaires qui sont à la base.

Basé sur les observations précédentes qui révèlent que les cellules mutants *rim15Δ*, après un traitement avec rapamycine, ont un défaut dans l'arrêt en phase G1 du cycle cellulaire, on montre dans le premier chapitre que la régulation négative de TORC1 après traitement avec rapamycine ou après la privation des nutriments, se traduit par l'enlèvement des cyclines G1 et l'accumulation de Sic1, l'inhibiteur de Cdk1, en manière Rim15-Igo1/2-dépendente. Dans ce travail, on montre que l'accumulation de Sic1, conséquent à l'inactivation de TORC1, demande la phosphorylation spécifique de l'acide

aminé Thr¹⁷³, événement qui stabilise Sic1 et qui est réglé par la protéine kinase mitogen-activée Mpk1. Cette phosphorylation est contrebalancée par PP2A^{Cdc55} qui est inhibée, pendant les conditions de inactivation de TORC1, par les endosulfines greatwall kinase-activées. À travers ce double mécanisme, TORC1 coordonne le START checkpoint et la disponibilité des nutriments.

Dans le deuxième chapitre on étudie les mécanismes moléculaires avec les quels Thr¹⁷³ favorise la stabilité de Sic1. Nous avons accompli une analyse de co-immunoprécipitation suivie par spectrométrie de masse des partenaires, co-immunoprécipités, de Sic1 et de Sic1^{T173A}, qui sont été tirées à partir de cellules traitées avec rapamycine. Cette approche nous a permis de conclure que la phosphorylation de la Thr¹⁷³ en Sic1 promeut la liaison de Sic1 à Cks1, la sous-unités adaptatrice et régulatrice de la protéine kinase dépendante de les cyclines, en prévenant ainsi la phosphorylation, dépendante de Cdk1, du domaine N-terminal de Sic1. Bien que les détails de ce mécanisme de contrôle doivent être encore déchiffrés, c'est évident que ce mode de contrôle empêche, en fin, l'ubiquitination de Sic1 par le complexe SCF^{Cdc4} et sa suivante dégradation.

Dans le troisième chapitre on enquête sur les mécanismes à travers les quels Rim15-Igo1/2 contribuent au contrôle de la régulation négative des cyclines G1, pendant l'inactivation de TORC1. Dans cette partie, on montre que la voie de signalisation de greatwall contrôle la transcription des cyclines G1 et/ou la stabilité de leur mARN, probablement en régulant les facteurs de transcription comme Xbp1 and Msa1 qui jouent en rôle dans le contrôle de la transcription des cyclines G1. Les résultats présentés dans ce chapitre, confirment l'importance de Rim15 et Igo1/2 dans la machinerie du contrôle de la phase G1 du cycle cellulaire. Cependant, leur rôle précis dans le contrôle des cyclines G1 reste à élucider.

En fin, dans le quatrième chapitre, nous accomplissons un screen génétique dans le quel on essaye d'identifier des supprimeurs du défaut que les souches JK9-3D wild type ont, en sortant dans la quiescence après un traitement avec rapamycine. À travers l'identification des mutations responsables de la suppression de ce phénotype, on se propose d'identifier des nouveaux régulateurs potentiels et/ou des cibles de TORC1 qui peuvent nous permettre de mieux comprendre les mécanismes qui contrôlent la sortie de la quiescence.

Dans le chapitre final on discute nos résultats des chapitre I, II, III et IV dans le contexte de la littérature actuelle, en fournissant le profil des expériences les plus importantes qui pourront suivre à partir des découvertes résultant de cette étude.

Introduction

1. The cell cycle

Cell reproduction is fundamental for the development and survival of all life. The different regulated events that give rise to two daughter cells from a single mother cell are collectively coined the cell cycle, which includes key processes such as DNA replication, mitosis and cytokinesis. The various stages of the cell cycle are tightly regulated to ensure proper genome integrity during cell division. In proliferating cells, cell growth is typically coordinated with cell division by mechanisms that ensure that DNA replication does not take place before cells reach a critical cell size and that genome duplication occurs only once per cell cycle. In contrast to genome duplication, cell growth (including the synthesis of cytoplasmic organelles, membranes, structural proteins, and RNAs) occurs steadily throughout the cell cycle.

The cell cycle is divided into four phases on the basis of chromosomal events. The DNA replication phase (S phase) and mitosis (M phase) are separated by gaps of varying length called G1 and G2. The first gap phase, G1, occurs before S phase and it is where cells grow and prepare themselves for genome duplication. G1 is a particularly important regulatory period because cells decide in this phase whether to enter into a new round of cell division or exit from the cell cycle. During the G2 phase, which occurs before M phase, the accuracy of DNA replication is checked as cells prepare for division (Forsburg & Nurse, 1991). All eukaryotic cell types follow some version of this basic cell cycle, although the length, the structure, and the regulatory details of the different phases may differ considerably between cell types.

2. *Saccharomyces cerevisiae* as a model organism

Classic model systems for cell cycle studies include the fission yeast *Schizosaccharomyces pombe* and the budding yeast *Saccharomyces cerevisiae*. The experimental part of this thesis is focused on the latter type of yeast. *S. cerevisiae*, the yeast used for baking, winemaking and brewing, has become a powerful biological model for eukaryotic organisms and it has been used by many laboratories for molecular and cellular biology studies in several fields of biomedical research. Of note, the first complete DNA sequence of a eukaryotic genome available was the one of the yeast *S. cerevisiae* (Goffeau et al, 1996). This organism presents several advantages for

its utilization in the laboratory: it poses little ethical and experimental constraints when compared to other model organisms, it is easy and relatively cheap to culture, it is small and has a short generation time (doubling time 1.30 hours), it allows the development and optimization of analytical methods, and it is easy to manipulate genetically. More interestingly, despite the evolutionary divergence, 31% of all the potential protein-encoding genes of yeast have a human ortholog (Botstein et al, 1997). Probably the best example of the value of yeast as a model system has been elucidated in the studies of cell cycle division, where many of the genes and the function of their products have been conserved throughout evolution (O Morgan, 2007).

S. cerevisiae can follow two different reproductive strategies in response to different environmental conditions. Under poor nutrient sources, haploid cells have the ability to arrest in G1 and enter into stationary phase where they become more resistant to different stresses. This gives them the ability to survive for extended periods of starvation and to resume growth when more favorable conditions appear. In addition, in cases where there is another yeast of opposite mating type in the proximity they can undergo mating. *S. cerevisiae* can have either of two different mating types, a and α (genotypes *MATa* and *MAT α*), which secrete different pheromones that are sensed by cells of the opposite mating type. *MAT α* cells secrete α -factor and *MATa* cells secrete a-factor pheromones. During the mating process, yeast cells are stimulated by the pheromone secreted by the cell of the opposite mating type, which induces several physiological changes required for mating. These include changes in expression of about 200 genes, synchronization of the two cell cycles with a transient G1 arrest, and cellular growth oriented towards the mating partner followed by fusion of the plasma membranes and subsequent fusion of the two nuclei (Bardwell, 2005). After the fusion of the two haploid cells, a stable diploid is formed which may continue division by mitosis (Herskowitz, 1988). If yeast cells are diploid, they can enter into meiosis under nutrient depletion (*i.e.* nitrogen starvation on a non-fermentable carbon source) and produce four haploid spores that are highly resistant to stress.

When grown under optimal nutrient conditions, haploid and diploid cells can proceed through the cell cycle and divide by mitosis, in an asymmetric process of asexual reproduction by budding off progenies that are smaller than the mother cells (Hartwell & Unger, 1977; Keaton & Lew, 2006; Lord & Wheals, 1980). One of the main advantages of *S. cerevisiae* is that progression through the cell cycle can be monitored at least

approximately by light microscopy since the size of the bud can serve as a marker of the cell cycle position. Buds appear at the end of the G1 phase and enlargement occurs through the S and M phase until the buds reach a size that is a bit smaller than the mother cells. Hence, the daughter cells must increase in size before initiating a new cell division (Herskowitz, 1988).

3. Cell cycle regulation in *Saccharomyces cerevisiae*

As stated above, cell cycle progression is tightly regulated by several switches, which guarantee the order and timing of all cell cycle events. These transition points ensure that cells move unidirectionally through the cell cycle (Elledge, 1996). In the presence of sufficient nutrients, *S. cerevisiae* cells enter into a new round of cell division when they reach a critical size. This point occurs late in G1 phase and is known as Start (also known as restriction point in mammals). Passing through Start is an all-or-none response and once cells have gone through it, they initiate DNA replication, spindle pole body duplication, and bud growth (Fig. 1). All these processes are required for further cell cycle events such as mitosis and cytokinesis (Nishizawa et al, 1998). Cells divide rapidly when nutrients are abundant, but can exit the proliferation mode following nutrient deprivation upon which they arrest in the G1 phase of the cell cycle and enter into a quiescence state known as G0 phase (De Virgilio, 2012; Herskowitz, 1988). While Start is a nutrient- (and pheromone-) regulated cell cycle checkpoint, there are additional checkpoints that monitor the proper duplication of the genome (at G2/M) or attachment of spindles to chromosomes (at M).

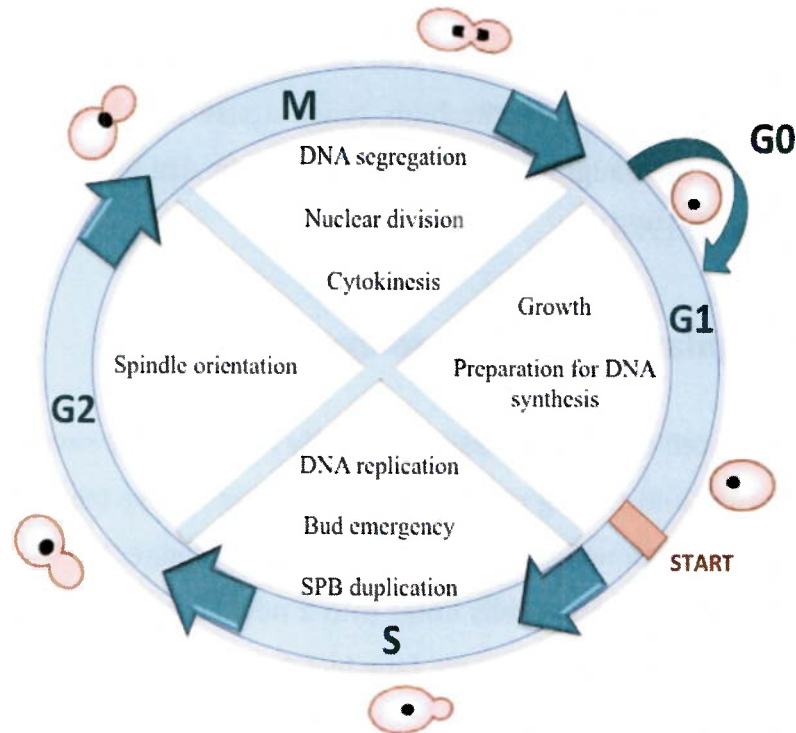


Figure 1. The *Saccharomyces cerevisiae* cell division cycle. The four cell cycle phases are represented: G1, S, G2 and M. Between the G1 and S phase, there is an event known as Start that is a point of commitment to the cell cycle. Although only annotated in the G1 phase, cell growth occurs throughout the whole cell cycle. Exit from cell cycle division into quiescence or G0 phase is shown. Cell cycle-dependent morphology is also represented.

During S phase, prior to DNA duplication, the DNA helix should be opened at specific sites known as replication origins. *S. cerevisiae* cells contain autonomous replication sequences (ARS) that are recognized by the origin recognition complex (ORC), which opens the DNA into a structure known as replication fork, where the replication machinery can be recruited. The cell cycle control systems activate replication origins under a strict temporal and spatial sequence throughout S phase to ensure that once DNA replication begins, it proceeds, only once, until its completion. This ensures that daughter cells inherit an appropriate amount of DNA (Donaldson & Blow, 1999). The budding yeast cell cycle is characterized by a relatively long G1 phase and no clearly defined gap (G2) between S and M phases (Hartwell et al, 1974). During M phase, the different cellular components are segregated into the daughter and mother cells in two major events, nuclear division, coined mitosis, and cellular division, also termed cytokinesis.

4. Cyclin dependent kinases: master regulators of the cell cycle.

Cyclin-dependent kinases (Cdks) control progression through the eukaryotic cell cycle. As the name implies, Cdks are a family of proline-directed serine/threonine (Ser/Thr) protein kinases that are dependent on the binding of a cyclin for their directed and specific activity (Morgan, 1995; Morgan, 1997). Cdks and cyclins are highly conserved from yeast to mammals (Malumbres, 2014). In the cyclin-free, monomeric form, the substrate binding site of a typical Cdk (*e.g.*, Cdk1) is blocked by the T-loop present in its carboxy-terminal (C-) lobe. In addition, the amino-terminal (N-) lobe, which contains the PSTAIRE motif, is displaced and partially disordered, which causes a misalignment of key catalytic residues in the ATP-binding thereby hampering efficient phospho-transfer (Jeffrey et al, 1995; Malumbres, 2014; Mendenhall & Hodge, 1998). Budding yeast express 6 cyclin-dependent protein kinases (Cdc28, Pho85, Kin28, Ssn3, Bur1, and Ctk1), which can be classified in two different groups. The first group includes the Cdks Cdc28 and Pho85 that bind several cyclins and regulate cell cycle events. The second group includes Kin28, Ssn3, Bur1 and Ctk1, which are activated by a single cyclin that is not usually regulated in a cell-cycle-dependent manner, and which are involved in the regulation of transcription (Malumbres, 2014). Unlike higher eukaryotes, budding yeast control all cell-cycle events mainly via a single essential cyclin dependent kinase called Cdk1 or Cdc28 (Nasmyth, 1993). Distinct cyclin-Cdk1 complexes are required at different stages of the cell cycle: in G1, Cln1-3-Cdk1 regulates the processes during the cell cycle interval between mitosis and DNA replication; in S phase, Clb5/6-Cdk1 is involved in DNA replication; and Clb1-4-Cdk1 is involved in G2 phase progression and mitosis. Typically, Cdk levels remain constant and in large excess over cyclin levels during the cell cycle, while the levels of cyclins oscillate (hence their name) during the different cell cycle phases (Nishizawa et al, 1998). Although cyclin binding is a key determinant event required for Cdk1 activity, additional regulatory mechanisms exist to ensure proper timing and coordination of cell cycle events (Mendenhall & Hodge, 1998). Accordingly, Cdk activity is also modulated by phosphorylation via other protein kinases, by cyclin dependent kinase inhibitors (CKIs), or by binding of specific adaptor subunits (such as Cks1).

4.1 Cyclins: key determinants of Cdk activity

Cyclins were initially identified as proteins whose levels oscillate synchronously with the early embryonic cleavage divisions of sea urchins (Evans et al, 1983). Binding of cyclins to Cdks is essential for their kinase activity as well as for their specificity as they mediate docking to specific substrates (Koivomagi et al, 2011b; Schulman et al, 1998). As their name implies, cyclins are highly unstable proteins that are synthesized and degraded periodically during the cell cycle. Cyclin expression is controlled by three different mechanisms that ensure proper timing: transcriptional control, subcellular localization, and ubiquitin mediated degradation. These mechanisms ensure that cyclin levels peak appropriately both temporally and spatially during the different cell cycle stages (Bloom & Cross, 2007; Murray, 2004).

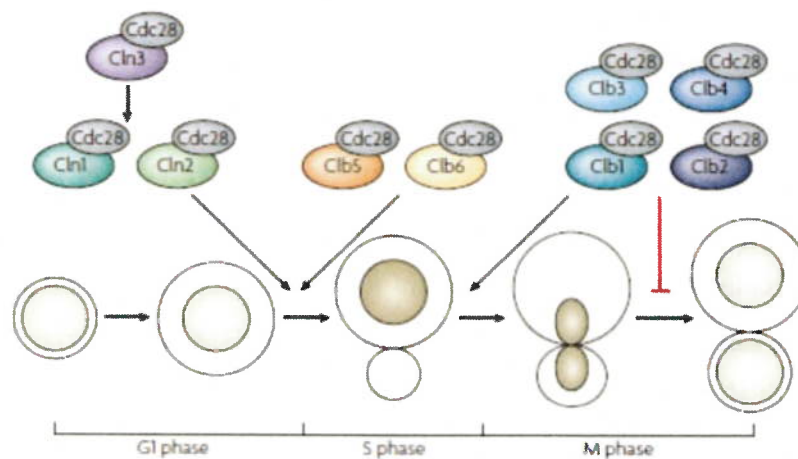


Figure 2. Cyclin binding to Cdc28 (Cdk1) regulates cell cycle progression in *S. cerevisiae*. The G1 phase Cln3 initiates Start and leads to the transcription of the other G1 cyclins Cln1 and Cln2 that promote bud emergence, spindle pole body duplication and activation of the B-type cyclins. The S-phase cyclins (Clb5 and Clb6) initiate DNA replication, and the M-phase cyclins (Clb1, Clb2, Clb3, and Clb4) promote spindle formation and mitosis initiation. Mitotic cyclins also prevent mitotic exit. From (Bloom & Cross, 2007).

Despite the very slow dissociation rates between Cdks and cyclins, Cdks can quickly associate with different cyclins as a result of the rapid ubiquitin-mediated degradation of cyclins (Glotzer et al, 1991; Kobayashi et al, 1994; Murray, 1995). Cyclins exhibit a high percentage of similarity at their N-termini in a specific conserved domain called

cyclin box (Kobayashi et al, 1992). Cyclin boxes contains a structural motif known as cyclin-fold (made up of five α -helices) and mediate binding between cyclins and Cdks (Noble et al, 1997). With the exception of Cln3, budding yeast expresses two functionally related paralogs of each other cyclin (Mendenhall & Hodge, 1998) (Fig. 2).

4.1.1. G1-Cyclins

CLN3

Cln3 initiates the transcription of the genes encoding the G1 cyclins Cln1 and Cln2. Since Cln3 is the most upstream activator of Cln1 and Cln2 at Start (Dirick et al, 1995; Dirick et al, 1998), it is not surprising that several signal transduction pathways control cell cycle progression by regulating Cln3 transcription, translation, stability, and function. Deletion of *CLN3* produces enlarged cells with an extended G1 phase, which exhibit normal growth rates (Dirick et al, 1995). Unlike other cyclins, the total amount of Cln3 does not oscillate strongly during the cell cycle, which is why additional post-translational mechanisms regulate Cln3-Cdk1 complexes to reach their maximal level in late G1. Nevertheless, there is a notable transcriptional periodicity that generates a small increase of *CLN3* mRNA late in G1 and this depends on the transcription factor Mcm1 that activates transcription from early cell cycle boxes (ECB) present in the promoter of *CLN3* (Cross & Blake, 1993; Mai et al, 2002; McInerney et al, 1997; Tyers et al, 1993). Cln3 is an unstable protein with a very short half-life whose levels are very sensitive to changes in translation initiation due to presence of an upstream open reading frame (uORF) in the 5' untranslated region (5' UTR) of the *CLN3* mRNA (Polymenis & Schmidt, 1997). This process renders Cln3 levels (and consequently Start) very sensitive to the nutritional status of the cell. Regarding subcellular localization, Cln3 contains a C-terminal nuclear localization signal (NLS) that is required for its nuclear import (Edgington & Futcher, 2001; Miller & Cross, 2001). When sufficiently high, nuclear levels of Cln3 may trigger passage through Start through a series of events that are presented below in more detail.

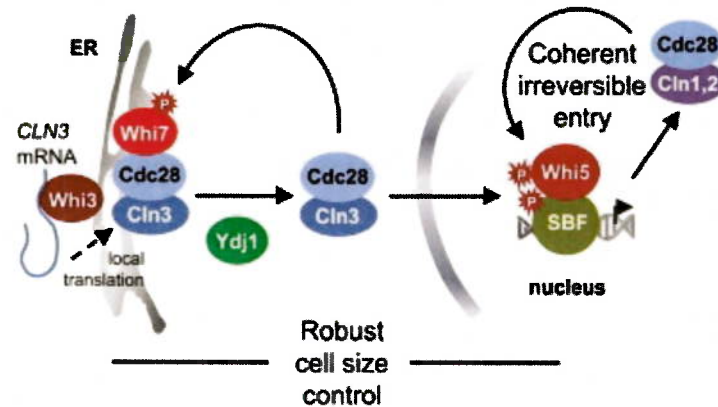


Figure 3. Cln3 regulation at the earliest steps of Start. Cln3 participates in a positive feedback loop to promote its own release from the ER. Whi3 and Whi7 are involved in the recruitment of *CLN3* mRNA, retaining newly formed Cln3-Cdk1 complexes at the ER in early G1. Initially, Cln3-Cdk1 is released by the Ydj1 chaperone, and then phosphorylates and inhibits Whi7, which releases further Cln3-Cdk1 complexes that enter into the nucleus to phosphorylate Whi5 and trigger Start. From (Yahya et al, 2014).

The mechanism of Cln3 nuclear translocation is regulated by a very complex mechanism (Fig. 3). In early G1, the Cln3-Cdk1 complex is regulated by an ER-retention/release mechanism. Cln3 ER-retention is mediated by the Ji domains of Cln3 and Ydj1 that compete for binding the ER-associated Ssa1/2 proteins, as well as by Whi3 that recruits Cdk1 to the ER membrane during early and mid G1 phase. In late G1, Ydj1 levels increase, achieving a specific threshold that promotes the release of Cln3 from Ssa1/2. Free Cln3-Cdk1 is then transported to the nucleus where it can exert its function (Gari et al, 2001; Verges et al, 2007; Wang et al, 2004). More recent studies also identified Whi7, a Whi5 paralog, as a novel negative regulator of Start that contributes to the recruitment of Cln3 to the ER. Whi7 associates with the ER in a Cdk1 phosphorylation-dependent manner. Once the first Cln3-Cdk1 complexes have been released by the Ydj1 chaperone, they are proposed to phosphorylate Whi7, thereby inhibiting its role in retaining Cln3 at the ER in a positive feedback loop (Yahya et al, 2014).

CLN1* and *CLN2

The second group of G1 cyclins includes Cln1 and Cln2 that were originally identified as high-dosage suppressors of the *cdc28-4^{ts}* mutation. They are only distantly related to Cln3 (Hadwiger et al, 1989b; Nash et al, 1988). These cyclins present high levels of homology among each other with 57% of identity that rises to 72% at their N-termini

where the cyclin box is located. The more divergent C-terminus contains destabilizing PEST regions that are involved in protein degradation by an ubiquitin dependent mechanism (see section 6.1) (Quilis & Igual, 2012). Deletion of each individual gene (*i.e.* *CLN1* or *CLN2*) does not cause a strong phenotype, but double mutant cells grow slowly and present an aberrant morphology (Hadwiger et al, 1989b) and have a delay in budding and DNA synthesis initiation (Dirick et al, 1995; Stuart & Wittenberg, 1995). Following Start, yeast cells initiate bud formation and spindle pole body duplication by mechanisms that involve cytoplasmic Cln1 and Cln2 (Miller & Cross, 2000; Polymenis & Schmidt, 1999). At Start, Cln1 and Cln2 are involved in proteolytic degradation of Sic1 (Verma et al, 1997a) and inactivation of Cdh1, both of which are negative regulators of Clb-Cdk1 activity (for a detailed description of Sic1 and Cdh1 see sections 4.3.4 and 6.2) (Schwab et al, 1997; Visintin et al, 1997; Zachariae et al, 1998). Cln1 and Cln2 are important for coordination of the transcriptional program and bud emergence at G1/S (Skotheim et al, 2008). Regarding their subcellular localization, Cln1 and Cln2 are mainly cytoplasmic, although Cln2 has also been found to be nuclear (Edgington & Futcher, 2001). In addition, some studies demonstrated that their function is affected when a nuclear export signal is included, suggesting that both cyclins may have also important roles in the nucleus (Bloom & Cross, 2007; Miller & Cross, 2001).

4.1.2. B-type cyclins

B-type cyclins form a family of six proteins commonly subdivided into three pairs based on their homology and transcriptional pattern.

CLB5* and *CLB6

The first pair of cyclins being expressed along the cell cycle is Clb5/6, which are 50% identical compared to each other (Mendenhall & Hodge, 1998). They are produced at Start and the respective protein levels peak at G1/S. Their primary roles are to inhibit Cln-Cdk1 complexes (Basco et al, 1995), to initiate S-phase and DNA replication and to prevent re-initiation of replication origins that have already fired (Dahmann et al, 1995; Masumoto et al, 2002; Schwob & Nasmyth, 1993). In addition, Clb5 and Clb6 may play a role in spindle formation (Schwob & Nasmyth, 1993). Cells deleted for *CLB5* present an extended S phase (Epstein & Cross, 1992), but deletion of *CLB6* has little or no

phenotype. Loss of Clb5 and Clb6 together causes a long S-phase initiation delay relative to bud emergence. Due to the high overlapping functional specificities of S and M phase cyclins, the mitotic Clb3 and Clb4 cyclins can trigger progression into S-phase in the absence of both Clb5 and Clb6 (Schwob & Nasmyth, 1993).

CLB3 and CLB4

Another pair of B-type cyclins is formed by Clb3/4, which are 62% identical compared to each other (Mendenhall & Hodge, 1998). Their levels increase at the beginning of the S-phase (after the Cln1/2 peak) and remain high until late in anaphase. Both proteins contribute to DNA replication and to drive spindle assembly with Clb3-Cdk1 complexes having a major role (Epstein & Cross, 1992; Fitch et al, 1992; Richardson et al, 1992). The mitotic Clb4-Cdk1 complex has been found to accumulate in the mother cell via a mechanism that is so far not well understood (Liakopoulos et al, 2003; Maekawa & Schiebel, 2004).

CLB1 and CLB2

The last wave of B-type cyclins appears before anaphase and includes the two highly homologous cyclins Clb1 and Clb2, which are 62% identical over their entire length. They promote bud growth, chromosome separation and inhibit G1-specific events (Amon et al, 1993; Fitch et al, 1992; Lew & Reed, 1993) with Clb2-Cdk1 complexes playing a major role (Bailly et al, 2003). Clb2 is present at the bud neck during budding (Hood et al, 2001).

4.2. Control of Cdk1 activity by phosphorylation

4.2.1. Cdk1-activating phosphorylation by the Cdk-activating kinase

Besides binding to cyclins, phosphorylation of Cdk1 at the position Thr¹⁶⁹ in its T-loop is required for full activation. In Cdks, phosphorylation at this position requires the Cdk activating kinase (CAK) Cak1 (also known as Civ1) (Fig. 4) (Espinoza et al, 1996; Kaldis et al, 1996; Thuret et al, 1996). Together with cyclin binding, the phosphorylation Thr¹⁶⁹ changes the three-dimensional structure of Cdks, affecting therefore their functionality. Binding of cyclins move the T-loop (containing Thr¹⁶⁹) to an opened conformation

where Thr¹⁶⁹ becomes accessible for Cak1 phosphorylation. This phosphorylation moves the T-loop such that the phosphate group can interact with several residues, which stabilizes the entire structure of the T-loop and the neighboring interactions in both the Cdk and cyclin. This explains the positive effect of Cdk1 phosphorylation on cyclin binding (Russo et al, 1996). In contrast to higher eukaryotes, in *S. cerevisiae* the activating phosphorylation of Cdk1 precedes cyclin binding, since the non-phosphorylatable Cdk1 mutants binds cyclins less efficiently compared to the wild type control *in vivo* (Ross et al, 2000).

4.2.2. Cdk1 inhibitory phosphorylation

Besides activation by phosphorylation, there is also a reversible inhibitory phosphorylation on the Cdk catalytic subunits at positions corresponding to Thr¹⁸ (Krek & Nigg, 1991; Norbury et al, 1991) and Tyr¹⁹ (Fig. 4) (Gould & Nurse, 1989). Although the mechanism by which phosphorylation at these sites inhibits Cdk activity has not been established, one proposed model is that the regulatory sites are located near the ATP-binding site and may interfere with the orientation of the ATP and reduce the affinity for its substrates (Welburn et al, 2007). In *S. cerevisiae*, the protein kinase Swe1 (the homolog of Wee1 in *S. pombe*) is responsible of Tyr¹⁹ phosphorylation and consequently the inhibition of the mitosis-promoting Cdk activity when actin polarization and bud formation are impaired and hence the morphogenesis checkpoint is activated. Different cyclin-Cdk1 complexes are differently susceptible to inhibition by Swe1, but Clb1/2-Cdk1 complexes are the best substrates in this respect (Cid et al, 2002; Kellogg, 2003; Lew, 2003; Rupes, 2002). Swe1 itself is also a substrate of Clb2-Cdk1 (McMillan et al, 2002). When Clb2-Cdk1 activity levels increase, Clb2-Cdk1-mediated phosphorylation of Swe1 serves as a priming site to promote the additional phosphorylation of Swe1 by the polo-like kinase Cdc5 at multiple sites, which then promotes Swe1 degradation and consequently progression to mitosis (Asano et al, 2005). The degradation of Swe1 is conducted by two different ubiquitin ligase complexes named the anaphase-promoting (APC) and the Skp1/Cdc53/F-box (SCF) complex (Kaiser et al, 1998; Thornton & Toczyski, 2003). Swe1 phosphorylation is opposed at mitosis by the Mih1 phosphatase (the ortholog of *S. pombe* Cdc25) (Russell et al, 1989).

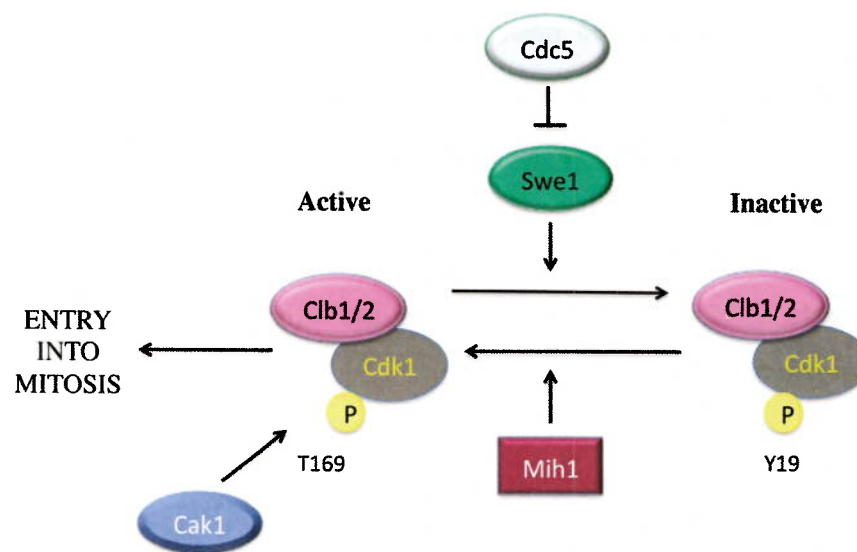


Figure 4. Regulation of Cdk1 by phosphorylation. The Cdk activating kinase Cak1 phosphorylates Cdk1 at Thr¹⁶⁹ contributing to its activation. On the contrary, Swe1 dependent phosphorylation at Tyr¹⁹ inhibits Clb1/2-Cdk1 complexes, which can be reverted by the phosphatase Mih1. Although Swe1 phosphorylation by Clb2-Cdk1 promotes its activity and therefore inhibition of Cdk1 (not shown), it also induces additional phosphorylation of Swe1 by Cdc5, which then causes its degradation.

4.3 Cdk1 inhibition by cyclin dependent kinase inhibitors

The cyclin dependent kinase inhibitors (CKI) antagonize the action of the cyclins. Mammalian CKIs can be classified in two families according to their sequence and functional similarities. The Kip/Cip family includes p27^{Kip1}, p21^{Cip1} and p57^{Kip2} that have a preference for G1/S-Cdk complexes over the mitotic ones (Chen et al, 1995; Harper et al, 1995; Lin et al, 1996; Toyoshima & Hunter, 1994). The second family includes p15, p16, p18 and p19 that have specificity for Cdk4 and Cdk6 isolated in complex with their partner cyclin D (Sherr & Roberts, 1995). In budding yeast, there are four known CKI that play important roles in cell cycle regulation. Far1 is an important regulator in the mating pathway that arrests cells at Start in response to mating pheromone; Sic1 regulates cell cycle at mitotic exit and antagonizes passage through Start; Cdc6 is involved in promoting mitotic exit by inhibiting mitotic cyclin Cdk1 complexes; and Pho81 inhibits Pho80-Pho85 to contribute to the inhibition of G1 progression. The following sections are focused on a more detailed description of these four CKIs.

4.3.1. *FAR1*

FAR1 was originally identified as a gene required for cell cycle arrest in response to mating pheromones (Chang & Herskowitz, 1990). Far1 plays two distinct roles in the pheromone response process: it acts as scaffold to stimulate the polarized growth of the cells towards their mating partner (Butty et al, 1998; Nern & Arkowitz, 1999) and as Cdk1 inhibitor to mediate pheromone-imposed cell cycle arrest (Chang & Herskowitz, 1990; Peter et al, 1993; Peter & Herskowitz, 1994). Although Far1 was initially reported as inhibitor of Cln1/2-Cdk1 protein kinase activity (Chang & Herskowitz, 1990; Peter & Herskowitz, 1994), successive studies have established that Far1 has inhibitory activity against the Cln3-Cdk1 complex as well (Jeoung et al, 1998). The respective inhibition seems to be specific for G1 cyclins, since Clb5-Cdk1 and Clb2-Cdk1 complexes cannot be inhibited by Far1 *in vitro* (Peter & Herskowitz, 1994). Several reports have described that Far1 is bound to Cln1/2-Cdk1 complexes even in the absence of pheromone and that *far1Δ* cells exhibit a shortened G1 phase relative to the wild-type cells, which is indicative of a constitutive role of Far1 in regulation of Cln-Cdk1 activity at Start that is independent of its role in mating (McKinney & Cross, 1995). In particular, it has been proposed that Far1, together with Cln3, may act as threshold-like, nutritionally modulated cell sizer. Cln3 levels have to overcome the ones of Far1 in order to trigger Cln1/2-Cdk1 activation (Alberghina et al, 2004; Barberis et al, 2007; Di Talia et al, 2007). Recent results further suggest that Far1 may also regulate cell cycle progression in mitotic cells (Alberghina et al, 2004; Fu et al, 2003).

In G1 cells, Far1 is predominantly nuclear, although it shuttles constantly between nucleus and cytoplasm (Blondel et al, 1999; Pines, 1999). Far1 localization is associated with different cellular functions: nuclear localization is thought to be required for cell cycle arrest, whereas cytoplasmic localization promotes polarized growth towards higher pheromone concentration (Blondel et al, 1999; Verma et al, 1997a). Pheromone addition stimulates *FAR1* transcription (Chang & Herskowitz, 1990), but the respective elevated Far1 protein levels are not sufficient to arrest cells in G1. Far1 inhibitory activity is acquired by post-translational modifications. Phosphorylation of Far1 at Thr³⁰⁶ by the mitogen-activated protein (MAP) kinase homolog Fus3 (which is also involved in boosting *FAR1* transcription) (Elion et al, 1993) is required for full activation of Far1 and this leads to the inhibition of Cln-Cdk1 complexes. The exact mechanism of

inhibition remains unclear, but it seems probable that Far1 mediates substrate exclusion, since Cln-Cdk1 resumes its activity *in vitro* following removal of Far1 (Peter & Herskowitz, 1994). In a regulated feedback inhibition loop, Cln-Cdk1 complexes phosphorylate and consequently trigger Far1 degradation (McKinney et al, 1993; Peter et al, 1993). This process is regulated via the phosphorylation of Ser⁸⁷ on Far1, which results in SCF^{Cdc4}-dependent ubiquitination and its subsequent degradation (Blondel et al, 2000; Henchoz et al, 1997). This negative feedback loop between Far1 and Cln-Cdk1 makes mitosis and mating mutually exclusive: cells commit to either a mitotic cycle or to mating (Doncic et al, 2011; McKinney et al, 1993).

4.3.2. *PHO81*

In response to phosphate levels, Pho81 inhibits Pho85-Pho80/Pcl7 complexes that control in part G1 cell-cycle progression (Lee et al, 2000; Schneider et al, 1994). Pho81 exhibits six repeats of ankyrin-like sequence in its terminal region, with high similarity to p16INK4 that inhibits human CycD-Cdk4 complexes (Ogawa et al, 1995).

4.3.3. *SIC1*

Sic1 is a potent inhibitor of Clb-Cdk1 complexes playing a role in the timing and robustness of DNA replication by setting a threshold for Clb-Cdk1 activation (Cross et al, 2007). Sic1 was first identified as a 40-kDa protein that co-precipitated with Cdk1, inhibiting its kinase activity (Mendenhall, 1993; Reed et al, 1985). The *SIC1* open reading frame codes for a protein of a predicted molecular weight of 32,2 kDa and 284 residues. Sic1 is intrinsically disordered throughout the polypeptide chain, although its C-terminus is slightly more ordered than its N-terminus (Brocca et al, 2009; Brocca et al, 2011; Lambrughi et al, 2012). Sic1 transcripts and protein levels are detectable throughout the cell cycle (Aerne et al, 1998; Archambault et al, 2003; Coccetti et al, 2004; Knapp et al, 1996), but peak at the M/G1 transition (Schwob et al, 1994; Thornton & Toczyski, 2003; Verma et al, 1997a). Sic1 has at least two specific roles in cell-cycle regulation. On one hand it inhibits Clb2-Cdk1 activity, in parallel to the APC^{Cdh1} dependent destruction of Clb2, to allow spindle degradation and mitosis exit (see section 6.2) (Lopez-Aviles et al, 2009). On the other hand, it inhibits Clb5/6-Cdk1

complexes at the G1/S transition. This is crucial for the proper timing of DNA replication initiation and for maintaining a G1 temporal window free of Clb5/6-Cdk1 activity that is required for origin licensing (Lengronne & Schwob, 2002; Mendenhall, 1993; Schwob et al, 1994).

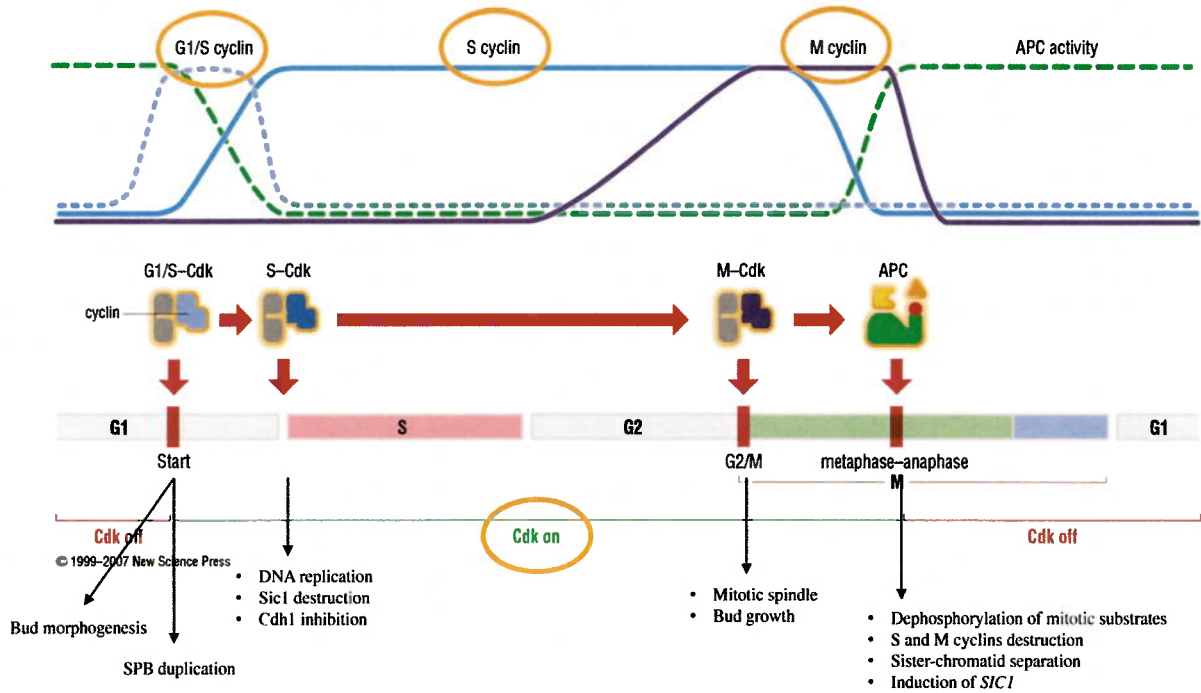


Figure 5. A simplified view of the cell cycle control system. Levels of the three cyclin types oscillate during the cell cycle. G1/S cyclin-Cdk1 complexes initiate bud morphogenesis and activate S cyclin-Cdk complexes that promote Sic1 destruction and DNA replication. M cyclin-Cdk complexes control mitotic spindle assembly and APC activation that triggers sister-chromatid separation and mitotic cyclin destruction. Adapted from (Morgan, 2007).

Sic1 has been described as the main regulator of the timing of Clb waves (Fig. 5) (Barberis, 2012; Barberis et al, 2011). In early G1, Cdk1 activity is low due to the scarce levels of Clbs that are prone to APC^{Cdh1}-mediated ubiquitination that is activated late in mitosis. This also allows the accumulation of the G1-cyclin-inhibitory Sic1 (see also section 6.2) (Cross, 2003). As cells progress through G1, Cln1/2-Cdk1 activity raises, phosphorylates Cdh1, and consequently reduces the APC activity. At the same time *CLB5/6* expression increases, although Clb5/6-Cdk1 activity is initially inhibited by the presence of Sic1. At the onset of S phase, Sic1 is phosphorylated by Cln1/2-Cdk1, ubiquitinated, and degraded by the proteasome. This releases the pool of inactive

Clb5/6-Cdk1 and promotes DNA synthesis and entry into S phase (Nash et al, 2001; Verma et al, 1997a)(Fig. 6).

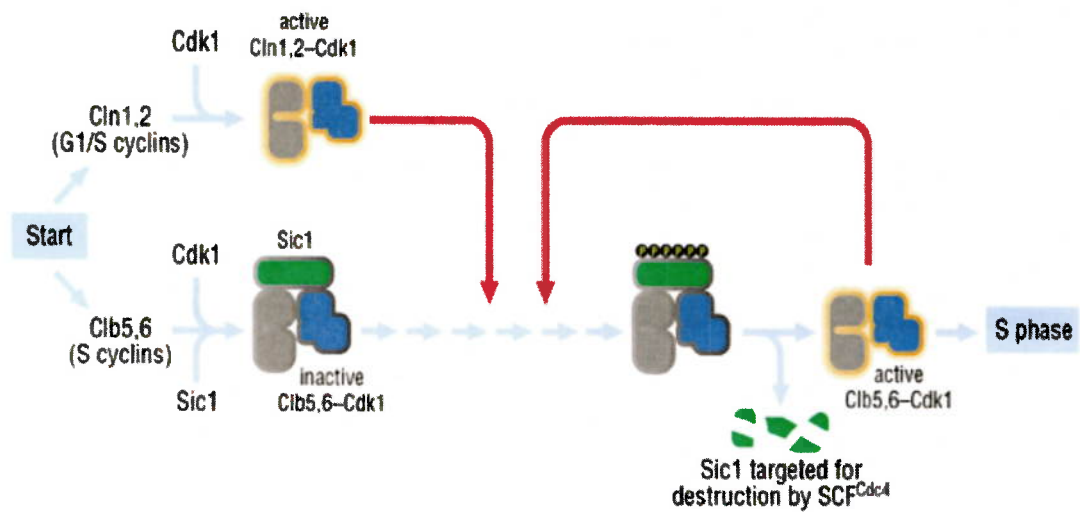


Figure 6. Sic1 regulation at the G1 to S phase transition. Passing through Start results in increased formation of G1/S cyclin-Cdk1 and S cyclin-Cdk1 complexes. However, S cyclin-Cdk1 complexes are initially inhibited by Sic1. Further accumulation of G1/S cyclin-Cdk1 complexes leads to multisite Sic1 phosphorylation, ubiquitination and destruction, releasing active S cyclin-Cdk1 complexes that can initiate DNA replication. From (Morgan, 2007).

SIC1 is not an essential gene, but its deletion causes a prematurely and uncontrolled activation of DNA synthesis where origins of replication are fired as a result of premature activation of Clb5/6-Cdk1 complexes in early G1. As a consequence, *sic1Δ* cells exhibit an extended S phase, a high frequency of broken and lost chromosomes, and inefficient chromosome separation during anaphase, which can lead to gross chromosomal rearrangements (Lengronne & Schwob, 2002; Nugroho & Mendenhall, 1994). Loss of Sic1 may therefore cause cells to arrest in anaphase and telophase transition with elongated buds (Lengronne & Schwob, 2002; Nugroho & Mendenhall, 1994). Delaying S-Cdk1 activation can rescue the defects of such cells in both S and M phases (Lengronne & Schwob, 2002). In contrast to loss of Sic1, overexpression of Sic1 causes cell cycle arrest at the transition between Start and the initiation of DNA replication, giving rise to cells with elongated buds (Barberis et al, 2005a; Schwob et al, 1994). The respective cell cycle arrest is dependent of total Clb-Cdk1 levels - if the latter exceed the ones of Sic1, cells can drive through cell cycle progression despite Sic1

overproduction (Barberis, 2012). Interestingly, a positive functional role of Sic1 in the G1/S transition has also been described (Rossi et al, 2005). Accordingly, Sic1 facilitates the transport of Clb5-Cdk1 complexes to the nucleus prior to the onset of DNA replication. A similar mechanism has been described for p21^{Cip1} and p27^{Kip1} that promote the nuclear import and the assembly of CycD1-Cdk4 (Cheng et al, 1999; LaBaer et al, 1997).

4.3.3.1. Molecular mechanism of Sic1 inhibition of Clb-Cdk1 complexes

Despite the well studied Clb-Cdk1 inhibitory role of Sic1 and its relevance for cell cycle and genomic stability control, the details of the molecular mechanisms of this inhibition remain largely unknown since any attempt to crystallize Sic1 was successful until now (Chouard, 2011). Verma and colleagues performed deletion analyses of Sic1, which indicated that the C-terminal fragment of Sic1 is able to bind Clb-Cdk1 complexes *in vitro* and that the N-terminal 160 residues are both necessary and sufficient for Cln2- and Cdc34-dependent Sic1 ubiquitination *in vitro* (Verma et al, 1997b). These results suggest a modular structure for Sic1 where the Cdk binding and the instability domains are spatially distinct (Verma et al, 1997b). Further studies of (Hodge & Mendenhall, 1999) mapped the C-terminal 70 amino acids (from residues 215 to 284) as a minimal domain required for Clb-Cdk1 inhibition *in vivo*. This sequence has high levels of homology to the minimal inhibitory domain of Rum1, the functional Sic1 ortholog from *S. pombe* (Sanchez-Diaz et al, 1998). In another study, Sic1 was described as functional ortholog of mammalian Cki p21^{Cip1} (Peter & Herskowitz, 1994), which has 42% of sequence similarity with Cki p27^{Kip1} (Barberis et al, 2005a). In mammalian cells, p27^{Kip1} inhibits progression through S phase by inhibiting CycA-Cdk2 complexes (Russo et al, 1996). The inhibitory mechanism proposed for p27^{Kip1} implies first occupation of a substrate binding site on cyclin A, followed by binding to the N-terminal lobe of Cdk2, which disrupts the active site. In addition, p27^{Kip1} blocks the ATP binding of Cdk2 by inserting itself into the ATP binding pocket (Russo et al, 1996)(Fig. 7). The fact that the inhibitory domain of Sic1 is functionally and structurally related to p27^{Kip1} suggests that Sic1 may inhibit G1/S cyclin-Cdk complexes in a similar manner (Barberis, 2012; Barberis et al, 2005a).

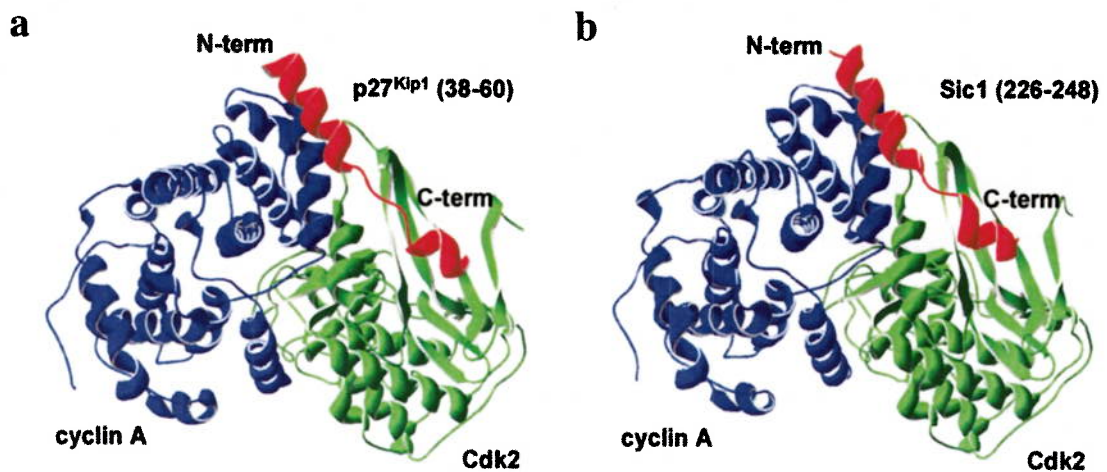


Figure 7. Molecular visualization of surface interactions of p27^{Kip1} and Sic1 inhibitory domains with the Cdk2-cyclin A complex. α -Helices of p27^{Kip1} (residues 38-60) (a) and Sic1 (residues 226-248) (b) are shown in red; Cdk2 and cyclin A are visualized in green and blue respectively. Secondary structure predictions were obtained for the sequence corresponding to the inhibitory domain of Sic1 and p27^{Kip1}, computed and compared with the secondary structure deduced from the X-ray structure of p27^{Kip1}, and finally modeled *in silico*. From (Russo et al, 1996).

4.3.3.2. Sic1 regulation at the M/G1 transition

SIC1 mRNA expression oscillates during the cell cycle, peaking in late anaphase (Schwob et al, 1994). *SIC1* transcription is regulated mainly by two transcription factors: Swi5 that is responsible for the majority of its periodicity and Ace2 that is responsible for the residual periodicity. Deletion of *SWI5* reduces *SIC1* transcription to 50% while deletion of *ACE2* decreases it to 80% of wild-type levels. Deletion of both *SWI5* and *ACE2* genes together reduces *SIC1* transcription to 20% of that of the wild type (Knapp et al, 1996; Toyn et al, 1997). Swi5 is a substrate for the SCF^{Cdc4} ubiquitin ligase complex and its consequent degradation stops *SIC1* transcription in early G1 phase to ensure proper entry into S phase (Kishi et al, 2008). Swi5 subcellular localization and activity is dependent on its phosphorylation state. When Clb2-Cdk1 activity is high, Swi5 is phosphorylated (inactive) in the cytoplasm, but when Clb2-Cdk1 activity is low, Swi5 is dephosphorylated (active) and is driven into the nucleus. The first accumulation of nuclear Swi5 produces a positive-feedback loop since the newly synthesized Sic1 inhibits any residual Clb2-Cdk1 not destroyed in anaphase, therefore reducing Swi5 phosphorylation and promoting nuclear transition even further (Irniger et al, 1995).

The phosphorylation state of Swi5 it is also controlled by the phosphatase Cdc14, which is required for mitotic exit as it dephosphorylates not only Swi5, but also Sic1 to favor its stabilization. The accumulation of Sic1 in anaphase plays a key role in a feedback loop that ensures that mitotic exit is irreversible (Lopez-Aviles et al, 2009; Visintin et al, 1998). Of note, besides Cdc14, the protein phosphatase Drc2 also seems to play a role in dephosphorylation and stabilization of Sic1 (Pathak et al, 2007; Visintin et al, 1998).

4.3.3.3. Sic1 regulation at the G1/S transition

At the G1/S transition there is a rapid turnover of Sic1 levels mediated by multisite phosphorylation that determines a threshold for Cln1/2-Cdk1 activity providing a switch-like activation mechanism of Clb5/6-Cdk1 complexes (Nash et al, 2001). Interestingly, it has been shown that free Clb5-Cdk1 complexes are able to phosphorylate Sic1 thereby promoting further its degradation in a positive feedback loop (Feldman et al, 1997; Koivomagi et al, 2011a; Skowyra et al, 1997). Sic1 contains nine Cdk1 consensus phosphorylation sites and the molecular mechanism by which it is phosphorylated at multiple sites has been subject of many studies (Fig. 8). In an original model, six or more residues needed to be simultaneously phosphorylated *in vivo* to induce Sic1 binding to the SCF subunit Cdc4 (Borg et al, 2007; Mittag et al, 2010; Nash et al, 2001; Verma et al, 1997b). Later binding studies showed that closely positioned pairs of phosphorylated residues in the right position might be sufficient for Sic1 degradation (Hao et al, 2007). Yet further studies have provided a more complex picture of this Sic1 multisite phosphorylation mechanism (Koivomagi et al, 2011b). Accordingly, Cln2-Cdk1 and Clb5-Cdk1 act in a processive multiphosphorylation cascade that leads to the phosphorylation of a small number of specific phosphodegrons. These phosphorylation cascades are shaped by precisely oriented docking interactions mediated by cyclin-specific docking motifs in Sic1 and by Cks1, the phospho-adaptor subunit of Cdk1. These results reveal a higher level of complexity in Cdk1-dependent regulation of cell cycle transitions.

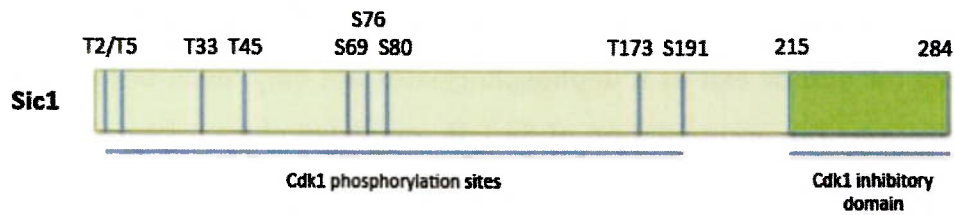


Figure 8. Schematic view of phosphorylation sites in Sic1. S/T-P Cdk1 phosphorylation sites and Cdk1 inhibitory domain are represented.

4.3.3.4. Sic1 regulation by kinases and phosphatases

There are several observations that demonstrate that Sic1 controls Clb waves in response to different stresses. These mechanisms of regulation involve several kinases and phosphatases in addition to Cdk1 and Cdc14. Upon hyperosmotic stress conditions, for instance, the stress activated protein kinase (SAPK) Hog1 (High Osmolarity Glycerol) is activated. Hog1 is the main kinase that regulates the high osmolarity response by activating a program that elicits cellular adaptation to this specific stress. This program regulates transcription, translation and post-translational processes, and elicits a delay in cell cycle progression in G1 (Clotet & Posas, 2007). Hog1 promotes G1 cell cycle arrest through two different mechanisms both of which affect Sic1 stability. On one hand, Hog1 downregulates *CLN1*, *CLN2*, and *CLB5* transcription, preventing therefore the degradation of Sic1 (Adrover et al, 2011; Clotet & Posas, 2007; Escote et al, 2004). On the other hand, Hog1 stabilizes Sic1 by phosphorylating it at Thr¹⁷³, thereby promoting a transient G1 arrest that prevents premature entry into the S phase until cells have adapted to the osmotic stress (Escote et al, 2004; Zapater et al, 2005). In line with these findings, *sic1Δ* or *sic1^{T173A}* cells do not arrest properly in G1 and are prone to genomic instability due to premature entry into S phase when challenged with osmotic stress (Escote et al, 2004). The mechanism by which the phosphorylation at Thr¹⁷³ promotes protein stability remains unknown, but based on a yeast two hybrid binding assay it has been proposed that the Thr¹⁷³ phosphorylation prevents Sic1 degradation by preventing its binding to the SCF^{Cdc4} complex (Escote et al, 2004).

Inhibition of the nutrient-sensitive target of rapamycin complex 1 (TORC1) following nutrient starvation treatment with its specific inhibitory macrolide rapamycin both causes cells to arrest in G1 (Wullschleger et al, 2006)(please see section 8.1 below for a detailed description of the TORC1 pathway). Interestingly, TORC1 regulates G1/S cell

cycle progression by controlling Sic1 expression and function at different levels. TORC1 favors G1 cyclin expression and hence Sic1 destabilization and inhibits *SIC1* transcription. Moreover, TORC1 also curtails, via unknown mechanisms, phosphorylation of the Thr¹⁷³ residue in Sic1 to promote its instability. Inhibition of TORC1 therefore results in Sic1 stabilization and inhibition of Clb5/6-Cdk1 complexes, which prevents inappropriate DNA replication under unfavorable nutrient conditions. Supporting these observations, loss of Sic1 prevents rapamycin induced G1 arrest and renders cells sensitive to nutrient starvation (Zinzalla et al, 2007). As stated previously, the regulatory mechanism of this phosphorylation remains unknown.

The Cdk Pho85 also regulates the phosphorylation status and stability of Sic1 in response to phosphate availability (Toh-e et al, 1988). Pho85 associates with Pcl1, Pcl2, Pcl7 and Pcl9 that are G1 cyclin homologues and whose expression is also cell cycle regulated (Nishizawa et al, 1998). Pcl1/Pcl2 cyclins likely activate Pho85 to promote Sic1 phosphorylation (and instability) and loss of Pho85 causes Sic1 stabilization (Nishizawa et al, 1998). Curiously, however, loss of Pcl1/2 had no effect on Sic1 stability (Moffat & Andrews, 2004). Supporting a negative regulatory role of Pho85 in Sic1 control, loss of Sic1 was found to partially rescue the synthetic lethality of a *cln1Δ cln2Δ pho85Δ* triple mutant (Nishizawa et al, 1998). Pho85 is also required for cells to recover from a DNA damage-induced G1 arrest by promoting Sic1 degradation, release of Cdk1 activity, and subsequent onset of S phase (Wysocki et al, 2006). Finally, Pho85 has also been recently shown to promote Cln3 stability as long as sufficiently high levels of phosphate are present. This raises the possibility that destabilizing effects of Pho85 on Sic1 might at least in part be an indirect effect of its stabilizing effect towards Cln3, which activates (indirectly) transcription of *CLN1/2* and *CLB5/6*, the products of which induce Sic1 phosphorylation and subsequent degradation (Menoyo et al, 2013).

Sic1 has also been described as a target of casein kinase 2 (CK2) (Barberis et al, 2005b; Coccetti et al, 2004; Coccetti et al, 2006; Tripodi et al, 2007). CK2 is a highly conserved serine/threonine kinase that phosphorylates a broad spectrum of targets with important roles in several processes: transcription, translation, signal transduction, cell cycle regulation, and cell death (Meggio & Pinna, 2003). CK2 has been shown to phosphorylate Sic1 on Ser²⁰¹ *in vivo*. This phosphorylation dramatically increases the affinity of Sic1 for Clb5-Cdk1 complexes, altering the timing of the G1/S transition (Coccetti et al, 2006). In addition, CK2 phosphorylates also Cdc34 (see section 6.1),

which affects the dynamics of Sic1 degradation (Sadowski et al, 2007).

4.4. Cdk1 kinase subunits: Cks

The Cdk complex is composed of the Cdk, the cyclin subunit, and the family members of the “cyclin-dependent kinase subunits” (Cks). Cks are small molecular weight proteins (9-18 kDa) that interact genetically and physically with Cdks. Despite intensive studies for over 20 years since their initial discovery, their effect on Cdk activity and precise biological function has not been clarified. This is in part due to the discrepancies in the results obtained in studies performed in different model organisms, as illustrated in the following paragraphs (Tang & Reed, 1993). Since Cks have been described to be linked to cancer (Inui et al, 2003; Kitajima et al, 2004; Shapira et al, 2005; Urbanowicz-Kachnowicz et al, 1999), understanding their functional role in regulation of cell cycle transitions is of potential medical interest (Malumbres et al, 2008).

Cks1 (p13^{Suc1}, hereafter referred as Suc1) was originally identified in *S. pombe* as a suppressor of defective alleles of the cyclin dependent kinase p34^{Cdc2} (Hayles et al, 1986). In the case of budding yeast, Cks1 was also discovered as a suppressor of *cdc28* mutations (Hadwiger et al, 1989a). Both Suc1 and Cks1 bind directly to Cdk1 with high affinity (Bourne et al, 2000; Brizuela et al, 1987). Co-immunoprecipitation studies have also shown that Cks bind to cyclin-Cdk complexes in frog eggs (Patra & Dunphy, 1996). The human homologues CksHs1 and CksHs2 of a molecular size of 9 kDa (sharing 81% sequence identity; (Richardson et al, 1990)) were identified by immunoprecipitation with affinity-purified anti-p13^{Suc1} polyclonal serum in HeLa cells (Draetta et al, 1987). Interestingly, human Cks can functionally complement normal growth in *cks1Δ S. cerevisiae* mutant cells indicating that the function of Cks has been evolutionarily conserved (Richardson et al, 1990). Regarding their structure, Cks can crystallize as monomers or as strand-exchanged dimers. The structure of human CksHs2 was obtained in 1993 (Parge et al, 1993). Apparently CksHs2 forms strand-exchanged dimers, unlike CksHs1 that forms monomers (Arvai et al, 1995). The crystal structure of Suc1, similar to the one of *S. cerevisiae* (Balog et al, 2011; Bourne et al, 2000), revealed that it can also crystallize as monomer or dimer (Khazanovich et al, 1996). The resolution of the crystal structures in the case of the human CksHs1 together with Cdk2, has given further clues regarding the function of the Cks (Bourne et al, 1996). CksHs1

interacts with the Cdk2 C-terminal lobe opposite to the Cdk2 N-terminal lobe and the cyclin binding surface. CksHs1 binding to Cdk2 does not provoke a conformational change in Cdk2 structure, suggesting that it has little effect on the formation of cyclin-Cdk complexes, or in the binding of other regulatory proteins. However, CksHs1 binding restricts CAK-dependent phosphorylation of Thr¹⁶⁹ in Cdk2, which indicates that this activating phosphorylation may temporally precede the event of Cks binding to Cdk (Bourne et al, 1996).

Several genetic analyses in fission and budding yeast suggested that loss of Cks1 promotes mitotic arrest (Basi & Draetta, 1995; Hayles et al, 1986; Moreno et al, 1989; Tang & Reed, 1993). Results obtained in these studies lead to the proposal of a role of Cks as adaptor proteins that promote multiple substrate phosphorylation by enhancing the binding of Cdks to their previously phosphorylated substrates in mitosis (Pines, 1996). In fact, several Cks-dependent multiphosphorylation events have been observed in some cell cycle regulatory proteins like Cdc25, Myt1, Wee1 and Cdc27, and Apc1 (Ganoth et al, 2001; Patra & Dunphy, 1996; Patra et al, 1999).

Several studies have also tried to clarify the role of Cks1 in G2/M transition. Initially, it was shown that Cdc28 and Cks1 interact with different components of the 26S proteasome. Cks1 function is required for degradation of the anaphase inhibitor Pds1, the stabilization of which is in part responsible of the metaphase arrest observed in *cks1* mutant cells. In addition, Cks1 inactivation or prevention of Cdk1-Cks1 binding confers stability to already ubiquitinated Clb2, suggesting that Cks are not essential for APC activity but for some aspects of the proteasome function during M-phase proteolysis (Kaiser et al, 1999). Another role of Cks1 in mitosis implies a function as a positive regulator of the APC activator Cdc20 (Morris et al, 2003). Accordingly, Cks1 is required to recruit the proteasome to the *CDC20* promoter (independently of Cdk1 kinase activity), facilitating *CDC20* transcription. Interestingly, the proteasomal function required in this process is not proteolytic; it could promote transcription by remodeling transcriptional complexes or chromatin associated with the *CDC20* gene. These results suggest that together with mitotic substrate degradation, induction of *CDC20* transcription is a double regulatory mechanism important for Cks1-dependent mitotic progression. Some other roles of Cks1 in transcriptional regulation control as well as in growth signaling pathways have also been proposed (Chaves et al, 2010; Holic et al, 2010; Morris et al, 2003; Simon et al, 1995; Suzuki et al, 2011; Yu et al, 2005; Zhang et al,

2004).

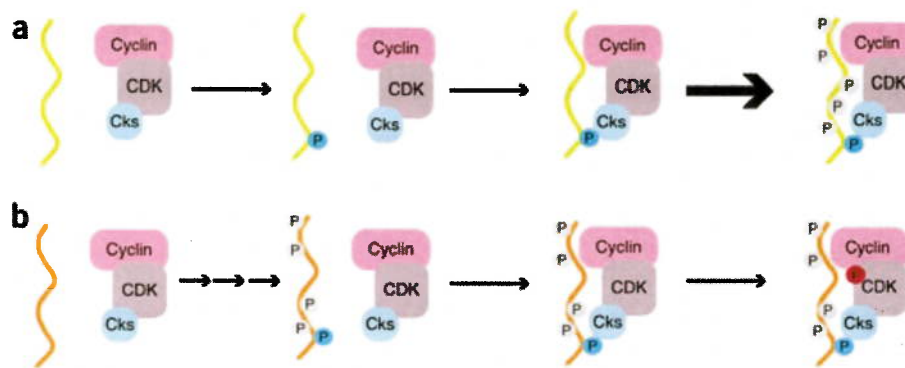


Figure 9. Cks mediates Cdk-substrate association for multiple functions. (a) Cks bind substrates phosphorylated at specific consensus (blue phosphate) sites to prime further phosphorylation events, as it has been described for Sic1. **(b)** Cks act as adaptors for Cdk regulators that target Cdk. Specifically, in the case of Wee1, Cks1 association induces the inhibitory Tyr¹⁹ phosphorylation (red phosphorylation) in Cdk. From (McGrath et al, 2013).

In mammals Cks1 has also been identified as a player in the degradation of mitotic substrates by controlling the APC/C ubiquitin ligase and spindle assembly checkpoint (SAC) important for mitotic control (Fry & Yamano, 2006; Kim & Yu, 2011; Song & Rape, 2010; Wasch & Engelbert, 2005). In addition, CksHs1 has a Cdk-independent function as a factor of the SCF-Skp2 complex that is responsible of p27^{Kip1} degradation. Interestingly, in the case of Sic1 it was described that a priming phosphorylation event facilitates the processive phosphorylation of specific phosphodegrons involved in Sic1 degradation, and this was completely dependent on Cks1 (Koivomagi et al, 2011b). Further studies corroborated the relevance of Cks1 association with specific priming sites in Sic1 (McGrath et al, 2013). Crystal structures of Cks have evidenced also the presence of an anion-binding site able to interact with phosphates that direct Cdk complexes to other phosphoproteins. In *S. cerevisiae* the residues Arg³³, Arg⁴², Ser⁸², Trp⁸⁵, and Arg¹⁰² in Cks1 form a conserved anion-binding site (Balog et al, 2011; Bourne et al, 2000). In several studies performed in mammals, *Xenopus* egg extracts, and budding yeast cells it has been proposed that Cks1 binds Cdk substrates following a priming phosphorylation event that facilitates further processive phosphorylation events (Fig. 9). This highlights a role of Cks in regulation of Cdks by directing their interactions with specific targets (McGrath et al, 2013).

5. Cell cycle transcriptional regulation

Oscillatory activity of Cdc28 during the cell cycle is not only regulated by protein phosphorylation, Cks, and cyclin binding, but also by transcriptional changes in regulatory genes. Sequential waves of transcription ensure periodicity of cyclin expression to maintain the organization of cell cycle events. In *S. cerevisiae*, about 800 genes (more than 10% of all protein-encoding genes) exhibit a cell-cycle periodic expression pattern (Spellman et al, 1998). These genes can be divided into three different clusters according to the stage of the cell cycle where peak expression occurs: the Start checkpoint cluster in late G1/S, the S/G2 cluster, and the M to early-G1 cluster (Fig. 10).

Cell-Cycle Transcription Factors		
Factor	Subunits	Gene example
Start		
SBF	Swi6 + Swi4	<i>CLN1,2</i>
MBF	Swi6 + Mbp1	<i>CLB5,6</i>
G2/M transition		
Mcm1-Fkh (SFF complex)	Mcm1 + Fkh1/2 + Ndd1	<i>CLB1,2</i>
Late mitosis		
Ace2	Ace2	<i>SIC1</i>
Swi5	Swi5	<i>SIC1</i>
Mcm1	Mcm1	<i>CLN3, SWI4</i>

Figure 10. Table of major cell-cycle transcription factors controlling Cdk activity in yeast. From (Morgan, 2007).

5.1. The Start checkpoint cluster

Cell cycle initiation during G1 phase occurs after approximately 200 genes involved in cell cycle progression are transcriptionally activated (Cho et al, 1998; Spellman et al, 1998). Gene expression at Start is regulated by two heterodimeric transcription factors called Swi4 cell-cycle box binding factor (SBF) and Mlu1 cell-cycle box binding factor

(MBF), which bind to the promoter regions of their target genes by recognizing specific DNA sequence elements called Swi4 cell cycle boxes (SCBs) and Mlu cell cycle boxes (MCBs) (Fig. 11). Both complexes contain a DNA-binding protein (Swi4 and Mpb1) and a common regulatory subunit (Swi6). MBF regulates processes controlling DNA replication and repair (via expression of *POL2*, *CDC2*, *RNR1*, and *CLB5/6*, for instance), whereas SBF orchestrates growth related processes, cell morphogenesis, and spindle pole body duplication (via expression of *CLN1/2*, *PCL1/2*, *GIN4*, and *FKS1/2*, for instance) (Wittenberg & Reed, 2005). In early G1 before Start, a transcriptional inhibitor protein called Whi5, analogous to retinoblastoma protein (pRB) in mammals, represses both transcription factors. However, this does not suppress the growth dependent accumulation of Cln3 that gradually increases Cln3-Cdk1 activity in G1 phase. When Cln3-Cdk1 activity reaches a threshold, it phosphorylates and inactivates Whi5, which releases it from the nucleus and unleashes the inhibition of the SBF and MBF transcription factors (Costanzo et al, 2004; de Bruin et al, 2004; Stuart & Wittenberg, 1995; Tyers et al, 1993). This then allows the expression of around 200 G1/S genes, including the G1 and S phase cyclins (Eser et al, 2011; Skotheim et al, 2008). The accumulation of Cln1/2-Cdk1 activity further activates SBF- and MBF-dependent transcription by accelerating the nuclear exclusion of Whi5 through a potent positive feedback loop, which is essential for the synchrony of the G1/S transcription regulon (Cross & Tinkelenberg, 1991; Dirick et al, 1995; Skotheim et al, 2008).

5.2. The S/G2 cluster

During S phase, Hcm1, a transcription factor of the Forkhead family, is controlling the timing of transcription of the genes involved in chromosome segregation, spindle dynamics and budding (Fig. 10). In addition, it drives the transcription of the M-phase specific transcription factor-encoding *FKH1*, *FKH2* and *NDD1* genes and of the two cell-cycle transcriptional repressor-encoding *WHI5* and *YPH1* genes (Horak & Snyder, 2002; Pramila et al, 2006). From the end of S-phase until nuclear division, the Mcm1-Fkh1/2-Ndd1 regulatory complex promotes the expression of additional 35 G2/M genes whose products are required for proper mitotic progression. These include the mitotic cyclins Clb1/2, the yeast polo like kinase homolog Cdc5, the APC activator Cdc20, which is required for proper mitotic exit, and the Swi5 and Ace2 transcription factors involved in

the regulation of M/early G1 gene expression (Spellman et al, 1998). In addition, rising levels of Clb2-Cdk1 also mediate SBF inactivation (Amon et al, 1993).

5.3. The M to early-G1 cluster

In late mitosis, the activation of the Swi5 and Ace2 transcription factors leads to the expression of the M/G1 genes that are involved in mitotic exit and the preparation of the next G1 phase (Fig. 11). Among these genes there is *PCL2*, *PCL9*, *ASH1*, *HO*, and *SIC1* that ensure absence of Cdk activity in the time frame period between late mitosis and early G1. Mcm1 also recognizes a specific DNA sequence known as early cell cycle box (ECB) present in the promoter of several M/G1 genes (McInerny et al, 1997). Yox1 and Yhp1 repress the expression of those genes from late G1 to early mitosis by binding to ECBs (Pramila et al, 2002). Removal of these repressors in late mitosis, leaves an interval from M phase to early G1 that allows Mcm1 to favor expression of genes such as *CLN3* and *SWI4* whose products prepare the cell for the next cell cycle entry.

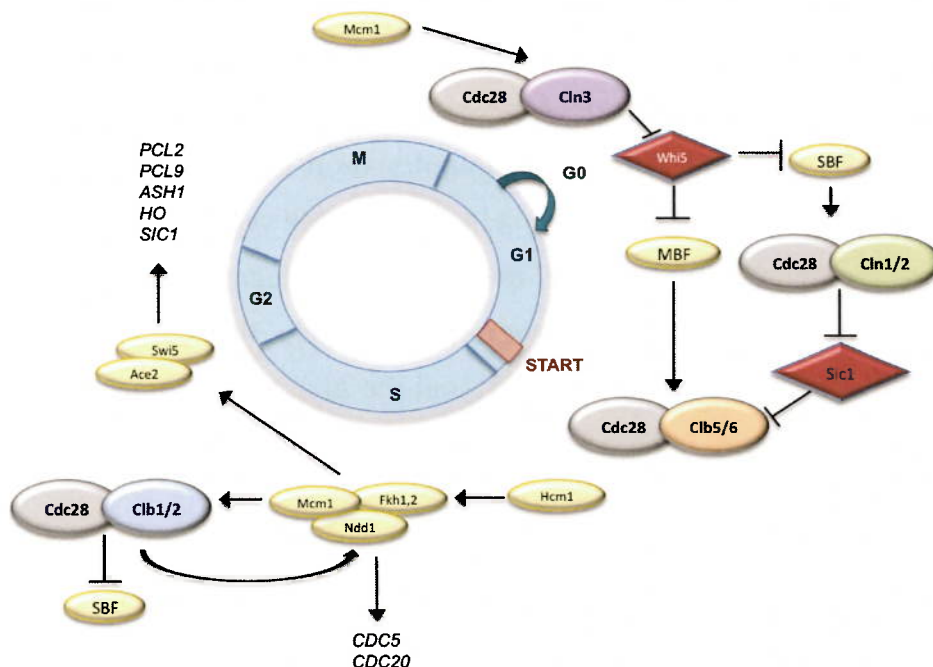


Figure 11. Transcriptional regulation during the cell cycle. At early G1, the transcription repressor Whi5 inhibits the activity of the SBF/MBF transcription factors that induces the transcription of G1/S phase cyclins (*CLN1*, *CLN2*, *CLB5* and *CLB6*). During S-phase the transcription factor Hcm1 induces the transcription of genes encoding the Mcm1-Fkh1/2-Ndd1 complex that further activates *CLB1/2*, *SWI5* and

ACE2 expression, whose products are required for further mitotic events. In late mitosis-early G1, Mcm1 promotes ECB dependent transcription (of *CLN3*, *SWI4*, and *CDC6*, for instance).

6. Cell cycle proteolytic regulation

Besides transcriptional regulation, cell cycle proteins are also timely regulated by ubiquitin proteasome-dependent proteolysis (Hershko & Ciechanover, 1998). The process of ubiquitination includes three enzymes. First, ubiquitin (a small, conserved 76 amino-acid protein) is activated at its C-terminus forming an ATP-dependent thio-ester bond with an ubiquitin-activating E1 enzyme. Subsequently, ubiquitin is transferred to the Cys active-site of a ubiquitin-conjugating E2 enzyme that takes the ubiquitin to the target protein. In the last step, the formation of an isopeptide bond between the C-terminus of ubiquitin with the lysine residue of a target protein may occur either directly, or with the assistance of an E3 ubiquitin ligase enzyme that provides substrate specificity. E3s recognize E2s and by forming thiol-esters with ubiquitin promote the transfer of ubiquitin from E2 to the target protein. Several rounds of ubiquitin transfer to one another via their Lys⁴⁸, gives rise to an assembly of a multiubiquitin chain on the substrate that converts it into a target of the 26S proteasome for degradation into small peptides (Verma et al, 1997b). This ubiquitin regulatory cascade is evolutionarily conserved from yeast to mammals. Almost all short-lived cell cycle regulatory proteins are regulated by phosphorylation and ubiquitination via a set of different E2 and E3 enzymes that promote their degradation in different cell cycle phases. The most relevant E3 enzyme complexes with HECT domains (Homologous to the E6-AP Carboxyl Terminus) controlling cell cycle progression include the Skp1/Cullin/F-box (SCF) complex that controls proteolysis at Start and the Anaphase Promoting Complex (APC) that is turned on during anaphase to promote exit from mitosis (DeSalle & Pagano, 2001; Jorgensen & Tyers, 1999; Zachariae & Nasmyth, 1999)(Fig. 12).

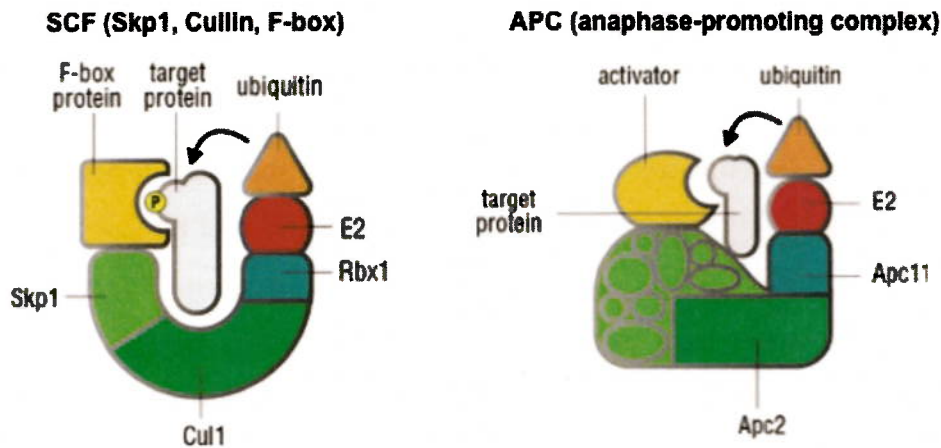


Figure 12. Control of substrate stability by the SCF and APC ubiquitin ligase complexes. The different components of the SCF and APC complexes are represented. SCF promotes substrate degradation at the G1/S transition, with the two different F-boxes Cdc4 and Grr1 having affinity for Sic1 and G1 phase cyclins, respectively. The APC promotes degradation at the metaphase/anaphase transition, with the two activators Ccd20 and Cdh1 performing sequential events in sister-chromatid separation and S and M phase cyclin degradation. From (Morgan, 2007).

6.1. Proteolysis at Start

SCF complexes are formed by an F-box binding protein (Skp1), a scaffold protein (Cdc53 or cullin) and an F-box protein (Cdc4, Grr1, Met30, Skp2, or Ctf13). SCF complexes catalyze the ubiquitination of phosphorylated cell-cycle regulating proteins including the G1 cyclins, Cdk inhibitors (Sic1 and Far1), and proteins involved in DNA replication like Cdc6 and Clb6 (Barral & Mann, 1995; Henchoz et al, 1997; Schwob et al, 1994; Tyers & Jorgensen, 2000). Differential localization of F-box proteins (FBPs) participates in cell cycle regulation: while Cdc4 is localized in the nucleus, Grr1 is both nuclear and cytoplasmic (Jackson et al, 2006; Willems et al, 1996). SCF complexes are active throughout the cell cycle and ubiquitin protein ligation (and therefore protein degradation) is coupled to Cdk1-mediated phosphorylation (Lanker et al, 1996). A good example of an SCF-regulated event is the degradation of Sic1 and Far1 at the G1/S transition. Cdc4 recognizes Cln1/2-Cdk1 dependent phosphorylation on those proteins and promotes their ubiquitination by Cdc34. Following phosphorylation and ubiquitination, Sic1 is recognized by the ubiquitin-binding proteins Rpn10 and Rad23, as well as the Ran-binding protein Yrb1, which target it to the proteasome (Skowyra et al, 1997) for degradation at the G1/S transition (Verma et al, 2001; Verma et al, 2004).

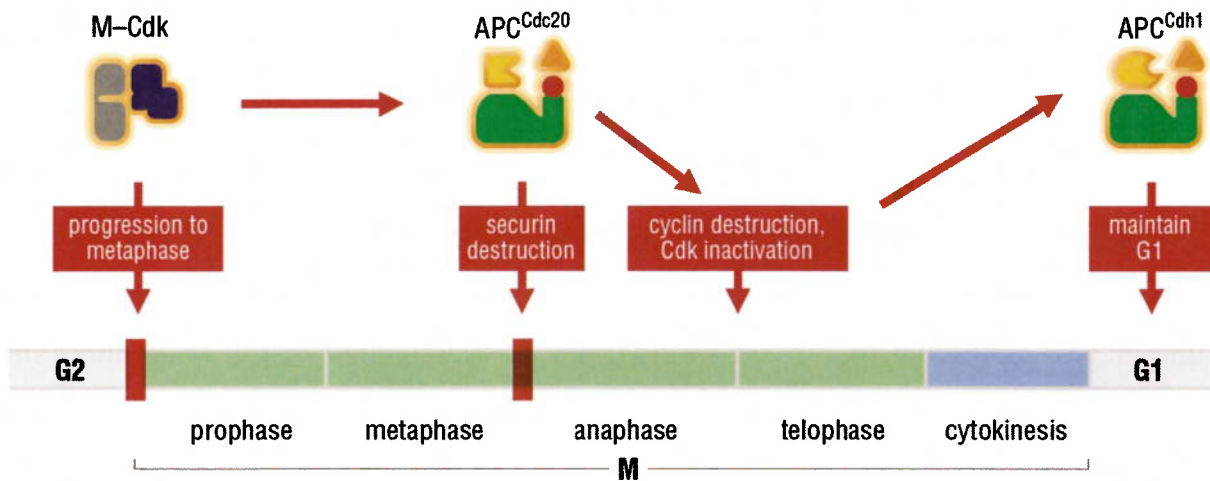
The majority of the known SCF substrates need to be phosphorylated at specific phosphodegron sites to be able to bind their respective F-box protein (Deshaies, 1997; Nash et al, 2001).

Distinct types of cyclins are controlled by different ubiquitin-dependent proteolysis mechanisms. The G1 cyclins are targets of SCF complexes and phosphorylation of their destabilizing C-terminal PEST regions is a key event in targeting them for degradation. For example, autophosphorylation of Cln1/2-Cdk1 at PEST regions incites Cln1/2 to bind the F-box protein Grr1 that will mediate their ubiquitination and degradation. Ubiquitination of Cln3, following its Cdk1-dependent phosphorylation, is mediated by both SCF^{Grr1} but SCF^{Cdc4} complexes (Landry et al, 2012; Yaglom et al, 1995). In addition, the B-type cyclin Clb6 is also targeted by the SCF^{Cdc4} system (Jackson et al, 2006).

6.2. Proteolysis at anaphase

With the exception of Clb6, the other B-type cyclins are degraded by the APC. This complex is required for progression through anaphase, exit from mitosis, and maintenance of the G1 phase (Zachariae & Nasmyth, 1999). This complex is inactivated at the S phase and activated during anaphase and its regulatory activity depends on its association with two conserved accessory activators, Cdc20 and Cdh1 that are responsible for substrate specificity (Fang et al, 1998; Kitamura et al, 1998; Lorca et al, 1998; Visintin et al, 1997). At the beginning of mitosis, cells initiate anaphase by activation of the APC^{Cdc20} complex that destroys the inhibitor of sister chromatid separation (Pds1 in budding yeast and Cut2 in fission yeast) and targets Clb5 and mitotic cyclins for degradation (Rudner & Murray, 2000; Shirayama et al, 1999; Visintin et al, 1997; Wasch & Cross, 2002). This activation requires mitotic Cdk1 dependent phosphorylation: Clb2-Cdk1 phosphorylates APC^{Cdc20} components to activate the APC and facilitate the binding of Cdc20 to the APC *in vivo* (Rudner & Murray, 2000). During the exit from mitosis, Cdc20 is exchanged for Cdh1 that mediates APC activation from the end of anaphase until the late G1 phase (Fig. 13). The APC^{Cdh1} complex destroys the securin Pds1, other substrates like Ase1, Cdc23, Cdc27, Cdc5 and Cdc20, and promotes complete destruction of Clb1-Clb4 (Funabiki et al, 1996; Ghiara et al, 1991; Holloway et al, 1993; Juang et al, 1997; Lim & Surana, 1996; Prinz et al, 1998; Shirayama et al, 1998; Yamamoto et al, 1996). Together with the cyclin-dependent kinase inhibitor Sic1, Cdh1

decreases Cdk1 activity to allow cells to exit from mitosis and drive them to the next G1 phase (Donovan et al, 1994; Li & Cai, 1997; Mendenhall, 1993).



© 1999–2007 New Science Press

Figure 13. Regulation of late mitotic events by the APC. M-Cdk1 activity promotes progression to metaphase and activates the APC^{Cdc20}, which destroys securin and mitotic cyclins thereby promoting anaphase and mitotic exit. Mitotic cyclin destruction results in activation of APC^{Cdh1}, which ensures S and M cyclin destruction until the cell is committed to another cell cycle. From (Morgan, 2007).

7. Cell cycle regulation in quiescent cells

Cell growth and cell cycle progression, as introduced in detail above (sections 1-6), are regulated by the presence of essential nutrients. In their absence, all living cells are able to exit the normal proliferating state and enter into an alternative non proliferative, but metabolically active state known as quiescence or G0. Most microorganisms remain in this quiescent state for the majority of their natural lifetime. Entrance into this resting state is accompanied by the acquisition of physiological, biochemical and morphological characteristics that allow cells to reduce their overall growth rate, increase their stress resistance, and survive long periods of starvation. However, under favorable conditions, these cells are able to detect and respond quickly to nutritional cues in order to resume growth and proliferation upon refeeding (Lillie & Pringle, 1980).

The quiescent state in yeast is often defined as the state of the cells that were grown to saturation in liquid rich media cultures (Gray et al, 2004). Several adaptive growth phases have been described that precede entry into G0. Initially, cells obtain energy from fermentation, the process in which glucose is metabolized via glycolysis to

nonfermentable carbon compounds, mainly ethanol. Cells divide rapidly in this exponential or logarithmic growth phase until half of the glucose gets consumed, at which time cells start to synthesize the reserve carbohydrate glycogen (Lillie & Pringle, 1980). This is followed by a stress resistance response that leads to specific transcriptional changes. Once glucose is exhausted in the medium, cells start to synthesize the stress protectant and reserve carbohydrate trehalose and enter the diauxic shift phase, a period of slower growth and metabolic adaptation to respiratory growth during which the nonfermentable carbon sources ethanol and acetate serve as carbohydrate sources. After the diauxic shift, cells in batch cultures typically undergo one or two additional rounds of cell divisions until depletion of the remaining non-fermentable carbon sources (Lillie & Pringle, 1980). Transition into the quiescent state in response to starvation for distinct essential nutrients requires a tightly coordinated program that includes downregulation of the expression of translational genes at both the level of transcription and translation (Gray et al, 2004) and seems not to be simply a consequence of growth cessation (De Virgilio, 2012; Klosinska et al, 2011). In addition, during the transition into G₀, cells induce a typical transcriptional program that includes induction of genes involved in respiration, fatty acid metabolism, glyoxylate cycle reactions, and antioxidant protective responses (De Virgilio, 2012). It is important to note that stationary phase yeast cultures are heterogeneous and contain both quiescent and non-quiescent cells (Allen et al, 2006; Werner-Washburne et al, 1993). Quiescent cells are unbudded and can come back to the proliferative cell cycle after prolonged starvation periods, whereas non-quiescent cells accumulate reactive oxygen species over short periods of time and lose rapidly viability in the absence of nutrients (Galdieri et al, 2010).

The cell division cycle and the cell quiescent cycle (entry into, survival in, and exit from quiescence) coincide at the G₁ phase (Gray et al, 2004). At this stage, after checking the environmental clues, cells take the decision whether to continue into a proliferative state in the cell division cycle or to enter into the quiescence cycle. In *S. cerevisiae*, entry into quiescence from G₁ is preferred probably due to selective advantages. It has been shown that quiescent cells arrested in other phases than G₁ present a diminished ability to survive longer periods of starvation (Laporte et al, 2011). However, whether cells have access to quiescence only via G₁ arrest at Start A has been a matter of intensive debate. It appears possible, depending also on the organism and

environmental conditions, that cells can enter into quiescence either at G1 or at G2 (Cameron & Bols, 1975; Takeo et al, 1995). In addition, quiescent cells in other cell cycle phases than G1 have also been described in human carcinomas and specific cell lines (Baisch, 1988; Drewinko et al, 1984). Thus, some cells may have the option to stably arrest in cell-cycle phases other than in G1 (Wei et al, 1993).

Yeast cells deprived for carbon, nitrogen, or phosphate, fail to go through the Start checkpoint and arrest in G0 phase (Gray et al, 2004; Klosinska et al, 2011; Swinnen et al, 2006; Wanke et al, 2005). Like all eukaryotic cells, yeast cells have developed several signaling pathways that detect changes in nutrient availability and regulate cell proliferation. The protein kinase A, Pho85 and TORC1 kinases are central elements of these signaling pathways that regulate cell division in response to glucose, phosphate and nitrogen availability, respectively. Consequently, inactivation of any of these major pathways upon nutrient deprivation leads to a cell cycle arrest and to the induction of typical phenotypes of the G0 program. Although the underlying mechanisms by which nutrient sensing pathways regulate the cell cycle machinery remain mostly unknown, the current knowledge will be briefly described in the following section. The TORC1 signaling pathway, which is a central element in the experimental part of this thesis, will be discussed in more detail in this context.

8. Nutrient signaling pathways control the decision between proliferation and entry into quiescence

Interestingly, proper cell cycle arrest and entry into the G0 phase following nutrient depletion has been described to depend on the protein kinase Rim15 that controls entry into G0 in response to glucose, nitrogen or phosphate starvation. Rim15 is a protein kinase that is key for proper establishment of most aspects of the yeast G0 program including proper G1 arrest (De Virgilio, 2012). Notably, Rim15 represents a regulatory node that is negatively controlled by TORC1, PKA, and the Pho80-Pho85 cyclin-CDK when the respective protein kinases are stimulated by the nutrients to which they respond. Rim15 is a serine/threonine kinase that is distantly related to the conserved nuclear Dbf2-related (NDR) family and large tumor suppressor subclass of the AGC (protein kinases A, G, and C) group of kinases (Cameroni et al, 2004). A typical feature of these kinases is that they all carry an insert of at least 30 amino acids between the

protein kinase subdomains VII and VIII. In the case of the human Ndr1, this insert contains a non-consensus nuclear localization signal (Tamaskovic et al, 2003). While it is currently not known whether Rim15 contains a nuclear localization signal in this kinase insert domain, it has been shown to contain a single 14-3-3 binding motif (RSXpS/TXP) (Yaffe & Elia, 2001) that is key for its cytoplasmic retention (see below). The Rim15 domain organization includes the N-terminal PAS and C₂HC type zinc finger domains, the central protein kinase domain (with its insert), and a C-terminal receiver domain (Fig. 14).

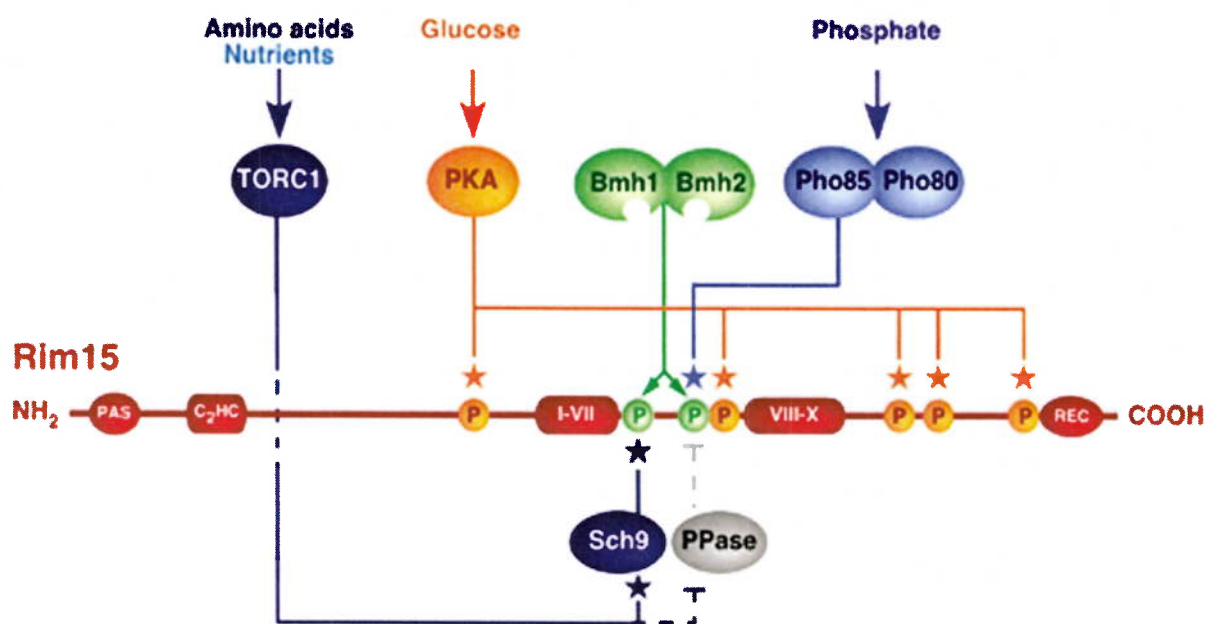


Figure 14. Convergence of nutrient signaling pathways on Rim15. PKA phosphorylates at least five amino-acid residues in Rim15 to mediate its inactivation (orange circles) (Reinders et al, 1998). Phosphorylation of Thr¹⁰⁷⁵ and Ser¹⁰⁶¹ (green circles) favors Rim15 binding to the two monomeric subunits within a single 14-3-3 protein dimer that anchors it to the cytoplasm. The TORC1 target Sch9 directly phosphorylates Ser¹⁰⁶¹ whereas Thr¹⁰⁷⁵ is phosphorylated by the Pho80-Pho85 cyclin-Cdk. Dephosphorylation of pThr¹⁰⁷⁵ is likely also regulated by TORC1 via its inhibition of a protein phosphatase (PPase) (Pedruzzi et al, 2003a; Wanke et al, 2008; Wanke et al, 2005). From (De Virgilio, 2012).

The role of TORC1, PKA and Pho85 nutrient signaling pathways in cell cycle control and their convergence on Rim15 to regulate the G₀ program will be introduced in the following sections.

8.1. TORC1

The highly conserved TOR (target of rapamycin) proteins are central components of a key signaling pathway that transduce nutrient signals to regulate cell growth (De Virgilio & Loewith, 2006; Santangelo, 2006; Soulard et al, 2009). Tor1 and Tor2 are 67% identical (and 82% similar), partially redundant protein kinases and members of the family of phosphatidylinositol protein kinases (or phosphatidyl inositol 3'kinase-related kinases (PI3 kinase)) (Keith & Schreiber, 1995). Despite their similarity to lipid kinases, Tor proteins are Ser/Thr protein kinases (Alarcon et al, 1999). All eukaryotes express a TOR ortholog; in contrast to yeast, higher eukaryotes such as mammals express typically only one TOR kinase (called mTOR) (Keith & Schreiber, 1995). Tor proteins were initially identified by mutations that confer resistance to rapamycin, a lipophilic macrolide with immune-suppressive properties produced by *Streptomyces hygroscopicus* (Heitman et al, 1991). TOR is found in two highly conserved and functionally distinct complexes. The rapamycin-sensitive TOR Complex 1 (TORC1), which localizes at the vacuolar membrane (Aronova et al, 2007; Cardenas & Heitman, 1995; Sturgill et al, 2008) and controls cell growth in response to nutrients by promoting translation and ribosomal protein gene expression and by antagonizing autophagy, mRNA degradation, and ubiquitin-dependent protein degradation (Crespo & Hall, 2002; De Virgilio & Loewith, 2006; Loewith et al, 2002). The rapamycin-insensitive TOR Complex 2 (TORC2) localizes at discrete dots at the plasma membrane (Cardenas & Heitman, 1995; Kunz et al, 2000; Sturgill et al, 2008) and regulates spatial control of cell growth by controlling the actin cytoskeleton, cell polarity, ceramide metabolism, and cell wall integrity (Aronova et al, 2008; Cybulski & Hall, 2009; De Virgilio & Loewith, 2006). During this thesis I have worked exclusively on TORC1. This introduction will therefore be focused on this complex.

In yeast, TORC1 is formed by a core dimer of Tor1 and/or Tor2 together with the additional subunits Lst8, Kog1, and Tco89 (Wullschleger et al, 2006) (Fig. 15). The function of these latter three proteins is not clear, but they might be involved in substrate binding, localization of the complex, or in the reception of upstream signals (Fadri et al, 2005; Loewith et al, 2002). The mode of action of rapamycin is highly conserved from yeast to humans: rapamycin binds to the co-factor peptidylprolyl isomerase Fpr1 (known as FK506-binding protein 12 (FKBP12) in mammals) to bind

and inhibit the kinase activity of TORC1. The position of the FRB (FKB12-rapamycin-binding) domain in the structure of TORC1 suggests that the Fpr1-rapamycin complex inhibits TOR by preventing the access of targets to the kinase domain (Alessi & Kulathu, 2013; Aylett et al, 2016; Gaubitz et al, 2015).

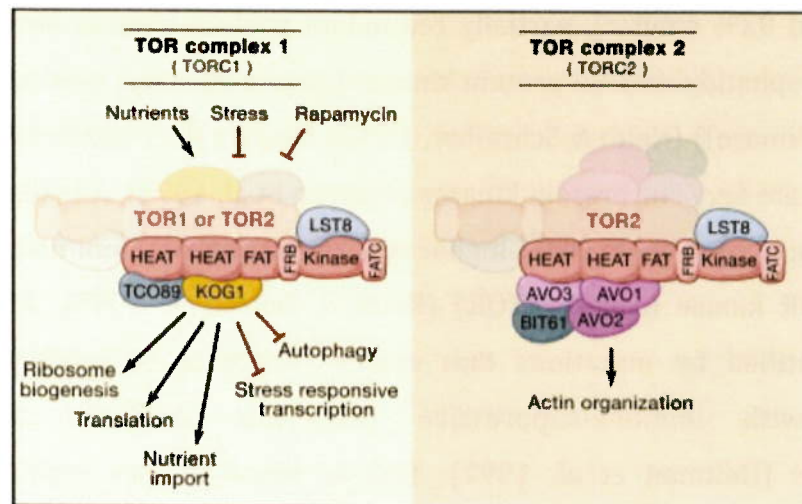


Figure 15. Composition of *Saccharomyces cerevisiae* TORC1 and TORC2. Tor associated proteins and domains are represented. Black arrows and red bars indicate positive and negative TORC1 inputs and outputs, respectively. From (Wullschlegel et al, 2006).

TORC1 activity is regulated in response to several environmental cues. TORC1 is responsive to both the abundance and the quality of nutrients in the environment; but, with few exceptions (see EGO complex in Chapter IV), the mechanisms of nutrient sensing and how this information is transmitted to TORC1 is still one of the major challenges in the TORC1 field (Binda et al, 2009; Urban et al, 2007). TORC1 activity is downregulated in response to various stress conditions, including high salt, redox stress, heat shock, rapamycin, and caffeine treatment (Kuranda et al, 2006; Urban et al, 2007). With the exception of rapamycin and caffeine, which directly inhibit TORC1 kinase activity, (Gaubitz et al, 2015; Kuranda et al, 2006; Reinke et al, 2006; Wanke et al, 2008), the mechanisms by which stress signals are transduced to TORC1 are still unclear.

Under favorable growth conditions, yeast TORC1 transmits signals via two main effector branches which include (1) the mammalian S6 kinase (S6K) ortholog Sch9 (Pearce et al, 2010; Powers et al, 2006) whose activity is regulated by TORC1 mediated phosphorylation at five to six C-terminal serine and threonine residues (Urban et al,

2007) and (2) the PP2A catalytic subunits Pph21/22 or the related Sit4 protein phosphatase when associated with Tap42 and the regulatory proteins Rrd12 or Rrd1, respectively (Di Como & Arndt, 1996; Jiang & Broach, 1999).

TORC1 inhibition by rapamycin and nutrient starvation triggers many downstream events that result in gene transcription reprogramming, decreased protein synthesis, induction of autophagy, cell cycle arrest in late G1 and entry into the G0 state (De Virgilio & Loewith, 2006; Hara et al, 2002; Kim et al, 2002; Smets et al, 2010) (Fig. 16). Regarding the role of TORC1 in cell cycle control in response to nutrient availability, TORC1 induces protein synthesis globally by regulating RNA Pol I, II, and III and promotes the G1/S transition by favoring the transcription and translation of G1 cyclins. With respect to the latter, Cln3 is special as its levels are very sensitive to changes in translation initiation rates due to a short upstream open reading frame (uORF) in the 5' UTR of the *CLN3* mRNA that represses its translation (Polymenis & Schmidt, 1997). Accordingly, inhibition of TORC1 by rapamycin and consequently reduction in translation initiation causes a G1 arrest as a result of the rapid decrease in Cln3 translation. This phenotype can be suppressed by replacement of the endogenous 5' UTR of the *CLN3* transcript with the one of *UBI4*, the expression of which is induced in G0 phase (Barbet et al, 1996; Zaragoza et al, 1998). In mammalian cells, mTORC1 also controls translation (and mRNA stability) of the cyclins D1, D3, E, and A (mainly through its effectors 4E-BP and S6K1) (Averous et al, 2008; Fingar et al, 2004; Hashemolhosseini et al, 1998; Hleb et al, 2004).

TORC1 further couples cell growth with cell cycle events at the G1/S boundary of the cell cycle by inhibiting the expression and/or function of Ckis. Although the underlying mechanisms remains poorly understood, some progress has been made in this area with respect to the yeast Cki Sic1. TORC1 triggers Sic1 degradation by two means. First, it ensures Cln-Cdk1 activation that promotes Sic1 N-terminal phosphorylation and its subsequent ubiquitination by the SCF^{Cdc4} ubiquitin ligase complex, followed by its degradation via the proteasome (Feldman et al, 1997). Secondly, it prevents the phosphorylation of the specific residue Thr¹⁷³ in Sic1 that seems to be required for its stability (see above) (Zinzalla et al, 2007). Similarly, TORC1 in mammals antagonizes p27 levels that otherwise inhibit cyclinE/Cdk2 complexes to block G1/S cell cycle progression. In addition, mTORC1 favors downregulation of p27^{Kip1} and destabilization of p27 and p21 mRNAs (Leung-Pineda et al, 2004; Luo et al, 1996), and controls

subcellular localization of p27^{kip1}. In the presence of growth factors, active mTORC1 indirectly promotes phosphorylation and consequently cytoplasmic sequestration of p27^{kip1}. This renders p27^{kip1} unable to inhibit nuclear Cdk, which is then free to promote DNA replication (Medema et al, 2000).

Interestingly, TORC1 also plays (still poorly defined) roles in controlling cell cycle events other than the ones at G1. For instance, TORC1 has been reported to promote S-phase progression and control mitotic entry by regulating the nuclear translocation of the polo kinase Cdc5, which is essential for mitosis and cytokinesis (Shen et al, 2007). The latter observation fits also with the finding that temperature-sensitive *kog1^{ts}* mutants or rapamycin treated cells are significantly delayed in mitotic entry (Nakashima et al, 2008). More recent studies elaborated on the role of TORC1 in controlling events during M phase. Accordingly, TORC1 was found to control the mRNA stability of the M phase cyclin Clb2. Under optimal growing conditions, the Dbf2 protein kinase phosphorylates the arginine methyltransferase Hmt1, which promotes Hmt1-dependent methylation of specific mRNA binding proteins that stabilize the *CLB2* mRNA. Following TORC1 inactivation by rapamycin or following nutrient starvation, the protein phosphatase Pph22 dephosphorylates and inactivates Hmt1, which then results in destabilization of *CLB2* mRNA transcripts and consequently a delay in anaphase transit and completion of mitosis (Messier et al, 2013). A further observation supporting a role of TORC1 during mitosis is that loss Tco89 leads to a decrease in the levels of nuclear PP1 phosphatase Glc7, which is required to antagonize Ipl1-mediated substrate phosphorylation during mitosis (Tatchell et al, 2011). Finally, a defined set of experiments in fission yeast (Hartmuth & Petersen, 2009), as well as various less well characterized observations in other organisms, generally suggest additional roles of TORC1/mTORC1 in controlling the G2/M transition. For further details, the reader is referred to a more comprehensive overview in the chapter 7 of the book *TORC1 and cell cycle control* (Noguchi et al, 2014).

Concerning the role of TORC1 towards Rim15 regulation, TORC1 inhibits Rim15 function in a PKA-independent manner. It was observed that cells deleted for *RIM15* are impaired in the entry into G0 following rapamycin treatment or nitrogen starvation. Under these conditions, they are defective in proper G1 arrest, in transcriptional induction of stress and G0 genes, and in trehalose and glycogen accumulation, indicating that Rim15 is required for G0 entry following TORC1 inactivation. Accordingly, TORC1

inhibits Rim15 function by antagonizing its nuclear accumulation by promoting the phosphorylation of the Rim15 residues Thr¹⁰⁷⁵ and Ser¹⁰⁶¹ to guarantee optimal Rim15 anchorage in the cytoplasm via the 14-3-3 proteins Bmh1 and Bmh2 (Wanke et al, 2005; Zapater et al, 2005). TORC1 regulates the phosphorylation of Ser¹⁰⁶¹ in Rim15 via its direct downstream target Sch9 (Wanke et al, 2008) and the phosphorylation status of Thr¹⁰⁷⁵ via inhibition of a yet unidentified protein phosphatase (Pedruzzi et al, 2003a).

8.2. PKA

Besides the TORC1 pathway, the PKA pathway constitutes another key signaling pathway that controls growth of proliferating yeast in response to nutrients. The heterotetrameric PKA complex is formed by a combination of two out of three closely related Tpk1, Tpk2, and Tpk3 catalytic subunits and two regulatory Bcy1 subunits, which restrict the activity of the catalytic subunits. In response to high glucose levels, binding of cyclic AMP (cAMP) to Bcy1 subunits alleviates their inhibitory activity and releases the catalytic subunits (Ptacek et al, 2005; Robertson & Fink, 1998). Interestingly, loss of Rim15 renders cells devoid of PKA activity (*i.e.* *tpk1Δ tpk2Δ tpk3Δ* mutant cells) viable (Reinders et al, 1998), while overproduction of Rim15 rescues the defect in induction of stationary phase traits in strains with hyperactive PKA (*e.g.*, in mutants deleted for the gene that encodes the PKA-inhibitory Bcy1 subunit). Collectively, these genetic epistasis analyses indicated that Rim15 is negatively regulated by PKA. This assumption could be confirmed by *in vitro* kinase assays, which demonstrated that Rim15 is directly phosphorylated and inhibited by PKA-mediated phosphorylation at five PKA consensus sites (*i.e.* RRXS/T; Ser⁷⁰⁹, Ser¹⁰⁹⁴, Ser¹⁴¹⁶, Ser¹⁴⁶³, Ser¹⁶⁶¹) (Reinders et al, 1998).

In response to nutrient limitation, downregulation of PKA and of TORC1 liberates Rim15 from PKA-inhibition and allows it to translocate to the nucleus where Rim15 is required to induce cell cycle arrest in early G1 and activation of the G0 program (Pedruzzi et al, 2003a; Reinders et al, 1998).

In addition to Rim15 regulation, the PKA pathway also plays a crucial role in connecting nutrient availability with G1/S cell cycle transition via the inhibitory phosphorylation of Whi3. This protein inhibits Cln3 function in the G1 phase by binding to *CLN3* mRNA (Wang et al, 2004). Phosphorylation of Whi3 by PKA plays an inhibitory

role in Whi3 function by decreasing its interaction with *CLN3* mRNA and therefore allowing G1/S progression (Mizunuma et al, 2013).

8.3. Pho85

Phosphate is sensed by the PHO signaling pathway whose central element is the Pho85 CDK that associates with a family of 10 cyclins, each of which directs Pho85 towards different substrates. Nutrient sensing by Pho85 is mainly dependent on Pho80, a main cyclin of the PHO pathway that controls entry into G0 under phosphate deprivation conditions (Menoyo et al, 2013). It has been shown that Pho80/Pho85 directly phosphorylates and thereby contributes to sequestering Rim15 into in the cytoplasm. Under high inorganic phosphate (Pi) conditions, Pho80-Pho85 phosphorylates Thr¹⁰⁷⁵ within the 14-3-3 binding site of Rim15, thereby promoting its cytoplasmic retention via its association with Bmh1 and Bmh2 (Wanke et al, 2005). Upon Pi starvation, the CDK inhibitor Pho81, inactivates the Pho80-Pho85 complex (O'Neill et al, 1996; Schneider et al, 1994), which causes dephosphorylation of Thr¹⁰⁷⁵ in Rim15 and subsequent nuclear import of Rim15 and induction of the Rim15-controlled G0 program, including proper G1 arrest (Wanke et al, 2005).

It has also been demonstrated that Pho80-Pho85 is essential to restart the cell cycle by targeting the CDK inhibitor Sic1, specially following DNA damage-induced G1 arrest (Huang et al, 2007; Wysocki et al, 2006). Furthermore, it has been shown that the Pho85 also phosphorylates and inactivates Swi5, the transcription factor responsible for the expression of Sic1 in late M phase (Measday et al, 2000). More recently it has been demonstrated that Pho80-Pho85 complex also controls Cln3 stability, probably by its direct phosphorylation in response to phosphate levels. This later study shows that either the absence of Cln3 or low Pho85 activity hinders reentry into the cell cycle following phosphate starvation reinforcing the idea that Pho85 becomes indispensable for exiting from nutrient-induced G0 arrest (Menoyo et al, 2013). Taken together, Pho85 impinges by various means on cell cycle decisions. Given the fact that Rim15 is not essential, its functions in cell cycle control are largely of modulatory nature.

Distinct nutrient signaling pathways differentially regulate distinct cell cycle processes. Importantly, Rim15 integrates signals from TORC1, PKA and Pho80-Pho85, and hence plays a role in connecting nutrient-induced signaling cues with cell cycle

regulation. Although the mechanisms by which Rim15 controls cell cycle division at G1/S boundary remain unknown, some progress has been made in the last years regarding the identification of downstream effectors of this protein kinase. This will be described in the following sections.

9. Rim15 regulates transcription factors

Rim15 integrates signals from different nutrient sensing pathways to activate the expression of a variety of genes whose expression depends mainly on three transcription factors Msn2, Msn4, and Gis1. Gis1 is a zinc-finger transcription factor that binds the post-diauxic shift (PDS; TT/AAGGGAT) element in the promoter region of genes activated upon glucose exhaustion. The two partially redundant transcriptional activators Msn2 and Msn4 regulate the expression of genes that contain stress response elements (STREs, AGGGG) mainly in response to heat shock, oxidative stress and nutrient starvation. Msn2/4 and Gis1 functionally overlap, regulating many common targets (Cameroni et al, 2004; Pedruzzi et al, 2000). It has been shown that Rim15 phosphorylates *in vitro* Msn2 at both its N-terminal domain (1-400) and C-terminal domain (401-704), but not Gis1 that is consistent with recent results, which show an indirect regulation of Gis1 by Rim15 via its effectors Igo1/2 that will be introduced in more detail below (Bontron et al, 2013). Genome-wide transcriptional profiling indicated that the Rim15-dependent effects on transcription upon glucose limitation depend almost entirely on the three transcription factors Gis1, Msn2 and Msn4 (Cameroni et al, 2004). More recent studies in retenostat cultures showed that the expression of one fifth of the yeast genome is affected by loss of Rim15 under calorie restriction. However, a substantial fraction (55%) of the affected genes does not contain STRE or PDS binding elements in their promoter regions, which suggests that additional regulatory proteins may act downstream of Rim15 in response to nutrient signals (Bisschops et al, 2014). Consistent with this assumption, Rim15 also appears to regulate the expression of Hsf1-dependent genes by regulating the phosphorylation status and activity of Hsf1 as well as the stability of mRNAs of Hsf1 target genes (Lee et al, 2013).

10. Rim15 coordinates transcription with posttranscriptional mRNA protection

In order to understand the molecular mechanism by which Rim15 regulates initiation of the quiescence program, Rim15 target proteins were identified using the proteome chip array technology (Ptacek et al, 2005). The best candidate was Igo1 that shares 58% identity with its paralog Igo2. Further results demonstrated that Igo1 and Igo2 proteins play an essential, redundant role in proper initiation of the G0 program, hence their name Igo. Both proteins present high homology with small (16-20 kDa) proteins of the α -endosulfine family in higher eukaryotes, such as the cAMP-regulated phosphoprotein 19 (ARPP-19) and the α -endosulfine (ENSA). Both human ARPP-19 and ENSA are able to partially complement Igo1/2 function in yeast, suggesting that their role has been conserved throughout evolution (Dulubova et al, 2001; Talarek et al, 2010). Igo1/2 are required for the initiation of the G0 program, since cells deleted for both genes had a defect in glycogen and trehalose accumulation, a dramatically reduced chronological life span, and an important defect in gene expression. In other words, loss of Igo1/2 phenocopies the one of Rim15.

Igo1 interacts with Pbp1, Pbp4, Lsm12, and Dhh1 that are all involved in regulating mRNA stability. Dhh1, a DEAD-box RNA helicase, is a decapping activator of the 5'-3' mRNA decay pathway (Coller & Parker, 2005). Pbp1, together with the poly-adenine (A) binding protein Pab1 and its partner Pbp4, regulates mRNA polyadenylation (Mangus et al, 1998; Mangus et al, 2004a; Mangus et al, 2004b). Lsm12, interacts with Pbp1 and Pbp4 (Fleischer et al, 2006) and binds the 3'UTR of mRNAs (Albrecht & Lengauer, 2004). Igo1 is recruited to Pbp1-/Pbp4-containing mRNA-protein complexes specifically in rapamycin-treated cells and this event requires its direct phosphorylation by Rim15 on Ser⁶⁴, which lies in a conserved sequence motif in endosulfine-family proteins (Tolarek et al, 2010). Genetic experiments further suggested that phosphorylated Igo1 (on Ser⁶⁴) plays a specific role in stabilization of a subset of mRNAs by preventing their degradation via the 5'-3' mRNA decay pathway. Accordingly, inactivation of the 5'-3' mRNA decay pathway could fully restore the levels of the respective set of rapamycin-induced mRNAs in *igo1/2Δ* cells, but not in *rim15Δ* cells that likely have an additional defect in transcriptional induction of these genes (Tolarek et al, 2010). How Igo1/2 protect mRNAs from 5'-3' mRNA decay is currently not known. It is likely, however, that

the underlying mechanism involves the indirect control of the phosphorylation status (see below) and consequently inhibition of a key factor within 5'-3' mRNA decay pathway that may operate in P bodies (Luo et al, 2011). Interestingly, mammalian ARPP-19 has been described to control axon growth and synaptic plasticity by stabilizing the growth-associated protein-43 (GAP-43) mRNA in response to nerve growth factor treatment (Irwin et al, 2002). Thus, endosulfines may have an evolutionarily conserved role in mRNA stability control.

11. Yeast endosulfines Igo1/2 inhibit protein phosphatase 2A

Recent data shed light on the mechanism by which Rim15 coordinates transcription and posttranscriptional stability of specific mRNAs. The Cdc55-protein phosphatase 2A (PP2A^{Cdc55}) was identified as the essential complex that links Rim15-Igo1/2-dependent nutrient signaling to downstream effectors to promote quiescence entry and proper chronological lifespan (Bontron et al, 2013). When phosphorylated by Rim15 on Ser⁶⁴, Igo1 directly binds and inhibits PP2A^{Cdc55} to prevent the dephosphorylation of several target proteins that include for instance the transcription factor Gis1. PP2A^{Cdc55} targets the phospho-residue Ser⁴²⁵ in Gis1 to inhibit its recruitment to promoter regions of nutrient regulated genes. Thus, Rim15-mediated phosphorylation of Igo1/2 serves to inhibit PP2A^{Cdc55} and consequently promote the recruitment of phosphorylated Gis1 to promoter regions of specific genes (Fig. 16). Interestingly, the Rim15-Igo1/2-PP2A^{Cdc55} yeast module is conserved in higher eukaryotes and coined the Gwl-Ensa/Arpp19-PP2A-B55 δ pathway.

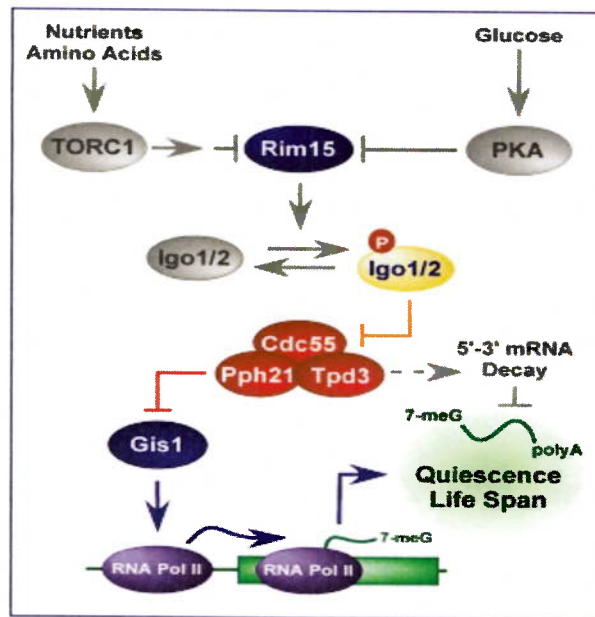


Figure 16. TORC1 and PKA control yeast cell proliferation in response to nutrients and/or growth factors. Inactivation of PKA and/or TORC1 results in Rim15 activation that orchestrates the initiation of the quiescence program via activation of the endosulfines Igo1/2 that inhibit the Cdc55-protein phosphatase 2A (PP2A^{Cdc55}). The latter phosphatase regulates the transcription of G0 genes in part via the transcription factors Gis1. From (Bontron et al, 2013).

12. The Gwl-Ensa/Arpp19-PP2A-B55 δ pathway controls mitosis

The protein kinase Gwl (human ortholog of Rim15) plays an important role in the regulation of cell cycle phosphorylation events. Gwl was first identified in *Drosophila*, where it was proposed to function in the control of mitotic progression (Bettencourt-Dias et al, 2004; Yu et al, 2004). Gwl depletion prevents cycling extracts to activate CycB-Cdk1 complexes and entry into mitosis (Yu et al, 2006). Several studies demonstrated that Gwl/MASTL inhibits PP2A (specifically the PP2A-B55 δ sub-complex) to prevent CycB-Cdk1 substrate dephosphorylation (Burgess et al, 2010; Mochida et al, 2009; Vigneron et al, 2009; Voets & Wolthuis, 2010). The missing link between Gwl and PP2A-B55 was provided when Gwl was found to phosphorylate Ser⁶³ in Arpp19 and Ser⁶⁷ in ENSA that promotes their binding to and inhibition of PP2A-B55 δ (Gharbi-Ayachi et al, 2010; Mochida et al, 2010). Genetic analyses in *Drosophila* fully supported these biochemical data (Rangone et al, 2011). Notably, additional protein kinases phosphorylate other residues in ENSA (Thr²⁸ and Ser¹⁰⁹) during different cell cycle states, probably to regulate PP2A-B55 as a 'stepwise tuner' in response to multiple

cellular signals (Mochida, 2014). Combined, the current data suggest a model in which Cdk-dependent activation of Gwl at mitotic entry leads to inhibition of PP2A-B55 via the ENSA/Arpp19, which is important to prevent futile phosphorylation/dephosphorylation cycles on mitotic Cdk1 substrates.

Gwl itself requires activation by CycB-Cdk1-mediated phosphorylation in its T-loop (Yu et al, 2006) and phosphorylation in its C-terminal tail that may lead to stabilization of its active conformation (Blake-Hodek et al, 2012; Vigneron et al, 2011). It has also been shown that Gwl stabilization involves the chaperones Hsp90 and Cdc37 (Yamamoto et al, 2014). Regarding its localization, Gwl contains a long insert region that separates the kinase domain into N- and C-terminal subdomains and that contains two nuclear localization signals (NLS) in *Drosophila* (Wang et al, 2013) and one in mammalian and *Xenopus* Gwl (Alvarez-Fernandez et al, 2013; Yamamoto et al, 2014). These NLS sequences are essential for Gwl relocation from the nucleus to the cytoplasm, where cytoplasmic endosulfines need to be activated to be able to antagonize PP2A-B55. This process is important for mitotic progression. Gwl also contains a putative nuclear export sequence (NES) that participates in Gwl shuttling between the nucleus and the cytoplasm. This relocation involves phosphorylation by CycB-Cdk1 and by Polo kinase that promotes the association of Gwl with 14-3-3 ϵ leading to its cytoplasmic retention (Alvarez-Fernandez et al, 2013; Wang et al, 2013). More recently, it has been described in *Drosophila* that Cdk1 specifically phosphorylates Gwl at Thr⁵⁶² that is adjacent to the NLS in the central region to antagonize its nuclear import in prophase (Fig. 17a). This phosphorylation is reverted by PP2A-Tws (ortholog of PP2A-B55 δ), which promote the return of Gwl to the nucleus prior to mitotic exit (Fig. 17b). Notably, since PP2A is inactive in the presence of active Gwl, PP2A cannot be responsible of the initial inactivation of Gwl during mitotic exit. This task is likely taken over by PP1, which dephosphorylates the auto-activation site in the C-terminal tail of Gwl (Heim et al, 2015). Most recent data unraveled a similarly important role of the greatwall kinase pathway in controlling mitosis in the model organism fission yeast (Chica et al, 2016). Curiously, this pathway seems to play only a marginal role in mitotic control in *S. cerevisiae* that is linked to favoring, rather than inhibiting, mitotic entry (Juanes et al, 2013; Rossio & Yoshida, 2011). Accordingly, *S. cerevisiae* PP2A^{Cdc55} appears to promote mitotic entry by favoring the nucleolar sequestration of Cdc14, which is the main protein phosphatase in budding yeast that antagonizes Cdk1-mediated

phosphorylation events (Queralt et al, 2006; Queralt & Uhlmann, 2008). Notably, Cdc14 orthologs have remained elusive in higher eukaryotes, which may explain why the greatwall kinase pathway may have been wired differently in *S. cerevisiae*. Besides the well-studied role of the greatwall kinase pathway in mitosis regulation, its potential role at other phases of the cell cycle has remained largely unexplored.

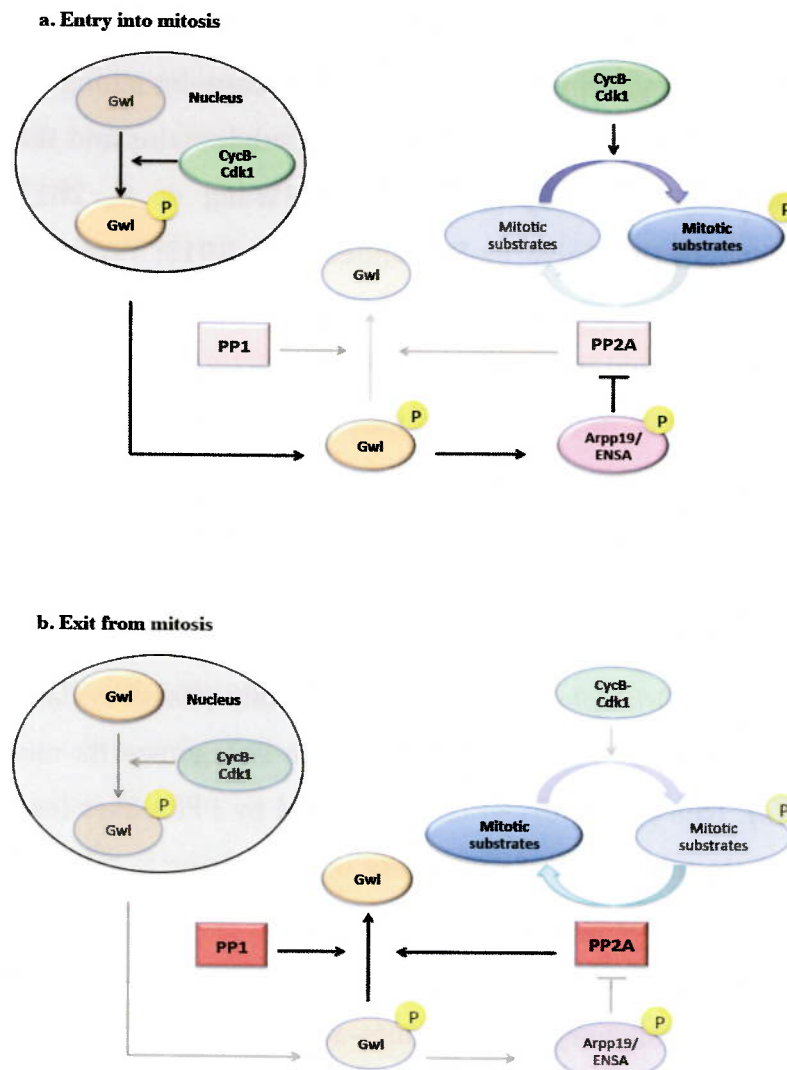


Figure 17. Mammalian Gwl control of mitosis. Gwl regulatory mechanism of mitotic entry **(a)** and mitotic exit **(b)** are shown. Black arrows and bars denote positive and negative interactions, respectively. For details see text.

Aim and outline

Aim and outline

Eukaryotic cell proliferation is controlled by growth factors and essential nutrients, in the absence of which cells enter into a quiescent state. These processes are fine-tuned by nutrient signaling pathways that coordinate nutrient availability with cell cycle division.

Nutrient signaling pathways have long been considered as linear pathways acting in parallel, however recent findings clearly show that such pathways exhibit extensive cross-talk between each other at different levels. A good example for a common effector of multiple nutrient-dependent signaling pathways is Rim15: cues from TORC1, PKA and Pho80/Pho85 protein kinases converge on Rim15.

The main goal of this thesis is to unravel the underlying mechanisms of Rim15-dependent TORC1 cell cycle regulation at G1 phase in response to nutrient availability. Current knowledge suggests that TORC1 may regulate cell decisions in G1 by controlling G1 cyclin expression and the stability of the cyclin-dependent kinase inhibitor Sic1. However, the exact mechanism remains elusive. Due to the high level of conservation of the TORC1-Rim15-Igo1/2-PP2A^{Cdc55} (Greatwall) signaling pathway among eukaryotes and to the relevance of Rim15 in promoting G1 arrest and entry into G0, we speculated that this signaling branch might affect G1 cell cycle events by controlling G1/S cyclins expression and/or Sic1 stability. This hypothesis will be addressed in the following chapters.

In Chapter I we describe the role of the Greatwall signaling pathway and the MAP kinase Mpk1 in the control of Sic1 stability by promoting Sic1^{Thr173} phosphorylation in response to rapamycin treatment and nitrogen starvation. Although the role of the Greatwall pathway in mitosis control has been extensively studied in various organisms, the data presented in this manuscript show a novel function of this pathway in G1/S cell cycle control.

In chapter II we attempt to understand the mechanistic details of Sic1 stabilization by Thr¹⁷³ phosphorylation. The idea that phosphorylation may prevent interaction with E3 ligases and therefore degradation has been suggested for several cell cycle-regulated proteins (Escote et al, 2004; Menoyo et al, 2013; Zinzalla et al, 2007) but no regulatory mechanism has been described so far. Here we demonstrate that Thr¹⁷³ phosphorylation

protects Sic1 from Cln/Clb-Cdk1-dependent phosphorylation, thereby preventing binding to Cdc4 and subsequent degradation.

In chapter III we show data that suggest a novel function of Rim15-Igo1/2-PP2A^{Cdc55} in the regulation of G1 cyclin expression. Rapamycin-induced G1 cyclin downregulation partially involves Rim15-Igo1/2 that impinge on G1 cyclin levels most likely via the regulation of Xbp1 and Msa1 transcription factors. Further studies are required to better understand the role of the Greatwall pathway in the regulation of cell cycle machinery.

In chapter IV, we introduce a genetic screening performed to identify potential new regulators and/or targets of TORC1 that may allow us to gain further insight into the mechanisms controlling exit from quiescence.

Finally, concluding remarks, open questions and the implications of the obtained results in higher eukaryotes will be presented.

CHAPTER I:
***TORC1 controls G1-S cell cycle
transition in yeast via Mpk1 and
the greatwall kinase pathway***

ARTICLE

Received 17 Mar 2015 | Accepted 3 Aug 2015 | Published 10 Sep 2015

DOI: 10.1038/ncomms9256

OPEN

TORC1 controls G₁-S cell cycle transition in yeast via Mpk1 and the greatwall kinase pathway

Marta Moreno-Torres¹, Malika Jaquenoud¹ & Claudio De Virgilio¹

The target of rapamycin complex 1 (TORC1) pathway couples nutrient, energy and hormonal signals with eukaryotic cell growth and division. In yeast, TORC1 coordinates growth with G₁-S cell cycle progression, also coined as START, by favouring the expression of G₁ cyclins that activate cyclin-dependent protein kinases (CDKs) and by destabilizing the CDK inhibitor Sic1. Following TORC1 downregulation by rapamycin treatment or nutrient limitation, clearance of G₁ cyclins and C-terminal phosphorylation of Sic1 by unknown protein kinases are both required for Sic1 to escape ubiquitin-dependent proteolysis prompted by its flagging via the SCF^{Cdc4} (Skp1/Cul1/F-box protein) ubiquitin ligase complex. Here we show that the stabilizing phosphorylation event within the C-terminus of Sic1 requires stimulation of the mitogen-activated protein kinase, Mpk1, and inhibition of the Cdc55 protein phosphatase 2A (PP2A^{Cdc55}) by greatwall kinase-activated endosulfines. Thus, Mpk1 and the greatwall kinase pathway serve TORC1 to coordinate the phosphorylation status of Sic1 and consequently START with nutrient availability.

¹Department of Biology, University of Fribourg, Chemin du Musée 10, Fribourg CH-1700, Switzerland. Correspondence and requests for materials should be addressed to C.D.V. (email: Claudio.DeVirgilio@unifr.ch).

Nutrient signalling drives protein kinase activity of target of rapamycin complex 1 (TORC1) to stimulate anabolic, growth-related processes (for example, protein biosynthesis) in concert with cell cycle transition events^{1,2}. TORC1 has primarily been appreciated for its role in coordinating growth with the G₁-S cell cycle transition, or START in yeast³, but recent data indicate that TORC1 also contributes to the fine-tuning of other cell cycle events (for example, G₂-M transition) to environmental cues^{4,5}. TORC1 favours the G₁-S transition in part by promoting transcription and translation of the cell cycle regulatory G₁ cyclins^{4,6-8}. However, detailed mechanistic insight into TORC1-regulated G₁ cyclin expression is still sporadic and incomplete. A well-studied example in yeast indicates that the Cln3 G₁ cyclin levels, and consequently START-promoting G₁ cyclin-dependent protein kinase (CDK; Cln-Cdc28) activity, are specifically sustained by TORC1-mediated stimulation of translation initiation. The latter is required for ribosomes to bypass a translational repressive upstream open reading frame and reach the start codon of the 5'-untranslated region within the *CLN3* messenger RNA (mRNA)^{7,9}. In parallel to favouring G₁ cyclin expression, TORC1 further couples cell growth with cell cycle progression by antagonizing the expression and/or function of CDK inhibitors (CDKIs) that restrain CDK-mediated G₁-S transition⁴. Although the underlying mechanistic details remain poorly understood, progress has also been made in this area. An example in yeast, again, is the CDKI Sic1, which binds, following G₁ CDK-dependent multi-site phosphorylation, the F-box protein Cdc4 of the SCF^{Cdc4} ubiquitin ligase complex that flags it for ubiquitin-dependent proteolysis¹⁰⁻¹³. TORC1 apparently triggers Sic1 degradation not only by ensuring G₁ CDK activation but also by confining the phosphorylation of specific residue(s) (for example, Thr¹⁷³) in Sic1 (ref. 6). The details of the latter regulatory mechanism, however, are still elusive.

Attenuation of signalling through TORC1 (for example, following carbon and/or nitrogen limitation) incites yeast cells to arrest in G₁ of the cell cycle and enter a quiescent state that is characterized by a distinct array of physiological, biochemical and morphological traits^{14,15}. The protein kinase Rim15 orchestrates quiescence (including proper G₁ arrest) when released from inhibition by the AGC family kinase, Sch9, which requires, analogously to mammalian S6 kinase (S6K), activation by TORC1 (refs 16-19). Like the orthologous greatwall kinases (Gwl) in higher eukaryotes, Rim15 controls some of its distal readouts by phosphorylating a conserved residue within endosulfines (that is, Igo1/2 in yeast), thereby converting them to inhibitors of the Cdc55 protein phosphatase 2A (PP2A^{Cdc55}, or PP2A-B55 in higher eukaryotes)²⁰⁻²². The Gwl signalling branch in yeast (Rim15-Igo1/2-PP2A^{Cdc55}) mediates the activation of a quiescence-specific gene expression programme in part via the transcriptional activator Gis1 and likely additional factors that protect specific mRNAs from degradation via the 5'-3' mRNA decay pathway²²⁻²⁵. Whether Rim15 also controls cell cycle arrest in G₁ via Igo1/2-PP2A^{Cdc55} is currently not known. Interestingly, in this context, *Xenopus*, *Drosophila* and likely human cells employ their respective greatwall kinase pathway (Gwl-endosulfine-B55) to maintain high-level phosphorylation of cyclin B-CDKI substrates, thereby promoting mitotic entry^{26,27}. In yeast, however, the Gwl signalling branch contributes only marginally to the regulation of mitotic entry^{28,29}, likely because TORC1 curtails signalling through Rim15 in exponentially growing cells.

Here we show that TORC1 inhibition and consequently activation of Igo1/2 by the Gwl Rim15 serves to antagonize PP2A^{Cdc55} and prevent it from dephosphorylating pThr¹⁷³ within the CDKI Sic1. This specific phosphorylation event depends on the mitogen-activated protein kinase (MAPK)

Mpk1 and ensures protection of Sic1 from SCF^{Cdc4}-mediated ubiquitination and subsequent proteolysis to enable it to grant proper G₁ arrest when TORC1 is downregulated. Thus, TORC1 coordinates the phosphorylation status of Sic1 and consequently G₁-S cell cycle progression with nutrient availability via Mpk1 and the greatwall kinase pathway.

Results

The greatwall kinase pathway controls Sic1 stability. To study whether Rim15 mediates G₁ cell cycle arrest via activation of endosulfines and consequently inhibition of PP2A^{Cdc55}, we treated wild-type (WT) BY4741 cells with rapamycin and examined the cells by standard fluorescence-activated cell sorting (FACS) analyses. Unexpectedly, we found that BY4741 WT cells, like the ones from other commonly used WT strains such as W303-1A and SP1 (ref. 30), exhibited a significant delay in rapamycin-induced G₁ arrest that contrasted with the quite rapid G₁ arrest observed in JK9-3D WT cells (Fig. 1a,b). In trying to understand the different behaviour of JK9-3D cells, which have been instrumental for the discovery of TORC1 (ref. 31), we noticed that they carry a genomic *rme1* mutation that (on the basis of our complementation analysis) is in part responsible for their expedited rapamycin-induced G₁ arrest (Fig. 1b). Of note, Rme1 contributes to G₁ cyclin gene expression and has been assigned a specific role in preventing premature entry of cells into an off-cycle stationary phase (at G₁) in response to nutrient limitation³². While this issue deserves to be addressed in more detail elsewhere, we decided to take advantage of the robust rapamycin-induced G₁ arrest in JK9-3D cells to address our question whether Rim15 mediates G₁ cell cycle arrest via activation of endosulfines. Accordingly, we found that a large fraction of *rim15Δ* and *igo1/2Δ* cells was significantly impaired in proper G₁ arrest following rapamycin treatment when compared with their isogenic JK9-3D WT cells (Fig. 1c). This defect of *rim15Δ* and *igo1/2Δ* cells was even more pronounced following nitrogen starvation, a physiological condition that results in rapid TORC1 downregulation and subsequent G₁ arrest in WT cells (Fig. 1d)³³.

Since our results suggested a role for Rim15/Igo1/2 in cell cycle control, we next examined whether the expression of G₁ cyclins (Cln1, Cln2 and Cln3) or of the CDKI Sic1 was altered in rapamycin-treated *rim15Δ* or *igo1/2Δ* mutant cells. In agreement with previous reports^{6,7}, the *CLN1-3* transcripts and their corresponding proteins were progressively depleted in rapamycin-treated WT cells (Fig. 1e,f). In parallel, and consistent with the notion that TORC1 inhibition entails post-translational Sic1 stabilization⁶, Sic1 protein levels strongly increased despite the fact that the respective *SIC1* transcript levels remained relatively constant over the entire period of the rapamycin treatment. In rapamycin-treated *rim15Δ* and *igo1/2Δ* mutant cells, clearance of *CLN1-3* transcripts and of Cln1-3 proteins was noticeably delayed when compared with WT cells (Fig. 1e-h). In addition, loss of Rim15 or of Igo1/2, while only marginally affecting *SIC1* mRNA levels (Fig. 1e), severely and persistently compromised the ability of rapamycin-treated cells to accumulate Sic1 (Fig. 1f,i). This latter defect, which was also observed in respective BY4741, W303-1A and SP1 *rim15Δ* mutants (Supplementary Fig. 1), may in part be due to the delayed elimination of G₁ cyclins that favour CDK-mediated multi-site phosphorylation and consequently SCF^{Cdc4}-dependent ubiquitination and degradation of Sic1. However, both the transient nature of the G₁ cyclin downregulation defect and the rather persistent Sic1 accumulation defect in rapamycin-treated *rim15Δ* and *igo1/2Δ* cells indicate that the Rim15-Igo1/2 signalling branch controls Sic1 stability also via an additional

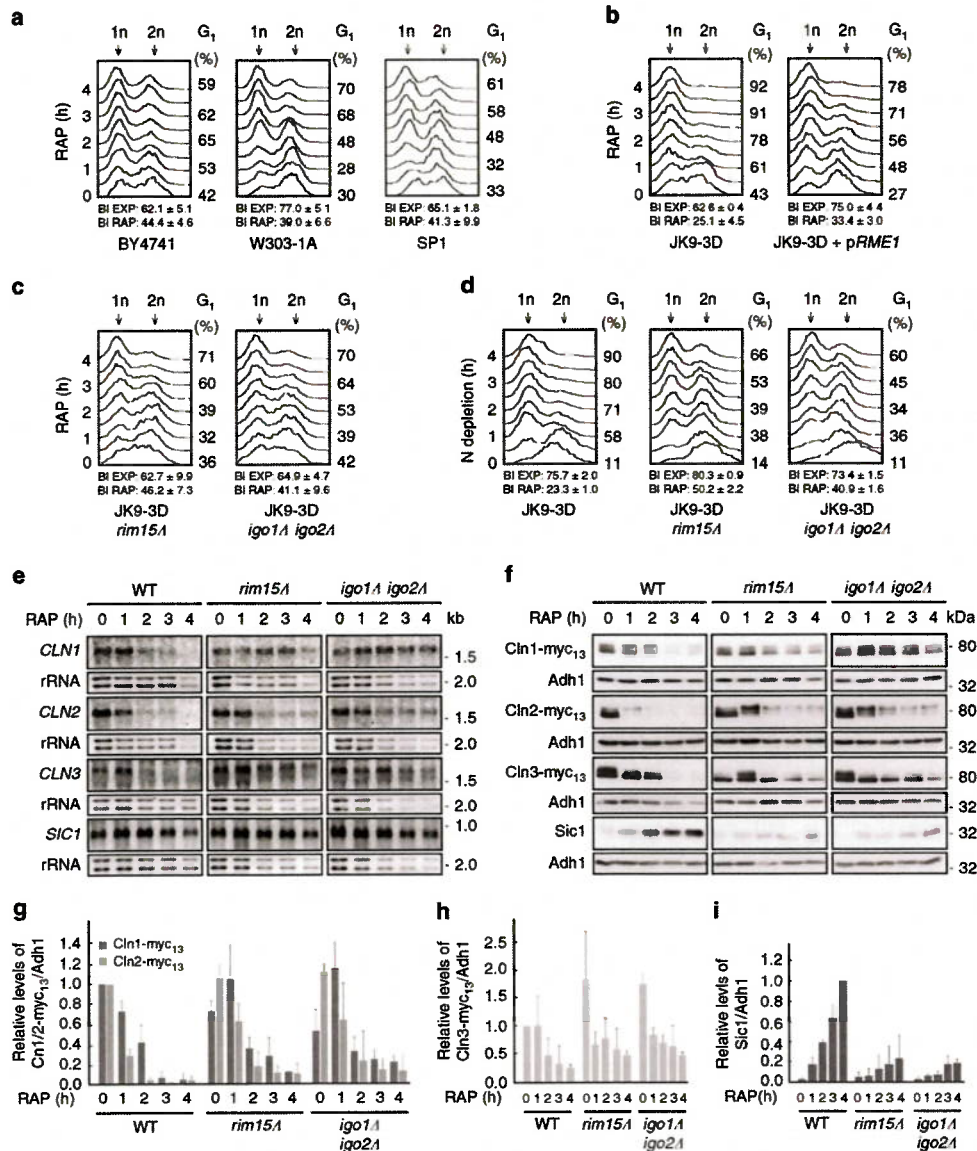


Figure 1 | The greatwall kinase pathway ensures proper G₁ arrest following TORC1 inactivation. (a) Cells of commonly used *Saccharomyces cerevisiae* wild-type strains (that is, BY4741, W303-1A and SP1) exhibit a delay in G₁ arrest following rapamycin-mediated TORC1 inactivation. Fluorescence-activated cell sorting (FACS) analyses of the DNA content of wild-type cells treated for the indicated times with rapamycin are shown. The relative number of budded cells (budding index, BI) was determined in exponentially growing (EXP) and rapamycin-treated (RAP; 4 h) cultures. Numbers are means \pm s.d. from three independent experiments in which at least 300 cells were assessed. Populations of cells contain both 1n (G₁; left-hand peak) and 2n (G₂/M; right-hand peak) DNA. The relative level of 1n cells within the populations is indicated on the right of the graphs (G₁ (%)). (b) JK9-3D cells promptly and uniformly arrest in G₁ following rapamycin treatment. Expression of plasmid-encoded *RME1* from its own promoter (*pRME1*) delays the rapamycin-mediated G₁ arrest in JK9-3D cells, indicating that the *rme1* mutation in JK9-3D contributes significantly to the observed phenotype. (c,d) Swift G₁ arrest in rapamycin-treated (c) or nitrogen-starved (d) JK9-3D cells requires Rim15 and Igo1/2. (e) Northern blot analyses of the expression of the indicated cell cycle regulatory genes in exponentially growing (0 h) and rapamycin-treated (1–4 h) wild-type (WT; JK9-3D), *rim15Δ* and *igo1/2Δ* mutant cells. Ribosomal RNA served as loading control. (f–i) The levels of genomically myc₁₃-tagged cyclins (f–h), or of endogenous Sic1 (i), in exponentially growing (0 h) and rapamycin-treated (1–4 h) WT (JK9-3D), *rim15Δ* and *igo1/2Δ* mutant cells, were determined by immunoblot analyses using monoclonal anti-myc or polyclonal anti-Sic1 antibodies, respectively. Adh1 levels served as loading controls. The experiments were performed independently three times (one representative blot is shown in f). The myc₁₃-tagged cyclin (g,h) or Sic1 (i) levels were normalized to the Adh1 levels in each case, calculated relative to the value in exponentially growing WT cells (set to 1.0 (g,h)) or to the value in 4-h rapamycin-treated WT cells (set to 1.0 (i)), respectively, and expressed as mean values ($n = 3; \pm$ s.d.).

mechanism(s) that is not directly related to G₁ cyclin expression control.

Following their activation by Rim15, Igo1/2 mediate some, if not all, of their effects via the inhibition of PP2A^{Cdc55}. Supporting this notion, we also found that loss of the regulatory Cdc55 subunit of the heterotrimeric PP2A^{Cdc55} complex rescued the Sic1 stabilization defect in rapamycin-treated *rim15Δ* and *igo1/2Δ* cells (Fig. 2a). Loss of Cdc55 alone, however, was not sufficient to drive Sic1 accumulation in exponentially growing cells, indicating that TORC1 antagonizes Sic1 by additional Cdc55-independent means. We were not able to examine whether loss of Cdc55 also suppresses the G₁ arrest defect in rapamycin-treated *rim15Δ* or *igo1/2Δ* cells because all of the respective *cdc55Δ* mutants exhibited an extended G₂/M delay that reflects an additional crucial role of PP2A^{Cdc55} in mitotic entry and spindle assembly checkpoint control³⁴. Expectedly, however, overexpression of Cdc55 under the control of the constitutive *ADH1* promoter destabilized Sic1 (Fig. 2a) and caused a G₁ arrest defect in rapamycin-treated cells (Fig. 2b) to a similar extent as loss of Rim15 or of Igo1/2 (Fig. 1c). Together with the current literature, these data could be unified in a model in which PP2A^{Cdc55} and Cln-CDK antagonize G₁ arrest by favouring Sic1 destabilization via dephosphorylation and phosphorylation, respectively, of different, specific residues within Sic1.

The greatwall kinase pathway impinges on Thr¹⁷³ in Sic1. To begin to study how many residues in Sic1, if any, are targeted by PP2A^{Cdc55}, we examined the migration pattern of Sic1-myc₁₃ by phosphate affinity gel electrophoresis in different yeast strains. When analysed in extracts of exponentially growing WT, *rim15Δ* and *igo1/2Δ* cells, the weakly expressed Sic1-myc₁₃ migrated in at least four distinct bands (labelled isoforms 1–4; Fig. 2c,d). Following rapamycin treatment (Fig. 2c), and similarly following nitrogen starvation (Fig. 2d), two additional slow-migrating Sic1-myc₁₃ isoforms (labelled 5 and 6) were detectable in WT cell extracts. These were either absent (isoform 6) or reduced in intensity (isoform 5) in rapamycin-treated and in nitrogen-starved *rim15Δ* and *igo1/2Δ* cells, which likely explains the relative increase in the intensity of the faster migrating isoforms in the extracts of the respective strains (Fig. 2c,d). Loss of Cdc55, however, rendered *rim15Δ* and *igo1/2Δ* mutant cells capable again of expressing both isoforms (that is, isoforms 5 and 6) at levels comparably (or even higher) to the ones in WT cells under the same conditions. Of note, in exponentially growing, rapamycin-treated and nitrogen-starved cells, and independently of the presence or absence of Rim15 or Igo1/2, Sic1-myc₁₃ preferentially migrated as isoforms 4, 5 and 6 when Cdc55 was

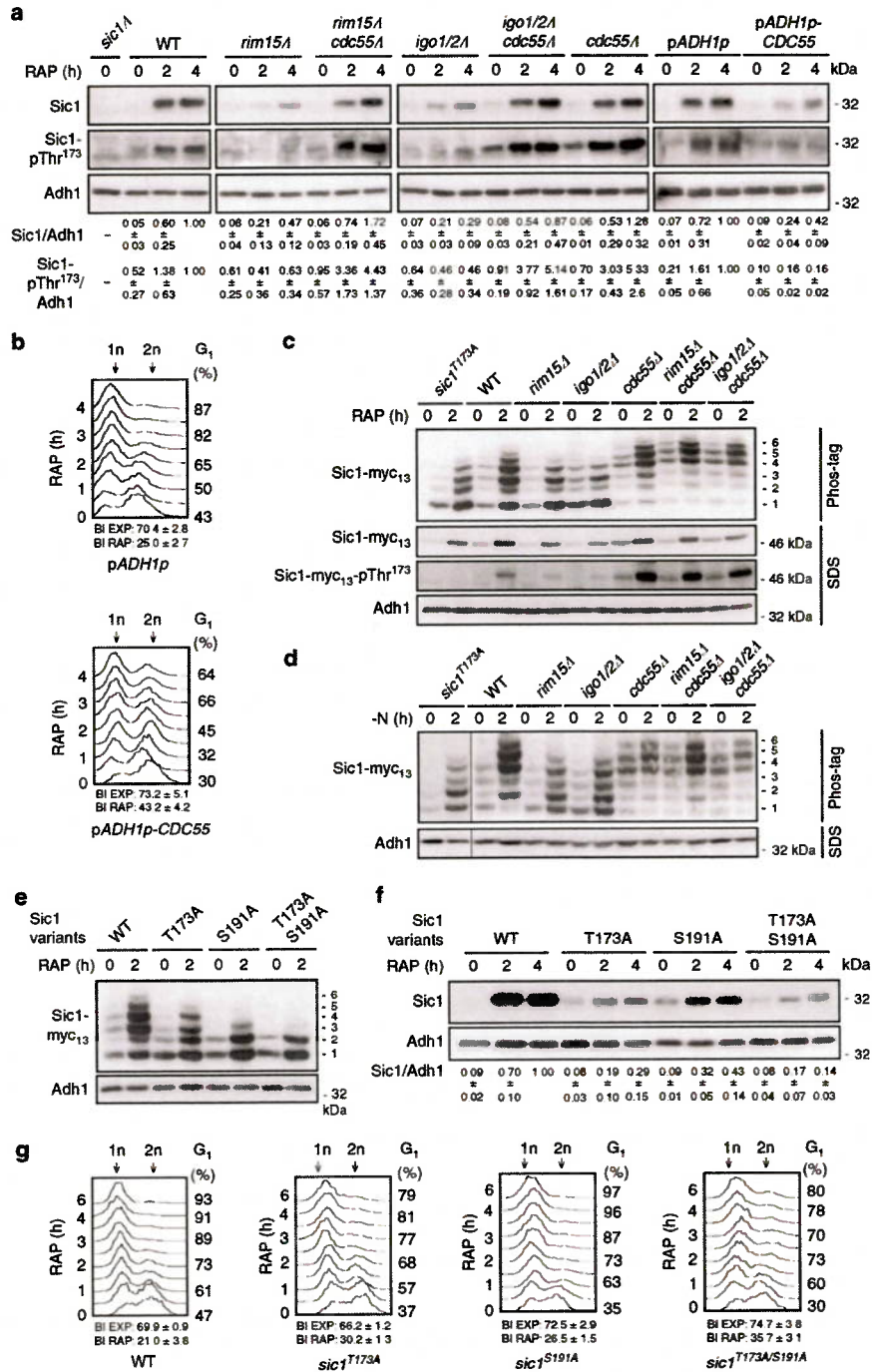
absent. Together, these results indicate that PP2A^{Cdc55} targets at least two Sic1 phosphoresidues (to various degrees), and that activation of Rim15/Igo1/2 following rapamycin treatment or nitrogen starvation restrains the respective PP2A^{Cdc55} activity. To examine whether one of the respective residues corresponded to phosphorylated Thr¹⁷³ (pThr¹⁷³), which is critical for Sic1 stability in rapamycin-treated cells⁶ (Supplementary Fig. 2), we also analysed the migration pattern of a Sic1^{T173A} mutant allele via phosphate affinity gel electrophoresis in extracts of rapamycin-treated or nitrogen-starved cells. The Sic1^{T173A}-myc₁₃ migration pattern specifically lacked isoform 6 and was overall very similar to the one observed for Sic1-myc₁₃ in extracts of rapamycin-treated or nitrogen-starved *rim15Δ* and *igo1/2Δ* mutant cells (Fig. 2c,d; Supplementary Fig. 3), indicating that pThr¹⁷³ in Sic1 may indeed represent a PP2A^{Cdc55} target. Moreover, the previously identified phosphoresidue pSer¹⁹¹ in Sic1 (ref. 35) was required for the formation of three of the observed 6 isoforms (as Sic1^{S191A}-myc₁₃ migrated only in three (two major and one weaker) bands in rapamycin-treated cells; isoforms 1–3; Fig. 2e). Interestingly, mutation of Thr¹⁷³ to Ala in Sic1 destabilized Sic1 and compromised proper G₁ arrest in rapamycin-treated cells, and both of these defects were marginally enhanced by combined mutation of Thr¹⁷³ and Ser¹⁹¹ to Ala in Sic1 (Fig. 2f,g; see budding indices; Supplementary Fig. 4). The Sic1^{S191A} allele *per se*, albeit less stable than WT Sic1, was able to ensure normal rapamycin-induced G₁ arrest *in vivo* (Fig. 2f,g; Supplementary Fig. 4). The stability of Sic1 and hence proper G₁ arrest in rapamycin-treated cells therefore primarily depend on the phosphorylation of Thr¹⁷³ with at most accessory contributions from pSer¹⁹¹ (as well as potentially additional, less significant phosphoresidues). To further verify this assumption, we decided to focus our subsequent analyses on Thr¹⁷³ in Sic1. Using phospho-specific antibodies against pThr¹⁷³ in Sic1 (see below), we found that the Sic1-pThr¹⁷³ signal strongly increased in rapamycin-treated WT cells, but not in Cdc55 overproducing nor in *rim15Δ*, or *igo1/2Δ* cells, unless the latter two mutant strains were additionally deleted for *CDC55* (Fig. 2a). In control experiments (corroborating the *in vivo* specificity of the anti-Sic1-pThr¹⁷³ antibodies), mutation of Thr¹⁷³ to Ala in Sic1 totally abolished the Sic1-pThr¹⁷³ signal, and eliminated the Sic1-myc₁₃ isoform 6 on phos-tag gels, even when Cdc55 was absent (Supplementary Fig. 3). Notably, Sic1-Thr¹⁷³ phosphorylation signals closely mirrored the overall Sic1 levels in rapamycin-treated WT and all, except the Sic1^{T173A} mutant strains tested (Fig. 2a). Together, these data corroborate a model in which activation of Rim15/Igo1/2 following TORC1 inhibition serves to antagonize PP2A^{Cdc55} and prevent it from dephosphorylating pThr¹⁷³ (and possibly additional

Figure 2 | The greatwall kinase pathway regulates phosphorylation and stability of Sic1. (a) Loss of Cdc55 suppresses the defect of rapamycin-treated *rim15Δ* and *igo1/2Δ* cells in Sic1 accumulation. Sic1 levels and phosphorylation of Thr¹⁷³ in Sic1 (Sic1-pThr¹⁷³) were determined by immunoblot analyses using polyclonal anti-Sic1 and phospho-specific anti-Sic1-pThr¹⁷³ antibodies, respectively. Overexpression of plasmid-encoded *CDC55* from the strong constitutive *ADH1* promoter (*ADH1p*) prevents normal Sic1 accumulation and reduces the total amount of Sic1-pThr¹⁷³ in WT cells. Relevant genotypes are indicated. The experiments were performed independently three times (one representative blot is shown). The respective Sic1 levels or Sic1-pThr¹⁷³ signals were normalized to the Adh1 levels in each case, calculated relative to the value in 4-h rapamycin-treated wild-type cells (set to 1.0), except for the values of the *CDC55*-overexpressing cells (*pADH1p-CDC55*), which were calculated relative to the control cells carrying the empty vector (*pADH1p*), and expressed as mean values ($n = 3; \pm$ s.d.). (b) Overexpression of plasmid-encoded *CDC55* from the *ADH1* promoter causes a substantial defect in G₁ arrest in rapamycin-treated WT cells. (c–e) Phos-tag phosphate affinity gel electrophoresis analyses of genomically myc₁₃-tagged Sic1, Sic1^{T173A}, Sic1^{S191A} and/or Sic1^{T173A/S191A} in extracts from exponentially growing (time 0 h) and rapamycin-treated (RAP; 2 h; (c,e)) or nitrogen-deprived (–N; 2 h; (d)) strains with the indicated genotype. The six differentially phosphorylated Sic1-myc₁₃ isoforms are numbered sequentially from 1 to 6 (right side of the panels). In c, samples were also subjected to SDS-gel electrophoresis to detect the Sic1-myc₁₃ levels and Sic1-myc₁₃-pThr¹⁷³ signals by immunoblot analyses using monoclonal anti-myc and phospho-specific anti-Sic1-pThr¹⁷³ antibodies, respectively. (f,g) The Sic1^{T173A} allele is unstable (f) and compromises timely G₁ arrest in rapamycin-treated cells (g). Levels of Sic1 in f were determined in exponentially growing (time 0 h) and rapamycin-treated (2 and 4 h) WT, *sic1^{T173A}*, *sic1^{S191A}* and *sic1^{T173A/S191A}* cells and quantified as in a. For quantifications of FACS profiles, see Supplementary Fig. 4. FACS and BI analyses in b and g were performed as in Fig. 1a. Adh1 levels in a,c,d,e and f served as loading controls. FACS, fluorescence-activated cell sorting.

phosphoresidues) in Sic1, which presumably exposes Sic1 to a proteolytic degradation mechanism.

Inactivation of SCF^{Cdc4} stabilizes Sic1^{T173A}. To examine whether phosphorylation of Thr¹⁷³ in Sic1 may serve to protect

Sic1 from SCF^{Cdc4}-mediated ubiquitination and subsequent proteolysis, we introduced the temperature-sensitive *cdc4-2⁵* allele in our WT, *rim15Δ*, *igo1/2Δ* and *sic1^{T173A}* strains, and measured their capacity to accumulate Sic1 during exponential growth or following rapamycin treatment at the permissive



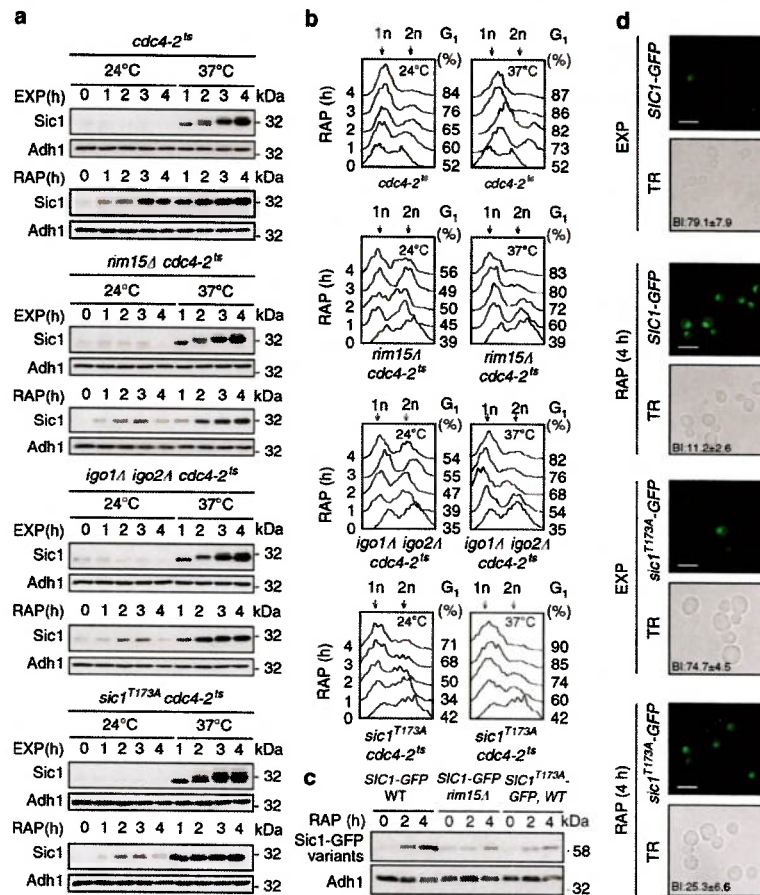


Figure 3 | Inactivation of SCF^{Cdc4} stabilizes Sic1^{T173A}. (a) Levels of endogenous Sic1 were determined by immunoblot analyses as in Fig. 2a. Cells (genotypes indicated) were pre-grown exponentially at 24 °C (time 0 h) and then grown up to 4 h at either 24 °C or 37 °C (to inactivate Cdc4-2^{ts}) in the absence (EXP) or presence of rapamycin (RAP). Samples were taken at the indicated time points. (b) FACS analyses from cells treated as in a. (c,d) Sic1-Thr¹⁷³ phosphorylation primarily serves to control Sic1 stability, but not Sic1 subcellular localization. In c, levels of endogenously tagged Sic1-GFP and Sic1^{T173A}-GFP were determined in exponentially growing (time 0 h) and rapamycin-treated (2 h and 4 h) WT and/or *rim15Δ* cells by immunoblot analyses using polyclonal anti-GFP antibodies. In d, exponentially growing (EXP) or rapamycin-treated (RAP; 4 h) cells expressing endogenously tagged versions of Sic1-GFP or Sic1^{T173A}-GFP were analysed by fluorescence microscopy. Scale bars, 5 μm (white); TR, transmission; BI, budding index. Adh1 levels in a and c served as loading controls. FACS, fluorescence-activated cell sorting.

(24 °C) and the non-permissive temperature (37 °C). At 24 °C, the *cdc4-2^{ts}* allele did not noticeably alter the Sic1 expression pattern in any of the strains studied, whether they were grown exponentially or subjected to rapamycin treatment (that is, specifically *rim15Δ cdc4-2^{ts}*, *igo1/2Δ cdc4-2^{ts}* and *sic1^{T173A} cdc4-2^{ts}* cells were still defective for normal Sic1 accumulation following rapamycin treatment when compared with *cdc4-2^{ts}* cells; Fig. 3a). Temperature inactivation of Cdc4-2^{ts} (at 37 °C), however, prompted Sic1 accumulation to a similarly strong extent in all strains, independently of the presence or absence of rapamycin, and could thus override the defect in Sic1 accumulation, but not in Sic1-Thr¹⁷³ phosphorylation (Supplementary Fig. 5a,b), in rapamycin-treated *rim15Δ cdc4-2^{ts}*, *igo1/2Δ cdc4-2^{ts}*, and *sic1^{T173A} cdc4-2^{ts}* cells. As expected, the latter mutant strains also regained their capacity to timely arrest in G₁ following rapamycin treatment at 37 °C, but not at 24 °C (Fig. 3b). Rim15-Igo1/2-mediated inhibition of PP2A^{Cdc55} therefore likely serves to preserve the phosphorylation status of

Thr¹⁷³ (and other residues) in Sic1, thereby preventing SCF^{Cdc4}-mediated ubiquitination and subsequent proteolysis of Sic1. To address the possibility that Sic1-Thr¹⁷³ phosphorylation plays an additional role in nutrient-regulated nucleo-cytoplasmic distribution of Sic1 (ref. 36), we examined the localization of endogenously tagged Sic1-green fluorescent protein (GFP) and of Sic1^{T173A}-GFP. These GFP fusions behaved like the respective untagged versions in terms of their stability (that is, Sic1-GFP accumulated in rapamycin-treated WT, but not in *rim15Δ* cells, and Sic1^{T173A}-GFP was intrinsically unstable in a WT context under the same conditions; Fig. 3c). Sic1^{T173A}-GFP, although expressed at lower levels and compromised in ensuring proper G₁ arrest to a larger fraction of the population, was able to accumulate like Sic1-GFP within the nuclei of those cells that were still able to arrest in an unbudded state, specifically also following rapamycin treatment (Fig. 3d). Thus, Sic1-Thr¹⁷³ phosphorylation likely serves to primarily control Sic1 stability, but not Sic1 subcellular localization.

Mpk1 phosphorylates Thr¹⁷³ in Sic1. Since rapamycin treatment was able to strongly increase the Sic1-pThr¹⁷³ signal in *cdc55Δ* cells (Fig. 2a), we reasoned that TORC1 is additionally involved in downregulation of a Sic1-Thr¹⁷³-targeting protein kinase(s). In this context, the MAPK Hog1 has previously been proposed to mediate Sic1-Thr¹⁷³ phosphorylation following exposure of cells to osmotic stress³⁷. Whether TORC1 impinges on Hog1 is not known, but TORC1 indirectly inhibits the closely related MAPK Slt2/Mpk1 (refs 38,39). Intriguingly, and consistent with a role of Mpk1 in Sic1-Thr¹⁷³ phosphorylation, loss of Mpk1, but not of Hog1, significantly reduced the Sic1-pThr¹⁷³ signal and rendered Sic1 unstable in rapamycin-treated cells (Fig. 4a). Moreover, the migration pattern of Sic1-myc₁₃ (analysed by phosphate affinity gel electrophoresis) in extracts of rapamycin-treated WT, *mpk1Δ* and *hog1Δ* cells indicated that

Mpk1, but not Hog1, might (directly or indirectly) target one major residue in Sic1 (compare the levels of isoforms 5 and 6 in WT and *hog1Δ* versus *mpk1Δ* cells in Fig. 4b). Together, these data pinpoint a potential role for Mpk1 in direct phosphorylation of Thr¹⁷³ in Sic1. Corroborating this assumption, we further found that Mpk1-HA₃, but not kinase-dead Mpk1^{KD}-HA₃, strongly phosphorylated Sic1-Thr¹⁷³ *in vitro* (Fig. 4c; notably, the respective signal was almost entirely abrogated by introduction of the Thr¹⁷³ to Ala mutation in Sic1, indicating that the anti-Sic1-pThr¹⁷³ antibodies are also exquisitely specific *in vitro*). In addition, rapamycin treatment not only stimulated the activity of Mpk1 towards Thr¹⁷³ in Sic1 10.4-fold (± 2.6 s.d.; three independent time-course experiments; Fig. 4d), but also significantly boosted the interaction of Mpk1 with Sic1 *in vivo* (Fig. 4e). From these studies, we infer that Mpk1 directly

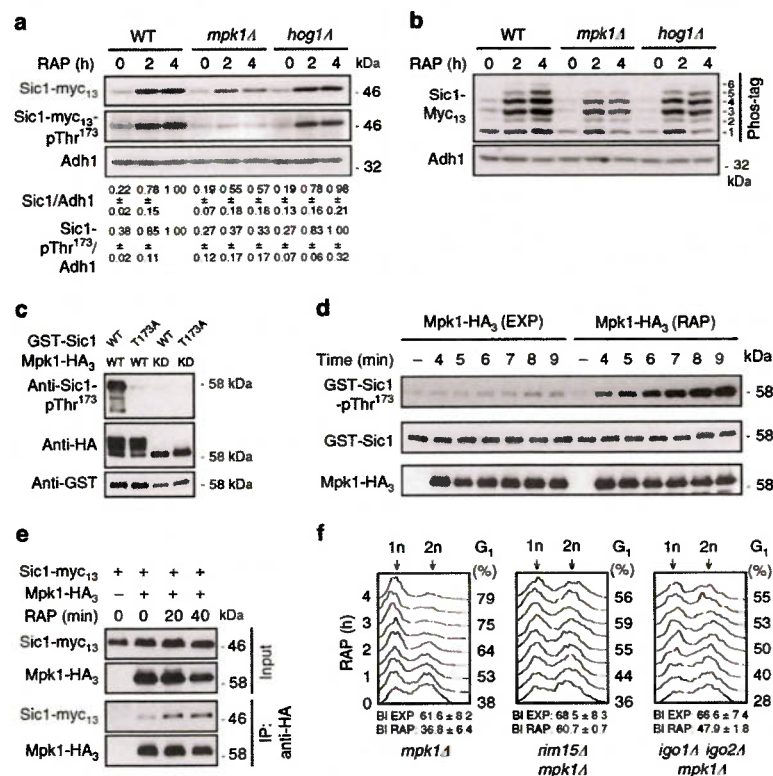


Figure 4 | Mpk1 phosphorylates Thr¹⁷³ in Sic1. (a) Mpk1, but not Hog1, is required for normal Sic1 accumulation in rapamycin-treated cells. Levels of Sic1-myc₁₃ and of Sic1-myc₁₃-pThr¹⁷³ signals were determined in cells with the indicated genotypes before (0 h) and following a rapamycin treatment (for 2 and 4 h). The Sic1-myc₁₃ levels or Sic1-myc₁₃-pThr¹⁷³ signals (three independent experiments) were normalized to Adh1 in each case, calculated relative to the value in 4-h rapamycin-treated wild-type cells (set to 1.0), and expressed as mean values (± s.d.). (b) Phos-tag phosphate affinity gel electrophoresis analysis of genomically myc₁₃-tagged Sic1 from exponentially growing (time 0 h) and rapamycin-treated (2 and 4 h) WT, *mpk1Δ* and *hog1Δ* cells were carried out as in Fig. 2c. (c) Mpk1 phosphorylates Thr¹⁷³ in Sic1 *in vitro*. Mpk1-HA₃ and kinase-dead Mpk1^{KD}-HA₃ (carrying the K54R mutation) were purified from rapamycin-treated (1 h) cells and used for *in vitro* protein kinase assays on bacterially purified GST-Sic1 or GST-Sic1^{T173A}. Levels of Sic1 protein and of Sic1-pThr¹⁷³ signals were determined using anti-GST and anti-Sic1-pThr¹⁷³ antibodies, respectively. Immunoblot analysis using anti-HA antibodies served as input control for Mpk1-HA₃ variants. Mpk1-HA₃, but not Mpk1^{KD}-HA₃, displayed slow-migrating isoforms due to post-translational modifications. (d) Rapamycin treatment strongly stimulates Mpk1 protein kinase activity towards Thr¹⁷³ in Sic1. *In vitro* protein kinase assays were carried out as in c for the indicated times using Mpk1-HA₃ preparations from exponentially growing (EXP) or rapamycin-treated (1 h; RAP) cells. (e) Rapamycin treatment stimulates the interaction between Sic1-myc₁₃ and Mpk1-HA₃. Plasmid-encoded Mpk1-HA₃ was immunoprecipitated from extracts of untreated (0 min) and rapamycin-treated (RAP; 20 and 40 min) Sic1-myc₁₃-expressing WT cells. Cells carrying an empty vector (-) were used as control. The co-precipitated Sic1-myc₁₃ levels were detected by immunoblot analysis using anti-myc antibodies. (f) Proper G₁ arrest in rapamycin-treated cells requires Mpk1. FACS analyses (see Supplementary Fig. 6 for quantifications of triplicates) and BI determinations were performed as in Fig. 1a. All strains (relevant genotypes indicated) are isogenic to JK9-3D (see Fig. 1b,c for comparison). FACS, fluorescence-activated cell sorting.

phosphorylates Sic1-Thr¹⁷³ *in vivo*, thereby contributing to Sic1 stability when TORC1 is attenuated. Expectedly, therefore, loss of Mpk1, but not of Hog1, also caused a significant G₁ arrest defect in rapamycin-treated cells (Fig. 4f; Supplementary Fig. 6).

Mpk1 and PP2A^{Cdc55} reciprocally control Sic1-pThr¹⁷³. Since we were able to phosphorylate Sic1-Thr¹⁷³ with Mpk1, we also examined whether PP2A^{Cdc55} could directly dephosphorylate this residue *in vitro*. As illustrated in Fig. 5a, PP2A^{Cdc55} indeed very efficiently dephosphorylated pThr¹⁷³ in Sic1 in these assays (Fig. 5a, lane 1 versus lane 5). In addition, following prior activation by Rim15, Igo1 (Igo1-pSer⁶⁴; Fig. 5a, lanes 2–4), but not inactive Igo1 (Fig. 5a, lane 7), efficiently inhibited the respective PP2A^{Cdc55} activity in a concentration-dependent manner. Thus, Mpk1 and PP2A^{Cdc55} directly and antagonistically control the phosphorylation status of Thr¹⁷³ in Sic1 both *in vitro* and within cells. Of note, since Sic1-Thr¹⁷³ phosphorylation was not fully abolished in the absence of Mpk1 (in *mpk1Δ*), nor in the presence of unrestricted PP2A^{Cdc55} (in *rim15Δ* or *igo1/2Δ* cells), we expected the combination of *mpk1Δ* with either *rim15Δ* or *igo1/2Δ* to cause an additive G₁ arrest defect in rapamycin-treated cells. This was indeed the case (Fig. 4f).

Discussion

TORC1 coordinates START with nutrient availability in part by tightly regulating the phosphorylation status of Thr¹⁷³ within the CDKI Sic1 (Fig. 5b). Together with the previous observations (i) that Sic1 only marginally interacts with the catalytic SCF^{Cdc4} subunit Cdc34 in rapamycin-treated cells⁶ and (ii) that the introduction of a phosphomimetic Glu at position 173 of Sic1 compromises its capacity to interact with Cdc4 (ref. 37), our present data are best explained in a model in which phosphorylation of Thr¹⁷³ in Sic1 serves to stabilize Sic1 by preventing (directly or indirectly) its association with SCF^{Cdc4}. Of note, Cln-CDK downregulation following TORC1 inhibition, which transiently relies on Rim15 and Igo1/2 (Fig. 1e,f),

presumably also contributes to the latter process. It will therefore be interesting in future studies to decipher the respective Rim15- and Igo1/2-dependent and -independent mechanism(s) by which TORC1 controls transcriptional and/or post-transcriptional control of G₁ cyclin expression.

Finally, Sic1 is functionally and structurally related to the mammalian CDKI p27^{Kip1}, an atypical tumour suppressor that regulates the G₀-S cell cycle transition by inhibiting cyclin-CDK2-containing complexes⁴⁰. Similar to Sic1, p27^{Kip1} turnover is stimulated by direct cyclin-CDK2-mediated phosphorylation, followed by SCF^{Skp2}-dependent ubiquitination and proteasomal degradation in proliferating cells. In quiescent G₀ cells, in contrast, phosphorylation of specific alternative residues ensures p27^{Kip1} stability⁴⁰. Since p27^{Kip1} also mediates in part the anti-proliferative effects of rapamycin⁴, it will be interesting to study whether and to what extent our findings in yeast may have been evolutionarily conserved.

Methods

Strains, plasmids and growth conditions. *Saccharomyces cerevisiae* yeast cells were pre-grown overnight at 30 °C in standard synthetic defined (SD) medium with 2% glucose and supplemented with the appropriate amino acids for maintenance of plasmids. Before the experiments, cells were diluted to an OD₆₀₀ of 0.001 in SD and grown until they reached an OD₆₀₀ of 0.4. Rapamycin was dissolved in 10% Tween-20/90% ethanol and used at a final concentration of 200 ng ml⁻¹. Strains and plasmids used in this study are listed in Supplementary Tables 1 and 2, respectively. Epitope-tagged proteins studied were expressed from their genomic locus, except GST-Sic1, Mpk1-HA₃ and Cdc55-HA₃ that were expressed from plasmids (under the control of their own promoter) to be used for the *in vitro* protein kinase and phosphatase assays.

Fluorescence-activated cell sorting analysis. A measure of 1.5 ml samples were collected at the indicated time points after rapamycin treatment, centrifuged and resuspended in 1 ml 70% ethanol. Following overnight incubation at 4 °C, cells were washed once with H₂O, centrifuged, resuspended in 250 μl of RNase solution (50 mM Tris (pH 7.4), 200 μg ml⁻¹ RNase A (Axonlab AG)) and incubated for 3 h at 37 °C. Subsequently, cells were centrifuged again, resuspended in 250 μl of propidium iodide solution (50 mM Na⁺-citrate (pH 7.0) and 10 μg ml⁻¹ propidium iodide (Sigma)) and analysed in a CyFlow (PARTEC) flow cytometer. Data were processed using the FlowJo software.

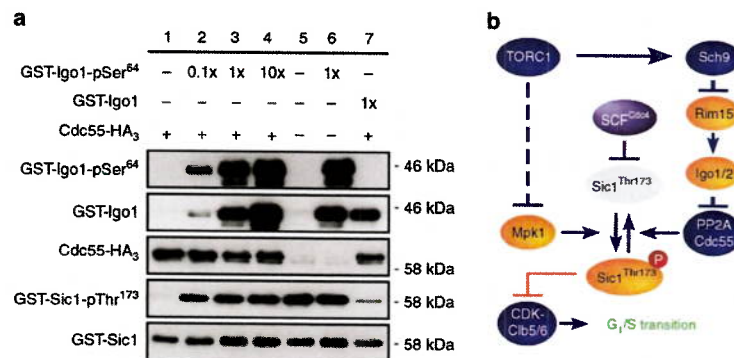


Figure 5 | TORC1 coordinates G₁-S cell cycle progression via Mpk1 and PP2A^{Cdc55}. (a) PP2A^{Cdc55} dephosphorylates pThr¹⁷³ in Sic1 and this activity is inhibited in a concentration-dependent manner by activated Igo1 (Igo1-pSer⁶⁴), but not inactive Igo1. GST-Sic1 was phosphorylated by Mpk1 *in vitro* before being used as a substrate for the PP2A^{Cdc55} phosphatase assay. Phosphatase activity of PP2A^{Cdc55} was analysed in the absence (lane 1) and in the presence of increasing amounts (lanes 2, 3 and 4, respectively) of recombinant Igo1-pSer⁶⁴, which had been subjected to thio-phosphorylation by Rim15 previously. Assays without both PP2A^{Cdc55} and Igo1-pSer⁶⁴ (lane 5), without PP2A^{Cdc55} but with Igo1-pSer⁶⁴ (lane 6), and with PP2A^{Cdc55} combined with inactive Igo1 (lane 7) were included as additional controls. The levels of Ser⁶⁴ phosphorylation in GST-Igo1 (GST-Igo1-pSer⁶⁴), GST-Igo1, Cdc55-HA₃, Thr¹⁷³ phosphorylation in GST-Sic1 (GST-Sic1-pThr¹⁷³) and GST-Sic1 were determined by immunoblot analyses using phospho-specific anti-Igo1-pSer⁶⁴, anti-GST, anti-HA, phospho-specific anti-Sic1-pThr¹⁷³ and anti-GST antibodies, respectively. (b) Model for the role of TORC1 in regulating the phosphorylation status and stability of the CDKI Sic1. For the sake of clarity, we have not schematically depicted the additional role of Rim15-Igo1/2 in G₁ cyclin downregulation that may transiently favour CDK-mediated multi-site phosphorylation and consequently SCF^{Cdc4}-dependent ubiquitination and degradation of Sic1 following TORC1 inactivation. Sic1 inhibits the CDK-Cln5/6 complexes to prevent transition into S phase⁴³. Arrows and bars denote positive and negative interactions, respectively. Solid arrows and bars refer to direct interactions, the dashed bar refers to an indirect interaction. For details see text.

Northern blot and immunoblot analyses. Northern blot analyses were performed according to our standard protocol¹⁸ and the respective uncropped scans have been included in Supplementary Fig. 7. Total protein extracts were prepared by mild alkali treatment of cells followed by boiling in standard electrophoresis buffer⁴¹. SDS-polyacrylamide gel electrophoresis and immunoblot analyses were performed according to standard protocols. For the analysis of protein phosphorylation states, we used Phos-tag acrylamide gel electrophoresis⁴². Anti-Sic1, (sc-50441; Santa Cruz), anti-c-Myc (9E10; sc-40; Santa Cruz), anti-Adh1 (Calbiochem), phospho-specific anti-Sic1-pThr¹⁷³ (produced by GenScript), anti-GFP (Roche), phospho-specific anti-Igo1-pSer⁶⁴ (ref. 24), anti-GST (Lubio) and anti-HA antibodies (Enzo) were used at 1:1,000, 1:3,000, 1:200,000, 1:1,000, 1:3,000, 1:1,000, 1:1,000 and 1:1,000 dilutions, respectively. Goat anti-rabbit/anti-mouse IgG-horse-radish peroxidase-conjugated antibodies (BioRad) were used at a 1:3,000 dilution. All immunoblots presented in the main text have been included as uncropped scans in Supplementary Figs 8–25.

Co-immunoprecipitation. For co-immunoprecipitation analyses, Sic1-myc₁₃ and Mpk1-HA₃-expressing cells were fixed for 20 min with 1% formaldehyde, quenched with 0.3 M glycine, washed once with Tris-buffered saline, centrifuged and subsequently frozen (–80 °C). Lysates were prepared by disruption of frozen cells in lysis buffer (50 mM TRIS (pH 7.5), 1 mM EDTA, 150 mM NaCl, 0.5% NP40 and 1 × protease and phosphatase inhibitor cocktails (Roche)) with glass beads (0.5-mm diameter) using a Precellys cell disruptor and subsequent clarification by centrifugation (5 min at 14,000 r.p.m.; 4 °C). Mpk1-HA₃ was immunoprecipitated with anti-HA magnetic matrix (Pierce) and co-immunoprecipitated Sic1-myc₁₃ was determined by immunoblot analysis using anti-c-Myc antibodies.

Mpk1 protein kinase assays. Mpk1-HA₃ or Mpk1^{K54R}-HA₃ was immunopurified from yeast cells using anti-HA magnetic matrix (Pierce). The respective matrices were incubated for 30 min at 30 °C with 3 μl of bacterially purified GST-Sic1 or GST-Sic1^{T173A} in 50 μl of kinase buffer mix (125 mM Tris (pH 7.5), 50 mM MgCl₂, 2.5 mM dithiothreitol and 10 mM ATP). The reactions were stopped by addition of loading buffer, boiled at 95 °C and analysed by immunoblot analyses. For the Mpk1 kinase time-course experiment, Mpk1-HA₃ was purified from exponentially growing or rapamycin-treated (1 h) cells. The protein kinase reactions (with bacterially purified GST-Sic1 as substrate) were stopped at the indicated time points by addition of loading buffer and subsequent boiling (5 min).

PP2A^{Cdc55} protein phosphatase assay. Cdc55-HA₃ was isolated from exponentially growing *cdc55Δ* cells carrying the pRS416-CDC55-HA₃ plasmid. Cdc55-HA₃ was immunoprecipitated from total extracts in lysis buffer (50 mM Tris (pH 7.5), 1 mM EDTA, 150 mM NaCl, 0.5% NP40 and 1 × protease and phosphatase inhibitor cocktails from Roche) using anti-HA magnetic matrix (Pierce). Igo1-GST and Igo1^{S64A}-GST were isolated from bacteria using glutathione sepharose (GE Healthcare) and phosphorylated where indicated by yeast-purified GST-Rim15-HA₃ using 1 mM adenosine 5'-[γ-thio] triphosphate^{17,22}. The *in vitro* phosphatase assay (30 min at 30 °C) was performed in phosphatase buffer (10 mM Tris (pH 7.5), 5 mM MgCl₂ and 1 mM EGTA) with purified PP2A^{Cdc55}, bacterially purified Sic1-GST that was phosphorylated by Mpk1 *in vitro* as substrate, and different concentrations of Igo1, which was, or was not, subjected to *in vitro* phosphorylation by Rim15 before the use. To assess PP2A^{Cdc55} activity, the decrease in Sic1^{T173} phosphorylation was detected using phospho-specific anti-Sic1-pThr¹⁷³ antibodies. Levels of immunoprecipitated Cdc55-HA₃ were assessed using anti-HA antibodies.

References

- Soulard, A., Cohen, A. & Hall, M. N. TOR signaling in invertebrates. *Curr. Opin. Cell Biol.* **21**, 825–836 (2009).
- Zoncu, R., Efeyan, A. & Sabatini, D. M. mTOR: from growth signal integration to cancer, diabetes and ageing. *Nat. Rev. Mol. Cell Biol.* **12**, 21–35 (2011).
- Hartwell, L. H., Culotti, J., Pringle, J. R. & Reid, B. J. Genetic control of the cell division cycle in yeast. *Science* **183**, 46–51 (1974).
- Wang, X. & Proud, C. G. Nutrient control of TORC1, a cell-cycle regulator. *Trends Cell Biol.* **19**, 260–267 (2009).
- Workman, J. J., Chen, H. & Larabee, R. N. Environmental signaling through the mechanistic target of rapamycin complex 1: mTORC1 goes nuclear. *Cell Cycle* **13**, 714–725 (2014).
- Zinzalla, V., Graziola, M., Mastriani, A., Vanoni, M. & Alberghina, L. Rapamycin-mediated G1 arrest involves regulation of the Cdk inhibitor Sic1 in *Saccharomyces cerevisiae*. *Mol. Microbiol.* **63**, 1482–1494 (2007).
- Barbet, N. C. *et al.* TOR controls translation initiation and early G1 progression in yeast. *Mol. Biol. Cell* **7**, 25–42 (1996).
- Beretta, L., Gingras, A. C., Svitkin, Y. V., Hall, M. N. & Sonenberg, N. Rapamycin blocks the phosphorylation of 4E-BP1 and inhibits cap-dependent initiation of translation. *EMBO J.* **15**, 658–664 (1996).
- Polymenis, M. & Schmidt, E. V. Coupling of cell division to cell growth by translational control of the G₁ cyclin *CLN3* in yeast. *Genes Dev.* **11**, 2522–2531 (1997).
- Feldman, R. M., Correll, C. C., Kaplan, K. B. & Deshaies, R. J. A complex of Cdc4p, Skp1p, and Cdc53p/cullin catalyzes ubiquitination of the phosphorylated CDK inhibitor Sic1p. *Cell* **91**, 221–230 (1997).
- Bai, C. *et al.* SKP1 connects cell cycle regulators to the ubiquitin proteolysis machinery through a novel motif, the P-box. *Cell* **86**, 263–274 (1996).
- Skowyra, D., Craig, K. L., Tyers, M., Elledge, S. J. & Harper, J. W. P-box proteins are receptors that recruit phosphorylated substrates to the SCF ubiquitin-ligase complex. *Cell* **91**, 209–219 (1997).
- Petroski, M. D. & Deshaies, R. J. Function and regulation of cullin-RING ubiquitin ligases. *Nat. Rev. Mol. Cell Biol.* **6**, 9–20 (2005).
- De Virgilio, C. The essence of yeast quiescence. *FEMS Microbiol. Rev.* **36**, 306–339 (2012).
- Zaragoza, D., Ghavidel, A., Heitman, J. & Schultz, M. C. Rapamycin induces the G₀ program of transcriptional repression in yeast by interfering with the TOR signaling pathway. *Mol. Cell Biol.* **18**, 4463–4470 (1998).
- Wanke, V., Pedruzzi, L., Cameroni, E., Dubouloz, F. & De Virgilio, C. Regulation of G₀ entry by the Pho80-Pho85 cyclin-CDK complex. *EMBO J.* **24**, 4271–4278 (2005).
- Reinders, A., Bürckert, N., Boller, T., Wiemken, A. & De Virgilio, C. *Saccharomyces cerevisiae* cAMP-dependent protein kinase controls entry into stationary phase through the Rim15p protein kinase. *Genes Dev.* **12**, 2943–2955 (1998).
- Pedruzzi, L. *et al.* TOR and PKA signaling pathways converge on the protein kinase Rim15 to control entry into G₀. *Mol. Cell* **12**, 1607–1613 (2003).
- Urban, J. *et al.* Sch9 is a major target of TORC1 in *Saccharomyces cerevisiae*. *Mol. Cell* **26**, 663–674 (2007).
- Gharbi-Ayachi, A. *et al.* The substrate of Greatwall kinase, Arpp19, controls mitosis by inhibiting protein phosphatase 2A. *Science* **330**, 1673–1677 (2010).
- Mochida, S., Maslen, S. L., Skehel, M. & Hunt, T. Greatwall phosphorylates an inhibitor of protein phosphatase 2A that is essential for mitosis. *Science* **330**, 1670–1673 (2010).
- Bontron, S. *et al.* Yeast endosulfines control entry into quiescence and chronological life span by inhibiting protein phosphatase 2A. *Cell Rep.* **3**, 16–22 (2013).
- Luo, X., Talarek, N. & De Virgilio, C. Initiation of the yeast G₀ program requires Igo1 and Igo2, which antagonize activation of decapping of specific nutrient-regulated mRNAs. *RNA Biol.* **8**, 14–17 (2011).
- Talarek, N. *et al.* Initiation of the TORC1-regulated G₀ program requires Igo1/2, which license specific mRNAs to evade degradation via the 5'-3' mRNA decay pathway. *Mol. Cell* **38**, 345–355 (2010).
- Pedruzzi, L., Bürckert, N., Egger, P. & De Virgilio, C. *Saccharomyces cerevisiae* Ras/cAMP pathway controls post-diauxic shift element-dependent transcription through the zinc finger protein Gis1. *EMBO J.* **19**, 2569–2579 (2000).
- Mochida, S. & Hunt, T. Protein phosphatases and their regulation in the control of mitosis. *EMBO Rep.* **13**, 197–203 (2012).
- Wurzenberger, C. & Gerlich, D. W. Phosphatases: providing safe passage through mitotic exit. *Nat. Rev. Mol. Cell Biol.* **12**, 469–482 (2011).
- Juanes, M. A. *et al.* Budding yeast greatwall and endosulfines control activity and spatial regulation of PP2A^{Cdc55} for timely mitotic progression. *PLoS Genet.* **9**, e1003575 (2013).
- Rossio, V., Kazatskaya, A., Hirabayashi, M. & Yoshida, S. Comparative genetic analysis of PP2A-Cdc55 regulators in budding yeast. *Cell Cycle* **13**, 2073–2083 (2014).
- Cohen, R. & Engelberg, D. Commonly used *Saccharomyces cerevisiae* strains (e.g. BY4741, W303) are growth sensitive on synthetic complete medium due to poor leucine uptake. *FEMS Microbiol. Lett.* **273**, 239–243 (2007).
- Heitman, J., Movva, N. R. & Hall, M. N. Targets for cell cycle arrest by the immunosuppressant rapamycin in yeast. *Science* **253**, 905–909 (1991).
- Toone, W. M. *et al.* Rme1, a negative regulator of meiosis, is also a positive activator of G₁ cyclin gene expression. *EMBO J.* **14**, 5824–5832 (1995).
- De Virgilio, C. & Loewith, R. Cell growth control: little eukaryotes make big contributions. *Oncogene* **25**, 6392–6415 (2006).
- Jiang, Y. Regulation of the cell cycle by protein phosphatase 2A in *Saccharomyces cerevisiae*. *Mol. Biol. Cell.* **17**, 440–449 (2006).
- Verma, R. Phosphorylation of Sic1p by G₁ Cdk required for its degradation and entry into S phase. *Science* **278**, 455–460 (1997).
- Rossi, R. L., Zinzalla, V., Mastriani, A., Vanoni, M. & Alberghina, L. Subcellular localization of the cyclin dependent kinase inhibitor Sic1 is modulated by the carbon source in budding yeast. *Cell Cycle* **4**, 1798–1807 (2005).
- Escoté, X., Zapater, M., Clotet, J. & Posas, F. Hog1 mediates cell-cycle arrest in G₁ phase by the dual targeting of Sic1. *Nat. Cell Biol.* **6**, 997–1002 (2004).
- Soulard, A. *et al.* The rapamycin-sensitive phosphoproteome reveals that TOR controls protein kinase A toward some but not all substrates. *Mol. Biol. Cell* **21**, 3475–3486 (2010).
- Torres, J., Di Como, C. J., Herrero, E. & De La Torre-Ruiz, M. A. Regulation of the cell integrity pathway by rapamycin-sensitive TOR function in budding yeast. *J. Biol. Chem.* **277**, 43495–43504 (2002).
- Chu, I. M., Hengst, L. & Slingerland, J. M. The Cdk inhibitor p27 in human cancer: prognostic potential and relevance to anticancer therapy. *Nat. Rev. Cancer* **8**, 253–267 (2008).

41. Kushnirov, V. V. Rapid and reliable protein extraction from yeast. *Yeast* **16**, 857–860 (2000).
42. Kinoshita, E., Kinoshita-Kikuta, E., Takiyama, K. & Koike, T. Phosphate-binding tag, a new tool to visualize phosphorylated proteins. *Mol. Cell. Proteomics* **5**, 749–757 (2006).
43. Barberis, M. Sic1 as a timer of Clb cyclin waves in the yeast cell cycle—design principle of not just an inhibitor. *FEBS J.* **279**, 3386–3410 (2012).

Acknowledgements

We thank Séverine Bontron for strains, plasmids and discussions, and Louis-Félix Bersier for advice regarding statistical analyses. This research was supported by the Canton of Fribourg and grants from the Swiss National Science Foundation and the Novartis Foundation (C.D.V).

Author contributions

M.M.-T. designed and performed experiments. M.J. helped with experimental design and procedures. C.D.V. conceived and directed the project and wrote the manuscript. All authors discussed and interpreted the data together.

Additional information

Supplementary Information accompanies this paper at <http://www.nature.com/naturecommunications>

Competing financial interests: The authors declare no competing financial interests.

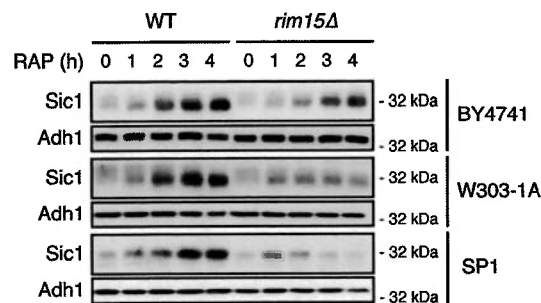
Reprints and permission information is available online at <http://npg.nature.com/reprintsandpermissions/>

How to cite this article: Moreno-Torres, M. *et al.* TORC1 controls G1–S cell cycle transition in yeast via Mpk1 and the greatwall kinase pathway. *Nat. Commun.* **6**:8256 doi: 10.1038/ncomms9256 (2015).

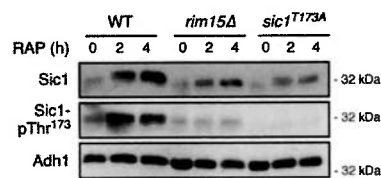


This work is licensed under a Creative Commons Attribution 4.0 International License. The images or other third party material in this article are included in the article's Creative Commons license, unless indicated otherwise in the credit line; if the material is not included under the Creative Commons license, users will need to obtain permission from the license holder to reproduce the material. To view a copy of this license, visit <http://creativecommons.org/licenses/by/4.0/>

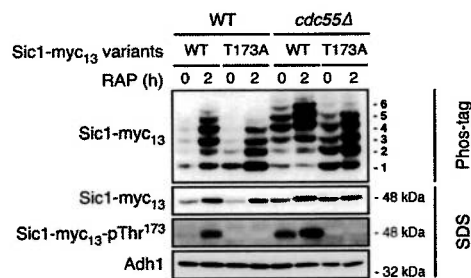
Supplementary Figures



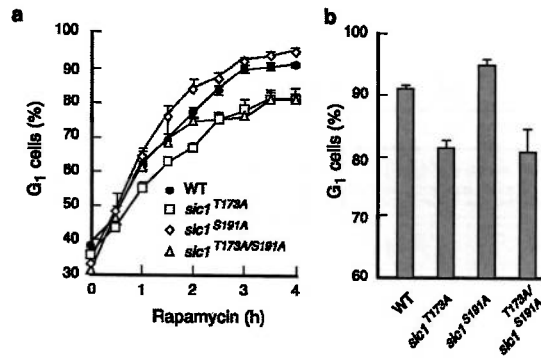
Supplementary Figure 1 | Rim15 ensures Sic1 accumulation following TORC1 inactivation independently of the yeast strain background. The levels of endogenous Sic1, in exponentially growing (0 h) and rapamycin-treated (RAP; 1-4 h) BY4741, W303-1A, and SP1 wild-type (WT) and respective isogenic *rim15Δ* mutant cells, were determined by immunoblot analyses using polyclonal anti-Sic1 antibodies. Adh1 levels served as loading controls.



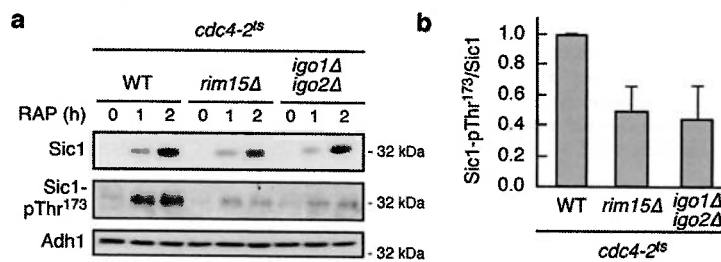
Supplementary Figure 2 | Mutation of Thr¹⁷³ to Ala in Sic1, like loss of Rim15, compromises normal Sic1 accumulation in rapamycin-treated cells. Sic1 levels and phosphorylation of Thr¹⁷³ in Sic1 (Sic1-pThr¹⁷³) were determined in exponentially growing (0 h) and rapamycin-treated (RAP; 2 and 4 h) cells with the indicated genotypes by immunoblot analyses using polyclonal anti-Sic1 and phosphospecific anti-Sic1-pThr¹⁷³ antibodies, respectively. Adh1 levels served as loading controls.



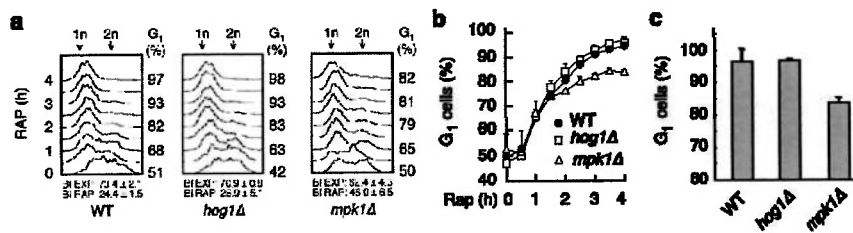
Supplementary Figure 3 | Phos-tag phosphate affinity gel electrophoresis analysis of genomically myc₁₃-tagged Sic1 or Sic1^{T173A}. Sic1-myc₁₃ or Sic1^{T173A}-myc₁₃ were analyzed by phos-tag phosphate affinity and SDS gel electrophoresis (followed by immunoblot analysis using anti-myc or anti-Sic1-pThr¹⁷³ antibodies) in extracts from exponentially growing (0 h) and rapamycin-treated (RAP; 2 h) WT and *cdc55Δ* strains. The 6 differentially phosphorylated Sic1-myc₁₃ isoforms are numbered sequentially from 1 to 6 (right side of the panels). Adh1 levels served as loading controls.



Supplementary Figure 4 | The Sic1^{T173A} allele compromises G₁ arrest in rapamycin-treated cells. (a) FACS analyses were performed in exponentially growing (0 h) and rapamycin-treated (times indicated) WT, *sic1*^{T173A}, *sic1*^{S191A}, and *sic1*^{T173A/S191A} cells. The experiments were performed independently 3 times for each strain (one representative FACS profile is shown in Fig. 2g) and the quantifications (means ± SD) of the percentage of G₁ cells in the respective populations are presented. (b) Bar graphs show the percentage of G₁ cells in the populations of rapamycin-treated (4 h) strains with the indicated genotypes with error bars indicating the 95% confidence interval. The data points from the 4-h rapamycin treatment were further used to perform an ANOVA analysis, which was followed by a Tukey's post-hoc test to examine the differences for each pair of strains. We found a highly significant difference among the four strains (ANOVA, p-value <0.001). Tukey's post-hoc test indicated that the values for WT and *sic1*^{S191A} cells were not significantly different from each other (p-value=0.133); similarly the values for *sic1*^{T173A} and *sic1*^{T173A/S191A} cells were also not significantly different from each other (p-value=0.97). All other pairwise comparisons were statistically significant (all p-values <0.001), showing that the values for WT and *sic1*^{S191A} cells significantly diverged from the ones of the *sic1*^{T173A} and *sic1*^{T173A/S191A} cells.



Supplementary Figure 5 | Inactivation of the SCF^{Cdc4} ubiquitin ligase suppresses the defect in Sic1 accumulation, but not in Sic1-Thr¹⁷³ phosphorylation, in rapamycin-treated *rim15Δ cdc4-2^{ts}* and *igo1Δ igo2Δ cdc4-2^{ts}* mutant cells. (a) Sic1 levels and phosphorylation of Thr¹⁷³ in Sic1 (Sic1-pThr¹⁷³) were determined by immunoblot analyses using polyclonal anti-Sic1 and phosphospecific anti-Sic1-pThr¹⁷³ antibodies, respectively. Cells (genotypes indicated) were pre-grown exponentially at 24°C (0 h) and then shifted to 37°C for 1 or 2 h (to inactivate Cdc4-2^{ts}) in the presence of rapamycin (RAP). Adh1 levels served as loading controls. The experiment was performed independently 3 times and one representative set of blots is shown. (b) Bars represent the ratio between the mean Sic1-pThr¹⁷³ levels and Sic1 protein levels (± SD; 3 independent experiments), determined in rapamycin-treated (2h at 37°C) *cdc4-2^{ts}*, *rim15Δ cdc4-2^{ts}*, and *igo1Δ igo2Δ cdc4-2^{ts}* cells and expressed relative to the value in *cdc4-2^{ts}* cells (set to 1.0).

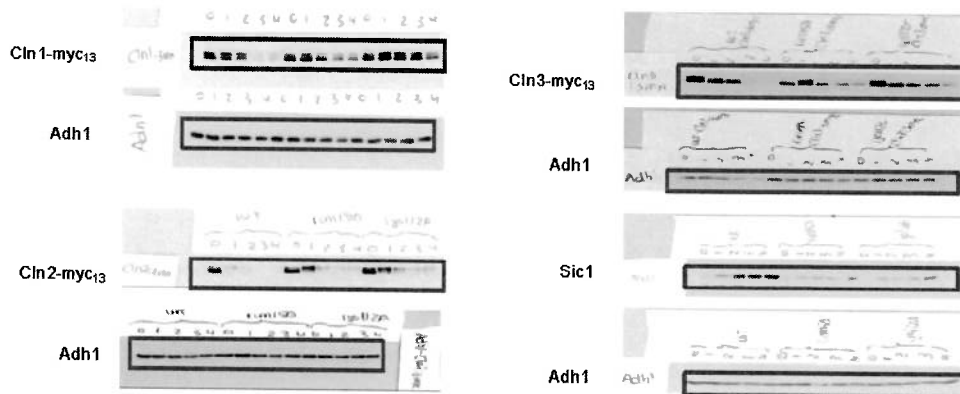


Supplementary Figure 6 | Loss of Mpk1, but not of Hog1, compromises timely G₁ arrest in rapamycin-treated cells. (a) FACS analyses were performed in exponentially growing (time 0 h) and rapamycin-treated (times indicated) WT, *hog1Δ*, and *mpk1Δ* cells. FACS and BI analyses were performed as in Fig. 1a. The experiments were performed independently 3 times for each strain (one representative FACS profile is shown). (b) Quantifications (means ± SD) of the percentage of G₁ cells in the respective populations in (a) are presented. (c) Bar graphs showing the percentage of G₁ cells in the populations of rapamycin-treated (4 h) strains with the indicated genotypes with error bars indicating the 95% confidence interval. The data points from the 4-h rapamycin treatment were further used to perform an ANOVA analysis, which was followed by a Tukey's post-hoc test to examine the differences for each pair of strains. We found a highly significant difference among the three strains (ANOVA, p-value <0.001). Tukey's post-hoc test indicated that the values for WT and *hog1Δ* cells were not significantly different from each other (p-value=0.53), but that the values for the *mpk1Δ* cells were significantly different from the other two strains (both p-values <0.002).

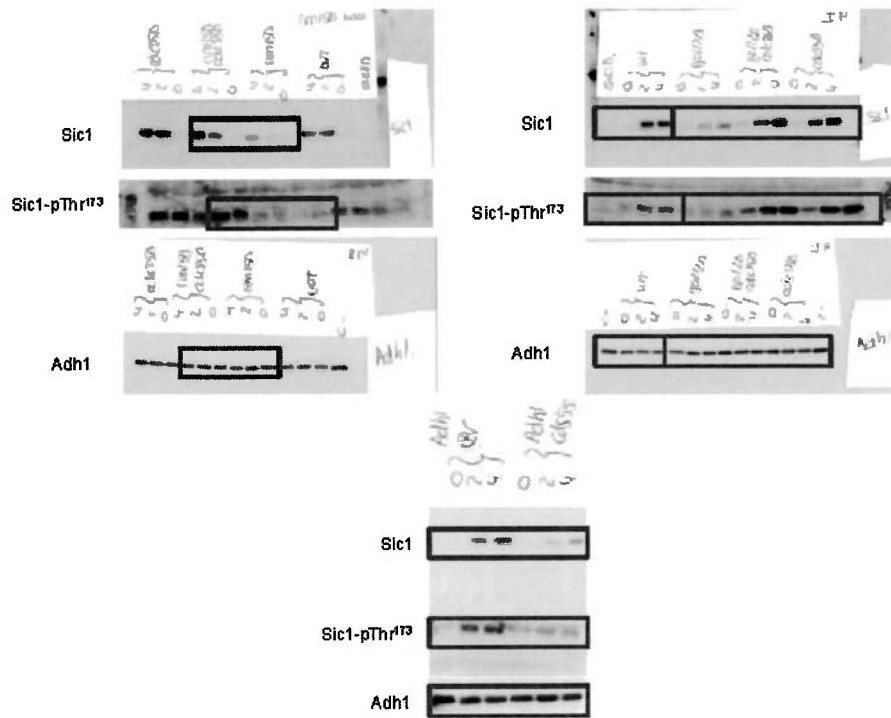
Supplementary Figures 7-25: Original Blots



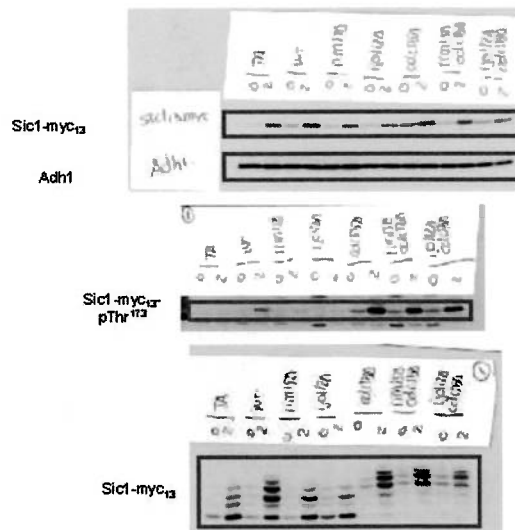
Supplementary Figure 7 | Full-sized scans of Northern blots in Figure 1e.



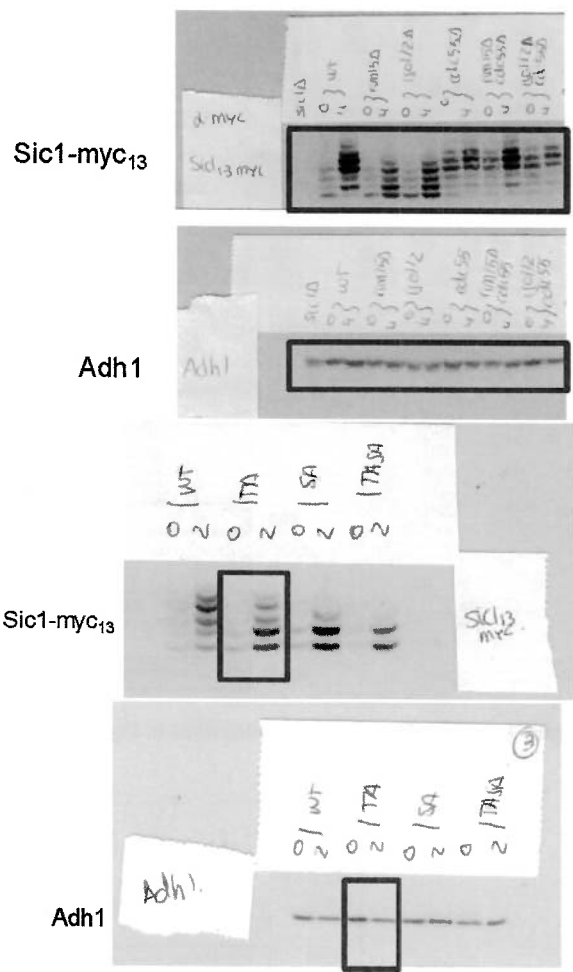
Supplementary Figure 8 | Full-sized scans of Western blots in Figure 1f.



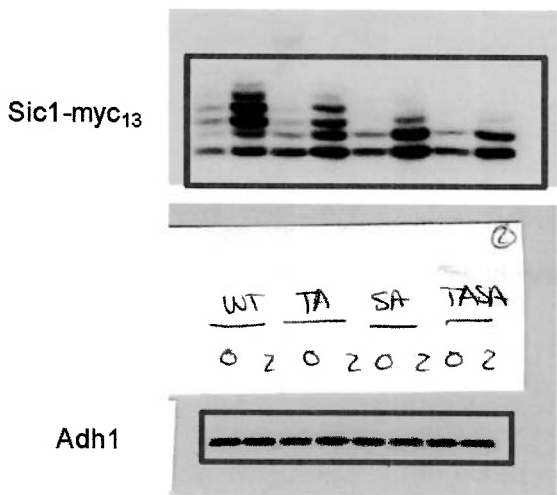
Supplementary Figure 9 | Full-sized scans of Western blots in Figure 2a.



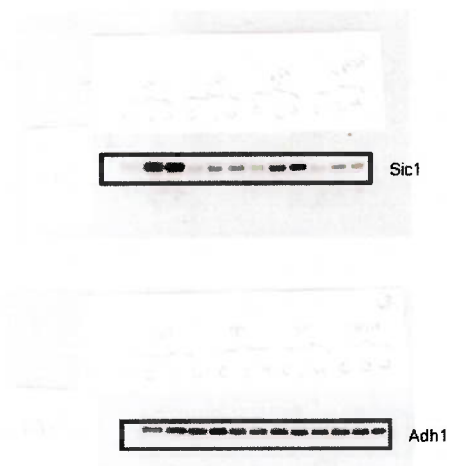
Supplementary Figure 10 | Full-sized scans of Western blots in Figure 2c.



Supplementary Figure 11 | Full-sized scans of Western blots in Figure 2d.



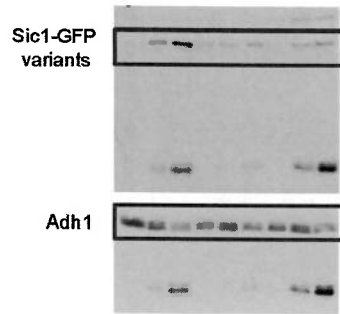
Supplementary Figure 12 | Full-sized scans of Western blots in Figure 2e.



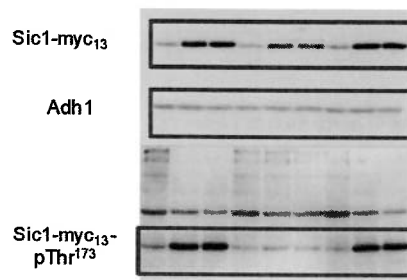
Supplementary Figure 13 | Full-sized scans of Western blots in Figure 2f.



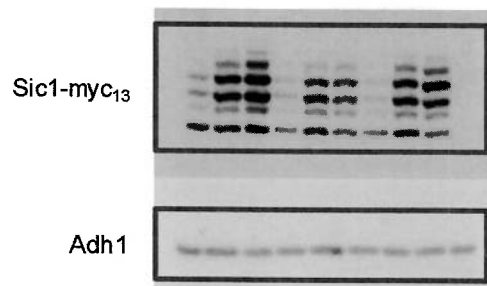
Supplementary Figure 14 | Full-sized scans of Western blots in Figure 3a.



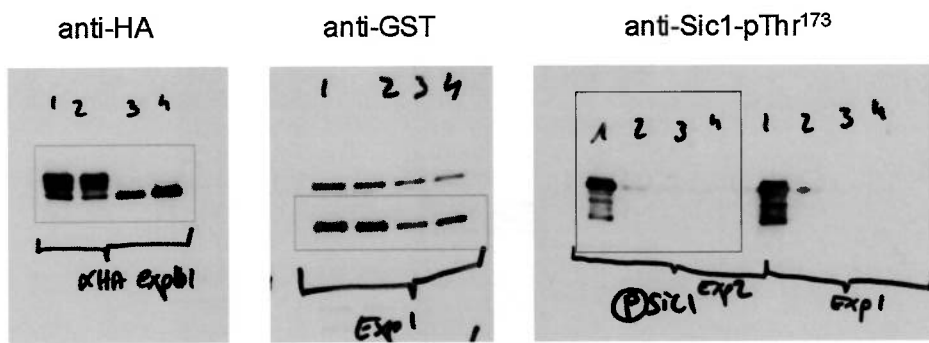
Supplementary Figure 15 | Full-sized scans of Western blots in Figure 3c.



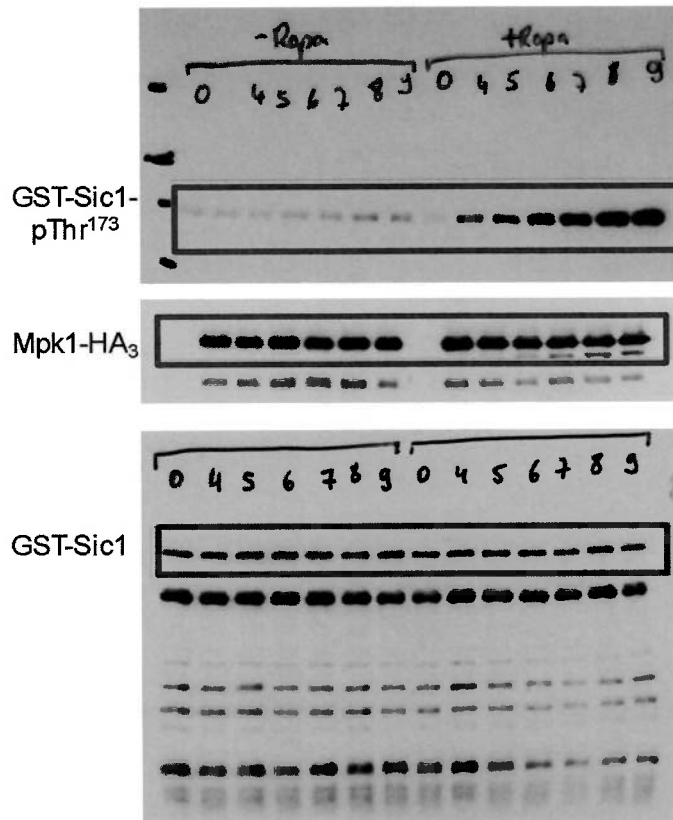
Supplementary Figure 16 | Full-sized scans of Western blots in Figure 4a.



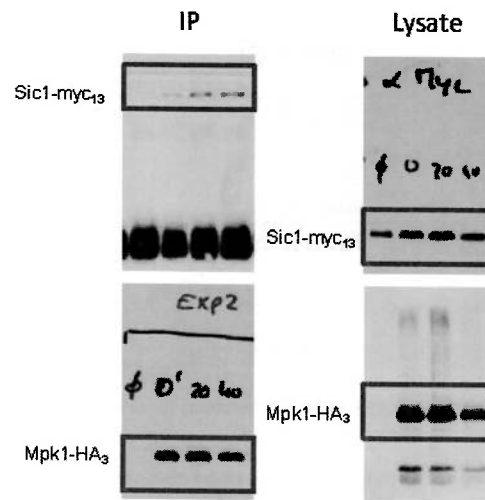
Supplementary Figure 17 | Full-sized scans of Western blots in Figure 4b.



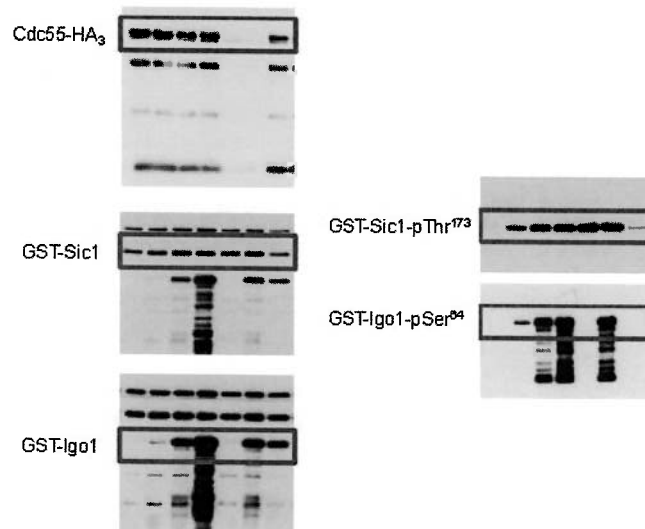
Supplementary Figure 18 | Full-sized scans of Western blots in Figure 4c.



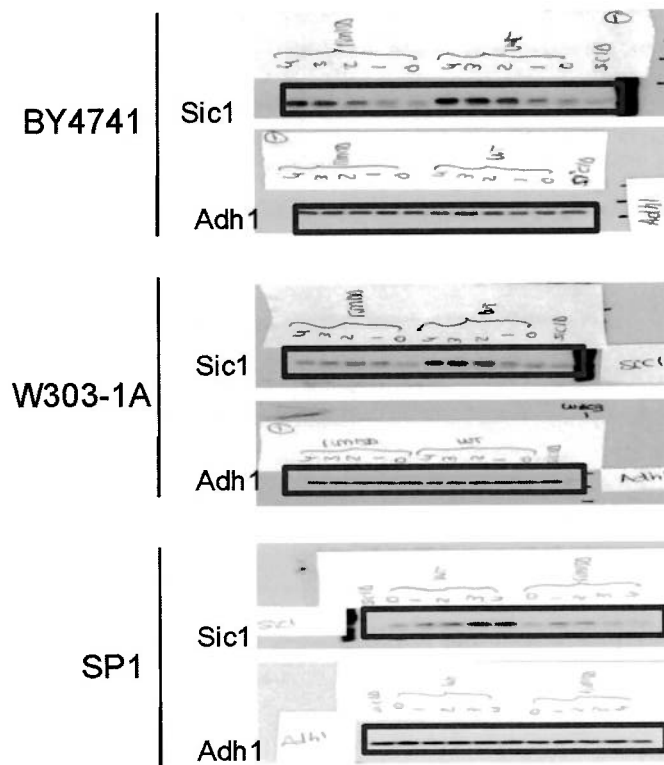
Supplementary Figure 19 | Full-sized scans of Western blots in Figure 4d.



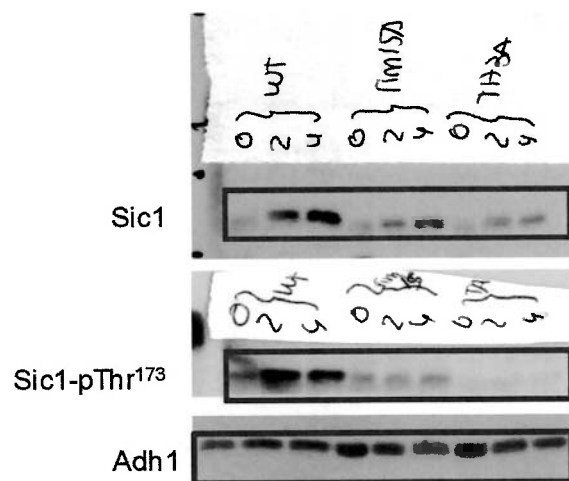
Supplementary Figure 20 | Full-sized scans of Western blots in Figure 4e.



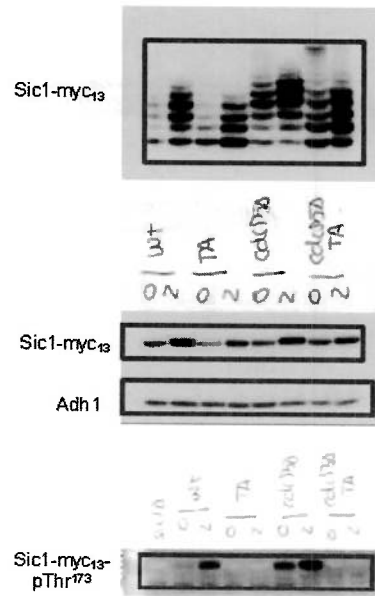
Supplementary Figure 21 | Full-sized scans of Western blots in Figure 5a.



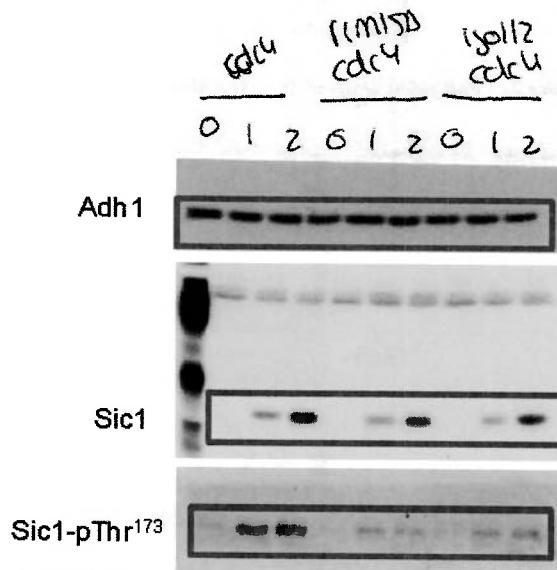
Supplementary Figure 22 | Full-sized scans of Western blots in Supplementary Figure 1.



Supplementary Figure 23 | Full-sized scans of Western blots in Supplementary Figure 2.



Supplementary Figure 24 | Full-sized scans of Western blots in Supplementary Figure 3.



Supplementary Figure 25 | Full-sized scans of Western blots in Supplementary Figure 5.

Supplementary Tables

Supplementary Table 1 | Strains Used in This Study.

Strain	Genotype	Source	Figure
BY4741	<i>MATa; his3Δ1, leu2Δ0, met15Δ0, ura3Δ0</i>	reference ¹	1a, S1
W303-1A	<i>MATa; ade2-1, trp1-1, can1-100, leu2-3,112, his3-11,15, ura3-1</i>		1a, S1
SP1	<i>MATa; leu2, his3, trp1, ade8, ura3, can1</i>	reference ²	1a, S1
JK9-3D	<i>MATa; leu2, his4, trp1, ura3, rme1, GAL,HMLa</i>	reference ³	1b,1d-f,1i, 2a-b, 2f-g, S2, S4, S6
YMM203	[SP1] <i>rim15Δ::kanMX</i>	this study	S1
YSB147	[BY4741] <i>rim15Δ::natMX, MET15</i>	reference ⁵	S1
CDV95-4A	[W303-1A] <i>rim15Δ::kanMX</i>	this study	S1
IP11	[JK9-3D] <i>rim15Δ::kanMX</i>	reference ⁴	1c-f, 1i, 2a, S2
YMM57-2A	[JK9-3D] <i>igo1Δ::natMX, igo2Δ::Hph-NT1</i>	this study	1c-f, 1i, 2a
YMM59	[JK9-3D] <i>CLN1-myc₁₃::kanMX</i>	this study	1f-g
YMM60	[JK9-3D] <i>CLN2-myc₁₃::kanMX</i>	this study	1f-g
YMM61	[JK9-3D] <i>CLN3-myc₁₃::kanMX</i>	this study	1f, 1h
YMM87-2D	[JK9-3D] <i>rim15Δ::kanMX, CLN1-myc₁₃::kanMX</i>	this study	1f-g
YMM88-12B	[JK9-3D] <i>rim15Δ::kanMX, CLN2-myc₁₃::kanMX</i>	this study	1f-g
YMM78-2A	[JK9-3D] <i>rim15Δ::kanMX, CLN3-myc₁₃::kanMX</i>	this study	1f, 1h
YMM85-5D	[JK9-3D] <i>igo1Δ::natMX, igo2Δ::Hph-NT1, CLN1-myc₁₃::kanMX</i>	this study	1f-g
YMM79-9A	[JK9-3D] <i>igo1Δ::natMX, igo2Δ::Hph-NT1, CLN2-myc₁₃::kanMX</i>	this study	1f-g
YMM80-5C	[JK9-3D] <i>igo1Δ::natMX, igo2Δ::Hph-NT1, CLN3-myc₁₃::kanMX</i>	this study	1f, 1h
YMM55-1C	[JK9-3D] <i>rim15Δ::kanMX, cdc55Δ::natMX</i>	this study	2a
YMM90-3D	[JK9-3D] <i>igo1Δ::natMX, igo2Δ::Hph-NT1, cdc55Δ::natMX</i>	this study	2a
YMM46	[JK9-3D] <i>cdc55Δ::natMX</i>	this study	2a, 5a
YMM98	[JK9-3D] <i>sic1^{T173A}-myc₁₃::kanMX, EMP46::natMX</i>	this study	2c-e, S3
YMM143-2A	[JK9-3D] <i>sic1^{T173A}-myc₁₃::kanMX, cdc55Δ::natMX, EMP46::natMX</i>	this study	S3
YMM63	[JK9-3D] <i>SIC1-myc₁₃::kanMX</i>	this study	2c-e, S3
YMM68-9D	[JK9-3D] <i>rim15Δ::kanMX, SIC1-myc₁₃::kanMX</i>	this study	2c-d
YMM70-6B	[JK9-3D] <i>igo1Δ::natMX, igo2Δ::Hph-NT1, SIC1-myc₁₃::kanMX</i>	this study	2c-d
YMM69-1C	[JK9-3D] <i>cdc55Δ::natMX, SIC1-myc₁₃::kanMX</i>	this study	2c-d, S3
YMM100-9D	[JK9-3D] <i>rim15Δ::kanMX, cdc55Δ::natMX, SIC1-myc₁₃::kanMX</i>	this study	2c-d
YMM96	[JK9-3D] <i>igo1Δ::natMX, igo2Δ::Hph-NT1, cdc55Δ::natMX, SIC1-myc₁₃::kanMX</i>	this study	2c-d
YMM91	[JK9-3D] <i>sic1^{T173A}, EMP46::natMX</i>	this study	2f-g, S2, S4
YMM101	[JK9-3D] <i>sic1^{S191A}, EMP46::natMX</i>	this study	2f-g, S4
YMM103	[JK9-3D] <i>sic1^{T173AS191A}, EMP46::natMX</i>	this study	2f-g, S4
YMM105	[JK9-3D] <i>sic1^{S191A}-myc₁₃::kanMX, EMP46::natMX</i>	this study	2e
YMM133	[JK9-3D] <i>sic1^{T173AS191A}-myc₁₃::kanMX, EMP46::natMX</i>	this study	2e
YMM114	[JK9-3D] <i>cdc4-2::kanMX</i>	this study	3a-b, S5
YMM117-3A	[JK9-3D] <i>rim15Δ::kanMX, cdc4-2::kanMX</i>	this study	3a-b, S5
YMM116-4A	[JK9-3D] <i>igo1Δ::natMX, igo2Δ::Hph-NT1, cdc4-2::kanMX</i>	this study	3a-b, S5
YMM118-2D	[JK9-3D] <i>sic1^{T173A}, EMP46::natMX, cdc4-2::kanMX</i>	this study	3a-b
YMM77	[JK9-3D] <i>SIC1-GFP(S65T)::kanMX</i>	this study	3c-d
YMM97-7B	[JK9-3D] <i>rim15Δ::kanMX, SIC1-GFP(S65T)::kanMX</i>	this study	3c
YMM99	[JK9-3D] <i>sic1^{T173A}-GFP(S65T)::kanMX</i>	this study	3c-d
YMM67-1C	[JK9-3D] <i>sic1Δ::kanMX</i>	this study	2a
YMM53	[JK9-3D] <i>mpk1Δ::kanMX</i>	this study	4c-f, S6
YMM65-2D	[JK9-3D] <i>mpk1Δ::kanMX, SIC1-myc₁₃::kanMX</i>	this study	4a-b
YMM204-14C	[JK9-3D] <i>hog1Δ::kanMX, SIC1-myc₁₃::kanMX</i>	this study	4a-b
YMM64-3C	[JK9-3D] <i>rim15Δ::kanMX, mpk1Δ::kanMX</i>	this study	4f
YMM111-2A	[JK9-3D] <i>igo1Δ::natMX, igo2Δ::Hph-NT1, mpk1Δ::kanMX</i>	this study	4f
YMM130	[JK9-3D] <i>hog1Δ::kanMX</i>	this study	S6

Supplementary Table 2 | Plasmids Used in This Study.

Plasmid	Genotype	Source	Figure
pRS416	<i>CEN/ARS, URA3</i>	reference ¹	1b
pMM5	[pRS416] <i>RME1</i>	this study	1b
p1308	[pRS414]	reference ¹	1d, 2d
p1309	[pRS415]	reference ¹	1d, 2d
p1310	[pRS416]	reference ¹	1d, 2d
pMM10	[pRS415] <i>HIS4</i>	this study	1d, 2d
pSB004	[pRS416] <i>ADH1p-CDC55</i>	reference ⁵	2a-b
p834	[pRS416] <i>ADH1p</i>	reference ⁶	2a-b
pMM6	[pRS416] <i>MPK1-HA₃</i>	this study	4c-e
pMM7	[pRS416] <i>mpk1^{K54R}-HA₃</i>	this study	4c
pMM8	pGEX- <i>SIC1</i>	this study	4c-d, 5a
pMM9	pGEX- <i>sic1^{T173A}</i>	this study	4c
pMJA2610	[pRS416] <i>CDC55-HA₃</i>	this study	5a
pCDV487	pHAC195- <i>GAL1-GST-RIM15, 2 μ, URA3</i>	reference ⁴	5a
pLC1092	pGEX- <i>IGO1</i>	reference ⁷	5a
pLC1134	pGEX- <i>igo1^{S64A}</i>	reference ⁷	5a

Supplementary References

1. Brachmann, C.B. *et al.* Designer deletion strains derived from *Saccharomyces cerevisiae* S288C: a useful set of strains and plasmids for PCR-mediated gene disruption and other applications. *Yeast* **14**, 115-132 (1998).
2. Toda, T. *et al.* In yeast, RAS proteins are controlling elements of adenylate cyclase. *Cell* **40**, 27-36 (1985).
3. Heitman, J., Movva, N.R. & Hall, M.N. Targets for cell cycle arrest by the immunosuppressant rapamycin in yeast. *Science* **253**, 905-909 (1991).
4. Pedruzzi, I. *et al.* TOR and PKA signaling pathways converge on the protein kinase Rim15 to control entry into G₀. *Mol. Cell* **12**, 1607-1613 (2003).
5. Bontron, S. *et al.* Yeast endosulfines control entry into quiescence and chronological life span by inhibiting protein phosphatase 2A. *Cell Rep* **3**, 16-22 (2013).
6. Mumberg, D., Müller, R. & Funk, M. Yeast vectors for the controlled expression of heterologous proteins in different genetic backgrounds. *Gene* **156**, 119-122 (1995).
7. Talarek, N. *et al.* Initiation of the TORC1-regulated G₀ program requires Igo1/2, which license specific mRNAs to evade degradation via the 5'-3' mRNA decay pathway. *Mol Cell* **38**, 345-355 (2010).

CHAPTER II:
***Regulatory mechanisms of Sic1
stabilization by Thr¹⁷³
phosphorylation***

2.1 Introduction

As stated in the previous chapter, the target of rapamycin complex 1 (TORC1) pathway couples cellular growth with proliferation in response to nutrient availability. TORC1 inhibition by rapamycin treatment or nitrogen starvation causes cells to arrest growth in the G1 phase of the cell cycle by controlling a dual mechanism: downregulation of the expression of G1 cyclins required for cyclin-dependent protein kinase activity (Barbet et al, 1996) and stabilization of the cyclin dependent kinase inhibitor Sic1 (Zinzalla et al, 2007). Stabilization of Sic1 under different stress conditions has been shown to be essential to prevent premature entry into the S-phase. In the case of hyperosmotic stress, cells arrest transiently in G1 to adapt metabolically and/or physiologically to this unfavorable condition and to avoid detrimental consequences such as for instance erroneous DNA replication (Escote et al, 2004). Upon nutrient deprivation, this arrest in G1 persists and cells enter into the G0 phase where they will remain until more favorable nutrient conditions may incite them to enter back again into a proliferative state.

Sic1 stabilization involves phosphorylation at Thr¹⁷³, which is favored by direct Mpk1-mediated phosphorylation and inhibition of PP2A^{Cdc55} as shown in Chapter I. However, the mechanism by which Thr¹⁷³ phosphorylation promotes Sic1 stability remains still elusive. Previous analyses showed that Sic1 has less affinity for the catalytic SCF^{Cdc4} subunit Cdc34 in rapamycin-treated cells (Zinzalla et al, 2007) and that the introduction of a phospho-mimetic glutamate at position 173 of Sic1 reduces its ability to bind Cdc4 in a yeast two-hybrid assay (Escote et al, 2004).

The results presented in Chapter I (Fig. 3a) showed that temperature-inactivation of the Cdc4-2^{ts} allele caused Sic1 accumulation and that the respective protein migrated on SDS-PAGE in at least two different bands, but at least three in the case of Sic1^{T173A}. The appearance of these distinct isoforms did not occur when cells were shifted to the non-permissive temperature concomitantly with rapamycin treatment, suggesting that the different bands might be a consequence of G1/S-Cdk1 dependent phosphorylation events on Sic1. This observation suggests that Sic1 phosphorylation at Thr¹⁷³ may not necessarily directly prevent its interaction with E3 ligases as it has been previously proposed (Escote et al, 2004; Zinzalla et al, 2007), but may instead play a role in the

inhibition of Cln/Clb-Cdk1 complexes. Such a mechanism could downregulate any remaining phosphorylation activity towards the N-terminal domain of Sic1 and, as a consequence, prevent SCF^{Cdc4} binding (and subsequent Sic1 degradation by proteolysis). In this chapter, I will describe a set of preliminary data that aim to address the mechanistic details of this process.

2.2 Results

2.2.1. Sic1 Thr¹⁷³ phosphorylation promotes binding to Cks1

To understand the regulatory mechanisms controlling Sic1 stability by Thr¹⁷³ phosphorylation, we decided to check whether this phosphorylation event affects binding of different Sic1 partners. For that purpose, Sic1-HA₃ and Sic1^{T173A}-HA₃ were immunoprecipitated from rapamycin-treated cells and samples were processed for mass spectrometry analyses. As a negative control, Lst7-HA₃, a subunit of the Lst4-Lst7 GTPase activating protein complex for Gtr2, was included (Peli-Gulli et al, 2015) (Fig. 2.1a). Among all the different partners identified, we found three proteins that did not interact with Lst7-HA₃ and presented stronger binding to Sic1-HA₃ than to Sic1^{T173A}-HA₃: the cyclin-dependent protein kinase regulatory subunit and adaptor Cks1, and the mitotic cyclins Clb3 and Clb4.

To validate these interactions, co-immunoprecipitation analyses were performed. Cks1 and Clb3 were genomically HA₃-tagged and Sic1 interaction was analyzed in the absence or presence of rapamycin. In exponentially growing cells, Sic1 strongly bound to Cks1 and this interaction was significantly boosted upon rapamycin treatment. However, only a weak interaction with Cks1 was observed for Sic1^{T173A} in exponentially growing cells that was barely detectable upon rapamycin treatment (Fig. 2.1.b). These results confirmed our mass spectrometry data for Cks1, but this was not the case for Clb3-HA₃, were no evident difference in binding of Clb3-HA₃ to Sic1 or Sic1^{T173A} was observed (data not shown).

Since Thr¹⁷³ phosphorylation seems to promote Cks1 binding to Sic1, we analyzed the interaction between Sic1 and Cks1 in the absence of key regulatory proteins involved in Thr¹⁷³ phosphorylation control: the protein phosphatase Cdc55 and the protein kinase

Mpk1. The Sic1 interaction with Cks1 was significantly increased in cells deleted for *CDC55* even in the absence of rapamycin (Fig. 2.1c,d). This increase was completely prevented in *cdc55Δ* mutant cells containing the Sic1^{T173A} allele (data not shown). On the contrary, no increase in Sic1 binding to Cks1 was observed upon rapamycin treatment in the absence of Mpk1 (Fig. 2.1c,d). From these results we conclude that Thr¹⁷³ phosphorylation promotes Sic1 binding to Cks1.

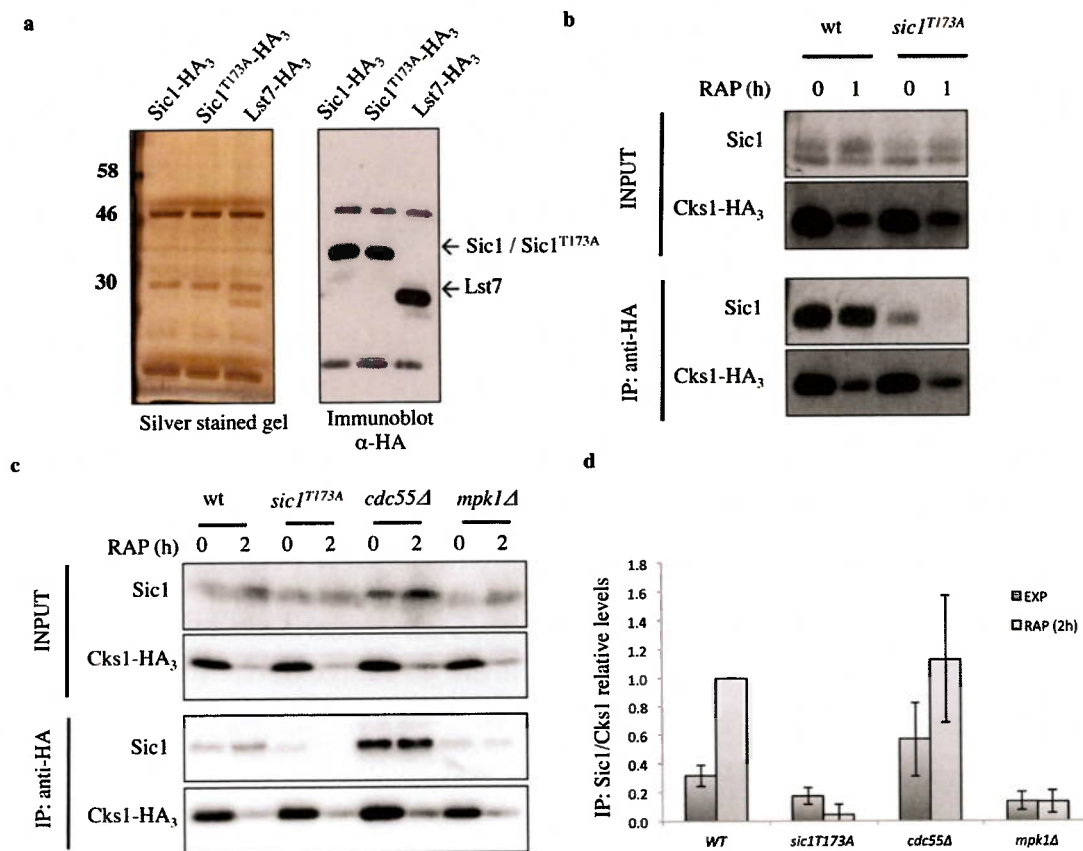


Figure 2.1. Phosphorylation of Sic1 at Thr¹⁷³ promotes its binding to Cks1. **(a)** Sic1-HA₃, Sic1^{T173A}-HA₃ and Lst7-HA₃ were immunoprecipitated from 18 mg of total protein extract from rapamycin treated WT and *sic1^{T173A}* cells. Approximately 10% of the IP was run on an SDS gel and Sic1-HA₃, Sic1^{T173A}-HA₃ and Lst7-HA₃ proteins were detected by silver staining and immunoblot analysis using monoclonal anti-HA antibodies. Samples were further analyzed by mass spectrometry. **(b)** Rapamycin treatment promotes the interaction between Cks1-HA₃ and Sic1. Genomically HA₃-tagged Cks1 was immunoprecipitated from extracts of untreated (RAP, 0 h) and rapamycin-treated (RAP, 1 or 2 h) WT, *sic1^{T173A}* **(b, c)**, *cdc55Δ*, and *mpk1Δ* **(c)** cells. The co-immunoprecipitated Sic1 levels were detected by immunoblot analysis using polyclonal anti-Sic1 antibodies. The experiments were performed independently three times (one representative blot is shown in **(c)**). **(d)** The co-immunoprecipitated Sic1 levels from **(c)** were normalized

to the immunoprecipitated Cks1-HA₃ in each case, calculated relative to the value in 2-h rapamycin-treated WT cells (set to 1.0), and expressed as mean values (n=3; ± s.d.).

Previous studies demonstrated that the phospho-adaptor subunit Cks1 provides processivity for the multiphosphorylation of Sic1 by Cln2/Clb5-Cdk1 (Koivomagi et al, 2011a), which promotes its degradation. According to these data, our results may seem contradictory since Cks1 strongly binds to the stable form of Sic1-pThr¹⁷³ whereas a weak interaction is observed with unstable Sic1^{T173A}. However, most of the studies performed on Sic1 multisite phosphorylation by Cln/Clb-Cdk1 have been performed *in vitro* where phosphorylation of Thr¹⁷³ was not considered. Since rapamycin treatment strongly increased Cks1 binding to Sic1 but not to Sic1^{T173A}, we hypothesized that this interaction may be important for Sic1 stability control.

To gain further insight into the mechanistic details of the impact of Cks1 on Sic1 stability, we examined whether Cks1 is able to interact with the region surrounding the p-Thr¹⁷³ or if this phosphorylation event plays an indirect role in regulating Cks1 binding to the N-terminal or C-terminal domains of Sic1. Co-immunoprecipitation analysis of Cks1-HA₃ with a series of truncated forms of Sic1-myc₁₃ and Sic1^{T173A}-myc₁₃ in exponentially growing and rapamycin-treated cells were performed (Fig. 2.2a,b). Full length Sic1-myc₁₃ and to a lower extent Sic1^{T173A}-myc₁₃, co-immunoprecipitated with Cks1-HA₃. As with the endogenous Sic1 form, rapamycin treatment increased the interaction between Sic1-myc₁₃ to Cks1-HA₃. However, no binding was observed for any of the Sic1-myc₁₃ and Sic1^{T173A}-myc₁₃ variants tested.

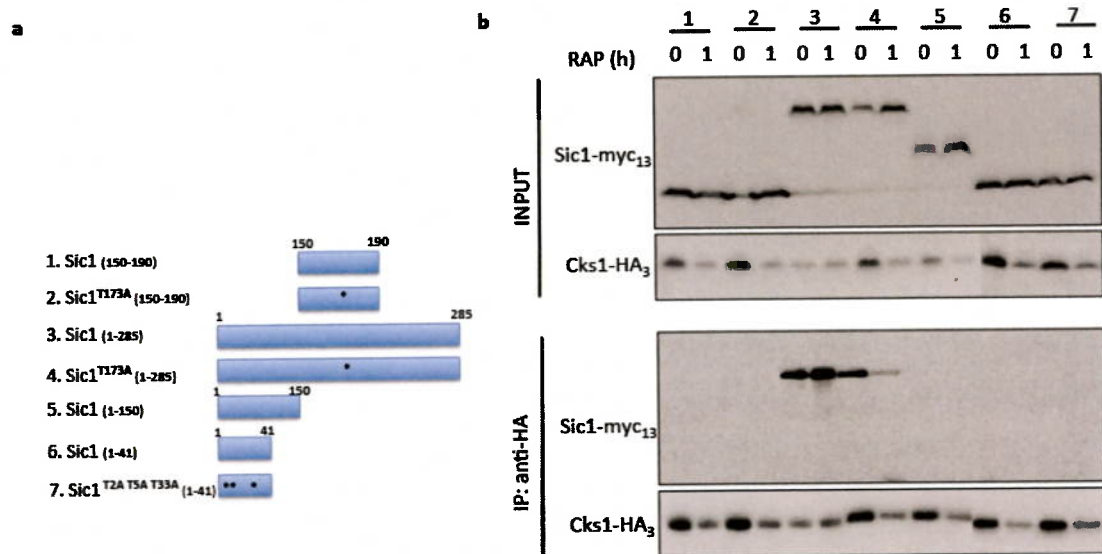


Figure 2.2. (a) Schematic representation of full length or truncated Sic1-myc₁₃ and Sic1^{T173A}-myc₁₃ variants. (b) Cks1-HA₃ co-immunoprecipitation analysis with plasmid-encoded Sic1-myc₁₃ and Sic1^{T173A}-myc₁₃ variants in exponentially growing (RAP, 0 h) and rapamycin-treated (RAP, 1 h) wild-type cells. Asterisks signal the presence of the indicated threonine to alanine substitutions. Cks1-HA₃ and Sic1-myc₁₃ variants were detected by immunoblot analysis using monoclonal anti-HA and anti-myc antibodies, respectively.

These results do not exclude the possibility that Cks1 binds to the pThr¹⁷³ residue since truncated Sic1-myc₁₃ and Sic1^{T173A}-myc₁₃ variants used may be too small to allow Cks1 binding, and potential additional regions like the Cdk1 inhibitory domain (215-285) may be required for the stabilization of this interaction. Therefore, new truncated versions of Sic1 were constructed from amino acids 150 to 285. Since plasmid-encoded expression under the control of the *ADH1* promoter of non-degradable forms of Sic1 variants (that lack Cdk1 phospho-sites at the N-terminal domain) containing the Cdk1 inhibitory domain (215-285) may be growth inhibitory, Sic1 versions with R262A and L264A inactivating mutations in the Cdk1 inhibitory domain were generated and included in the assay (Hodge & Mendenhall, 1999).

Preliminary results showed that Sic1-myc₁₃ truncations (150-285) co-immunoprecipitated with Cks1-HA₃ independently of the absence or presence of the inactivating alleles at the Cdk1 inhibitory domain. However, this interaction was completely lost in the variants containing the alanine substitution at Thr¹⁷³ (Fig. 2.3a,b,c).

Taken together, these results confirm that Sic1-pThr¹⁷³ is required for Cks1 binding to the C-terminal part of Sic1, independently of the N-terminal domain and the Cdk1 inhibitory activity.

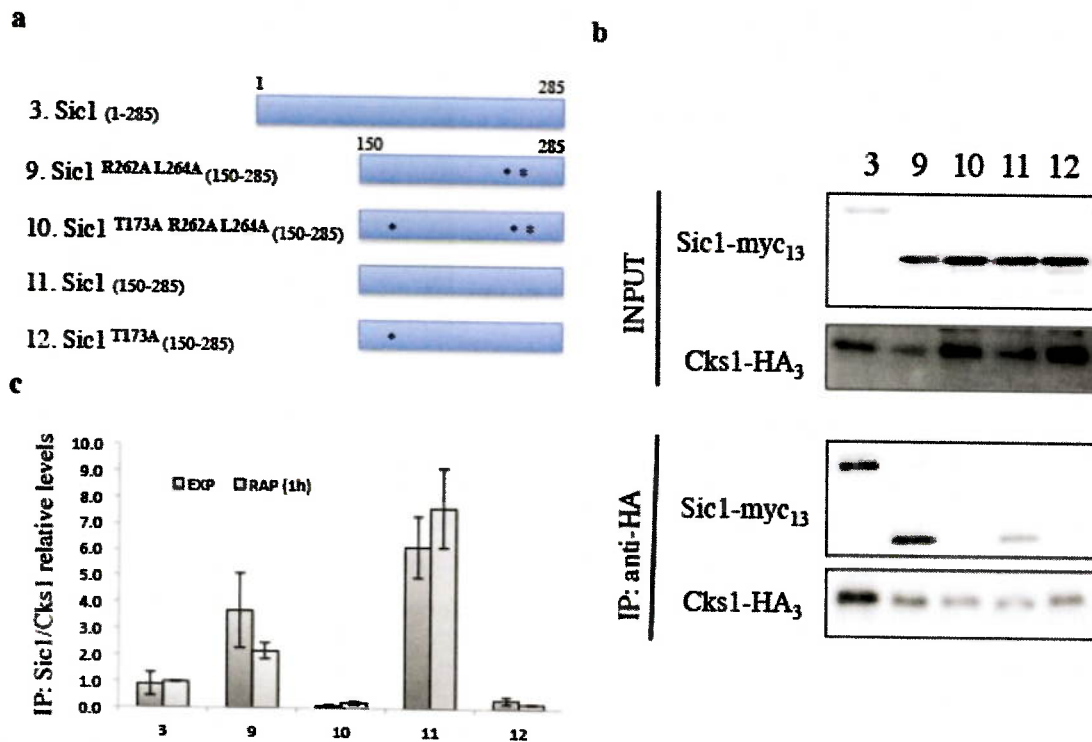


Figure 2.3. Sic1-pThr¹⁷³ is required for Cks1 binding to the C-terminal domain of Sic1. (a) Schematic representation of full length or truncated Sic1-myc₁₃ and Sic1^{T173A}-myc₁₃ variants. (b) Cks1-HA₃ co-immunoprecipitation analysis with plasmid-encoded Sic1-myc₁₃ and Sic1^{T173A}-myc₁₃ variants in rapamycin-treated (1 hour) wild-type cells. Asterisks signal the presence of the indicated threonine, arginine and/or leucine to alanine substitutions. Cks1-HA₃ and Sic1-myc₁₃ variants were detected by immunoblot analysis using monoclonal anti-HA and anti-myc antibodies, respectively. The experiments were performed independently two times (one representative blot is shown in (b)). (c) The co-immunoprecipitated Sic1 levels were normalized to the immunoprecipitated Cks1-HA₃ in each case, calculated relative to the value in 1-h rapamycin-treated wild-type cells (set to 1.0), and expressed as mean values (n=3; ± s.d.).

2.2.2. Sic1-Thr¹⁷³ phosphorylation prevents Cln/Clb-Cdk1-dependent multiphosphorylation of Sic1

To address if Thr¹⁷³ phosphorylation promotes Sic1 stability indirectly by preventing Cdk1-dependent phosphorylation events in the Sic1 N-terminal domain, we next examined whether expression (under the control of the constitutive *ADH1* promoter) of Sic1 myc₁₃-tagged mutant alleles carrying alanine substitutions in the CDK-target residues Thr², Thr⁵, Thr³³, Thr⁴⁵, Ser⁶⁹, Ser⁷⁶, and Ser⁸⁰, stabilized both Sic1 and Sic1^{T173A} in rapamycin-treated cells to the same extent. In control experiments, Sic1 and Sic1^{T173A}-myc₁₃ without alanine substitutions at the Cdk1 phosphorylation sites were also expressed (from the same construct plasmids). Unfortunately, plasmid-encoded Sic1 variants did not behave as the endogenous Sic1 and Sic1^{T173A} proteins. Sic1 expression was constitutive and no clear increase in Sic1 protein levels was observed upon rapamycin treatment. In addition, no difference in stability between Sic1-myc₁₃ and Sic1^{T173A}-myc₁₃ was observed (Fig. 2.4a,b). Since these control experiments did not work, no conclusion could be obtained from the N-terminal phospho-deficient forms. Therefore, further experiments will be performed, substituting the *ADH1* for the endogenous *SIC1* promoter and replacing myc₁₃ tag for a smaller one such as HA₃ that does not affect the stability of the protein.

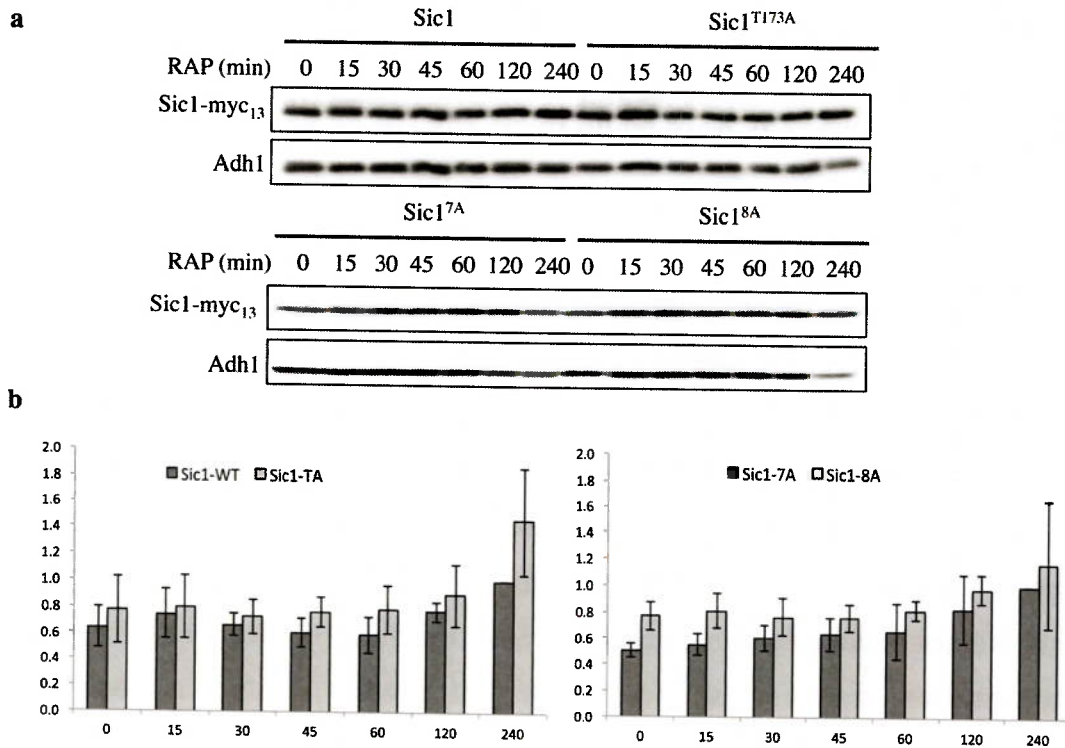


Figure 2.4. Analysis of protein stability of different Sic1 phospho-deficient mutants. (a) Levels of plasmid-encoded myc₁₃-tagged variants of Sic1, Sic1^{T173A}, Sic1^{7A} (T2A, T5A, T33A, T45A, S69A, S76, S80A) and Sic1^{8A} (T2A, T5A, T33A, T45A, S69A, S76, S80A, T173A) expressed under the *ADH1* promoter in exponentially growing (RAP; 0 min) and rapamycin-treated (RAP; 0-240 min) wild-type cells were determined by immunoblot analyses using polyclonal anti-myc antibodies. Adh1 levels served as loading controls. The experiments were performed independently three times (one representative blot is shown in (a)). **(b)** Sic1-myc₁₃ levels were normalized to the Adh1 levels in each case, calculated relative to the value in 4-h rapamycin-treated wild-type cells (set to 1.0), and expressed as mean values (n=3; ± s.d.).

As stated previously, temperature inactivation of Cdc4-2^{ts} (at 37°C) prompted the accumulation of Sic1 and Sic1^{T173A}, which migrated as several isoforms in SDS gels, with more abundant isoforms in the case of Sic1^{T173A}. To examine whether those bands correspond to different phosphorylation forms and whether Thr¹⁷³ phosphorylation impinges on the regulation of other Sic1 phosphorylation sites, we analyzed the migration pattern of Sic1 and Sic1^{T173A} by phosphate affinity gel electrophoresis in the absence and presence of rapamycin. In this assay, *cdc4-2^{ts}* and *cdc4-2^{ts} sic1^{T173A}* mutant cells were shifted for 3 hours at the non-permissive temperature (37°C) followed by rapamycin treatment. When analyzed in extracts of exponentially growing *cdc4-2^{ts}* mutant cells, Sic1 migrated as a slow-migrating isoform. Following rapamycin-

treatment, we observed a reduction in intensity of the slow-migrating isoform that correlated with the appearance of faster migrating isoforms that increased their intensity upon longer rapamycin treatment. Of note, although no clear difference of the Sic1/Sic1^{T173A} isoform patterns was observed in exponentially growing (3 hours at 37°C) *cdc4-2^{ts} sic1^{T173A}* in comparison with *cdc4-2^{ts}* mutant cells, the Sic1^{T173A} allele appeared to be strongly protected from the subsequent rapamycin-induced dephosphorylation that was observed in Sic1 (Fig. 2.5a). These results support a model in which Thr¹⁷³ phosphorylation promotes Sic1 stability by preventing most probably its Cln/Clb-Cdk1-dependent phosphorylation.

To further verify this assumption, we used phospho-specific antibodies against Thr⁵ and Thr³³ in Sic1, both residues previously described as priming sites for Cln/Clb-Cdk1-dependent phosphorylation (Koivomagi et al, 2011a). In control experiments, the specificity of the phospho-specific antibodies was assayed *in vivo* in wild-type cells expressing plasmid-encoded Sic1-myc₁₃ and Sic1^{7A}-myc₁₃ (with alanine substitutions in residues Thr², Thr⁵, Thr³³, Thr⁴⁵, Ser⁶⁹, Ser⁷⁶ and Ser⁸⁰). We identified both Sic1-pThr⁵ and Sic1-pThr³³ signals in wild-type cells expressing Sic1-myc₁₃, but not in Sic1^{7A}-myc₁₃, and both signals were strongly decreased upon rapamycin treatment (Fig. 2.5b).

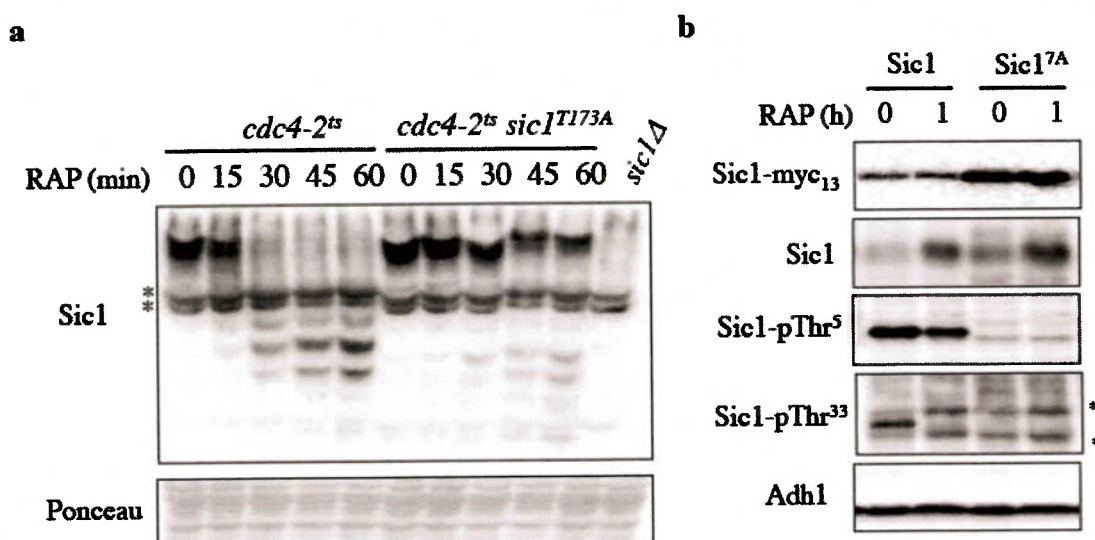


Figure 2.5. Thr¹⁷³ is required to protect Sic1 from other phosphorylation events in rapamycin-treated cells. (a) Phos-tag phosphate affinity gel electrophoresis analyses of Sic1 and Sic1^{T173A} in extracts from exponentially growing (RAP, 0 min; 3h at 37°C) and rapamycin-treated (RAP, 15-60 min) *cdc4-2^{ts}* and *cdc4-2^{ts} sic1^{T173A}* mutant cells. Sic1 signals were detected by immunoblot analyses using polyclonal

anti-Sic1 antibodies. Ponceau staining is shown as loading control. **(b)** Sic1-myc₁₃, Sic1, Sic1-pThr⁵ and Sic1-pThr³³ levels were determined by immunoblot analyses using monoclonal anti-myc and polyclonal anti-Sic1, and phospho-specific anti-Sic1-pThr⁵ and anti-Sic1-pThr³³, respectively, in extracts from wild-type cells expressing Sic1-myc₁₃ and Sic1^{7A}-myc₁₃ under the *ADH1* promoter. Adh1 levels served as loading control. Asterisks indicate two unspecific bands.

To address the possibility that phosphorylation of Thr¹⁷³ in Sic1 may serve to protect Sic1 from Cln/Clb-Cdk1-mediated phosphorylation we analyzed Sic1-pThr⁵ and Sic1-pThr³³ levels in *cdc4-2^{ts}* and *cdc4-2^{ts} sic1^{T173A}* strains during exponential growth at non-permissive temperature (37°C) (Fig. 2.6) followed by rapamycin treatment (Fig. 2.6). In agreement with previous results, temperature inactivation of Cdc4-2^{ts} during 3 hours caused Sic1 accumulation in *cdc4-2^{ts}* and *cdc4-2^{ts} sic1^{T173A}* cells with different phosphorylated isoforms (Fig. 2.6). When the levels of Sic1-pThr⁵ were analyzed upon rapamycin treatment, there was no difference in intensity but in the migration pattern in the two strains. The mobility of the band highlighted with anti-Sic1-pThr⁵ antibodies decreasing after rapamycin treatment in *cdc4-2^{ts}*, but not in *cdc4-2^{ts} sic1^{T173A}* cells. This suggests that the Thr¹⁷³ phosphorylation may not directly impinge on Sic1-pThr⁵ levels but on other Sic1 phosphorylation sites. Interestingly, Sic1-pThr³³ resulted to be one such site since a clear reduction was observed in Sic1-pThr³³ levels after rapamycin treatment in *cdc4-2^{ts}* cells that was strongly delayed in *cdc4-2^{ts} sic1^{T173A}* cells (Fig. 2.6). These results show that Sic1-pThr¹⁷³ prevents Cdk1-dependent phosphorylations, such as the one at Thr³³ and possibly others.

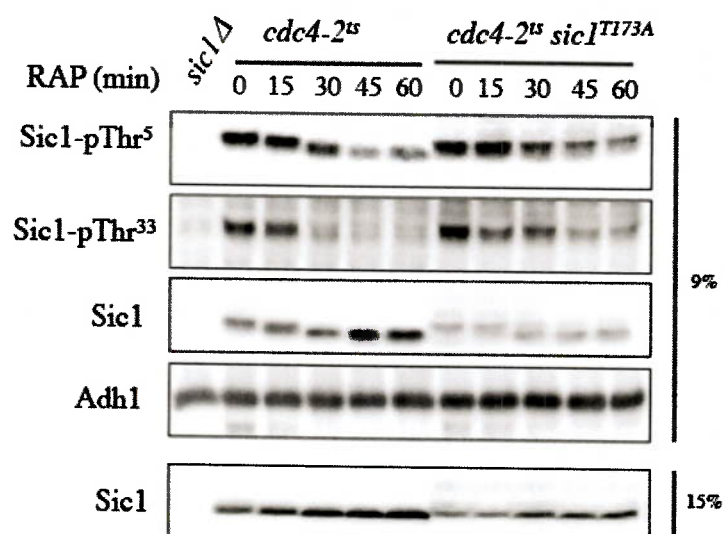


Figure 2.6. Thr¹⁷³ phosphorylation protects Sic1 from Cdk1-dependent phosphorylation. Sic1, Sic1-pThr⁵ and Sic1-pThr³³ levels were determined by immunoblot analyses using polyclonal anti-Sic1 and phospho-specific anti-Sic1-pThr⁵ and anti-Sic1-pThr³³, respectively, in extracts from exponentially growing (RAP, 0 h (3 hours 37°C) and rapamycin-treated (RAP, 15-60 min) *cdc4-2^{ts}* and *cdc4-2^{ts} sic1^{T173A}* cells. Adh1 levels served as loading control. 9% and 15% indicates the percentage of polyacrylamide of the gels.

To exclude the possibility that Sic1-Thr¹⁷³ phosphorylation affects Cdk1 dependent phosphorylation on Sic1 indirectly by controlling cyclin levels, we examined genomically HA₃-tagged Clb5 in *cdc4-2^{ts}* and *cdc4-2^{ts} sic1^{T173A}* cells (Fig. 2.7). In control experiments, we confirmed that these new strains behaved as the Clb5 non-tagged ones, with Sic1 and even more Sic1^{T173A} migrating as multiple phospho-isoforms when analyzed in cells grown at non-permissive temperature (Fig. 2.7a). Following rapamycin treatment, Clb5-HA₃ levels decreased to the same extent in *cdc4-2^{ts}* and *cdc4-2^{ts} sic1^{T173A}* cells, indicating that the higher Sic1-pThr³³ levels in *cdc4-2^{ts} sic1^{T173A}* (see above) are not an indirect consequence of increased Clb5 levels (Fig. 2.7b). Whether the Thr¹⁷³ phosphorylation is important for the Cdk1 inhibitory activity of Sic1 itself remains to be addressed in further experiments.

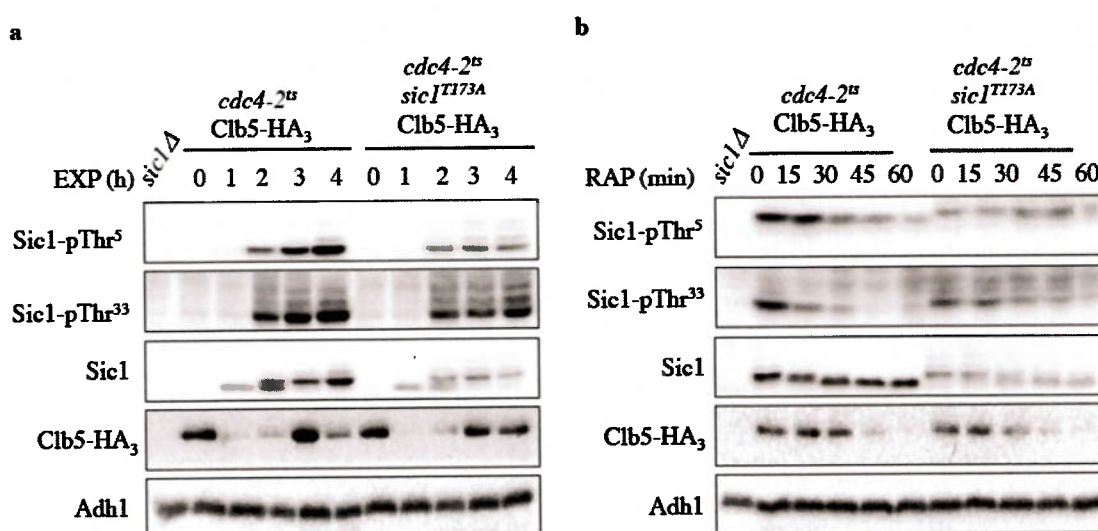


Figure 2.7. Mutation of Thr¹⁷³ in Sic1 does not affect Clb5 levels. (a) Cells (genotypes indicated) were pre-grown exponentially at 24°C (EXP, 0 h) and then grown up to 4 h at the non-permissive temperature 37°C (EXP, 1-4 h) or (b) were pre-grown exponentially at 37°C for 3 hours (RAP, 0 min)

followed by rapamycin treatment for up to 60 minutes (RAP, 15-60 min). **(a, b)** Samples were taken at the indicated time points. Clb5-HA₃, Sic1, Sic1-pThr⁵ and Sic1-pThr³³ levels were determined by immunoblot analyses using monoclonal anti-HA and polyclonal anti-Sic1 and phospho-specific anti-Sic1-pThr⁵ and anti-Sic1-pThr³³, respectively. Adh1 levels served as loading control.

2.3 Discussion

The involvement of the TORC1 pathway and of its targets in linking nutrient sensing to cell cycle progression has been previously described in this manuscript. One of the molecular mechanisms by which TORC1 leads to G1 arrest upon rapamycin treatment is by controlling Sic1-Thr¹⁷³ phosphorylation levels (Moreno-Torres et al, 2015; Zinzalla et al, 2007). Upon TORC1-inactivating conditions, cells expressing the Sic1^{T173A} mutant protein show strongly reduced Sic1 accumulation in comparison with wild-type cells and do not arrest properly in the G1 phase, an essential requirement to maintain high viability under stress conditions or nutrient depletion (Escote et al, 2004; Zinzalla et al, 2007).

The novelty of the results presented in this chapter lies in the evidence that the phosphorylation of Sic1 at Thr¹⁷³ upon rapamycin treatment protects Sic1 from Cln/Clb-Cdk1 dependent phosphorylation, thereby preventing SCF^{Cdc4} mediated ubiquitination and subsequent proteolysis. This finding explains previous data demonstrating that rapamycin treatment decreases the interaction between Sic1 with the catalytic SCF^{Cdc4} subunit Cdc34 (Zinzalla et al, 2007) and that binding to SCF^{Cdc4} was reduced in the Sic1^{T173E} allele when compared with wild-type Sic1 in a two-hybrid analysis (Escote et al, 2004).

Despite the insight provided by the presented results, many questions still need to be answered. Several results-driven hypotheses will be hereafter discussed.

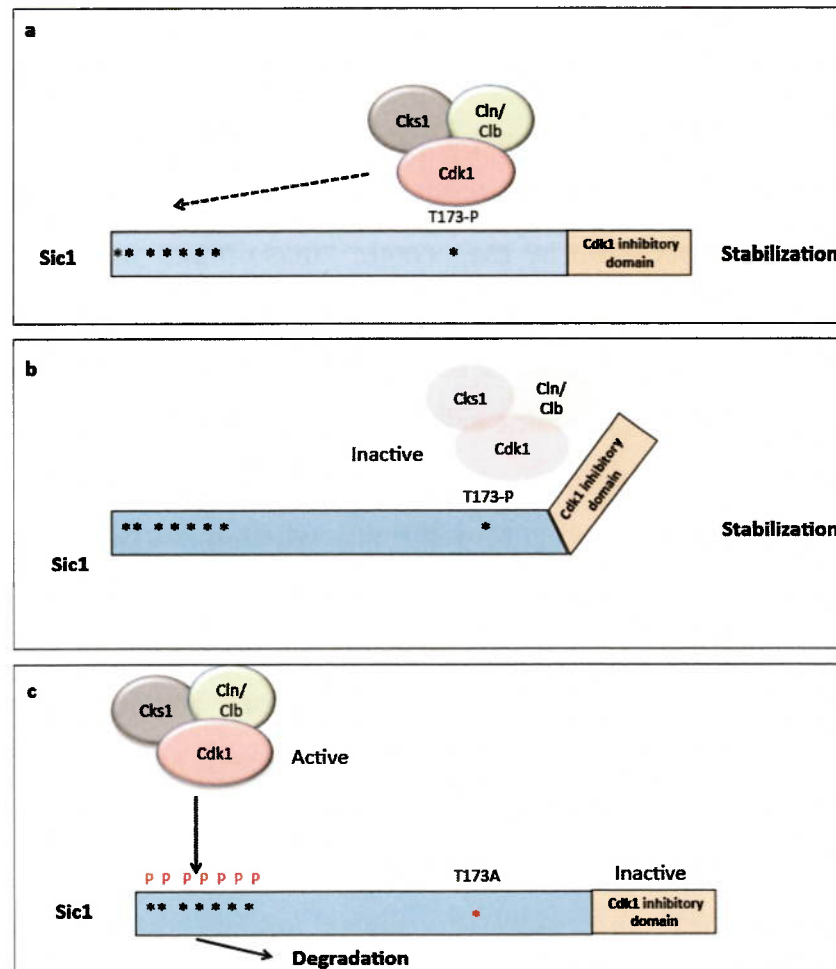


Figure 3.8. Schematic representation of the three putative models. For details see text.

Three different possibilities are listed here. (a) Sic1-pThr¹⁷³ recruits Cks1-Cln/Clb-Cdk1 complexes, thereby preventing the phosphorylation of the Cdk1-phosphosites at the Sic1 N-terminal domain. (b) Sic1-pThr¹⁷³ promotes Cks1-Cln/Clb-Cdk1 complex binding to the Thr¹⁷³ region and/or to the Cdk1 inhibitory domain, resulting in Cdk1 activity inhibition by the Cdk1 inhibitory domain. We hypothesize that under these specific conditions of Thr¹⁷³ phosphorylation, Sic1 might be able to inhibit not only Clb-Cdk1 complexes as it has so far been described (Schwob et al, 1994), but also Cln-Cdk1 ones. (c) Sic1-pThr¹⁷³ is itself important for the Sic1 inhibitory activity towards S-Cdk1 complexes. This possibility seems unlikely since it was previously described that cyclin-dependent kinase inhibitory domain is contained within the C-terminal 70 amino acids (215-286) (Hodge & Mendenhall, 1999).

Currently, we are addressing experimentally the suggested hypotheses. First, we will perform *in vitro* assays of the kinase activity of Cln2-HA₃-Cdk1 and Clb5-HA₃-Cdk1 towards the substrate Sic1 and Histone 1 (H1) in the presence of ATP or [γ -³²P] ATP. The cyclin-dependent kinase inhibitor Sic1, Sic1^{T173A}, Sic1^{T173E}, Sic1^{T173D} and Sic1 following prior phosphorylation by the protein kinase Mpk1 will be included in the assay. The inactive Cdk1 inhibitor Sic1^{R262A/L264A} will be used as a negative control. The *in vitro* kinase activity of Cln/Clb-Cdk1 complexes will be evaluated by separating the proteins on SDS/PAGE polyacrylamide gels and detecting the Sic1 phosphorylation with Sic1-pThr⁵ and Sic1-pThr³³ antibodies, and H1 phosphorylation by autoradiography. These experiments should allow us to determine whether the Sic1-pThr¹⁷³ residue is important for the Cdk1 inhibitory activity of Sic1 and if Sic1 is able to inhibit not only S-Cdk1 but also G1-Cdk1 complexes when phosphorylated at Thr¹⁷³.

If Sic1-pThr¹⁷³ is required for full Cdk1 inhibitory activity of Sic1, inefficient inhibition of Cdk1 complexes in *sic1*^{T173A} cells should result in increased levels of Sic1-free active Clb-Cdk1 complexes that would be able to promote Sic1 multiphosphorylation and degradation. This issue will be addressed by studying differently tagged Sic1 and Sic1^{T173A} alleles within diploid cells. If Thr¹⁷³ phosphorylation prompts Sic1 stability by promoting its Cdk1 inhibitory activity, the inefficient inhibition of Sic1^{T173A} towards S-Cdk1 complexes should affect similarly both tagged Sic1 alleles in a diploid cell and therefore they should be equally stable. If Thr¹⁷³ phosphorylation controls Sic1 stability independently of the Cdk1 inhibitory activity, there should be differences in the stability between Sic1 and Sic1^{T173A} alleles in diploid cells, and the introduction of the Cdk1 inhibitory inactive allele (Sic1^{R262A/L264A}) should not affect on Sic1 stability.

Taken together, these experiments will allow us to gain further insight into the mechanism by which phosphorylation of Thr¹⁷³ protects Sic1 from Cdk1-dependent multiphosphorylation, promoting its stability to block the activity of Clb-Cdk1 complexes (and maybe also Cln-Cdk1 complexes) upon nutrient stress.

Interestingly, as stated in the previous chapter, Sic1 is functionally and structurally related to the mammalian Cki p27^{Kip1} (Barberis et al, 2005a). Similar to Sic1, p27 phosphorylation controls binding to cyclin-CDK complexes that is important for CDK inhibition and for p27 turnover. In quiescent G0 cells, phosphorylation of Ser¹⁰

promotes p27 stability (Besson et al, 2006; Chu et al, 2008). The levels of p27^{S10A} protein have an accelerated turnover in G0 compared with wild-type p27, and mutation of Ser¹⁰ to Alanine or Glutamine destabilizes or stabilizes p27, respectively. However the mechanistic details of how Ser¹⁰ phosphorylation promotes p27 stability remain elusive. One hypothesis is that dephosphorylation of Ser¹⁰ promotes the assembly of heterotrimeric p27-cyclin-CDK complexes, thereby promoting p27 degradation. Alternatively, Ser¹⁰ phosphorylation may control the interaction of p27 with other proteins in quiescent cells that may regulate its interactions with cyclin-CDK complexes. One last hypothesis is that Ser¹⁰ phosphorylation directly affects the rate of degradation of p27 within cyclin-CDK complexes, by interfering with its recognition by an E3 ubiquitin ligase (Besson et al, 2006). Since the mechanisms leading to rapamycin-mediated G1 arrest may be conserved among eukaryotes and since misregulation of p27 is involved in tumor progression, it would be of great relevance to study whether the mechanisms described here for the regulation of Sic1 stability are also conserved in higher eukaryotes.

CHAPTER III:
***TORC1 controls G1 cyclins via the
greatwall kinase pathway***

3.1. Introduction

Previous studies implicated TORC1 in coordinating cell cycle at START with nutrient availability by controlling G1 cyclin transcription (Barbet et al, 1996). The mechanism by which TORC1 downregulates G1 cyclins is not completely understood, but it was suggested that G1 cyclin downregulation upon TORC1 inactivation is just a direct consequence of decreased translation initiation rates (Barbet et al, 1996). However, the data presented in Chapter I (Fig. 1e-h) show that the downregulation of G1 cyclin transcripts following rapamycin treatment depends partially on Rim15 and Igo1/2. This suggests that the TORC1-greatwall kinase pathway may also be implicated in the regulation of G1 cyclin transcription (or transcript stability). Accordingly, the Rim15-Igo1/2-PP2A^{Cdc55} signaling branch may ensure robust G1 arrest by exerting a dual role at START, namely by stabilizing Sic1 (via phosphorylation of Sic1-Thr¹⁷³; see chapter I) and by contributing to swift downregulation of G1 cyclin transcription (see chapter I). The main goal of the studies presented in this chapter is to identify the regulatory mechanism by which the Rim15-Igo1/2-PP2A^{Cdc55} signaling branch may impinge on G1/S transcriptional regulators.

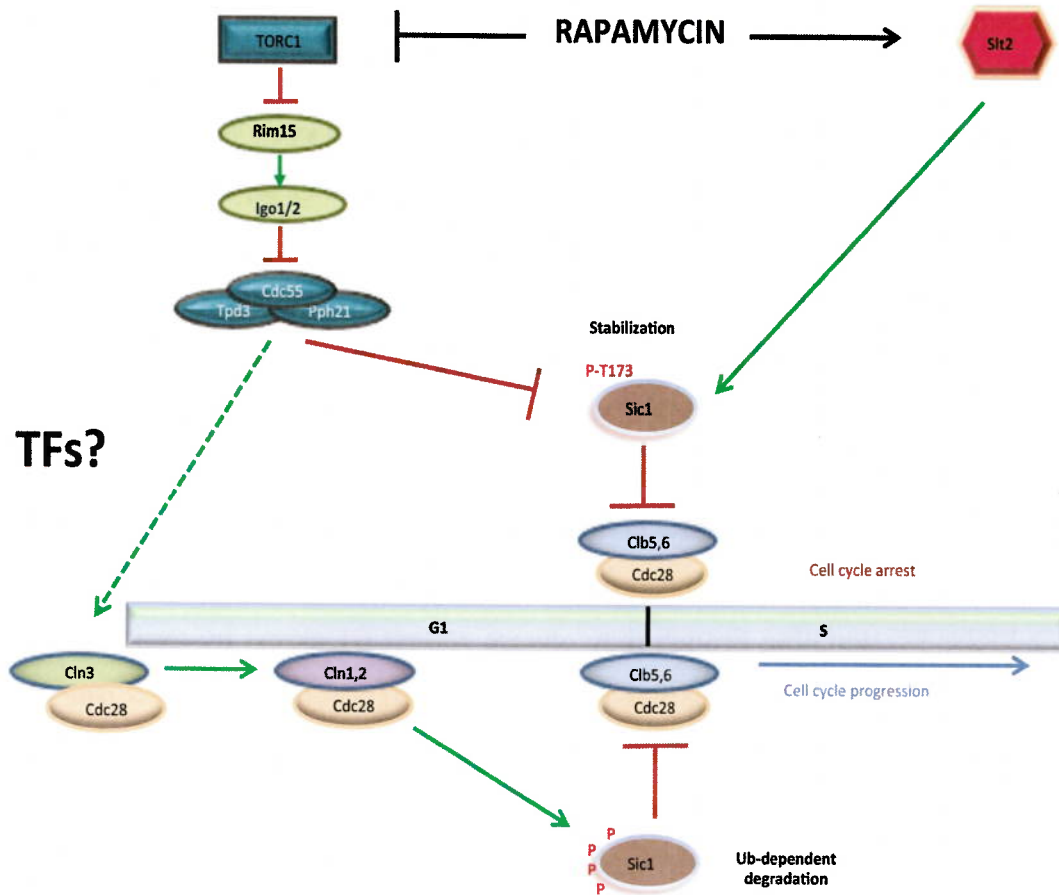


Figure 3.1. Model for a putative dual role of the greatwall kinase pathway in controlling G1/S transition. The Rim15-Igo1/2-PP2A^{Cdc55} pathway regulates G1/S cell cycle transition via its effects on Sic1 stability and potentially by contributing to downregulation of G1 cyclin transcription via a control of specific transcription factors (TFs). Arrows and bars denote positive and negative interactions. Solid arrows and bars refer to direct interactions, the dashed bar refers to potential interaction.

In order to understand whether and how Rim15-Igo1/2 affects G1 cyclin transcription, we decided to test whether several proteins involved in transcription of G1-specific genes were properly regulated (in terms of protein and phosphorylation levels) in rapamycin-treated *rim15Δ* and *igo1/2Δ* cells. Two transcription factor complexes are mainly responsible for transcription of G1-specific genes: the Swi4 cell cycle box binding factor (SBF) and the MluI cell cycle binding factor (MBF). SBF and MBF are composed of the DNA binding proteins Swi4 and Mbp1, respectively, and Swi6 that is shared between both complexes.

The SBF transcription factor is inhibited early in G1 by the transcriptional repressor Whi5, which is recruited to G1/S specific promoters via its interaction with SBF (de

Bruin et al, 2004). In late G1, phosphorylation of Whi5 by Cln3-Cdk1 leads to its dissociation from SBF and drives it out of the nucleus. The role of Whi5 in cell cycle control, like the one of mammalian pRb, is to repress G1-specific transcription in early G1 until its inactivation by Cln3-Cdk1 in late G1. At the end of mitosis, elimination of Cdk1 activity allows the entry of Whi5 back into the nucleus to repress transcription of the G1/S genes in the next cell cycle (Costanzo et al, 2004; de Bruin et al, 2004). In addition to SBF and MBF, several other proteins have also been found to participate in the regulation of G1-specific transcription. These include for instance Stb1, which binds to both SBF and MBF via Swi6 during the G1 phase (de Bruin et al, 2008). Whether Stb1 acts mainly as repressor or activator of SBF/MBF during the G1 phase is currently a matter of debate (Costanzo et al, 2003; de Bruin et al, 2008; Ho et al, 1999). Another factor is Nrm1, the levels of which increase as cell progress into the late G1 phase. This is likely due to the fact that Nmr1 is specifically protected from Cdh1-mediated degradation when cells exit mitosis (Ostapenko & Solomon, 2005; Ubersax et al, 2003). In contrast to Whi5 that acts early in G1 to inhibit SBF, Nmr1 assists MBF in repressing transcription as cells exit the G1 phase and progress into the S phase. Of note, expression of *NMR1* is also regulated by MBF as part of a negative feedback loop.

In addition to Whi5, Stb1 and Nrm1, the orthologous Msa1 and Msa2 proteins were also identified as SBF- and MBF-interactors, respectively. Their expression is cell cycle regulated with mRNA levels peaking in late M/early G1 and respective protein levels in early G1 (similarly as Cln3). Association of Msa1 with its target promoters increases during G1 phase and contributes to transcription of G1-specific genes (Ashe et al, 2008; Costanzo et al, 2003; de Bruin et al, 2006; Li et al, 2008; van der Felden et al, 2014). Finally, the Swi4/Mbp1 family transcription factor Xbp1 is also involved in transcriptional repression of specific cyclin-encoding genes (*e.g.*, *CLN1*, *CLN3*, *CLB1/2*, and *CLB5*) following exposure of cells to different stress conditions including nutrient starvation (Mai & Breeden, 1997; Miled et al, 2001; Miles et al, 2013). *XBP1* expression is regulated by the stress-responsive transcription factors Msn2/4 and is hence strongly induced under a variety of stress conditions.

In a first approach to analyze the potential role of the greatwall kinase pathway in regulating some of the transcription factors introduced above, we genomically tagged Xbp1, Msa1, Msa2, Whi5, Stb1, and Nmr1 and assessed the corresponding mRNA and/or

protein levels in exponentially growing and rapamycin-treated wild-type, *rim15Δ*, and *igo1/2Δ* cells.

3.2 Results

3.2.1. The greatwall kinase pathway regulates *XBP1* mRNA and Xbp1 protein levels

We started by analyzing the protein levels of myc₁₃-tagged Xbp1 in rapamycin treated and nitrogen-starved cells. Wild-type cells had significantly higher Xbp1 levels than *rim15Δ* and *igo1/2Δ* cells both before and after rapamycin treatment and rapamycin treatment did not significantly affect the Xbp1 levels in any of the strains during the first hour of rapamycin treatment (Fig. 3.2a). Interestingly, we observed that Xbp1 levels strongly increased in wild-type cells after nitrogen depletion, which was not observed in the case of cells deleted for *RIM15* or *IGO1/2* (Fig. 3.2b).

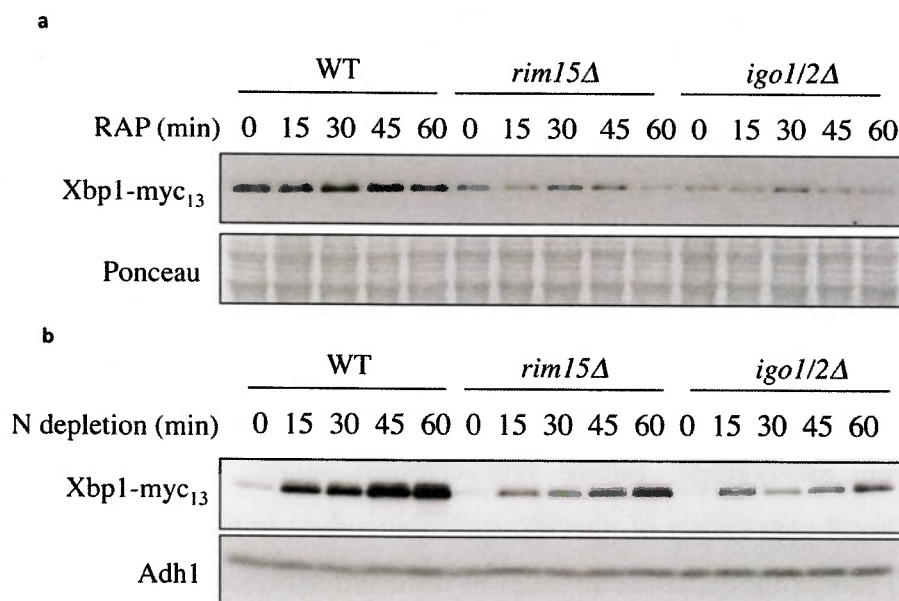


Figure 3.2. Rim15-Igo1/2 control Xbp1 protein levels. Xbp1-myc₁₃ levels were determined after rapamycin treatment (RAP) **(a)** and nitrogen depletion (N depletion) **(b)** by immunoblot analysis using polyclonal anti-myc antibodies at the indicated time points. Relevant genotypes are shown. Ponceau membrane staining and Adh1 levels served as loading controls.

In order to address whether the defect observed in the *rim15Δ* and *igo1/2Δ* cells was a consequence of higher PP2A^{Cdc55} activity in these strains, we combined these mutants with the deletion of *CDC55*. Of note, cells were then treated with rapamycin for up to 4 hours (since these were the conditions in which we observed complete depletion of G1 cyclin transcripts). Following prolonged rapamycin treatment, Xbp1-myc₁₃ levels also significantly increased in wild-type cells, but not in *rim15Δ* or *igo1/2Δ* cells. Interestingly, loss of Cdc55 not only resulted in higher constitutive Xbp1-myc₁₃ levels, but also fully rescued the Xbp1-myc₁₃ induction defect in both rapamycin treated *rim15Δ* (Fig. 3.3a,b) and *igo1/2Δ* (Fig. 3.3c,d) cells.

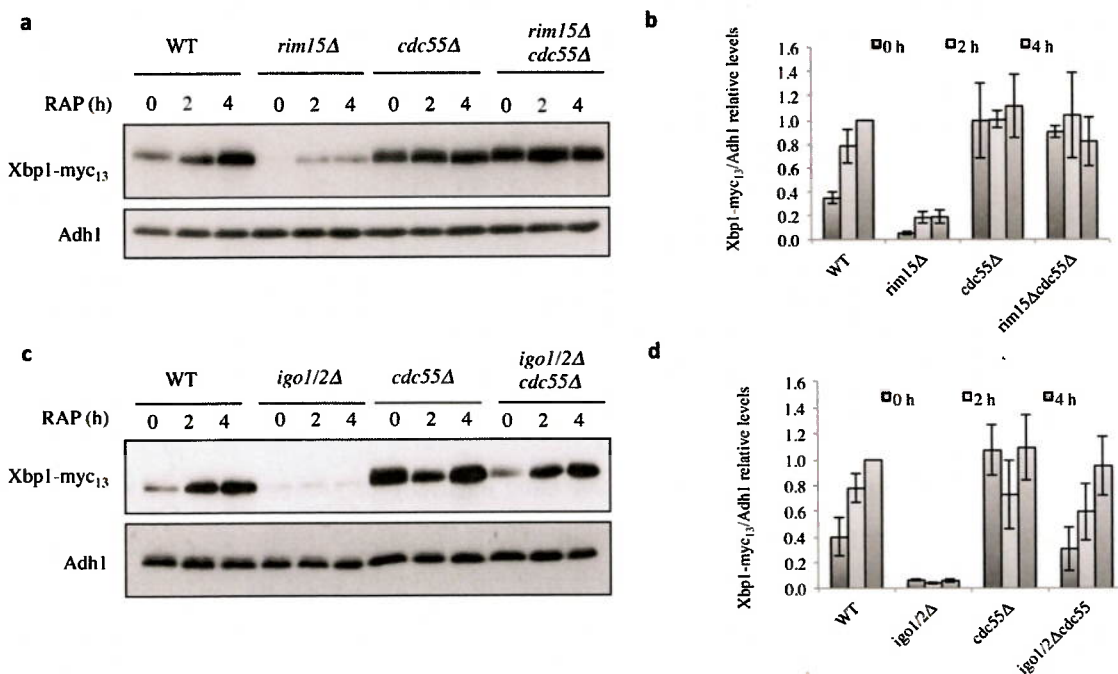


Figure 3.3. Loss of Cdc55 suppresses the defect of rapamycin-treated Xbp1 accumulation in *rim15Δ* and *igo1/2Δ* cells. (a,c) Xbp1-myc₁₃ levels were determined after rapamycin treatment (RAP; 0-4 h) by immunoblot analyses using polyclonal anti-myc antibodies. Genotypes of strains are indicated. The experiments were performed independently three times (one representative blot is shown). Adh1 levels served as loading control. (b, d) The respective Xbp1-myc₁₃ levels were normalized to the Adh1 levels in each case and calculated relative to the value in 4-h rapamycin treatment wild-type cells (set to 1.0). Each bar represents the mean \pm s.d. of three independent experiments.

To address whether Cdc55 regulates Xbp1 levels at the transcriptional or post-transcriptional level, we performed qRT-PCR analysis in rapamycin treated or nitrogen

starved wild-type, *rim15Δ*, and *igo1/2Δ*. Under both conditions, *XBP1* mRNA levels were highly induced in wild-type cells, while *rim15Δ* and *igo1/2Δ* cells were strongly or at least partially defective in *XBP1* mRNA induction following rapamycin treatment or nitrogen starvation, respectively, unless they were additionally deleted for *CDC55* (Fig. 3.4a,b). As observed for Xbp1-myc₁₃ levels (Fig. 3.3a,c), loss of Cdc55 alone also caused a constitutive increase of *XBP1* mRNA levels, independently of the presence or absence of Rim15 and Igo1/2 (Fig. 3.4a,b). It appears therefore that the Rim15-Igo1/2 play a significant role in favoring *XBP1* transcription (or transcript stability) specifically in rapamycin-treated cells.

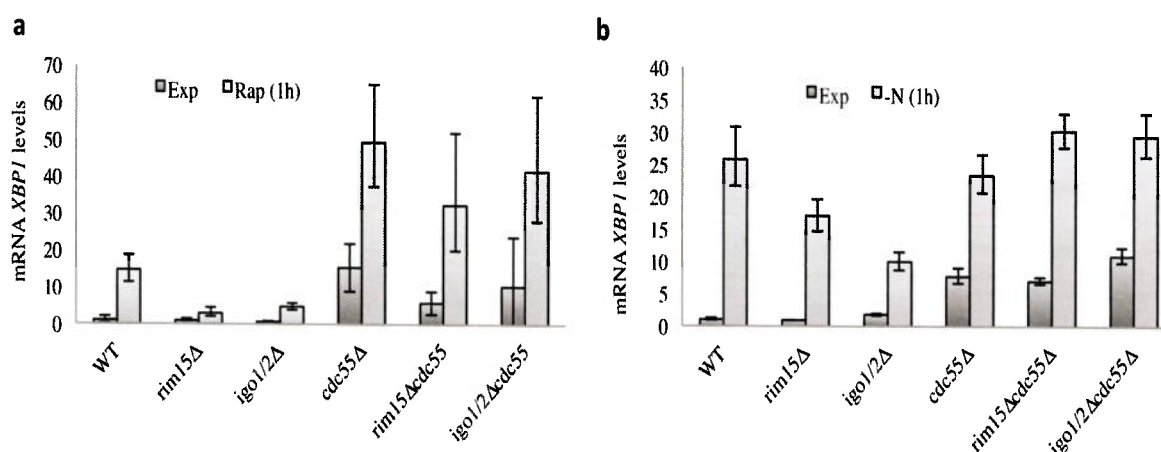


Figure 3.4. The Rim15-Igo1/2-PP2A^{Cdc55} signaling pathway regulates *XBP1* mRNA levels. qRT-PCR analyses of *XBP1* expression in rapamycin-treated (RAP, 1h) (a) or nitrogen starved (-N, 1h) (b) cells. The value for the reference sample (exponentially growing wild-type cells) was normalized to 1.0. Each bar represents the mean \pm s.d. of three experiments. Strains genotypes are indicated.

The defect of *rim15Δ* and *igo1/2Δ* cells in rapamycin or nitrogen starvation-induced G1 arrest may be partially due to lower levels of the G1 cyclin transcriptional repressor Xbp1 in these mutants. To test this hypothesis we overexpressed *XBP1* in *rim15Δ* and *igo1/2Δ* cells and studied whether this could overcome to a certain extent the G1 arrest defect following rapamycin treatment. To this end, we constructed a plasmid that expresses Xbp1-HA₃ under the control of the constitutive *ADH1* promoter. We transformed wild-type, *rim15Δ* and *igo1/2Δ* cells with either the empty vector or with the pADH1p-*XBP1*-HA₃ plasmid. While the latter plasmid appeared to drive strong expression of the fusion protein in exponentially growing cells, it was, unfortunately,

not competent to do so in rapamycin-treated cells (Fig. 3.5a). Not surprisingly, the respective plasmid was also not able to suppress the G1 arrest defect in rapamycin-treated *rim15Δ* and *igo1/2Δ* cells (Fig 3.5b). Notably, we found that the Xbp1-HA₃ levels expressed from the pADH1p-XBP1-HA₃ plasmid were overall significantly lower in the absence of Rim15 or Igo1/2, suggesting that Rim15 and Igo1/2 may play a role in controlling Xbp1 protein or XBP1 mRNA stability under the applied conditions. Consistent with this assumption, re-introduction of plasmid-encoded RIM15 or IGO1 partially reverted the observed effects on Xbp1-HA₃ levels in *rim15Δ* or *igo1/2Δ* cells, respectively (Fig. 3.5a).

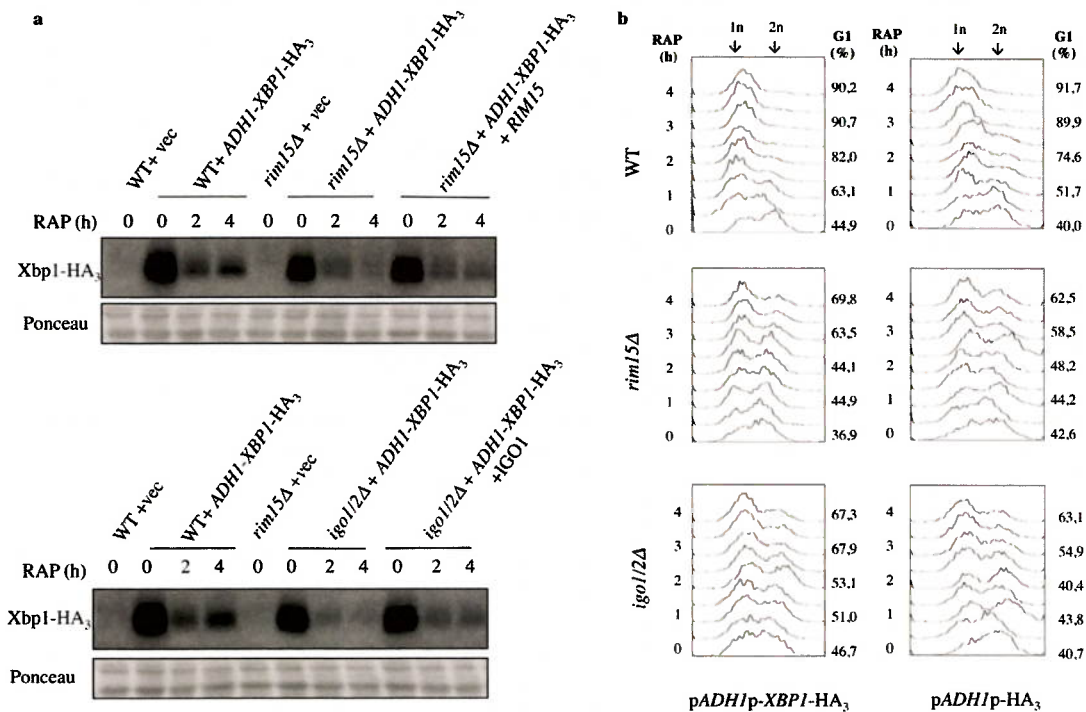


Figure 3.5. Rim15-Igo1/2 likely control Xbp1 protein stability. (a) Xbp1-HA₃ levels were determined by immunoblot analysis using polyclonal anti-HA antibodies. Overexpression of plasmid-encoded XBP1-HA₃ under the control of the ADH1 promoter did neither drive overproduction of Xbp1-HA₃ in rapamycin-treated cells (a), nor suppress the G1 arrest defect in *rim15Δ* and *igo1/2Δ* cells after rapamycin treatment (b). Fluorescence-activated cell sorting (FACS) analysis of the DNA content of wild-type, *rim15Δ* and *igo1/2Δ* cells transformed with pADH1p-HA₃ or pADH1p-XBP1-HA₃ treated for the indicated times with rapamycin are presented (one representative experiment shown from three independent ones). Populations of cells contain both 1n (G1; left-hand peak) and 2n (G2/M; right-hand peak) DNA. The relative level of cells with 1n DNA content is indicated on the right of the graphs (G1; (%)).

Since our first attempt to overproduce Xbp1 was not successful, we decided to change the *ADH1* promoter for the *UBI4* promoter that normally drives Ubi4 expression in nutrient-starved cells. The respective new plasmid (*pUBI4-XBP1-HA₃*) appeared to ensure high-level expression of Xbp1-HA₃ in rapamycin-treated wild-type cells, but the corresponding levels in *rim15Δ* and *igo1/2Δ* cells were still significantly lower when compared to the ones in wild-type cells (Fig. 3.6a). Therefore, not surprisingly, the *pUBI4-XBP1-HA₃* plasmid was also not able to suppress the G1 arrest defect in rapamycin-treated *rim15Δ* and *igo1/2Δ* cells (Fig. 3.6b). Combined with our data presented in Fig. 3.4, these studies corroborate the idea that Rim15 and Igo1/2 promote both Xbp1 protein (or *XBP1* mRNA) stability and *XBP1* transcription (in its wild-type promoter context).

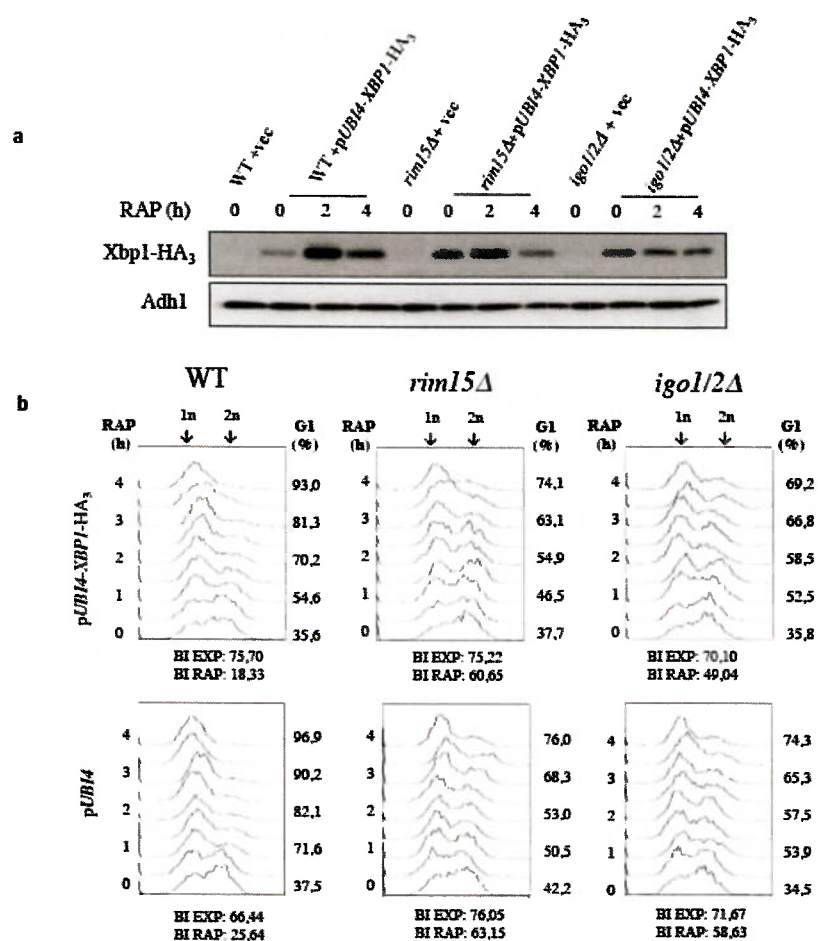


Figure 3.6. Expression of plasmid-encoded *XPB1* from the *UBI4* promoter does not rescue the defect in G1 arrest in rapamycin *rim15Δ* and *igo1/2Δ* cells. (a) Xbp1-HA₃ levels were determined in cells with the indicated genotype before (0h) and following rapamycin treatment (RAP; 2-4h) by immunoblot analysis using polyclonal anti-HA antibodies. (b) FACS analyses of the DNA content of wild-type, *rim15Δ* and *igo1/2Δ* cells transformed with *pUBI4p* or *pUBI4p-XPB1-HA₃* treated for the indicated times with rapamycin are shown. Populations of cells contain both 1n (G1; left-hand peak) and 2n (G2/M; right-hand peak) DNA content. The relative level of 1n cells within the populations is indicated on the right of the graphs (G1 (%)). The relative number of budded cells (budding index, BI) was determined in exponentially growing (EXP) and rapamycin-treated (RAP, 4h) cultures where at least 300 cells were assessed.

Previous data from our laboratory demonstrated that PP2A^{Cdc55} regulates transcription of G0 genes mainly via the control of three transcription factors: Gis1, Msn2, and Msn4 (Bontron et al, 2013). We therefore hypothesized that PP2A^{Cdc55} may regulate *XPB1* transcription via the control of those transcription factors. We found in the YEASTRACT database that Msn2 has been previously proposed (based on microarray and ChIP-on-chip analyses) to activate transcription of *XPB1* (Berry & Gasch, 2008; Huebert et al, 2012). Similar evidence was also obtained for Gis1 (Zhang et al, 2009). However, we found that loss of Gis1 did not affect Xbp1 protein levels in rapamycin-treated cells (Fig. 3.7a,b). Similarly, combined loss of Gis1, Msn2, and Msn4 only marginally (at the 2 hours rapamycin time point) affected the levels of Xbp1 under the same conditions. Although we have not measured directly *XPB1* mRNA levels in the triple *gis1Δ msn2/4Δ* cells, these results indicate that Gis1, Msn2, and Msn4 are not required for Xbp1 expression in rapamycin-treated cells.

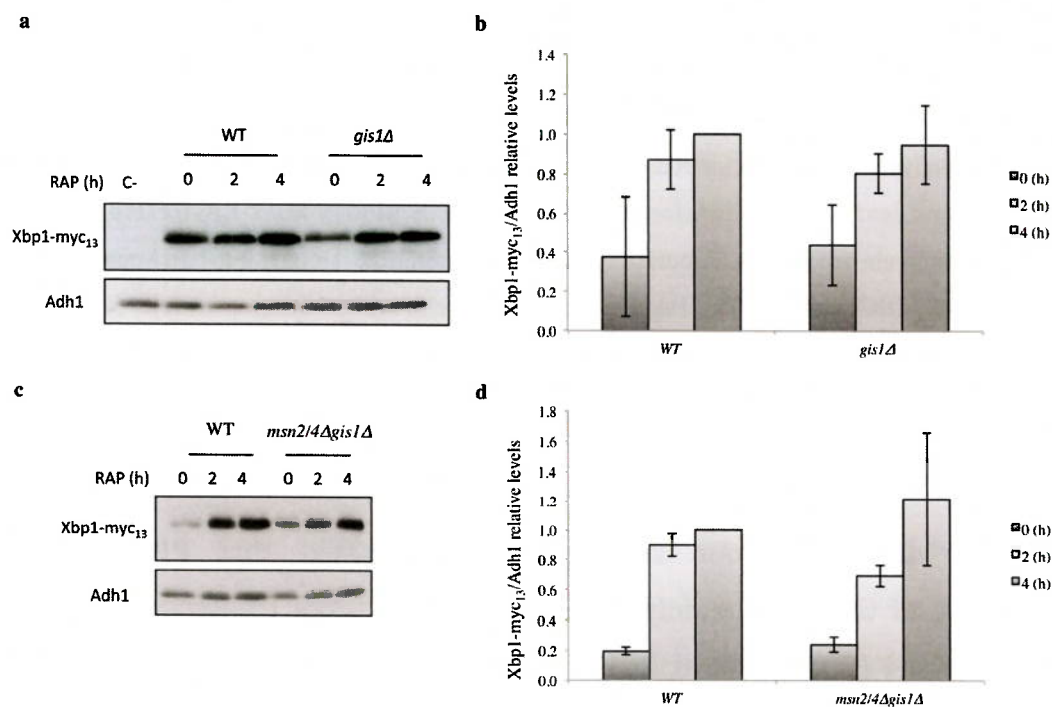


Figure 3.7. Gis1, Msn2, and Msn4 are not essential for Xbp1 accumulation after rapamycin treatment. (a, c) Xbp1-myc₁₃ levels were determined by immunoblot analyses using polyclonal anti-myc antibodies, in WT, *gis1Δ*, and *msn2/4Δ gis1Δ* cells that were grown exponentially (0h) or treated with rapamycin (RAP; 2-4h). The experiments were performed independently three times (one representative blot is shown). Adh1 levels served as loading control. (b, d) The respective Xbp1-myc₁₃ levels were normalized to the Adh1 levels in each case and calculated relative to the value in 4h rapamycin treatment wild-type cells (set to 1.0). Each bar represents mean \pm s.d. of three experiments.

3.2.2. The greatwall kinase pathway regulates Msa1, but not Msa2, protein levels

We next analyzed Msa1 and Msa2 protein levels in similar experiments as the ones outlined above for Xbp1. Loss of Rim15 or of Igo1/2 had no significant impact on Msa2 protein or *MSA2* mRNA levels, neither in rapamycin-treated (Fig. 3.8a,c), nor in nitrogen-depleted cells (Fig. 3.8b,d).

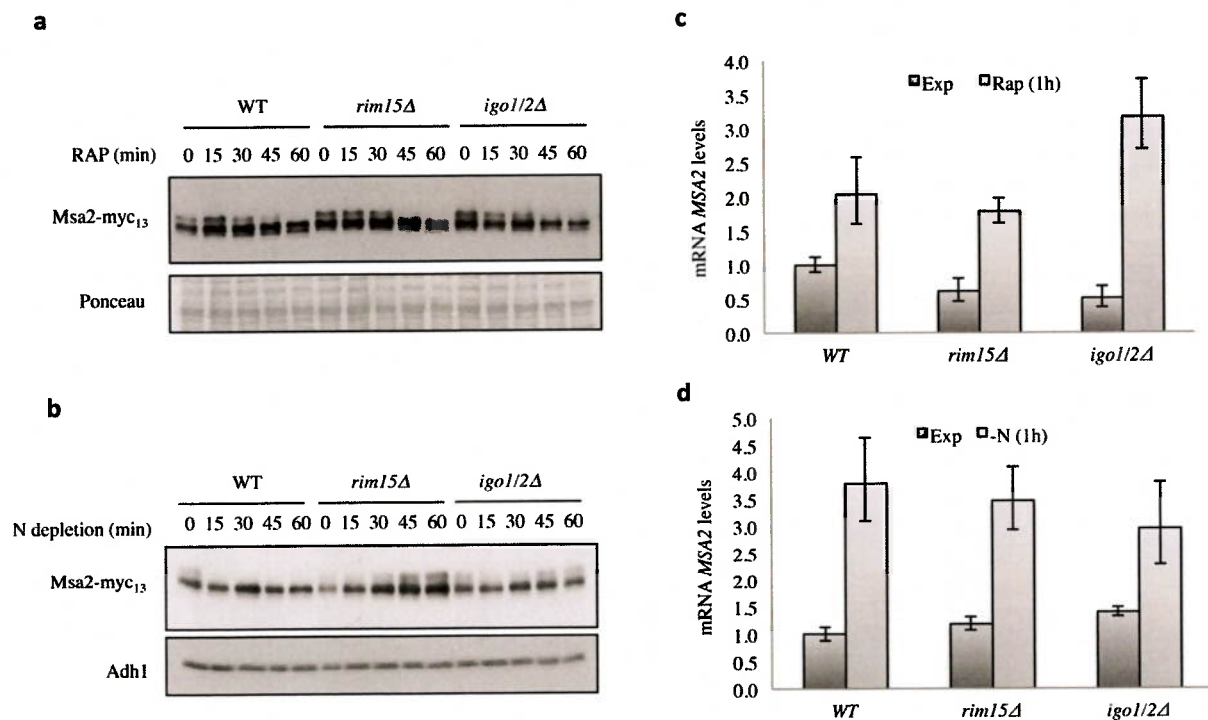


Figure 3.8. Msa2 levels are not regulated by Rim15-Igo1/2 after rapamycin treatment. Msa2-myc₁₃ levels were determined by immunoblot analyses using polyclonal anti-myc antibodies in rapamycin treated (RAP; 0-60 min) (a) and nitrogen-starved cells (N depletion; 0-60 min) (b). Relevant genotypes are indicated. Ponceau membrane staining and Adh1 levels served as loading controls. qRT-PCR analysis of *MSA2* expression were carried out in rapamycin-treated (1h) (c) or nitrogen-starved (1h) (d) cells. The value for the reference sample (exponentially-growing wild-type cells) was normalized to 1.0. Each bar represents the mean \pm s.d. of three experiments. Genotypes of strains are indicated.

Interestingly, loss of Rim15 caused significantly lower Msa1 protein expression levels in exponentially growing and rapamycin-treated cells, without any significant effect on *MSA1* mRNA levels under the same conditions. The defect in Msa1 protein expression in *rim15Δ* cells could be partially suppressed by loss of Cdc55 (Fig. 3.9a,b). Further experiments with *igo1/2Δ* and *igo1/2Δ cdc55Δ* strains will have to be carried to complete this set of experiments (please note that loss of Igo1/2, like loss of Rim15, had no significant effect on *MSA1* mRNA levels). As such, however, our results indicate that Rim15 (and likely Igo1/2) controls the levels of Msa1 at a post-transcriptional level.

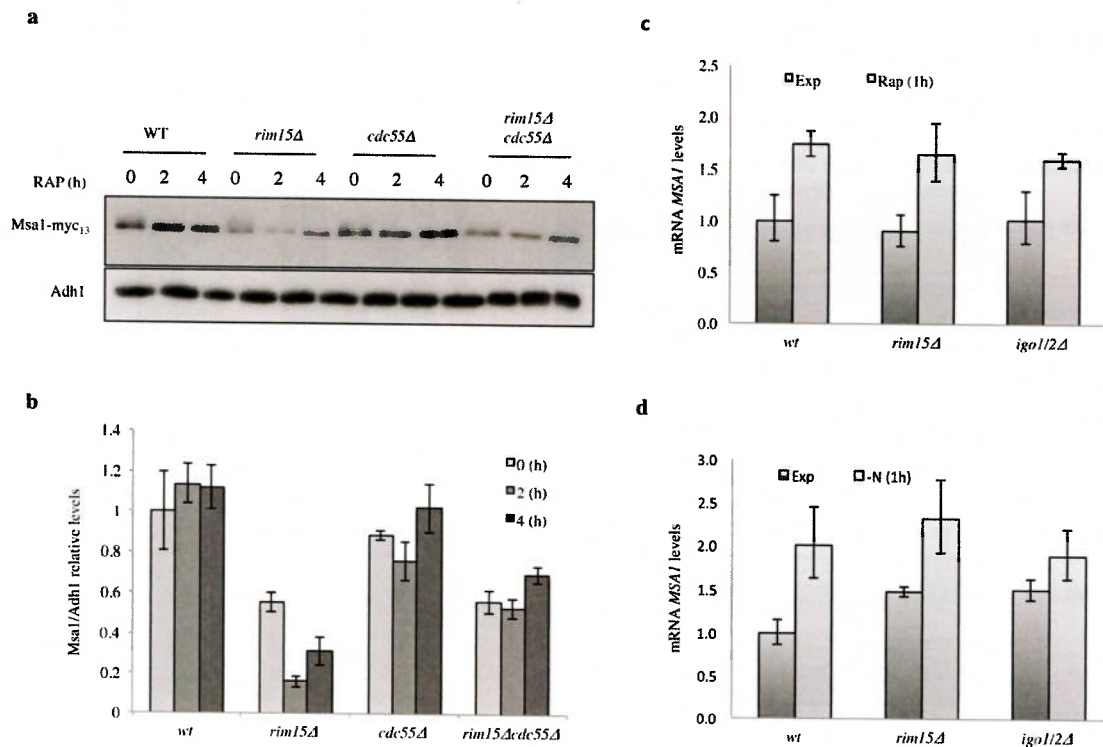


Figure 3.9. Rim15-Igo1/2 regulate Msa1 levels post-transcriptionally. (a) Msa1-myc₁₃ levels were determined by immunoblot analyses using polyclonal anti-myc antibodies in rapamycin treated cells (RAP; 0-4 h). The experiments were performed independently three times (one representative blot is shown). Adh1 levels served as loading control. Relevant genotypes are indicated. (b) Xbp1-myc₁₃ levels were normalized to the Adh1 levels for each strain and calculated relative to the value in exponentially growing wild-type cells (set to 1.0). qRT-PCR analysis of *MSA1* expression were carried out in rapamycin-treated (1h) (c) or nitrogen starved (1h) (d) cells. The value for the reference sample (exponentially growing wild-type cells) was normalized to 1.0. Each bar represents the mean \pm s.d. of three experiments.

3.2.3. The greatwall kinase pathway is not involved in the regulation of Whi5 protein levels

Our analyses of Whi5 indicated that it runs as two different isoforms on standard SDS-gels. The levels of the faster migrating isoform appeared to increase at the expense of the slower migrating isoform during the course of a 1 hour rapamycin treatment. Loss of Rim15 or of Igo1/2 did not significantly affect this pattern (Fig. 3.10a). In addition, Whi5 levels (and isoform migration pattern) were not affected by nitrogen starvation in any of the strains tested (Fig. 3.10b). It is likely therefore that Rim15 and Igo1/2 may not regulate G1 cyclin expression via a mechanism that implicates Whi5.

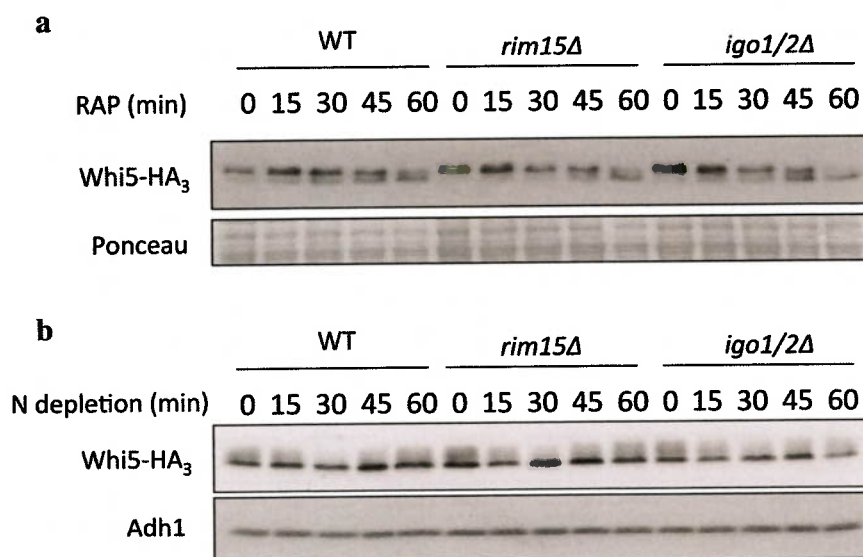


Figure 3.10. Rim15 and Igo1/2 have no significant impact on Whi5 protein levels. Whi5-HA₃ levels were determined by immunoblot analyses using polyclonal anti-HA antibodies in extracts from rapamycin-treated (RAP; 0-60 min) **(a)** and nitrogen-depleted cells (N depletion; 0-60 min) **(b)**. Ponceau membrane staining and Adh1 levels served as loading control. Relevant genotypes are indicated.

3.2.4. Loss of Rim15-Igo1/2 changes the Stb1 migration pattern independently of Cdc55

Next we studied Stb1, a protein with a role in the regulation of MBF-specific transcription at Start. This protein is phosphorylated by Cln-Cdk1 *in vitro* and its unphosphorylated form binds Swi6 to exert its function (Costanzo et al, 2003; Ho et al, 1999). Genomically myc₁₃-tagged Stb1 migrated as two isoforms on standard SDS-gels. As with Whi5, the levels of the faster migrating isoform of Stb1 appeared to increase at the expense of the slower migrating isoform during the course of a rapamycin treatment. Unlike in the case of Whi5, this rapamycin-induced change in the relative levels of the two Stb1 isoforms was significantly slower in *rim15Δ* or *igo1/2Δ* cells (Fig. 3.11a,b). This effect, however, could not be reversed by loss of Cdc55 and is hence not mediated by Cdc55 (Fig. 3.11c). It may therefore also be possible that the observed effect is simply a consequence of the G1 arrest defect in *rim15Δ* and *igo1/2Δ* cells.

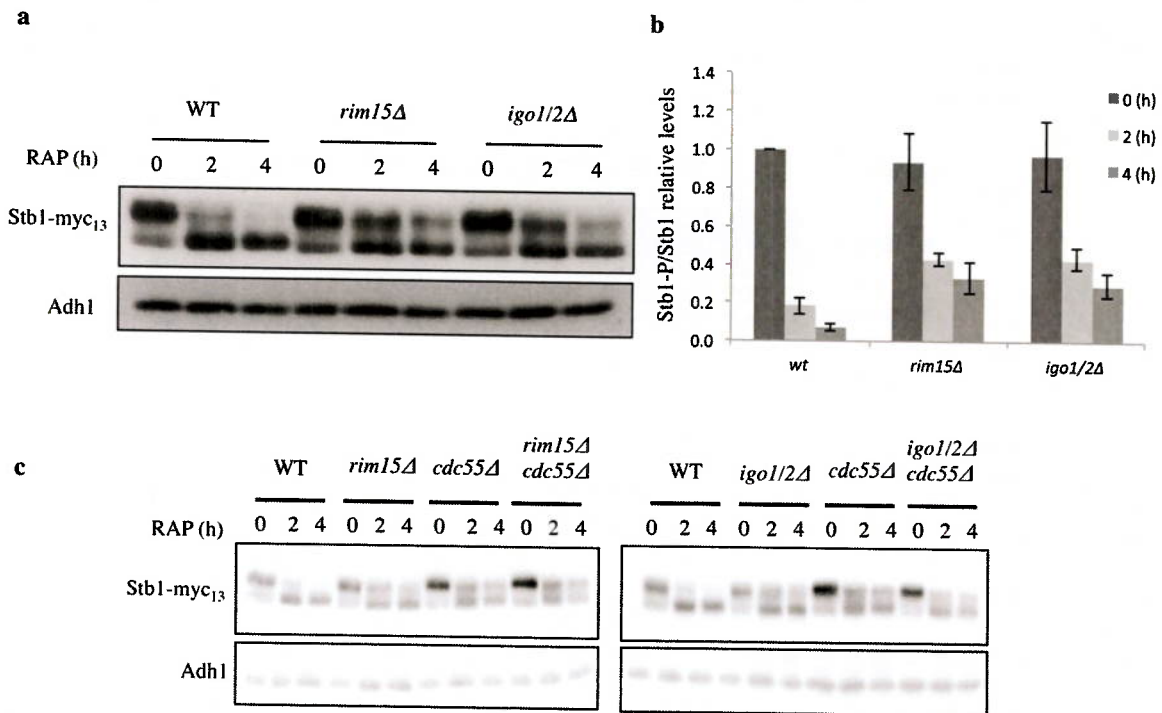


Figure 3.11. Loss of Rim15 or Igo1/2 affects the migration pattern of Stb1. (a, c) Stb1-myc₁₃ levels were determined by immunoblot analyses using polyclonal anti-myc antibodies in rapamycin-treated cells (RAP; 0-4 h). Adh1 levels served as loading control. (b) The experiment in (a) was performed independently three times (one representative blot is shown). The respective Xbp1-myc₁₃ levels of the slow migrating isoform were normalized to the levels of the fast migrating isoform and calculated relative to the value in exponentially growing wild-type cells (set to 1.0) Each bar represents the mean \pm s.d. of three experiments. Genotypes of strains are indicated.

3.2.5. Loss of Rim15-Igo1/2 alters Nmr1 protein levels in rapamycin-treated cells

Nrm1 protein levels were similar in exponentially growing wild-type, *rim15Δ*, and *igo1Δ igo2Δ* cells, and decreased significantly upon rapamycin treatment in wild-type, but to a much lower extent in *rim15Δ* and *igo1/2Δ* cells (Fig. 3.12a,b). We assumed that the enhanced Nmr1 levels in rapamycin-treated *rim15Δ* cells could be responsible for their defect in proper G1 arrest following rapamycin treatment. However, this was not the case, as loss of Nmr1 did not rescue the respective G1 arrest defect of *rim15Δ* (Fig. 3.12c). Therefore, we deem it possible that the observed differences in Nmr1 levels between wild-type and *rim15Δ* or *igo1/2Δ* cells may be rather a consequence than the

cause of the observed cell cycle arrest defect (*i.e.* the latter mutant cells may reach cell cycle stages past G1 during which Nmr1 expression is normally induced).

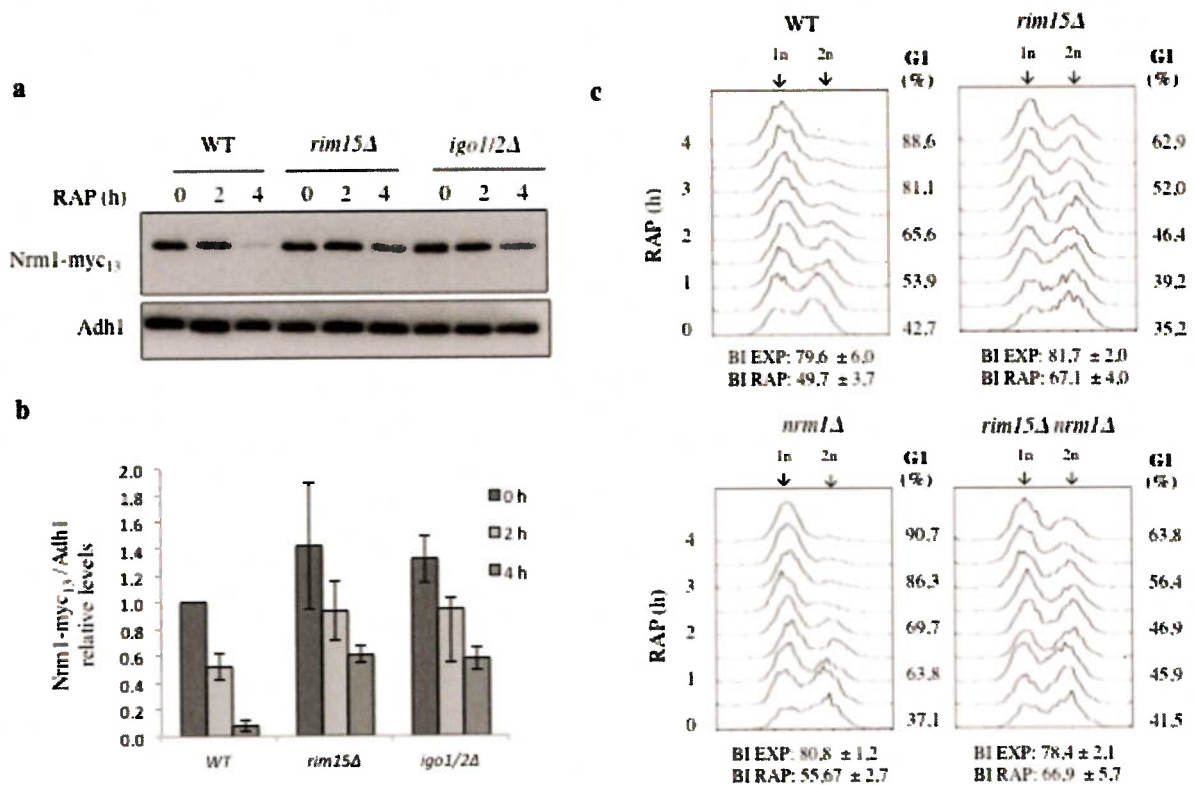


Figure 3.12. Loss of Rim15-Igo1/2 stabilizes Nmr1 in rapamycin-treated cells. (a) Nrm1-myc₁₃ levels were determined by immunoblot analyses using polyclonal anti-myc antibodies in rapamycin-treated cells (RAP; 0-4h). The experiments were performed independently three times (one representative blot is shown). Adh1 levels served as loading control. (b) The respective Nrm1-myc₁₃ levels were normalized to the Adh1 levels in each case and calculated relative to the value in exponentially growing wild-type cells (set to 1.0). Each bar represents the mean ± s.d. of three experiments. Genotypes of strains are indicated. (c) Fluorescence-activated cell sorting (FACS) analyses of the DNA content of cells treated for the indicated times with rapamycin are shown. The relative number of budded cells (budding index, BI) was determined in exponentially growing (EXP) and rapamycin-treated (RAP; 4 h) cultures. Numbers are means ± s.d. from three independent experiments in which at least 300 cells were assessed. Populations of cells contain both 1n (G1; left-hand peak) and 2n (G2/M; right-hand peak) DNA. The relative level of 1n cells within the populations is indicated on the right of the graphs (G1 (%)).

3.2.6. A combined role for Xbp1, Msa1/2 and Sic1 in rapamycin-induced G1 arrest

The above data suggested that the greatwall kinase pathway possibly impinges on Xbp1 and Msa1. We therefore studied whether Xbp1 or Msa1 (and, as a control, loss of

Msa2) may mediate G1 arrest in rapamycin-treated cells. Individual loss of Xbp1, Msa1, or Msa2 did not cause a G1 arrest defect in rapamycin-treated or nitrogen-starved cells (Fig. 3.13).

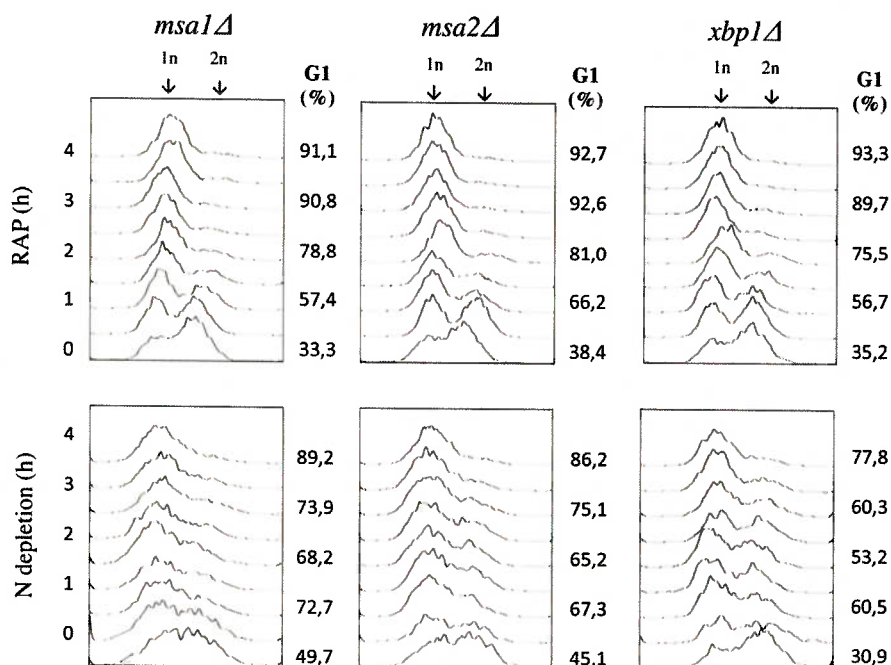


Figure 3.13. Individually, Msa1, Msa2, or Xbp1 are not essential for proper G1 arrest after rapamycin treatment. FACS analyses of the DNA content of the indicated strains were performed as in Fig. 3.5. after rapamycin treatment (RAP; 0-4 h) or nitrogen starvation (N depletion; 0-4 h). Genotypes of strains are indicated.

We therefore considered the possibility that Xbp1, Msa1, and Msa2 combined may play a role in G1 cyclin downregulation and hence G1 arrest in rapamycin-treated cells. But, combined loss of all three proteins did not cause any noticeable defect in rapamycin-mediated G1 arrest. Interestingly, however, the triple *xbp1Δ msa1Δ msa2Δ* strain exhibited a strong synthetic G1 arrest phenotype when combined with the *sic1^{T173A}* mutation, which on its own, or when only combined with *xbp1Δ* or with *msa1/2Δ* caused only a minor G1 arrest phenotype in rapamycin-treated cells. The observed synthetic G1 arrest defect was almost identical to the one observed in *rim15Δ* or *igo1Δ igo2Δ* cells. Together, these results support a model in which the greatwall kinase controls G1 arrest in rapamycin-treated cells via two branches, one that controls Sic1-Thr¹⁷³ phosphorylation and hence Sic1 stability and another that properly

represses G1 cyclin expression possibly via the combined action of Xbp1, Msa1, and Msa2.

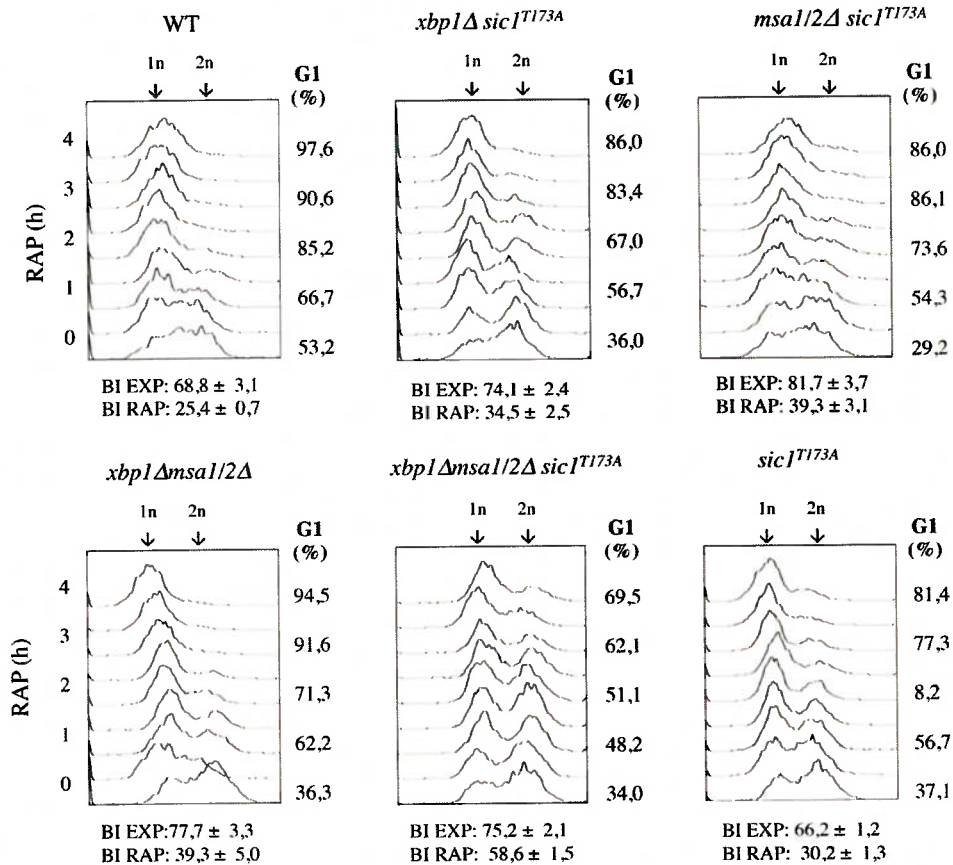


Figure 3.14. Deletion of *XBP1*, *MSA1*, and *MSA2* combined with *sic1^{T173A}* results in a G1 arrest defect after rapamycin treatment. FACS analyses of the DNA content and budding indexes (BI) of the strains with the indicated genotypes were performed as in Fig. 3.5.

3.3. Discussion

In this chapter we present our first attempt to understand the mechanisms by which the greatwall kinase pathway controls G1 cyclin transcription and/or mRNA stability. Our data suggest that Xbp1 and Msa1/2 may be potential target candidates for the Rim15-Igo1/2-PP2A^{Cdc55} signaling branch. Although loss of these transcriptional regulators did not have any effect in normal cell cycle progression (data not presented) or in G1 arrest following rapamycin treatment, we observed that the combination of the respective deletions with the Sic1-Thr¹⁷³ allele resulted in a synthetic G1 arrest defect in

rapamycin-treated cells. Our analyses are still preliminary and need to be complemented with experiments that corroborate our tentative model. Thus, in addition to also addressing a potential role of SBF and MBF components in mediating greatwall kinase pathway signals, we need to specifically assess whether Xbp1, Msa1, and Msa2 play a combined role in G1 cyclin expression. To this end, we plan to genomically tag Cln1-3 and measure the respective mRNA and protein levels in wild-type and *xbp1Δ msa1/2Δ* cells.

To discriminate if *XBP1* mRNA is regulated by Rim15-Igo1/2 transcriptionally and/or at the level of mRNA stability, mRNA levels will be quantified by qRT-PCR in *ccr4Δ* and *dhh1Δ* mutants. Ccr4 and Dhh1 have been shown to be involved in the decay of specific mRNAs during initiation of the G0 program in the absence of Igo1/2 (Luo et al, 2011) and we therefore hypothesize that the *XBP1* mRNA could be a potential target of 3'-5' mRNA decay machinery. If mRNA stability were not affected, we will try to identify the elusive transcription factors that control Xbp1 expression under the control of the greatwall kinase pathway. One approach could be the one-to-one study of transcription factors, which have been found to exhibit an altered phosphorylation pattern previously in our phosphoproteome analysis of rapamycin-treated *cdc55Δ* mutant cells (performed by Séverine Bontron, a former member of the group). Potential candidates could be further validated by ChiP analysis, qRT-PCR, and studies of deletion mutants.

Of note, Msa1 contains 25 potential SP/TP phosphorylation sites, 9 of which have already been shown to be phosphorylated by Hog1 upon osmotic stress and to play a role in controlling G1 cyclins transcription (Gonzalez-Novo et al, 2015). In addition, Msa1 is a phosphoprotein with cell cycle-dependent nucleocytoplasmic shuttling (Kosugi et al, 2009). Thus, it would be interesting to study whether the greatwall kinase pathway regulates Msa1 phosphorylation pattern and subcellular localization.

CHAPTER IV:
***Genetic screen for suppressors of
the defect in exit from the
rapamycin-induced G0 arrest***

4.1. Introduction

Binding of the rapamycin/Fpr1 complex to TORC1 inhibits the activity of TOR kinases and drives cells into G0 phase. Several proteins that are important for the transition from quiescence back to the proliferation state have been described during the last years. These include subunits of the EGO (exit from rapamycin-induced growth arrest) protein complex (EGOC) (Dubouloz et al, 2005), which mediates amino acid signals to TORC1 (Binda et al, 2009). The highly conserved EGOC (that is structurally similar to the Ragulator complex in mammals) colocalizes with TORC1 mainly at the vacuolar periphery and it is formed by Ego1, Ego2, Ego3, and the heterodimeric Rag GTPases Gtr1 and Gtr2 (Araki et al, 2005; Berchtold & Walther, 2009; Binda et al, 2009; Gao & Kaiser, 2006; Kogan et al, 2010; Powis et al, 2015; Reinke et al, 2004; Sancak et al, 2008). Rag GTPases have been described to mediate amino acid signals upstream of and towards TORC1 in yeast, *Drosophila* and mammalian cells (Binda et al, 2009; Sancak et al, 2008). In *S. cerevisiae*, the two small GTPases Gtr1 and Gtr2 interact directly with TORC1 in an amino acid-sensitive and nucleotide-dependent manner. Gtr1 bound to GTP and Gtr2 bound to GDP form the heterodimer that activates TORC1. The mechanistic details on how Gtr1/2 activate TORC1 in yeast, however, are unclear. Loss of any member of the EGOC results in cells deficient in resuming proliferation from quiescence when nutrient conditions become favorable.

Interestingly, we found that cells with the JK9-3D genetic background, unlike other wild-type cells of different origin, present an intrinsic defect in the exit from rapamycin-induced growth arrest (hereafter referred as “*EGO* phenotype”) that seems to be occasionally rescued by spontaneous suppressor mutations. Here, we aimed to perform a genetic selection to identify the mutations that are responsible of the latter suppressor phenotype. We hypothesized that this may allow us to identify potential new regulators and/or targets of TORC1 whose further characterization may help us to better understand the regulatory mechanisms of the TORC1 signaling pathway. Analyses of interesting novel candidates could be extrapolated to studies in higher eukaryotes where understanding how cells enter into and exit from quiescence is of key relevance since inappropriate exit from quiescence has dramatic medical consequences such as reactivation of latent infections or cancer.

4.2. Results

4.2.1. JK9-3D cells are defective in the exit from rapamycin-induced growth arrest

To confirm our previous observations that JK9-3D cells present an *EGO* phenotype, different JK9-3D strains including wild-type (*MATa*, *MAT α* , and diploid *MATa/ α*) and *rim15 Δ* mutant (*MATa* and diploid heterozygous *MATa/ α*) cells were rapamycin-treated for 4 hours. After washing out the rapamycin from the cultures, the ability of the cells to resume growth in rich or synthetic defined medium was tested (hereafter referred as “rapamycin recovery test”). Wild-type and *gtr1 Δ* BY4741 cells were used as positive and negative controls, respectively. As observed in Fig. 4.1., unlike wild-type cells of the BY4741 strain, none of the JK9-3D strains tested was able to restart growth after rapamycin treatment. In fact, the *EGO* phenotype of all of the JK9-3D strains was very similar to the one observed in *gtr1 Δ* BY4741 cells. These results confirmed that JK9-3D cells are defective in the exit from rapamycin-induced growth arrest.

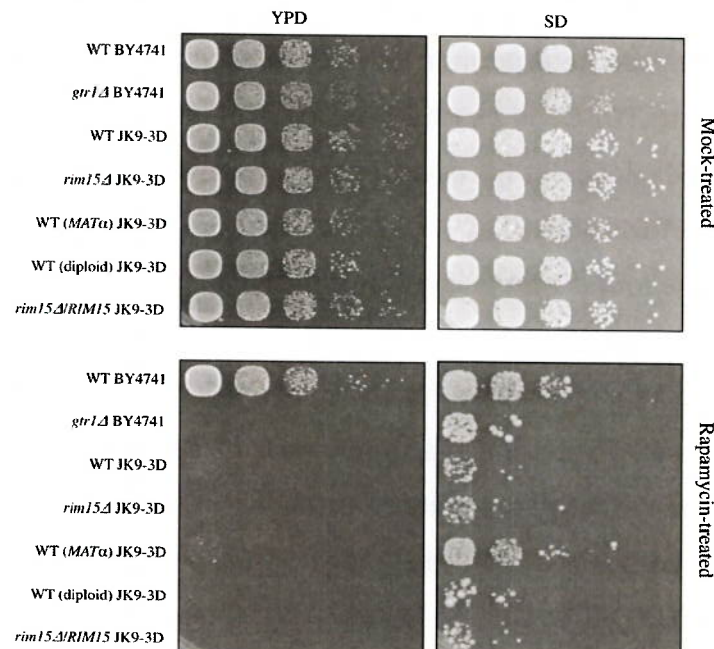


Figure 4.1. JK9-3D cells are defective in exit from rapamycin-induced growth arrest. JK9-3D and BY4741 cells with the indicated genotypes were treated with 200 ng/ml rapamycin or vehicle for 4 hours in liquid rich (YPD) medium. Cells were washed two times with YPD and serial 10-fold dilutions were

spotted onto YPD or synthetic defined medium (SD) and grown at 30°C for 2 days (rapamycin recovery test).

4.2.2. Hyperactive *TOR1* alleles suppress the *EGO* phenotype in JK9-3D cells

While this thesis was in progress, the complete genomic DNA sequence of the JK9-3D strain was published on SGD and many polymorphisms with respect to the most commonly used laboratory strain (BY4741) were identified. However, at the earlier stages of this specific project, the genomic DNA sequence of JK9-3D was not yet available. Initially we tried to complement wild-type JK9-3D cells with plasmids containing different genes (isolated from wild-type BY4741 cells) encoding proteins of the EGO to test whether the JK9-3D strain may have a specific defect in any of the corresponding genes that would explain the respective EGO phenotype of JK9-3D cells. Expression of the GTP-locked signaling competent *GTR1^{Q65L}* allele under control of its endogenous promoter (Fig. 4.2a) or the *Tet_{ON}* promoter (Fig. 4.2b) did not rescue the *EGO* phenotype of wild-type JK9-3D cells. Since the active GTPase heterodimer complex is formed with *Gtr1^{GTP}* and *Gtr2^{GDP}* signaling competent forms, the *GTR1^{Q65L}* allele was simultaneously transformed with *GTR2^{S23L}* allele (which has low affinity for nucleotides) in JK9-3D wild-type cells. However, similarly to the expression of plasmid-encoded *EGO1*, *EGO2*, or *EGO3*, this was not sufficient to overcome the defect in exit from rapamycin-induced growth arrest of JK9-3D wild-type cells (Fig. 4.2c,d). However, expression of the hyperactive *TOR1^{A1957V}* and *TOR1^{I1954V}* alleles (Reinke et al, 2006) suppressed the *EGO* phenotype of JK9-3D wild-type cells (Fig. 4.2e).

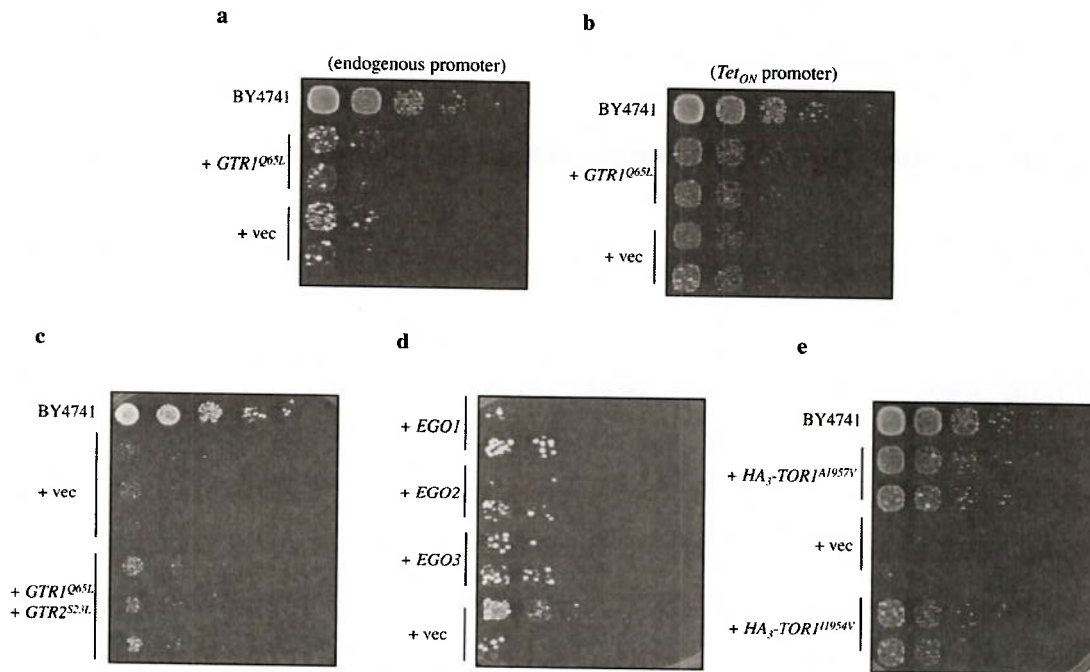


Figure 4.2. Expression of hyperactive *TOR1* alleles, but not of EGOC encoding genes, suppresses the *EGO* phenotype of JK9-3D wild-type cells. The rapamycin recovery test was performed as in Fig. 4.1 in wild-type JK9-3D cells complemented with plasmids expressing *GTR1^{Q65L}* under the endogenous (a) or the doxycycline-inducible *Tet_{ON}* promoter (b), the *GTR1^{Q65L}/GTR2^{S23L}* GTPase heterodimer (c), *EGO1* and *EGO2* (expressed under their own promoter) or *EGO3* (expressed under *ADH1* promoter) (d), or *TOR1^{A1957V}* or *TOR1^{I1954V}* hyperactive alleles (e). Wild-type BY4741 cells were included as positive controls whereas wild-type JK9-3D cells complemented with the corresponding empty vectors were used as negative controls. Expression of genes under the control of the *Tet_{ON}* promoter (b and c) was induced by adding 5 $\mu\text{g ml}^{-1}$ doxycycline to the medium.

Subsequent BLAST analyses between genomic DNA sequences of wild-type JK9-3D and all other laboratory strains available in the *Saccharomyces* Genome Database (SGD) identified many polymorphisms (in a total of 94 genes) that were unique in JK9-3D cells. None of these was present in any of the genes coding for EGOC subunits. Thus, the *EGO* phenotype of JK9-3D cells is not due to a defect in EGOC subunits.

4.2.3. Genetic selection for suppressors of the JK9-3D *EGO* phenotype

Interestingly, during the rapamycin recovery test after 2-3 days of incubation at 30°C, JK9-3D cells presented spontaneous appearance of individual colonies (see e.g. Fig. 4.2a). In order to further study these colonies, they were collected, cultured again,

treated for 4 hours in rapamycin containing liquid medium, and serially 10-fold diluted in plates without rapamycin. After 2 days of incubation at 30°C we observed that all the clones tested resumed growth after rapamycin treatment to the same extent as wild-type BY4741 cells (data not shown) indicating that these clones may have acquired a spontaneous mutation that suppresses the *EGO* phenotype of JK9-3D cells.

Since *TOR1* hyperactive alleles (Fig. 4.2e) were able to suppress the *EGO* phenotype of JK9-3D cells, we hypothesized that the majority of the presumed suppressor mutations may either cause hyperactive TORC1 or mimic the effects of hyperactive TORC1 on its downstream targets. Therefore, we performed a genetic selection assay to collect an array of different suppressors, whose genomic DNA was afterwards sequenced to potentially identify novel components of the TORC1 signaling pathway. To this end, we constructed JK9-3D (*leu2, his4, trp1, URA3, MAT α*) and JK9-3D (*leu2, trp1, ura3, HIS4, MAT α*) cells that allowed easy selection of JK9-3D diploids in further analyses (see Fig. 4.3e and Fig. 4.4a,b). We confirmed that these new strains, like the parental JK9-3D, presented a defect in exit from rapamycin-induced growth arrest (Fig. 4.3a). To obtain single suppressor colonies, cells were treated with rapamycin (4 h), washed twice with YPD, and 0.6×10^6 cells were plated on YPD plates containing 5 ng ml⁻¹ rapamycin. 30 suppressor colonies from each strain were retested/reconfirmed in a second *EGO* phenotype test (an example of two colonies of each strain shown in Fig. 4.3b). In order to exclude suppressors containing mutations in *FPR1*, we then generated JK9-3D *fpr1 Δ* (*MAT α , leu2, his4, trp1, URA3, or MAT α , leu2, trp1, ura3, HIS4*) cells that had no *EGO* phenotype (Fig. 4.3c,d) and that were then used to mate with the appropriate suppressor strains. Control experiments showed that the diploid heterozygous *fpr1 Δ /FPR1* cells had an *EGO* phenotype as expected (Fig. 4.3e).

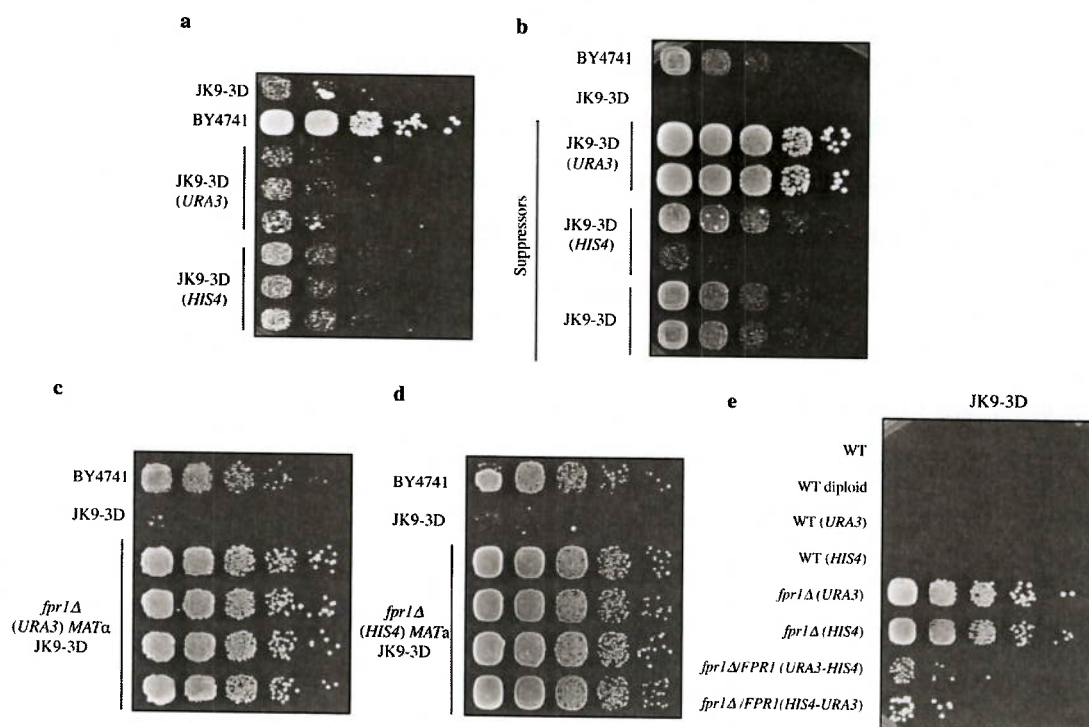


Figure 4.3. Rapamycin recovery growth test in control strains required for the screening. (a) JK9-3D cells present an *EGO* phenotype independently of their respective auxotrophies. (b) Two suppressor colonies from JK9-3D strains with different auxotrophies were re-tested for their *EGO* phenotype. (c, d) Deletion of *FPR1* in JK9-3D *MAT α URA3* (c) or *MAT α HIS4* cells (d) suppresses the *EGO* phenotype in haploid cells (4 independent clones tested). (e) Heterozygous diploids *fpr1Δ*/*FPR1* cells (2 independent clones tested) have an *EGO* phenotype. All rapamycin recovery tests were performed as in Fig. 4.1.

The *fpr1Δ* mutant cells were then mated with suppressor strains of the appropriate mating type and the respective diploids (selected via their different auxotrophic needs) were analyzed in the rapamycin recovery test. Two different results were obtained: some diploids had no *EGO* phenotype, being able to resume growth after rapamycin treatment at the same extent as single *fpr1Δ* cells (3 independent suppressors are shown in Fig. 4.4a) whereas others maintained the *EGO* phenotype behaving as the wild-type JK9-3D diploid strain (3 independent suppressors are shown in Fig. 4.4b). We considered that diploid cells that lost the *EGO* phenotype may contain with a high probability inactivating mutations in the *FPR1* gene and therefore they were eliminated from our study (36 suppressors), while all others (24 suppressors) were included in

further analyses. Of note, suppressors containing dominant suppressor mutations in any other gene than *FPR1* would also have been excluded by this procedure.

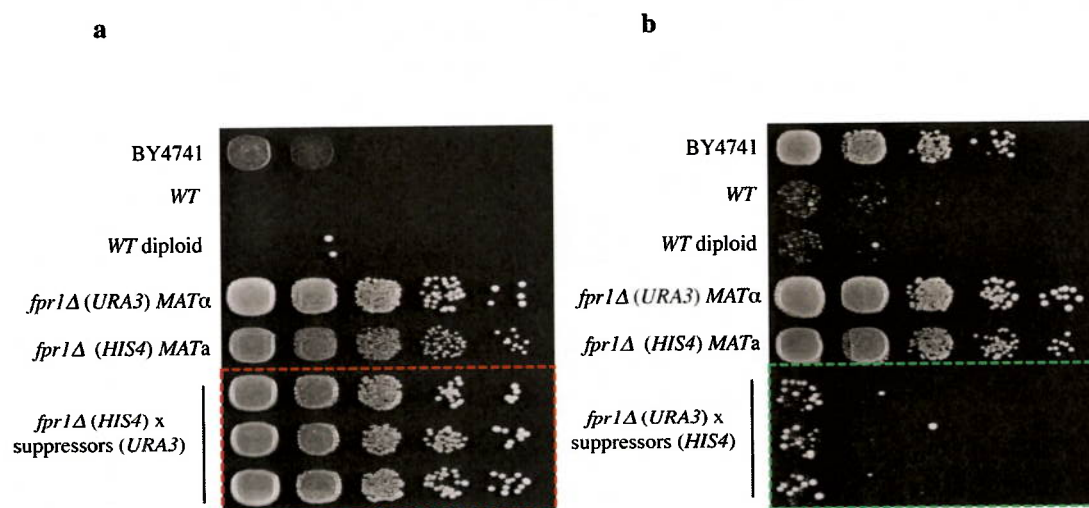


Figure 4.4. Exclusion of suppressors containing mutations in *FPR1* gene. The rapamycin recovery growth test performed as in Fig. 4.1. Three independent diploids (red rectangle) originating from a cross between an *fpr1Δ* and a suppressor strain that have no *EGO* phenotype are shown in (b). Three independent diploids (green rectangle) originating from a cross between an *fpr1Δ* and a suppressor strain that have an *EGO* phenotype are shown in (b). BY4741 and *fpr1Δ* JK9-3D mutant cells were included as positive controls while wild-type JK9-3D haploid and diploid cells were included as negative controls.

To confirm that the suppressor phenotype of the remaining clones was due to only one genetic mutation, we then mated all suppressor candidates with the wild-type strain. Diploids were sorted out on selective medium and placed into sporulation medium. For each diploid strain, several tetrads were dissected and the corresponding spores were analyzed for the rapamycin recovery test. All tetrads contained spores with a 2:2 segregation regarding their ability to resume growth after rapamycin-induced growth arrest (an example of two different tetrads analyzed for the rapamycin recovery test is shown in Fig. 4.5). These results confirmed the presence of one specific genetic mutation in all the 24 suppressor strains tested that might be responsible of reverting the defect in growth resumption after rapamycin treatment.

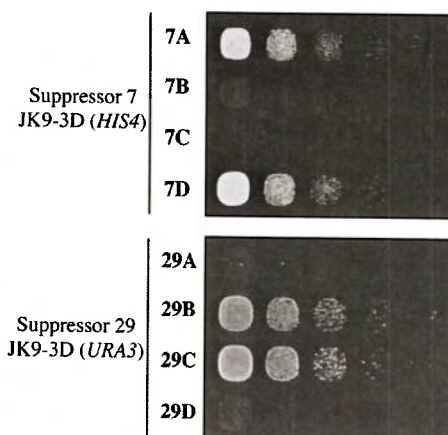


Figure 4.5. Genetic segregation analysis of heterozygous diploid strains. All suppressors clones were crossed with the wild-type strain and diploids were subjected to tetrad analysis. An example of the rapamycin recovery growth test of two different dissected tetrads is shown. Each tetrad contained two spores that exhibited (7B, 7C, 29A and 29D) and two that did not exhibit an *EGO* phenotype (7A, 7D, 29B and 29C). The rapamycin recovery test was performed as in Fig. 4.1.

Finally, genomic DNA from the remaining 24 candidates was extracted and sent for whole genome sequencing. The obtained Illumina data were analyzed by Dr. Falquet (University of Fribourg) and genomic variants with respect to the wild-type reference genome were identified and annotated. With the exception of one clone (n°. 20) all genomes sequenced contained a genetic variation in one of the following genes: *GLN3*, *PMR1*, *TOR1*, and *NPR1* (Fig. 4.6).

Mutation	Aminoacid substitution	Gene	Clones
cCg/cTg	P315L	<i>GLN3</i>	9
tgC/tgA	C327*	<i>GLN3</i>	1,17
tCc/tTc	S321F	<i>PMR1</i>	22,24
aTc/aCc	I1954T	<i>TOR1</i>	11
tCa/tGa	S710*	<i>NPR1</i>	23
cCg/cAg	P644Q	<i>NPR1</i>	13,18,19
Gag/Tag	E468*	<i>NPR1</i>	21
tTa/tGa	L444*	<i>NPR1</i>	2,3,4,5,6,7,8,10,12,14,15,16

Figure 4.6. Mutations identified that were able to suppress the *EGO* phenotype of JK9-3D wild-type cells. Mutations and deduced amino acid substitutions of respective gene products are shown.

4.3. Discussion

All of the mutations identified in the 24 suppressors that were identified in our genetic selection were in genes encoding proteins that have previously been described to be involved in the TORC1 signaling pathway. Firstly, *GLN3* codes for a transcriptional activator of genes regulated by nitrogen catabolite repression. TORC1 inhibition derepresses Gln3 and induces its translocation to the nucleus (Beck & Hall, 1999) where it induces a subset of nitrogen-repressed genes like *GAP1* and *MEP2* that encode the general amino acid and the ammonium permease, respectively (Magasanik & Kaiser, 2002). Both the C327* nonsense mutation and the P315L mutation located in the zinc finger domain of the Gln3 transcription factor likely totally abolish Gln3 function. Of note, loss of Gln3 has been found to increase the resistance of cells to rapamycin indicating that the *EGO* phenotype of JK9-3D wild-type cells is in part due to enhanced Gln3 activity (possibly as a result of lower TORC1 activity in this strain) (Beck & Hall, 1999). Secondly, *NPR1* codes for a Ser/Thr-protein kinase that stabilizes several plasma membrane amino acid transporters by antagonizing their ubiquitin-mediated degradation (De Craene et al, 2001; O'Donnell et al, 2010; Vandenbol et al, 1987). Npr1 activity is negatively regulated by TORC1. Inhibition of TORC1 upon nitrogen limitation or rapamycin treatment activates Npr1 by Sit4-dependent desphosphorylation (MacGurn et al, 2011; Schmidt et al, 1998). As a consequence, Gap1 is allowed to reach the plasma membrane and other specific amino acid permeases are endocytosed and targeted to the vacuole (Gander et al, 2008). The non-synonymous P644Q mutation and the S710*, E468*, and L444* nonsense mutations are located within protein kinase domain of Npr1 (438-742) and all likely also abolish the protein kinase function of Npr1. As with loss of Gln3, loss of Npr1 has also been reported to confer rapamycin resistance to wild-type cells indicating that the *EGO* phenotype of JK9-3D wild-type cells also is in part due to enhanced Npr1 activity (again, possibly as a result of lower TORC1 activity in this strain) (Schmidt et al, 1998). Thirdly, *PMR1* encodes a member of the P-type ATPase family of ion transporters and transports Ca²⁺ or Mn²⁺ ions with high affinity from the cytoplasmic space into the Golgi and thus functions in the secretory pathway also used by permeases (Rudolph et al, 1989). Several genetic epistasis analyses suggested that *PMR1* functions as negative regulator of TORC1 and that loss of *PMR1* confers rapamycin

resistance (Devasahayam et al, 2006). Thus, the S321F mutation may also render Pmr1 inactive and, by still unknown mechanisms, enhance the TORC1 activity and thus suppress the EGO phenotype in JK9-3D wild-type cells. Taken together, deletion of *GLN3*, *NPR1* or *PMR1* confers rapamycin resistance and the respective proteins have been described to be either negatively regulated by TORC1 (Npr1 and Gln3) or to negatively regulate TORC1 (Pmr1) (Cardenas et al, 1999; Devasahayam et al, 2006; Reinke et al, 2006; Schmidt et al, 1998).

Interestingly, the *TOR1^{1954T}* mutant allele codes for a Tor1 protein with a mutation within the FRB (FKBP12-rapamycin-binding) domain that has been previously characterized as a *TOR1* hyperactive allele (Reinke et al, 2006). We already previously observed that the expression of the *TOR1^{1954V}* allele rescued the defect in the exit from rapamycin-induced growth arrest in JK9-3D cells (Fig. 4.2e). The identification of this mutation in our unbiased selection proves the suitability of the applied suppressor selection system for the identification of new potential TORC1 regulators and/or targets. Overall, however, we were not able to identify any novel candidate genes in the analyses of our 24 suppressors chosen. Nevertheless, the selection procedure appears to be powerful in identifying TORC1 pathway components and, given the fact the selection procedure was far from being saturated (as we got some suppressor mutations only once or twice), isolation and analysis of more suppressor clones by whole genome sequencing is warranted. In a next round, we intend to first try to complement any new suppressor clone with plasmid-encoded *FPR1*, *GLN3*, *NPR1* and *PMR1* to eliminate these known suppressors from further analyses. We may also choose to select those suppressor clones that exhibit enhanced TORC1 activity. Currently we are also verifying whether the *in vivo* TORC1 activity (assessed by phosphorylation of Sch9) in *TOR1^{1954T}* cells is significantly higher than the one from wild-type cells as expected. It has been previously described that *tor1Δ* cells expressing the *TOR1^{1954V}* allele present approximately three times more TORC1 kinase activity than the corresponding wild-type (Reinke et al, 2006). In addition, overproduction of Gtr1^{GTP} (Binda et al, 2009) or expression of *TOR1^{1954T}* (data from this study; not shown) results in growth inhibition on nitrogen poor (urea-containing) media. To potentially enrich our selection for suppressors with enhanced TORC1 kinase activity, we may therefore also choose to test growth of the clones on nitrogen poor media. If genetic variations are identified in

potentially interesting new genes, further characterization analyses of those mutants will be performed.

Taken together, this project shows that combining an appropriate suppressor selection procedure with the potential of whole genome next-generation sequencing (NGS) technology, raises the possibility to obtain a high-resolution, base-by-base view of the genome detecting single nucleotide variants. These variations may be potential targets for further follow-up studies of gene expression and regulation processes, that in the case of our study, may allow to gain further insight into the mechanisms controlling exit from quiescence and the regulatory machinery of the TORC1 signaling pathway.

General Discussion

Concluding remarks

Nutrient signaling pathways allow yeast cells to benefit from rich nutrient environmental conditions by inducing cell proliferation, while ensuring long-term survival upon nutrient depletion conditions by promoting entry into a quiescent G0 phase. This switch between proliferation and quiescence is highly regulated by cell cycle mechanisms that are sensitive to the nutritional status in order to prevent cell cycle progression in the absence of essential nutrients, which may otherwise enhance DNA replication and chromosome segregation errors.

Glucose, phosphate, nitrogen and sulfur sources have been described as critical nutrients that control cell cycle progression in yeast, since their absence leads to a G1-phase cell cycle arrest. However, the underlying mechanisms by which cells coordinate cell division with cell growth in response to nutrient availability are so far poorly understood. In this context, the conserved target of rapamycin complex 1 (TORC1) nutrient signaling pathway plays a positive key role in the regulation of cell growth participating critically in the cells's decision whether to enter, or not, into the non-dividing resting state of quiescence. TORC1 negatively regulates the protein kinase Rim15 (orthologous to the Greatwall kinase [Gwl] in higher eukaryotes) that orchestrates most aspects of the G0 program including proper cell cycle arrest in G1. Previous studies from the laboratory demonstrated that upon TORC1 inactivating conditions, Rim15 inhibits (indirectly via the yeast endosulfines Igo1/2) PP2A^{Cdc55} activity to control several aspects of the initiation of the quiescence program that are relevant for the chronological lifespan (Bontron et al, 2013).

Combined, the findings of this thesis show that the TORC1-Rim15-Igo1/2-PP2A^{Cdc55} signaling pathway controls cell cycle progression at the G1/S transition in response to nutrient availability by several mechanisms. Firstly we confirmed that not only Rim15 but also Igo1/2 are required for G1 arrest after rapamycin treatment or nitrogen depletion. Interestingly, we observed that upon rapamycin treatment, cells deleted for *RIM15* or *IGO1/2* do not properly accumulate the Cdk1-inhibitor Sic1 and downregulation of G1 cyclins levels is delayed when compared with wild-type cells (Fig. 1.1e). These results suggested that TORC1-Rim15-Igo1/2 pathway regulates G1/S cell cycle transition in response to nutrient availability by controlling a dual mechanism: it

promotes Sic1 accumulation while ensuring a decrease of G1 cyclins levels to prevent Clb-Cdk1 activity. TORC1 inhibition results in the activation of the MAP kinase Mpk1 that phosphorylates Sic1 at residue Thr¹⁷³, which promotes Sic1 stability. The phosphorylated status of this residue is counterbalanced by the phosphatase PP2A^{Cdc55} that favors Sic1-pThr¹⁷³ dephosphorylation when nutrients are abundant. Overall, TORC1 inactivation results in stabilization of Sic1 by phosphorylation at Thr¹⁷³, which then allows proper inhibition of Clb-Cdk1 activity and ensures, together with G1 cyclin downregulation, proper G1 arrest. The data presented in this manuscript further show that phosphorylation at Thr¹⁷³ is required to prompt Cks1 binding to Sic1. This interaction protects Sic1 from G1/S-Cdk1-dependent phosphorylation by a so far unknown mechanism, thereby preventing SCF^{Cdc4}-mediated ubiquitination and subsequent degradation of Sic1 by the proteasome.

We further describe here that Rim15 and Igo1/2 are required for proper timing of G1 cyclin downregulation upon rapamycin treatment. Our data demonstrate that the greatwall kinase pathway controls G1 cyclin transcription and/or mRNA stability, probably by controlling potential target candidates such as the transcription factors Xbp1 and Msa1/2. Until now, it was generally assumed that the G1 arrest caused by TORC1 dysfunction (*e.g.*, following rapamycin treatment or nitrogen starvation) was mainly due to impaired protein synthesis, a consequence of inhibition of translation initiation that specifically affects *CLN3* mRNA translation (because ribosomes need to bypass a translational repressive upstream open reading frame to reach the 5' start codon of *CLN3* open reading frame). However, more recent studies have demonstrated the existence of a more tightly programmed response to starvation for essential nutrients that is not only a general consequence of blocked translation. It has for instance been reported that auxotrophic cells starved for essential compounds (*e.g.*, leucine, uracil, inositol, or fatty acids) downregulate translation, but are not able to arrest at the G1/0 phase and therefore rapidly lose their viability (Boer et al, 2008; Saldanha et al, 2004). Such a response to a stress that is virtually inexistent in nature obviously differs from the one that cells undergo when starved for individual nutrient and which allows them to survive for prolonged periods without nutrients (Coller et al, 2006). Nevertheless, these data demonstrate that simple inhibition of translation is not sufficient to cause appropriate G1 cell cycle arrest. It has also been shown that

phosphate starvation causes downregulation of Cln3 and leads to a G1 arrest. However, cells that express a Cln3 allele with aspartic acid substitutions at residues that are directly phosphorylated by the phosphate-responsive Pho85 protein kinase do not properly arrest in G1 when starved for phosphate and die prematurely. Thus, nutrients also impinge on cell cycle event independently from their role in translation regulation. These evidences, together with the results presented within this thesis, demonstrate that entry into the quiescent G0 state requires a tightly coordinated program of responses to growth inhibitory signals such as starvation of essential nutrients that ensures proper cell cycle arrest as a result of both downregulation of protein synthesis (and more specifically translation initiation) and more direct control mechanism of nutrient signaling pathways that impinge on key cell cycle regulators.

Open questions regarding the TORC1 regulatory mechanisms in cell cycle control

Despite these novel findings, many questions need to be addressed in order to better understand the mechanism of cell cycle regulation by TORC1. Our studies have been focused particularly on the phosphorylation of the Thr¹⁷³ residue, since the stability of Sic1 and hence proper G1 arrest in rapamycin-treated cells primarily depends on it. However, although the Sic1^{S191A} allele *per se* was able to ensure normal rapamycin-induced G1 arrest *in vivo*, the stability of Sic1 was partially affected by the respective mutation and the migration pattern of the Sic1^{S191A} mutant allele in phosphate affinity gel electrophoresis analyses using extracts of rapamycin-treated cells lacked several isoforms (*i.e.* 4-6; Fig. 1.2e). In addition, combined alanine substitution of Thr¹⁷³ and Ser¹⁹¹ in Sic1 resulted in additive effects with respect to the stability of Sic1 and the defect of cells expressing this allele in arresting uniformly in G1 upon rapamycin treatment (Fig. 1.2f,e). Thus, these results suggest that phosphorylation of Ser¹⁹¹ plays a role in the control of Sic1 stability upon TORC1 inactivation. Of note, our *in vitro* kinase assays with Mpk1 did not allow us to exclude the possibility that other residues in Sic1 besides Thr¹⁷³ could be also phosphorylated. Furthermore, the Sic1-myc₁₃ migration pattern in phostag analysis in extracts from *cdc55Δ* mutant cells revealed that Cdc55 does not only dephosphorylate Thr¹⁷³, but also other additional phosphorylation sites

(Fig. 1.2c,d). Moreover, co-immunoprecipitation experiments performed in rapamycin-treated cell extracts showed that the Sic1 domain 150-190 does not interact with Cks1 whereas the variant 150-286 does (always in the presence of Thr¹⁷³). These results suggest that either the Cdk1 inhibitory domain is important for the interaction, or other residues included in the domain 190-286, such as Ser¹⁹¹, contribute to promote or stabilize this interaction. Therefore, further analysis will be needed to better understand the role of the Ser¹⁹¹ in Sic1 phosphorylation and other potential phosphorylation sites in Sic1 stability control.

Despite the well-documented importance of Sic1 inhibition of S-Cdk1 activity for cell cycle control and genome stability, the molecular mechanism by which Sic1 inhibits S-Cdk1 activity and the molecular details of the distinct Sic1/Clb interactions are not well understood. All attempts to crystallize Sic1 have failed until now (Chouard, 2011), and structural studies for the interaction between Sic1 and Clb cyclins are also lacking due to the limitations regarding the analysis of large protein complexes. The only data available so far arises from homology modeling on the basis of the X-ray structure of the mammalian counterpart p27^{Kip1}-KID-Cdk2/cyclinA, which reveals that Sic1 and p27^{Kip1} are structural and functional homologues in their kinase inhibitory domains (KIDs) (Barberis et al, 2005a).

Surface plasmon resonance experiments showed that Sic1 binds to the cyclin subunit with high affinity, followed by low affinity binding to the kinase, indicating that its inhibitory function occurs via a two-step mechanism: firstly it interacts with the docking site on the cyclin and subsequently it binds into the catalytic site of the kinase (Barberis et al, 2005a). This specificity for the docking site of the cyclin may explain Sic1 inhibition of Clb-Cdk1 complexes, but not of Cln-Cdk1 ones. However, limited available information regarding molecular mechanism of Sic1-Clb-Cdk1 inhibition arises from *in vitro* assays. These studies have not considered *in vivo* processes such as phosphorylation events ongoing on particular stress conditions that promote Sic1 stabilization and G1 cell cycle arrest, as it is the case for the subject of our study. Hence, addressing the precise molecular mechanism by which Sic1 realizes its inhibitory function on cyclin-Cdk1 complexes *in vivo* is a challenge that will provide a great insight into the comprehension of Sic1 specificity towards different cyclins and of how the timing of cell cycle progression is accomplished.

Another crucial outstanding question that could not be addressed within the frame of this thesis is whether yeast cells have access to the quiescent state only after G1 arrest. The commonly accepted conclusion is that the best stage to arrest cell growth under nutrient-limiting conditions is at G1 phase, where in response to nutrient availability, cells stop proliferation prior DNA replication or commit to a new round of cell division. However, if nutrients become limiting after cells have exit G1, TORC1 inactivation results in a delay in the entry into mitosis by slowing down cell cycle progression at G2 until more favorable conditions reappear (Nakashima et al, 2008). This seems beneficial since it prevents cells to enter into mitosis (the most energy-consuming process in cell cycle division) without the presence of sufficient nutrient levels. In addition, it has been described that cells are able to induce some responses to nutrient depletion such as increased level of stress resistance at different cell cycle stages (Wei et al, 1993). However, it is still a matter of debate whether preventing G1 arrest (*e.g.*, by expressing hyperstable G1 cyclins (Hadwiger et al, 1989b)) may prevent setting up the quiescence program. Therefore, additional experiments need to be performed to address if cells have access to quiescence through different cell cycle stages. We could use temperature-sensitive or conditionally expressible alleles that arrest cells at these different stages of the cell cycle (*cdc28* (G1), *cdc8* (S), *cdc13* (G2) and *cdc15* (M)) and analyze their ability to properly induce the distinct array of physiological traits characteristics of G0 cells (*e.g.* glycogen and trehalose accumulation and/or expression of quiescent specific genes (*e.g.* Msn2/4 and Gis1)). In addition, since Rim15 activity is essential to promote entry into G0, we could measure the *in vivo* Rim15 activity under these conditions by measuring the phosphorylation levels of its direct target Ser⁶⁴ in Igo1.

Of note, an intriguing model posits that Rim15 (or any of its downstream effectors) could be feedback-controlled by Cln/Clb-Cdk1 to restrict the cell's access to G0 to the G1 phase of the cell cycle. In agreement with this model, our preliminary results (data not shown) demonstrate that Cdk1 inactivation by 1-NM-PP1 in *cdc28Δ* mutant cells expressing *cdc28-as1* allele, results in Rim15-dependent phosphorylation of Ser⁶⁴ in Igo1, without affecting TORC1 activity. These results suggest that the cell cycle machinery may also control nutrient signaling pathways via specific feedback control mechanisms.

In higher eukaryotes, Gwl translocation from the nucleus to the cytoplasm partially depends on its phosphorylation by CycB-Cdk1 that mediates phosphorylation of Gwl in its T-loop (Yu et al, 2006) and at Thr⁵⁶² that is adjacent to the nuclear localization signal (NLS) promoting nuclear exclusion. Gwl's relocalization in prophase allows the inhibition of PP2A complexes just before nuclear envelope breakdown (NEBD). This prevents dephosphorylation of essential mitotic substrates, which avoids the mitotic collapse that has been described in cells deleted for Gwl (Alvarez-Fernandez et al, 2013). Although Rim15 (the yeast orthologue of Gwl) is also regulated regarding its nucleo-cytoplasmic localization in response to phosphorylation (Pedruzzi et al, 2003a), the molecular mechanisms are not fully understood. However, the Rim15-Igo1/2-PP2A^{Cdc55} pathway seems to play only a minor role in mitotic control in yeast (Juanes et al, 2013; Rossio & Yoshida, 2011). This could be explained by the fact that Cdk1 and PP2A do not counterbalance the same substrates (as it occurs in mitosis in higher eukaryotes) in budding yeast, where Cdc14 and not PP2A^{Cdc55} has been described to be the main protein phosphatase that antagonizes Cdk1-mediated phosphorylation events (Queralt et al, 2006; Queralt & Uhlmann, 2008). These differences could also arise from evolutionary divergences such as the NEBD that does not occur in yeast cells during mitosis. However, the molecular mechanisms regulating Rim15 and Gwl may share general features. Therefore, further studies are required to analyze whether Cdk1 is able to phosphorylate Rim15 and whether if positive, this affects its localization or activity. Hence, we envisage a possible scenario in which Cdk1-dependent phosphorylation on Rim15 may lead to its inactivation by promoting nuclear exclusion and probably sequestering it to the cytoplasm via 14-3-3 proteins.

Significance in human diseases

The importance of tight regulation of cell proliferation in response to nutrient availability is evidenced by the available body of data that indicates that disruption of G0-entry/exit control mechanisms is often associated with either dramatically reduced lifespan (of unicellular organisms) or cellular transformation (particularly in multicellular organisms). Of note, mTORC1 is implicated in several cancers and cancer predisposition hypertrophic syndromes which highlights the importance of elucidating

the conserved mechanisms that are regulated by TORC1, such as the ones presented within this thesis. More precisely, the Sic1 functional homologue p27^{Kip1} functions as a tumor suppressor protein. It has been shown that p27 knockout mice spontaneously develop tumors and present increased mortality upon treatment with carcinogenic substances (Fero et al, 1996). Studies in human cancer tissues also showed a very significant correlation between low p27 expression levels and a worse prognosis of the affected patients (Kossatz & Malek, 2007). Since almost all studies report reduced p27 expression in more aggressive tumors, p27 expression has been shown to be an independent prognosis and/or diagnostic marker (Lloyd et al, 1999).

Interestingly, in contrast to other tumor suppressor proteins (*e.g.* p53 or p16) the genomic p27 locus is rarely mutated in human cancers. Levels of p27 protein decrease in some tissues during tumor development and progression, which mainly occurs at a post-translational level by degradation of the wild type protein by the ubiquitin proteasome pathway (Hershko & Shapira, 2006; Lloyd et al, 1999). The low frequency of mutations and other genetic alterations in the p27-encoding gene seems contradictory with its role as a tumor suppressor gene. Further studies need to be performed to analyze whether there are mutations or genetic alterations in other genes leading to increased degradation of p27 during tumor progression. Due to the high similarity in the functionality and the regulatory mechanisms of p27^{Kip1} and Sic1, and to the great conservation of the Greatwall pathway in higher eukaryotes, further studies addressing the potential conservation of the regulatory mechanism highlighted in this thesis are warranted.

Materials and Methods

Growth conditions

Standard conditions

Yeast and *Escherichia coli* media were prepared according to standard recipes (Amberg et al., 2005; Sambrook and Russel, 2001) unless otherwise stated.

Saccharomyces cerevisiae yeast cells were grown at 30°C in standard rich medium (YPD, 1% yeast extract, 2% peptone, and 2% glucose) or synthetic defined medium (SD, 2% glucose, 0.67% of yeast nitrogen base, and 0.2% drop out mix) supplemented with the appropriate amino acids for maintenance of plasmids. For solid media, 2% of agar was added.

For Kan^R selection, geneticin (Brunshwig, Cat. No. BRP25-011) was added to a final concentration of 200 µg ml⁻¹. For Nat^R selection, nourseothricin (WERNER BioAgents, Cat. No. 50000) was added to a final concentration of 100 µg ml⁻¹. For Hgy^R selection, hygromycin (Sigma, Cat. No. A2636) was added to a final concentration of 300 µg ml⁻¹. Expression of genes under the control of the *Tet_{ON}* promoter was induced by adding 5 µg ml⁻¹ doxycycline to the specified medium.

E. coli bacteria cells were grown at 37°C on LB medium (1% NaCl, 1% Bactotryptone, and 0.5% yeast extract). Solid medium was supplemented with 2% agar. For Amp^R selection, ampicillin was added to a final concentration of 100 µg ml⁻¹. Plasmid manipulations were performed in *E. coli* strain DH5α (Gibco BRL) using standard procedures (Sambrook and Russel, 2001).

Rapamycin treatments

For experiments with rapamycin, cell cultures in exponentially growing phase were treated with 200 ng ml⁻¹ rapamycin. The rapamycin stock solution was prepared dissolving rapamycin powder (LC Labs, Cat. No. R-5000) in an Ethanol:Tween 20 (90:10) solution to a concentration of 1 mg ml⁻¹. For FACS analyses, cells were grown in SD medium until OD₆₀₀ of 0.4 and rapamycin was added at the indicated concentration. Samples were collected at the corresponding time points. For rapamycin recovery test, cells were cultured in liquid YPD in presence of rapamycin during 4 hours and then

harvested by centrifugation, washed twice with fresh YPD medium, and plated onto YPD medium.

Nutrient starvation

For nitrogen starvation experiments, synthetic medium with 2% glucose and 0.2% yeast nitrogen base without ammonium sulfate (USBiological) was used. Nitrogen deprivation experiments were performed with prototrophic cells growing exponentially in SD-5aa (SD containing drop out mix minus adenine, histidine, leucine, tryptophan, and uracil) until they reached an OD₆₀₀ of 0.4. Cells were collected by centrifugation, washed two times with pre-warmed SD medium lacking nitrogen source, and grown on the same medium for the indicated time points. For experiments in poor nitrogen source medium, we prepared a synthetic medium with 2% glucose, 0.2% of yeast nitrogen base without ammonium sulfate, and 625 mM of urea. For solid media, 2% agar was added to the medium.

Fluorescence-activated cell sorting and budding index analyses

For the analysis of the cell-cycle arrest promoted by rapamycin or nitrogen starvation, cultures in the exponential phase of growth were treated with 200 ng ml⁻¹ rapamycin or shifted to nitrogen-depleted media. A measure of 1.5 ml samples were collected at the indicated time points, centrifuged and resuspended in 1 ml of 70% ethanol. Following overnight incubation at 4°C, cells were washed once with H₂O, centrifuged, resuspended in 250 µl of RNase solution (50 mM Tris [pH 7.4], 200 µg ml⁻¹ RNase A [Axonlab AG]) and incubated for 3 hours at 37°C. Subsequently, cells were centrifuged again, resuspended in 250 µl of propidium iodide solution (50 mM Na⁺-citrate [pH 7.0] and 10 µg ml⁻¹ propidium iodide [Sigma]). Cellular suspensions were sonicated for 5 seconds and analyzed in a CyFlow® Space (PARTEC) flow cytometer. Data were processed using the FlowJo software. Budding indexes were calculated by analyzing microscopically the cell morphology (presence and size of the bud) scoring a minimum of 300 cells. Mean values and standard deviations were calculated from three independent experiments.

Preparation of mRNAs for Northern blot and quantitative Real-Time PCR

Yeast cells were grown exponentially until an OD₆₀₀ of 0.4 and 50 ml samples were collected at the indicated time points after rapamycin treatment or nitrogen starvation. Cells were harvested by centrifugation and washed with DEPC-H₂O. Total RNA was extracted using the hot acidic phenol method and prepared as described by (Ausubel et al., 1999).

Northern blot analyses were performed according to our standard protocol (Pedruzzi et al, 2003a). An amount of 5 µg total RNA was separated in 1% agarose gels containing 5% formaldehyde, and transferred to nitrocellulose membranes. mRNAs were detected via specific DNA probes that were labeled with ($\alpha^{32}\text{P}$)-CTP using the PRIME-IT II Random Primer labeling kit (Stratagene, Cat. No. 300385). The labeled probes were purified through a spin column by size separation (Bio-Rad, Cat. No. 7326221). The radioactive signals on the hybridized membranes were revealed using the Typhoon FLA 9400 imaging system and the supplied software (GE Healthcare).

For qRT-PCR, DNA was removed from RNA samples with the DNA-free Kit (Ambion®, Life Technologies) and first-strand cDNA was synthesized with the PrimeScript RT Reagent Kit (TaKaRa) according to the manufacturer's instructions. For quantitative real-time PCR (qRT-PCR) the Rotor-Gene SYBR Green PCR kit (Qiagen) was used. qRT-PCR were run in the Rotor-Gene Q real-time PCR cycler (Qiagen). *XBP1*, *MSA1* and *MSA2* mRNA levels were normalized with respect to *TBP1* mRNA.

NaOH extraction of proteins for immunoblot analysis

Cell culture samples of 10 ml were treated with trichloroacetic acid (TCA; final concentration of 6.66%). After centrifugation, pellets were washed with 1 ml of cold acetone and frozen at -80°C. Total protein extracts were prepared by mild alkali-treatment of cells followed by boiling in standard loading sample buffer (350 mM Tris HCl [pH 6.8], SDS 10%, Glycerol 30%, bromophenol blue 0.02%, and DTT 9.3%). Pellets were resuspended in 300 µl of solution 1 (1.85 M NaOH and 2-mercaptoethanol 7.4%).

Afterwards, 300 μ l of solution 2 (50% TCA) was added. Samples were centrifuged (5 min, 13,000 r.p.m. at 4°C) and washed with acetone. Pellets were resuspended in 50 μ l of NaOH 0.1 M and 5 μ l were kept to determine protein concentration by the Bradford assay. Finally, 45 μ l of loading sample buffer was added and samples were boiled at 95°C for 5 minutes.

SDS-polyacrylamide gel electrophoresis and immunoblot analyses were performed according to standard protocols. For the analysis of protein phosphorylation, we used 7.5% acrylamide Phos-tag™ gels, containing 25 μ M Phos-tag™ (Wako, Cat. No. AAL-107) and 25 μ M MnCl₂. After protein migration, gels were treated for 10 min with transfer buffer containing 1 mM EDTA followed by one wash of 10 min with EDTA-free transfer buffer. Protein samples were then transferred to nitrocellulose membranes (Whatman, Cat. No. GT08123). The membranes were then probed successively with the appropriate primary and secondary antibodies: anti-Sic1, (sc-50441; Santa Cruz), anti-c-Myc (9E10; sc-40; Santa Cruz), anti-Adh1 (Calbiochem), phospho-specific anti-Sic1-pThr¹⁷³ (GenScript), anti-GFP (Roche), phospho-specific anti-Igo1-pSer⁶⁴, anti-GST (Lubio), anti-HA (Enzo), phospho-specific anti-Sic1-pThr⁵ (GenScript), and phospho-specific anti-Sic1-pThr³³ (GenScript) antibodies were used at 1:1,000, 1:3,000, 1:200,000, 1:1,000, 1:3,000, 1:1,000, 1:1,000, 1:1,000, 1:1,000 and 1:1,000 dilutions, respectively. Goat anti-rabbit/anti-mouse IgG-horseradish peroxidase-conjugated antibodies (BioRad) were used at a 1:3,000 dilution.

Phospho-specific antibodies were raised against the phosphorylated peptide of Igo1-pSer⁶⁴ (H2N-KRKYFDpSGDYALQC-CONH₂), Sic1-pThr¹⁷³ (CKIHKDVPGpTPSDKV), Sic1-pThr⁵ (MTPSpTPPRSRGTRYC) and Sic1-pThr³³ (QGQKpTPQKPSQNLVC) in rabbits and purified by double-affinity purification in order to separate phospho-specific antibodies from sequence specific.

Co-immunoprecipitation

Samples of 500 ml of yeast cell culture expressing the indicated fusion proteins were harvested by centrifugation. Pellets were washed once with cold Tris-buffered saline (TBS), centrifuged and subsequently frozen in liquid nitrogen. For co-immunoprecipitation analyses with extracts from Mpk1-HA₃-expressing cells, cells were

fixed for 20 min with 1% formaldehyde and quenched with 0.3 M glycine before pellet collection.

Lysates were prepared by disruption of frozen cells in lysis buffer (50 mM Tris pH 7.5, 1 mM EDTA, 150mM NaCl, 0.5% NP40 and 1 x protease and phosphatase inhibitor cocktails [Roche]) with glass beads (0.5 mm diameter) using a Precellys® homogenizer and subsequent clarification by centrifugation (5 min at 14,000 r.p.m.; 4°C). Mpk1-HA₃ and Cks1-HA₃ were immunoprecipated with anti-HA magnetic beads (Pierce®) and co-immunoprecipitated Sic1 or Sic1^{T173A}-myc₁₃ was determined by immunoblot analysis using polyclonal anti-Sic1 or monoclonal anti-c-Myc antibodies.

Recombinant protein purification

Plasmids encoding GST or GST-fusion proteins were transformed by electroporation in *E. coli* (Rosetta™ strain). Selection of transformants was performed on LB media containing 1 mg ml⁻¹ of ampicillin and 34 µg ml⁻¹ of chloramphenicol. Cells were grown until they reached an OD₆₀₀ of 0.6 and protein expression was induced with 1 mM of isopropyl-D-thiogalactopyranoside (IPTG) for 3 hours at 37°C. Samples of 400 ml of cells were collected by centrifugation. Cells were resuspended in lysis buffer (50 mM Tris pH 7.5, 5 mM EDTA, 150 mM NaCl, and 2 mM DTT) and sonicated 3 times for 15 seconds. Afterwards, 0.1% of Triton X-100 was added. Samples were incubated on ice for 15 minutes and centrifuged (15 min at 14,000 r.p.m.; 4°C). Supernatants were incubated with 500 µl of washed glutathione-Sepharose beads (GE Healthcare Life Sciences) for 1 hour at 4°C. Beads were washed 3 times with TBS containing 0.1% Triton X-100 and 2 times with TBS. GST-fusion proteins were eluted with 500 µl of 10 mM fresh glutathione for 10 minutes at room temperature. A second elution step was performed with 500 µl of 10 mM fresh glutathione for 20 min at room temperature. The beads were resuspended with 400 µl of sample buffer to check the non-eluted proteins bound to the beads.

Mpk1 protein kinase assays

Mpk1-HA₃ and Mpk1^{K54R}-HA₃ were immunopurified from yeast cells using anti-HA

magnetic matrix (Pierce). The respective matrices were incubated for 30 min at 30 °C with 3 µl of bacterially purified GST-Sic1 or GST-Sic1^{T173A} in 50 µl of kinase buffer mix (125 mM Tris [pH 7.5], 50 mM MgCl₂, 2.5 mM dithiothreitol and 10 mM ATP). The reactions were stopped by adding loading buffer and boiling the samples at 95 °C. For the Mpk1 kinase time-course experiment, Mpk1-HA₃ was purified from exponentially growing or rapamycin-treated (1 hour) cells. The protein kinase reactions (with bacterially purified GST-Sic1 as substrate) were stopped at the indicated time points by addition of loading buffer and subsequent boiling (5 min).

PP2A^{Cdc55} protein phosphatase assay

Cdc55-HA₃ was isolated from exponentially growing *cdc55Δ* cells carrying the pRS416-*CDC55-HA₃* plasmid. Cdc55-HA₃ was immunoprecipitated from total extracts in lysis buffer (50 mM Tris [pH 7.5], 1 mM EDTA, 150 mM NaCl, 0.5% NP40, and 1 x protease and phosphatase inhibitor cocktails from Roche) using anti-HA magnetic matrix (Pierce). Igo1-GST and Igo1^{S64A}-GST were isolated from bacteria using glutathione sepharose (GE Healthcare) and phosphorylated where indicated by yeast-purified GST-Rim15-HA₃ using 1 mM adenosine 5'-[γ-thio] triphosphate. The *in vitro* phosphatase assay (30 min at 30 °C) was performed in phosphatase buffer (10 mM Tris [pH 7.5], 5 mM MgCl₂, and 1 mM EDTA) with purified PP2A^{Cdc55}, bacterially purified Sic1-GST that was phosphorylated by Mpk1 *in vitro* as substrate, and different concentrations of Igo1, which was, or was not, subjected to *in vitro* phosphorylation by Rim15 before use. To assess PP2A^{Cdc55} activity, the decrease in Sic1^{T173} phosphorylation was detected using phospho-specific anti-Sic1-pThr¹⁷³ antibodies. Levels of immunoprecipitated Cdc55-HA₃ were assessed using anti-HA antibodies.

Microscopic analyses

Mid-log phase or rapamycin-treated cells for the indicated times cultured in SD medium were imaged using an Olympus BX51 microscope (Olympus) equipped with a piezo-positioner (Olympus), a XBO 75W Xenon light source (Atlanta Light Bulbs Inc. GA), 100X 1.45 Plan-Fluar objectives, and a three-position filter sliding rack containing a

complete set of filters: U-MWIBA, U-MWIG and U-MNUA2 (Olympus). Images were acquired in 3z-section separated from 0.5 μm , projected to two-dimensional images and analyzed with the CellM software (Olympus).

Mass Spectrometry

To identify binding partners of Sic1 and Sic1^{T173A}, yeast cells were harvested by centrifugation (5 min at 4,000 r.p.m., 4°C) and washed with cold TBS. Lysates were prepared by disruption of frozen cells in lysis buffer (50 mM Tris-HCl pH 7.5, 150 mM NaCl, 1 mM EDTA, 0.5 % NonidetP40, and 1x protease and phosphatase inhibitor cocktails from Roche) using a Precellys® Homogenizer. Sic1-HA₃ and Sic1^{T173A}-HA₃ were immunoprecipitated from total lysates using anti-HA magnetic beads (Pierce®). Loading sample buffer was added to the beads and they were boiled for 5 minutes at 95°C. Samples were loaded into a 12% acrylamide gel, which was stained with Candiano colloidal Coomassie after migration. The different bands were excised and digested with trypsin. Samples were outsourced to the protein analysis facility (PAF) at the University of Lausanne, where Dr. Quadroni loaded the digested proteins into a nano-HPLC and eluted directly into a tandem mass spectrometer. Results were analyzed with the software Mascot (version 2.5.1.).

Genomic DNA preparation

Samples of 20 ml of yeast cultures grown in YPD to an OD₆₀₀ of 1.0 were collected by centrifugation (3 min at 4,000 r.p.m.) and washed with dH₂O two times. Cells were resuspended in 200 μl of breaking buffer (2% Triton X-100, 1% SDS, 100 mM NaCl, 10 mM Tris-HCl pH 8.0, and 1 mM EDTA [pH 8.0]) and 0.3 g of glass beads and 200 μl of phenol/chloroform/isoamyl alcohol (25:24:1) were added. Cells were vortexed at highest speed for 3 minutes. After vortexing, 200 μl of TE buffer (10 mM Tris-HCl [pH 7.5] and 1 mM EDTA [pH 8.0]) was added and samples were centrifuged (5 min at 13'500 r.p.m.). The aqueous layer (upper phase) was transferred to a new eppendorf tube and 1 ml of absolute ethanol was added. After centrifugation (3 min at 13'5000 r.p.m.), the supernatant was removed and the pellet resuspended in 0.4 ml of TE buffer.

Samples were treated with 30 μl of 1 mg ml⁻¹ DNase-free RNaseA mix and incubated 5 minutes at 37°C. DNA was precipitated with 10 μl of 5 M ammonium acetate and 1 ml of absolute ethanol. After centrifugation (3 min at 13'500 r.p.m.), pellets were dried and resuspended in 100 μl TE buffer. A volume of 2.5 μl was loaded into a 1% agarose gel to check the quality and quantification of DNA concentration was performed with Qubit fluorometer (Qubit® 2.0 Fluorometer).

Analysis of Next Generation Sequencing data

Samples were subjected to Next Generation Sequencing (NGS). NGS Paired-End (100 bp) reads were analyzed to remove sources of error/bias with “FastQC” filtering by quality with “Sickle”. Reads were aligned to the reference genome (R64-1-1.79) remapping the reads with “bwa”. Afterwards, the likelihood of variation at each locus was predicted based on the quality scores and allele counts of the aligned reads at that locus. SNPs and small indels were called with “Samtools” and “bcftools”, and variants were annotated using “snpEFF”. The results were filtered with “SnpSift” to keep only good quality variants that are not common to all strains and that are responsible for critical effects (Stop-Gain, Non-Synonymous, Frameshift, etc.). Finally, manual inspection of the candidate variants was performed with integrative genomic viewer (IGV) to look for genes of interest.

Supplementary Tables

Table 1. Strains Used in Chapter I

Strain	Genotype	Source	Figure
BY4741	<i>MATa; his3Δ1, leu2Δ0, met15Δ0, ura3Δ0</i>	(Brachman et al, 1998)	1A,S1
W303-1A	<i>MATa; ade2-1, trp1-1, can1-100, leu2-3,112, his3-11,15, ura3-1</i>	(Reinders et al, 1997)	1A,S1
SP1	<i>MATa; leu2, his3, trp1, ade8, ura3, can1</i>	(Toda et al, 1985)	1A,S1
JK9-3D	<i>MATa; leu2, his4, trp1, ura3, rme1, GAL, HMLa</i>	(Heitman et al, 1991)	1B, 1D-F, 1I,2A-B,2F-G,S2,S4,S6
YMM03	[SP1] <i>rim15Δ::kanMX</i>	this study	S1
YSB147	[BY4741] <i>rim15Δ::kanMX MET15</i>	(Bontron et al, 2013)	S1
CDV95-4A	[W303-1A] <i>rim15Δ::kanMX</i>	this study	S1
IP11	[JK9-3D] <i>rim15Δ::kanMX</i>	(Pedruzzi et al, 2003b)	1CF,1I,2A,S2
YMM57-2A	[JK9-3D] <i>igo1Δ::natMX, igo2Δ::Hph-NT1</i>	this study	1C-F,1I,2A
YMM59	[JK9-3D] <i>CLN1-myc₁₃::kanMX</i>	this study	1F-G
YMM60	[JK9-3D] <i>CLN2-myc₁₃::kanMX</i>	this study	1F-G
YMM61	[JK9-3D] <i>CLN3-myc₁₃::kanMX</i>	this study	1F,1H
YMM87-2D	[JK9-3D] <i>rim15Δ::kanMX, CLN1-myc₁₃::kanMX</i>	this study	1F-G
YMM88-12B	[JK9-3D] <i>rim15Δ::kanMX, CLN2-myc₁₃::kanMX</i>	this study	1F-G
YMM78-2A	[JK9-3D] <i>rim15Δ::kanMX, CLN3-myc₁₃::kanMX</i>	this study	1F,1H
YMM85-5D	[JK9-3D] <i>igo1Δ::natMX, igo2Δ::Hph-NT1, CLN1-myc₁₃::kanMX</i>	this study	1F-G
YMM79-9A	[JK9-3D] <i>igo1Δ::natMX, igo2Δ::Hph-NT1, CLN2-myc₁₃::kanMX</i>	this study	1F-G
YMM80-5C	[JK9-3D] <i>igo1Δ::natMX, igo2Δ::Hph-NT1, CLN3-myc₁₃::kanMX</i>	this study	1F,1H
YMM55-1C	[JK9-3D] <i>rim15Δ::kanMX, cdc55Δ::natMX</i>	this study	2A
YMM90-3D	[JK9-3D] <i>igo1Δ::natMX, igo2Δ::Hph-NT1, cdc55Δ::natMX</i>	this study	2A
YMM46	[JK9-3D] <i>cdc55Δ::natMX</i>	this study	2A,5A
YMM98	[JK9-3D] <i>sic1^{T173A}-myc₁₃::kanMX, EMP46::natMX</i>	this study	2C-E,S3
YMM143-2A	[JK9-3D] <i>sic1^{T173A}-myc₁₃::kanMX, cdc55Δ::natMX, EMP46::natMX</i>	this study	S3
YMM63	[JK9-3D] <i>SIC1-myc₁₃::kanMX</i>	this study	2C-E,S3
YMM68-9D	[JK9-3D] <i>rim15Δ::kanMX, SIC1-myc₁₃::kanMX</i>	this study	2C-D
YMM70-6B	[JK9-3D] <i>igo1Δ::natMX, igo2Δ::Hph-NT1, SIC1-myc₁₃::kanMX</i>	this study	2C-D
YMM69-1C	[JK9-3D] <i>cdc55Δ::natMX, SIC1-myc₁₃::kanMX</i>	this study	2C-D,S3
YMM100-9D	[JK9-3D] <i>rim15Δ::kanMX, cdc55Δ::natMX, SIC1-myc₁₃::kanMX</i>	this study	2C-D
YMM96	[JK9-3D] <i>igo1Δ::natMX, igo2Δ::Hph-NT1, cdc55Δ::natMX, SIC1-myc₁₃::kanMX</i>	this study	2C-D
YMM91	[JK9-3D] <i>sic1^{T173A}, EMP46::natMX</i>	this study	2F-G,S2,S4
YMM101	[JK9-3D] <i>sic1^{S191A}, EMP46::natMX</i>	this study	2F-G,S4
YMM103	[JK9-3D] <i>sic1^{T173A S191A}, EMP46::natMX</i>	this study	2F-G,S4
YMM105	[JK9-3D] <i>sic1^{S191A}-myc₁₃::kanMX, EMP46::natMX</i>	this study	2E
YMM133	[JK9-3D] <i>sic1^{T173A S191A}-myc₁₃::kanMX, EMP46::natMX</i>	this study	2E

YMM114	[JK9-3D] <i>cdc4-2::kanMX</i>	this study	3A-B,S5
YMM117-3A	[JK9-3D] <i>rim15Δ::kanMX, cdc4-2::kanMX</i>	this study	3A-B,S5
YMM116-4A	[JK9-3D] <i>igo1Δ::natMX, igo2Δ::Hph-NT1, cdc4-2::kanMX</i>	this study	3A-B,S5
YMM118-2D	[JK9-3D] <i>sic1^{T173A}, EMP46::natMX, cdc4-2::kanMX</i>	this study	3A-B
YMM77	[JK9-3D] <i>SIC1-GFP(S65T)::kanMX</i>	this study	3C-D
YMM97-7B	[JK9-3D] <i>rim15Δ::kanMX, SIC1-GFP(S65T)::kanMX</i>	this study	3C
YMM99	[JK9-3D] <i>sic1^{T173A}-GFP(S65T)::kanMX</i>	this study	3C-D
YMM67-1C	[JK9-3D] <i>sic1Δ::kanMX</i>	this study	2A
YMM53	[JK9-3D] <i>mpk1Δ::kanMX</i>	this study	4C-F,S6
YMM65-2D	[JK9-3D] <i>mpk1Δ::kanMX, SIC1-myc₁₃::kanMX</i>	this study	4A-B
YMM204-14C	[JK9-3D] <i>hog1Δ::kanMX, SIC1-myc₁₃::kanMX</i>	this study	4A-B
YMM64-3C	[JK9-3D] <i>rim15Δ::kanMX, mpk1Δ::kanMX</i>	this study	4F
YMM111-2A	[JK9-3D] <i>igo1Δ::natMX, igo2Δ::Hph-NT1, mpk1Δ::kanMX</i>	this study	4F
YMM130	[JK9-3D] <i>hog1Δ::kanMX</i>	this study	S6

Table 2. Plasmids Used in Chapter I

Plasmid	Genotype	Source	Figure
pRS416	<i>CEN/ARS, URA3</i>	(Brachmann et al, 1998)	1B
pMM5	[pRS416] <i>RME1</i>	this study	1B
p1308	[pRS414]	(Brachmann et al, 1998)	1D,2D
p1309	[pRS415]	(Brachmann et al, 1998)	1D,2D
p1310	[pRS416]	(Brachmann et al, 1998)	1D, 2D
pMM10	[pRS415] <i>HIS4</i>	this study	1D,2D
pSB004	[pRS416] <i>ADHIp-CDC55</i>	(Bontron et al, 2013)	2A-B
p834	[pRS416] <i>ADHIp</i>	(Mumberg et al, 1995)	2A-B
pMM6	[pRS416] <i>MPK1-HA₃</i>	this study	4C-E
pMM7	[pRS416] <i>mpk1^{K54R}-HA₃</i>	this study	4C
pMM8	pGEX- <i>SIC1</i>	this study	4C-D,5A
pMM9	pGEX- <i>sic1^{T173A}</i>	this study	4C
pMJA2610	[pRS416] <i>CDC55-HA₃</i>	this study	5A
pCDV487	pHAC195- <i>GAL1-GST-RIM15, 2 μ,URA3</i>	(Pedruzzi et al, 2003b)	5A
pLC1092	pGEX- <i>IGO1</i>	(Talarek et al, 2010)	5A
pLC1134	pGEX- <i>igo1^{S64A}</i>	(Talarek et al, 2010)	5A

Table 3. Strains Used in Chapter II

Strain	Genotype	Source	Figure
JK9-3D	<i>MATα; leu2, his4, trp1, ura3, rme1, GAL,HMLα</i>	(Heitman et al, 1991)	4A,4B,5B
MP348-3C	[BY4742] <i>MATα; lst7Δ::kanMX</i>	(Peli-Gulli et al, 2015)	1A
SIC1-HA	[JK9-3D] <i>SIC1-HA$_3$::kanMX</i>	this study	1A,
SIC1TA-HA	[JK9-3D] <i>sic1^{T173A}-HA$_3$::kanMX, EMP46::natMX</i>	this study	1A,
MJA490	[JK9-3D] <i>CKS1-HA$_3$::kanMX</i>	this study	1B,1C,1D, 2B,3B-C
MJA491	[JK9-3D] <i>CKS1-HA$_3$::kanMX, sic1^{T173A}, EMP46::natMX</i>	this study	1B,1C,1D
YMM230-8A	[JK9-3D] <i>CKS1-HA$_3$::kanMX, cdc55Δ::natMX</i>	this study	1C,1D
YMM231-1A	[JK9-3D] <i>CKS1-HA$_3$::kanMX, mpk1Δ::kanMX</i>	this study	1C,1D
YMM114	[JK9-3D] <i>cdc4-2::kanMX</i>	this study	5A,6
YMM118-2D	[JK9-3D] <i>sic1^{T173A}, EMP46::natMX, cdc4-2::kanMX</i>	this study	5A,6
YMM67-1C	[JK9-3D] <i>sic1Δ::kanMX</i>	this study	5A,6A,6B
MJA 4090	[JK9-3D] <i>cdc4-2::kanMX, CLB5-HA$_3$::kanMX</i>	this study	7A,7B
MJA 4091	[JK9-3D] <i>cdc4-2::kanMX, CLB5-HA$_3$::kanMX, sic1^{T173A}, EMP46::natMX</i>	this study	7A,7B

Table 4. Plasmids Used in Chapter II

Plasmid	Genotype	Source	Figure
p2576	[pRS414] <i>LST7p-LST7-HA$_3$-CYC1ter</i>	MP.Peli-Gulli	1A
p2879	[pRS415] <i>ADH1p-sic1 (150-190)-myc$_{13}$</i>	this study	2A,2B
p2880	[pRS415] <i>ADH1p-sic1^{T173A} (150-190)-myc$_{13}$</i>	this study	2A,2B
p2881	[pRS415] <i>ADH1p-sic1 (1-285)-myc$_{13}$</i>	this study	2A,2B,3A,3 B,3C
p2882	[pRS415] <i>ADH1p-sic1^{T173A} (1-285)-myc$_{13}$</i>	this study	2A,2B,
p2883	[pRS415] <i>ADH1p-sic1 (1-150)-myc$_{13}$</i>	this study	2A,2B,
p2884	[pRS415] <i>ADH1p-sic1 (1-41)-myc$_{13}$</i>	this study	2A,2B,
p2886	[pRS415] <i>ADH1p-sic1^{T2A T5A T33A} (1-41)-myc$_{13}$</i>	this study	2A,2B,
p2993	[pRS415] <i>ADH1p-sic1^{R262A L264A} (150-285)-myc$_{13}$</i>	this study	3A,3B,3C
p2994	[pRS415] <i>ADH1p-sic1^{T173A R262A L264A} (150-285)-myc$_{13}$</i>	this study	3A,3B,3C
p2995	[pRS415] <i>ADH1p-sic1 (150-285)-myc$_{13}$</i>	this study	3A,3B,3C
p2996	[pRS415] <i>ADH1p-sic1^{T173A} (150-285)-myc$_{13}$</i>	this study	3A,3B,3C
p2919	[YCplac111] <i>ADH1p-sic1 (1-215)-myc$_{13}$</i>	this study	4A,4B
p2920	[YCplac111] <i>ADH1p-sic1^{T173A} (1-215)-myc$_{13}$</i>	this study	4A,4B
p2921	[YCplac111] <i>ADH1p-sic1^{T2A T5A T33A T45A S69A S76A S80A} (1-215)-myc$_{13}$</i>	this study	4A,4B
p2922	[YCplac111] <i>ADH1p-sic1^{T2A T5A T33A T45A S69A S76A S80A T173A} (1-215)-myc$_{13}$</i>	this study	4A,4B

Table 5. Strains Used in Chapter III

Strain	Genotype	Source	Figure
MJA457	[JK9-3D] <i>XBP1-myc₁₃::kanMX</i>	this study	2A-B,3A-D,7A-D
MJA477-B2	[JK9-3D] <i>rim15Δ::kanMX, XBP1-myc₁₃::kanMX</i>	this study	2A-B,3A-D
YMM195-12C	[JK9-3D] <i>igo1Δ::natMX, igo2Δ::kanMX, XBP1-myc₁₃::kanMX</i>	this study	2A-B
YMM159-3B	[JK9-3D] <i>cdc55Δ::natMX, XBP1-myc₁₃::kanMX</i>	this study	3A-D
YMM158-2B	[JK9-3D] <i>rim15Δ::kanMX, cdc55Δ::natMX, XBP1-myc₁₃::kanMX</i>	this study	3A-B
YMM195-7B	[JK9-3D] <i>igo1Δ::natMX, igo2Δ::kanMX, cdc55Δ::natMX, XBP1-myc₁₃::kanMX</i>	this study	3C-D
JK9-3D	<i>MATa; leu2, his4, trp1, ura3, rme1, GAL, HMLa</i>	reference(H eitman et al, 1991)	4A-B,5A-B,6A-B,9C-D,12C,13
IP11	[JK9-3D] <i>rim15Δ::kanMX</i>	(Pedruzzi et al, 2003a)	4A-B,5A-B,6A-B,9C-D,12C
YMM96	[JK9-3D] <i>igo1Δ::natMX, igo2Δ::Hph-NT1</i>	this study	4A-B,5A-B,6A-B,9C-D
YMM57-2A	[JK9-3D] <i>cdc55Δ::natMX</i>	this study	4A-B
YMM55-1C	[JK9-3D] <i>rim15Δ::kanMX, cdc55Δ::natMX</i>	this study	4A-B
YMM90-3D	[JK9-3D] <i>igo1Δ::natMX, igo2Δ::Hph-NT1, cdc55Δ::natMX</i>	this study	4A-B
YMM186-9D	[JK9-3D] <i>gis1Δ::natMX, XBP1-myc₁₃::kanMX</i>	this study	7A-B,
YMM211-7A	[JK9-3D] <i>msn2Δ::natMX, msn4Δ::kanMX, gis1Δ::natMX, XBP1-myc₁₃::kanMX</i>	this study	7C-D
MJA455	[JK9-3D] <i>MSA2-myc₁₃::kanMX</i>	this study	8A-D
MJA469-2B	[JK9-3D] <i>rim15Δ::kanMX, MSA2-myc₁₃::kanMX</i>	this study	8A-D
MJA472-14C	[JK9-3D] <i>igo1Δ::natMX, igo2Δ::Hph-NT1, MSA2-myc₁₃::kanMX</i>	this study	8A-D
MJA451	[JK9-3D] <i>MSA1-myc₁₃::kanMX</i>	this study	9A-B
MJA462-A2	[JK9-3D] <i>rim15Δ::kanMX, MSA1-myc₁₃::kanMX</i>	this study	9A-B
YMM183-2C	[JK9-3D] <i>cdc55Δ::natMX, MSA1-myc₁₃::kanMX</i>	this study	9A-B
YMM218-8A	[JK9-3D] <i>rim15Δ::kanMX, cdc55Δ::natMX, MSA1-myc₁₃::kanMX</i>	this study	9A-B
MJA457	[JK9-3D] <i>WHI5-HA₃::kanMX</i>	this study	10A-B
MJA474-D2	[JK9-3D] <i>rim15Δ::kanMX, WHI5-HA₃::kanMX</i>	this study	10A-B
MJA475-C2	[JK9-3D] <i>igo1Δ::natMX, igo2Δ::Hph-NT1, WHI5-HA₃::kanMX</i>	this study	10A-B
YMM196-1C	[JK9-3D] <i>STB1-myc₁₃::kanMX</i>	this study	11A-C
YMM199-4A	[JK9-3D] <i>rim15Δ::kanMX, STB1-myc₁₃::kanMX</i>	this study	11A-C
YMM200-2A	[JK9-3D] <i>igo1Δ::natMX, igo2Δ::Hph-NT1, STB1-myc₁₃::kanMX</i>	this study	11A-C
YMM234-6A	[JK9-3D] <i>cdc55Δ::natMX, STB1-myc₁₃::kanMX</i>	this study	11C
YMM210-6C	[JK9-3D] <i>rim15Δ::kanMX, cdc55Δ::natMX, STB1-myc₁₃::kanMX</i>	this study	11C
YMM225-8B	[JK9-3D] <i>igo1Δ::natMX, igo2Δ::Hph-NT1, cdc55Δ::natMX, STB1-myc₁₃::kanMX</i>	this study	11C
YMM172-2C	[JK9-3D] <i>NRM1-myc₁₃::kanMX</i>	this study	12A-B
YMM189-4C	[JK9-3D] <i>rim15Δ::kanMX, NRM1-myc₁₃::kanMX</i>	this study	12A-B
YMM190-3B	[JK9-3D] <i>igo1Δ::natMX, igo2Δ::Hph-NT1, NRM1-myc₁₃::kanMX</i>	this study	12A-B

Material and Methods

YMM171-3D	[JK9-3D] <i>nrm1Δ::kanMX</i>	this study	12C
YMM208-2D	[JK9-3D] <i>rim15Δ::kanMX, nrm1Δ::kanMX</i>	this study	12C
YMM151-1C	[JK9-3D] <i>msa1Δ::natMX</i>	this study	13
YMM152-1B	[JK9-3D] <i>msa2Δ::kanMX</i>	this study	13
YMM153-1C	[JK9-3D] <i>xbp1Δ::natMX</i>	this study	13
YMM187-3B	[JK9-3D] <i>xbp1Δ::natMX, sic1^{T173A}, EMP46::natMX</i>	this study	13
YMM229-5D	[JK9-3D] <i>msa1Δ::natMX, msa2Δ::kanMX, sic1^{T173A}, EMP46::natMX</i>	this study	13
YMM185-7B	[JK9-3D] <i>xbp1Δ::natMX, msa1Δ::natMX, msa2Δ::kanMX</i>	this study	13
YMM212-7D	[JK9-3D] <i>xbp1Δ::natMX, msa1Δ::natMX, msa2Δ::kanMX, sic1^{T173A}, EMP46::natMX</i>	this study	13

Table 6. Plasmids Used in Chapter III

Plasmid	Genotype	Source	Figure
p1308	[pRS414]	(Brachman n et al, 1998)	2B,4B,8B, 10B,13
p1309	[pRS415]	(Brachman n et al, 1998)	2B,4B,8B, 10B,13
p1310	[pRS416]	(Brachman n et al, 1998)	2B,4B,8B, 10B,13
pMM10	[pRS415] <i>HIS4</i>	this study	2B,4B,8B, 10B,13
pMM15	[pRS416] <i>ADH1p-XBP1-HA₃</i>	this study	5A-B
p2416	[pRS416] <i>ADH1p-HA₃</i>	S. Bontron	5A-B
pMM16	[pRS416] <i>UBI4p-XBP1-HA₃</i>	this study	6A-B
p222	[YCplac33] <i>UBI4p</i>	this study	6A-B

Table 7. Strains Used in Chapter IV

Strain	Genotype	Source	Figure
BY4741	<i>MATa; his3Δ1, leu2Δ0, met15Δ0, ura3Δ0</i>	(Brachmann et al, 1998)	1,2A-C,2E,3A-D,4A-B
JK9-3D	<i>MATa; leu2, his4, trp1, ura3, rme1, GAL, HMLa</i>	(Heitman et al, 1991)	1,2A-E,3A-E,4A-B
JK9-3D	<i>MATa/α, leu2/leu2, his4/his4, trp1/trp1, ura3/ura3, rme1/rme1, GAL/GAL</i>	this study	1,3E,4A-B
YMM47-1A	[JK9-3D] <i>MATα; leu2, his4, trp1, ura3, rme1, GAL, HMLa</i>	this study	1
YMM235	[JK9-3D] <i>MATa; leu2, his4, trp1, URA3, rme1, GAL, HMLa</i>	this study	3A,3B,3E
YMM236	[JK9-3D] <i>MATa; leu2, HIS4, trp1, ura3, rme1, GAL, HMLa</i>	this study	3A,3B,3E
MP02-1B	[BY4741] <i>gtr1Δ::kanMX</i>	MP.Peli-Gulli	1
IP11	[JK9-3D] <i>rim15Δ::kanMX</i>	this study	1
IP39	[JK9-3D] <i>MATa/α, leu2/leu2, his4/his4, trp1/trp1, ura3/ura3, rme1/rme1, GAL HMLa, rim15Δ::kanMX/RIM15</i>	I.Pedruzzi	1
YMM194	[JK9-3D] <i>MATα, fpr1Δ::kanMX, URA3</i>	this study	3C,3E,4A-B
YMM193	[JK9-3D] <i>MATa, fpr1Δ::kanMX, HIS4</i>	this study	3D-E,4A-B
<i>fpr1Δ/FPR1</i>	<i>MATa/α, leu2/leu2, his4/his4, trp1/trp1, ura3/ura3, rme1/rme1, GAL/GAL, fpr1Δ::kanMX/FPR1</i>	this study	3E

Table 8. Plasmids Used in Chapter IV

Plasmid	Genotype	Source	Figure
p2744	[pRS416] <i>GTR1p-GTR1^{Q65L}-GFP-ALP</i>	K.Powis	2A
p1284	[pCM252] <i>Tet_{ON}-GTR1^{Q65L}</i>	M.Binda	2B
p1394	[YCplac33] <i>Tet_{ON}-GTR1^{Q65L}</i>	(Binda et al, 2009)	2C
p1623	[YCplac111] <i>Tet_{ON}-GTR2^{S23L}</i>	(Bonfils et al, 2012)	2C
p2317	[YCplac111] <i>EGO1p-EGO1-HA₃</i>	F.Jaquier	2D
p2680	[YCplac111] <i>EGO2p-HA₂-EGO2</i>	K.Powis	2D
p2521	[YCplac111] <i>ADH1p-EGO3-His₆-TEV-ProtA</i>	N. Panchaud	2D
p1485	[pRS315] <i>HA₃-TOR1^{A1957V}</i>	(Reinke et al, 2006)	2E
p1486	[pRS315] <i>HA₃-TOR1^{I1954V}</i>	(Reinke et al, 2006)	2E
p1310	[pRS416]	(Brachman et al, 1998)	2A
p1272	[pCM252]	(Belli et al, 1998)	2B
p101	[YCplac33]	R.Gietz	2C
p102	[YCplac111]	R.Gietz	2C,2D
p127	[pRS315]	P.Hieter	2E

References

- Adrover MA, Zi Z, Duch A, Schaber J, Gonzalez-Novo A, Jimenez J, Nadal-Ribelles M, Clotet J, Klipp E, Posas F (2011) Time-dependent quantitative multicomponent control of the G(1)-S network by the stress-activated protein kinase Hog1 upon osmostress. *Sci Signal* **4**: ra63
- Aerne BL, Johnson AL, Toyn JH, Johnston LH (1998) Swi5 controls a novel wave of cyclin synthesis in late mitosis. *Mol Biol Cell* **9**: 945-956
- Alarcon CM, Heitman J, Cardenas ME (1999) Protein kinase activity and identification of a toxic effector domain of the target of rapamycin TOR proteins in yeast. *Mol Biol Cell* **10**: 2531-2546
- Alberghina L, Rossi RL, Querin L, Wanke V, Vanoni M (2004) A cell sizer network involving Cln3 and Far1 controls entrance into S phase in the mitotic cycle of budding yeast. *J Cell Biol* **167**: 433-443
- Albrecht M, Lengauer T (2004) Novel Sm-like proteins with long C-terminal tails and associated methyltransferases. *FEBS Lett* **569**: 18-26
- Alessi DR, Kulathu Y (2013) Structural biology: Security measures of a master regulator. *Nature* **497**: 193-194
- Allen C, Buttner S, Aragon AD, Thomas JA, Meirelles O, Jaetao JE, Benn D, Ruby SW, Veenhuis M, Madeo F, Werner-Washburne M (2006) Isolation of quiescent and nonquiescent cells from yeast stationary-phase cultures. *J Cell Biol* **174**: 89-100
- Alvarez-Fernandez M, Sanchez-Martinez R, Sanz-Castillo B, Gan PP, Sanz-Flores M, Trakala M, Ruiz-Torres M, Lorca T, Castro A, Malumbres M (2013) Greatwall is essential to prevent mitotic collapse after nuclear envelope breakdown in mammals. *Proc Natl Acad Sci U S A* **110**: 17374-17379
- Amberg, D.C., Burke, D.J. and Strathern, J.N. (2005) *Methods in Yeast Genetics* (Cold Spring Harbor, Cold Spring Harbor Laboratory Press)
- Amon A, Tyers M, Futcher B, Nasmyth K (1993) Mechanisms that help the yeast cell cycle clock tick: G2 cyclins transcriptionally activate G2 cyclins and repress G1 cyclins. *Cell* **74**: 993-1007
- Araki T, Uesono Y, Oguchi T, Toh EA (2005) LAS24/KOG1, a component of the TOR complex 1 (TORC1), is needed for resistance to local anesthetic tetracaine and normal distribution of actin cytoskeleton in yeast. *Genes Genet Syst* **80**: 325-343
- Archambault V, Li CX, Tackett AJ, Wasch R, Chait BT, Rout MP, Cross FR (2003) Genetic and biochemical evaluation of the importance of Cdc6 in regulating mitotic exit. *Mol Biol Cell* **14**: 4592-4604

- Aronova S, Wedaman K, Anderson S, Yates J, 3rd, Powers T (2007) Probing the membrane environment of the TOR kinases reveals functional interactions between TORC1, actin, and membrane trafficking in *Saccharomyces cerevisiae*. *Mol Biol Cell* **18**: 2779-2794
- Aronova S, Wedaman K, Aronov PA, Fontes K, Ramos K, Hammock BD, Powers T (2008) Regulation of ceramide biosynthesis by TOR complex 2. *Cell Metab* **7**: 148-158
- Arvai AS, Bourne Y, Hickey MJ, Tainer JA (1995) Crystal structure of the human cell cycle protein CksHs1: single domain fold with similarity to kinase N-lobe domain. *J Mol Biol* **249**: 835-842
- Asano S, Park JE, Sakchaisri K, Yu LR, Song S, Supavilai P, Veenstra TD, Lee KS (2005) Concerted mechanism of Swe1/Wee1 regulation by multiple kinases in budding yeast. *EMBO J* **24**: 2194-2204
- Ashe M, de Bruin RA, Kalashnikova T, McDonald WH, Yates JR, 3rd, Wittenberg C (2008) The SBF- and MBF-associated protein Msa1 is required for proper timing of G1-specific transcription in *Saccharomyces cerevisiae*. *J Biol Chem* **283**: 6040-6049
- Averous J, Fonseca BD, Proud CG (2008) Regulation of cyclin D1 expression by mTORC1 signaling requires eukaryotic initiation factor 4E-binding protein 1. *Oncogene* **27**: 1106-1113
- Aylett CH, Sauer E, Imseng S, Boehringer D, Hall MN, Ban N, Maier T (2016) Architecture of human mTOR complex 1. *Science* **351**: 48-52
- Bailly E, Cabantous S, Sondaz D, Bernadac A, Simon MN (2003) Differential cellular localization among mitotic cyclins from *Saccharomyces cerevisiae*: a new role for the axial budding protein Bud3 in targeting Clb2 to the mother-bud neck. *J Cell Sci* **116**: 4119-4130
- Baisch H (1988) Different quiescence states of three culture cell lines detected by acridine orange staining of cellular RNA. *Cytometry* **9**: 325-331
- Balog ER, Saetern OC, Finch W, Hoeft CO, Thai V, Harvey SL, Kellogg DR, Rubin SM (2011) The structure of a monomeric mutant Cks protein reveals multiple functions for a conserved hinge-region proline. *J Mol Biol* **411**: 520-528
- Barberis M (2012) Sic1 as a timer of Clb cyclin waves in the yeast cell cycle--design principle of not just an inhibitor. *FEBS J* **279**: 3386-3410
- Barberis M, Beck C, Amoussouvi A, Schreiber G, Diener C, Herrmann A, Klipp E (2011) A low number of SIC1 mRNA molecules ensures a low noise level in cell cycle progression of budding yeast. *Mol Biosyst* **7**: 2804-2812
- Barberis M, De Gioia L, Ruzzene M, Sarno S, Coccetti P, Fantucci P, Vanoni M, Alberghina L (2005a) The yeast cyclin-dependent kinase inhibitor Sic1 and mammalian p27Kip1

are functional homologues with a structurally conserved inhibitory domain. *Biochem J* **387**: 639-647

Barberis M, Klipp E, Vanoni M, Alberghina L (2007) Cell size at S phase initiation: an emergent property of the G1/S network. *PLoS Comput Biol* **3**: e64

Barberis M, Pagano MA, Gioia LD, Marin O, Vanoni M, Pinna LA, Alberghina L (2005b) CK2 regulates in vitro the activity of the yeast cyclin-dependent kinase inhibitor Sic1. *Biochem Biophys Res Commun* **336**: 1040-1048

Barbet NC, Schneider U, Helliwell SB, Stansfield I, Tuite MF, Hall MN (1996) TOR controls translation initiation and early G1 progression in yeast. *Mol Biol Cell* **7**: 25-42

Bardwell L (2005) A walk-through of the yeast mating pheromone response pathway. *Peptides* **26**: 339-350

Barral Y, Mann C (1995) [G1 cyclin degradation and cell differentiation in *Saccharomyces cerevisiae*]. *C R Acad Sci III* **318**: 43-50

Basco RD, Segal MD, Reed SI (1995) Negative regulation of G1 and G2 by S-phase cyclins of *Saccharomyces cerevisiae*. *Mol Cell Biol* **15**: 5030-5042

Basi G, Draetta G (1995) p13^{suc1} of *Schizosaccharomyces pombe* regulates two distinct forms of the mitotic cdc2 kinase. *Mol Cell Biol* **15**: 2028-2036

Beck T, Hall MN (1999) The TOR signalling pathway controls nuclear localization of nutrient-regulated transcription factors. *Nature* **402**: 689-692

Belli G, Gari E, Piedrafita L, Aldea M, Herrero E (1998) An activator/repressor dual system allows tight tetracycline-regulated gene expression in budding yeast. *Nucleic Acids Res* **26**: 942-947

Berchtold D, Walther TC (2009) TORC2 plasma membrane localization is essential for cell viability and restricted to a distinct domain. *Mol Biol Cell* **20**: 1565-1575

Berry DB, Gasch AP (2008) Stress-activated genomic expression changes serve a preparative role for impending stress in yeast. *Mol Biol Cell* **19**: 4580-4587

Besson A, Gurian-West M, Chen X, Kelly-Spratt KS, Kemp CJ, Roberts JM (2006) A pathway in quiescent cells that controls p27^{Kip1} stability, subcellular localization, and tumor suppression. *Genes Dev* **20**: 47-64

Bettencourt-Dias M, Giet R, Sinka R, Mazumdar A, Lock WG, Balloux F, Zafiroopoulos PJ, Yamaguchi S, Winter S, Carthew RW, Cooper M, Jones D, Frenz L, Glover DM (2004) Genome-wide survey of protein kinases required for cell cycle progression. *Nature* **432**: 980-987

- Binda M, Peli-Gulli MP, Bonfils G, Panchaud N, Urban J, Sturgill TW, Loewith R, De Virgilio C (2009) The Vam6 GEF controls TORC1 by activating the EGO complex. *Mol Cell* **35**: 563-573
- Bisschops MM, Zwartjens P, Keuter SG, Pronk JT, Daran-Lapujade P (2014) To divide or not to divide: a key role of Rim15 in calorie-restricted yeast cultures. *Biochim Biophys Acta* **1843**: 1020-1030
- Blake-Hodek KA, Williams BC, Zhao Y, Castilho PV, Chen W, Mao Y, Yamamoto TM, Goldberg ML (2012) Determinants for activation of the atypical AGC kinase Greatwall during M phase entry. *Mol Cell Biol* **32**: 1337-1353
- Blondel M, Alepuz PM, Huang LS, Shaham S, Ammerer G, Peter M (1999) Nuclear export of Far1p in response to pheromones requires the export receptor Msn5p/Ste21p. *Genes Dev* **13**: 2284-2300
- Blondel M, Galan JM, Chi Y, Lafourcade C, Longaretti C, Deshaies RJ, Peter M (2000) Nuclear-specific degradation of Far1 is controlled by the localization of the F-box protein Cdc4. *EMBO J* **19**: 6085-6097
- Bloom J, Cross FR (2007) Multiple levels of cyclin specificity in cell-cycle control. *Nat Rev Mol Cell Biol* **8**: 149-160
- Boer VM, Amini S, Botstein D (2008) Influence of genotype and nutrition on survival and metabolism of starving yeast. *Proc Natl Acad Sci U S A* **105**: 6930-6935
- Bonfils G, Jaquenoud M, Bontron S, Ostrowicz C, Ungermann C, De Virgilio C (2012) Leucyl-tRNA synthetase controls TORC1 via the EGO complex. *Mol Cell* **46**: 105-110
- Bontron S, Jaquenoud M, Vaga S, Talarek N, Bodenmiller B, Aebersold R, De Virgilio C (2013) Yeast endosulfines control entry into quiescence and chronological life span by inhibiting protein phosphatase 2A. *Cell Rep* **3**: 16-22
- Borg M, Mittag T, Pawson T, Tyers M, Forman-Kay JD, Chan HS (2007) Polyelectrostatic interactions of disordered ligands suggest a physical basis for ultrasensitivity. *Proc Natl Acad Sci U S A* **104**: 9650-9655
- Botstein D, Chervitz SA, Cherry JM (1997) Yeast as a model organism. *Science* **277**: 1259-1260
- Bourne Y, Watson MH, Arvai AS, Bernstein SL, Reed SI, Tainer JA (2000) Crystal structure and mutational analysis of the *Saccharomyces cerevisiae* cell cycle regulatory protein Cks1: implications for domain swapping, anion binding and protein interactions. *Structure* **8**: 841-850
- Bourne Y, Watson MH, Hickey MJ, Holmes W, Rocque W, Reed SI, Tainer JA (1996) Crystal structure and mutational analysis of the human CDK2 kinase complex with cell cycle-regulatory protein CksHs1. *Cell* **84**: 863-874

- Brachmann CB, Davies A, Cost GJ, Caputo E, Li J, Hieter P, Boeke JD (1998) Designer deletion strains derived from *Saccharomyces cerevisiae* S288C: a useful set of strains and plasmids for PCR-mediated gene disruption and other applications. *Yeast* **14**: 115-132
- Brizuela L, Draetta G, Beach D (1987) p13^{suc1} acts in the fission yeast cell division cycle as a component of the p34^{cdc2} protein kinase. *EMBO J* **6**: 3507-3514
- Brocca S, Samalikova M, Uversky VN, Lotti M, Vanoni M, Alberghina L, Grandori R (2009) Order propensity of an intrinsically disordered protein, the cyclin-dependent-kinase inhibitor Sic1. *Proteins* **76**: 731-746
- Brocca S, Testa L, Samalikova M, Grandori R, Lotti M (2011) Defining structural domains of an intrinsically disordered protein: Sic1, the cyclin-dependent kinase inhibitor of *Saccharomyces cerevisiae*. *Mol Biotechnol* **47**: 34-42
- Burgess A, Vigneron S, Brioudes E, Labbe JC, Lorca T, Castro A (2010) Loss of human Greatwall results in G2 arrest and multiple mitotic defects due to deregulation of the cyclin B-Cdc2/PP2A balance. *Proc Natl Acad Sci U S A* **107**: 12564-12569
- Butty AC, Pryciak PM, Huang LS, Herskowitz I, Peter M (1998) The role of Far1p in linking the heterotrimeric G protein to polarity establishment proteins during yeast mating. *Science* **282**: 1511-1516
- Calzada A, Sacristan M, Sanchez E, Bueno A (2001) Cdc6 cooperates with Sic1 and Hct1 to inactivate mitotic cyclin-dependent kinases. *Nature* **412**: 355-358
- Calzada A, Sanchez M, Sanchez E, Bueno A (2000) The stability of the Cdc6 protein is regulated by cyclin-dependent kinase/cyclin B complexes in *Saccharomyces cerevisiae*. *J Biol Chem* **275**: 9734-9741
- Cameron IL, Bols NC (1975) Effect of cell population density on G2 arrest in *Tetrahymena*. *J Cell Biol* **67**: 518-522
- Cameroni E, Hulo N, Roosen J, Winderickx J, De Virgilio C (2004) The novel yeast PAS kinase Rim 15 orchestrates G0-associated antioxidant defense mechanisms. *Cell Cycle* **3**: 462-468
- Cardenas ME, Cutler NS, Lorenz MC, Di Como CJ, Heitman J (1999) The TOR signaling cascade regulates gene expression in response to nutrients. *Genes Dev* **13**: 3271-3279
- Cardenas ME, Heitman J (1995) FKBP12-rapamycin target TOR2 is a vacuolar protein with an associated phosphatidylinositol-4 kinase activity. *EMBO J* **14**: 5892-5907
- Chang F, Herskowitz I (1990) Identification of a gene necessary for cell cycle arrest by a negative growth factor of yeast: FAR1 is an inhibitor of a G1 cyclin, CLN2. *Cell* **63**: 999-1011

- Chaves S, Baskerville C, Yu V, Reed SI (2010) Cks1, Cdk1, and the 19S proteasome collaborate to regulate gene induction-dependent nucleosome eviction in yeast. *Mol Cell Biol* **30**: 5284-5294
- Chen J, Jackson PK, Kirschner MW, Dutta A (1995) Separate domains of p21 involved in the inhibition of Cdk kinase and PCNA. *Nature* **374**: 386-388
- Cheng M, Olivier P, Diehl JA, Fero M, Roussel MF, Roberts JM, Sherr CJ (1999) The p21(Cip1) and p27(Kip1) CDK 'inhibitors' are essential activators of cyclin D-dependent kinases in murine fibroblasts. *EMBO J* **18**: 1571-1583
- Chica N, Rozalen AE, Perez-Hidalgo L, Rubio A, Novak B, Moreno S (2016) Nutritional Control of Cell Size by the Greatwall-Endosulfine-PP2A.B55 Pathway. *Curr Biol*
- Cho RJ, Campbell MJ, Winzeler EA, Steinmetz L, Conway A, Wodicka L, Wolfsberg TG, Gabrielian AE, Landsman D, Lockhart DJ, Davis RW (1998) A genome-wide transcriptional analysis of the mitotic cell cycle. *Mol Cell* **2**: 65-73
- Chouard T (2011) Structural biology: Breaking the protein rules. *Nature* **471**: 151-153
- Chu IM, Hengst L, Slingerland JM (2008) The Cdk inhibitor p27 in human cancer: prognostic potential and relevance to anticancer therapy. *Nat Rev Cancer* **8**: 253-267
- Cid VJ, Jimenez J, Molina M, Sanchez M, Nombela C, Thorner JW (2002) Orchestrating the cell cycle in yeast: sequential localization of key mitotic regulators at the spindle pole and the bud neck. *Microbiology* **148**: 2647-2659
- Clotet J, Posas F (2007) Control of cell cycle in response to osmotic stress: lessons from yeast. *Methods Enzymol* **428**: 63-76
- Cocchetti P, Rossi RL, Sternieri F, Porro D, Russo GL, di Fonzo A, Magni F, Vanoni M, Alberghina L (2004) Mutations of the CK2 phosphorylation site of Sic1 affect cell size and S-Cdk kinase activity in *Saccharomyces cerevisiae*. *Mol Microbiol* **51**: 447-460
- Cocchetti P, Zinzalla V, Tedeschi G, Russo GL, Fantinato S, Marin O, Pinna LA, Vanoni M, Alberghina L (2006) Sic1 is phosphorylated by CK2 on Ser201 in budding yeast cells. *Biochem Biophys Res Commun* **346**: 786-793
- Coller HA, Sang L, Roberts JM (2006) A new description of cellular quiescence. *PLoS Biol* **4**: e83
- Coller J, Parker R (2005) General translational repression by activators of mRNA decapping. *Cell* **122**: 875-886
- Costanzo M, Nishikawa JL, Tang X, Millman JS, Schub O, Breitkreuz K, Dewar D, Rupes I, Andrews B, Tyers M (2004) CDK activity antagonizes Whi5, an inhibitor of G1/S transcription in yeast. *Cell* **117**: 899-913

- Costanzo M, Schub O, Andrews B (2003) G1 transcription factors are differentially regulated in *Saccharomyces cerevisiae* by the Swi6-binding protein Stb1. *Mol Cell Biol* **23**: 5064-5077
- Crespo JL, Hall MN (2002) Elucidating TOR signaling and rapamycin action: lessons from *Saccharomyces cerevisiae*. *Microbiol Mol Biol Rev* **66**: 579-591, table of contents
- Cross FR (2003) Two redundant oscillatory mechanisms in the yeast cell cycle. *Dev Cell* **4**: 741-752
- Cross FR, Blake CM (1993) The yeast Cln3 protein is an unstable activator of Cdc28. *Mol Cell Biol* **13**: 3266-3271
- Cross FR, Schroeder L, Bean JM (2007) Phosphorylation of the Sic1 inhibitor of B-type cyclins in *Saccharomyces cerevisiae* is not essential but contributes to cell cycle robustness. *Genetics* **176**: 1541-1555
- Cross FR, Tinkelenberg AH (1991) A potential positive feedback loop controlling CLN1 and CLN2 gene expression at the start of the yeast cell cycle. *Cell* **65**: 875-883
- Cybulski N, Hall MN (2009) TOR complex 2: a signaling pathway of its own. *Trends Biochem Sci* **34**: 620-627
- Dahmann C, Diffley JF, Nasmyth KA (1995) S-phase-promoting cyclin-dependent kinases prevent re-replication by inhibiting the transition of replication origins to a pre-replicative state. *Curr Biol* **5**: 1257-1269
- de Bruin RA, Kalashnikova TI, Aslanian A, Wohlschlegel J, Chahwan C, Yates JR, 3rd, Russell P, Wittenberg C (2008) DNA replication checkpoint promotes G1-S transcription by inactivating the MBF repressor Nrm1. *Proc Natl Acad Sci U S A* **105**: 11230-11235
- de Bruin RA, Kalashnikova TI, Chahwan C, McDonald WH, Wohlschlegel J, Yates J, 3rd, Russell P, Wittenberg C (2006) Constraining G1-specific transcription to late G1 phase: the MBF-associated corepressor Nrm1 acts via negative feedback. *Mol Cell* **23**: 483-496
- de Bruin RA, McDonald WH, Kalashnikova TI, Yates J, 3rd, Wittenberg C (2004) Cln3 activates G1-specific transcription via phosphorylation of the SBF bound repressor Whi5. *Cell* **117**: 887-898
- De Craene JO, Soetens O, Andre B (2001) The Npr1 kinase controls biosynthetic and endocytic sorting of the yeast Gap1 permease. *J Biol Chem* **276**: 43939-43948
- De Virgilio C (2012) The essence of yeast quiescence. *FEMS Microbiol Rev* **36**: 306-339
- De Virgilio C, Loewith R (2006) Cell growth control: little eukaryotes make big contributions. *Oncogene* **25**: 6392-6415

- DeSalle LM, Pagano M (2001) Regulation of the G1 to S transition by the ubiquitin pathway. *FEBS Lett* **490**: 179-189
- Deshaies RJ (1997) Phosphorylation and proteolysis: partners in the regulation of cell division in budding yeast. *Curr Opin Genet Dev* **7**: 7-16
- Devasahayam G, Ritz D, Helliwell SB, Burke DJ, Sturgill TW (2006) Pmr1, a Golgi Ca²⁺/Mn²⁺-ATPase, is a regulator of the target of rapamycin (TOR) signaling pathway in yeast. *Proc Natl Acad Sci U S A* **103**: 17840-17845
- Di Como CJ, Arndt KT (1996) Nutrients, via the Tor proteins, stimulate the association of Tap42 with type 2A phosphatases. *Genes Dev* **10**: 1904-1916
- Di Talia S, Skotheim JM, Bean JM, Siggia ED, Cross FR (2007) The effects of molecular noise and size control on variability in the budding yeast cell cycle. *Nature* **448**: 947-951
- Dirick L, Bohm T, Nasmyth K (1995) Roles and regulation of Cln-Cdc28 kinases at the start of the cell cycle of *Saccharomyces cerevisiae*. *EMBO J* **14**: 4803-4813
- Dirick L, Goetsch L, Ammerer G, Byers B (1998) Regulation of meiotic S phase by Ime2 and a Clb5,6-associated kinase in *Saccharomyces cerevisiae*. *Science* **281**: 1854-1857
- Donaldson AD, Blow JJ (1999) The regulation of replication origin activation. *Curr Opin Genet Dev* **9**: 62-68
- Doncic A, Falleur-Fettig M, Skotheim JM (2011) Distinct interactions select and maintain a specific cell fate. *Mol Cell* **43**: 528-539
- Donovan JD, Toyn JH, Johnson AL, Johnston LH (1994) P40SDB25, a putative CDK inhibitor, has a role in the M/G1 transition in *Saccharomyces cerevisiae*. *Genes Dev* **8**: 1640-1653
- Draetta G, Brizuela L, Potashkin J, Beach D (1987) Identification of p34 and p13, human homologs of the cell cycle regulators of fission yeast encoded by *cdc2+* and *suc1+*. *Cell* **50**: 319-325
- Drewinko B, Yang LY, Barlogie B, Trujillo JM (1984) Cultured human tumour cells may be arrested in all stages of the cycle during stationary phase: demonstration of quiescent cells in G1, S and G2 phase. *Cell Tissue Kinet* **17**: 453-463
- Drury LS, Perkins G, Diffley JF (1997) The Cdc4/34/53 pathway targets Cdc6p for proteolysis in budding yeast. *EMBO J* **16**: 5966-5976
- Dubouloz F, Deloche O, Wanke V, Cameroni E, De Virgilio C (2005) The TOR and EGO protein complexes orchestrate microautophagy in yeast. *Mol Cell* **19**: 15-26

- Dulubova I, Horiuchi A, Snyder GL, Girault JA, Czernik AJ, Shao L, Ramabhadran R, Greengard P, Nairn AC (2001) ARPP-16/ARPP-19: a highly conserved family of cAMP-regulated phosphoproteins. *J Neurochem* **77**: 229-238
- Edgington NP, Futcher B (2001) Relationship between the function and the location of G1 cyclins in *S. cerevisiae*. *J Cell Sci* **114**: 4599-4611
- Elion EA, Satterberg B, Kranz JE (1993) FUS3 phosphorylates multiple components of the mating signal transduction cascade: evidence for STE12 and FAR1. *Mol Biol Cell* **4**: 495-510
- Elledge SJ (1996) Cell cycle checkpoints: preventing an identity crisis. *Science* **274**: 1664-1672
- Elsasser S, Lou F, Wang B, Campbell JL, Jong A (1996) Interaction between yeast Cdc6 protein and B-type cyclin/Cdc28 kinases. *Mol Biol Cell* **7**: 1723-1735
- Epstein CB, Cross FR (1992) CLB5: a novel B cyclin from budding yeast with a role in S phase. *Genes Dev* **6**: 1695-1706
- Escote X, Zapater M, Clotet J, Posas F (2004) Hog1 mediates cell-cycle arrest in G1 phase by the dual targeting of Sic1. *Nat Cell Biol* **6**: 997-1002
- Eser U, Falleur-Fettig M, Johnson A, Skotheim JM (2011) Commitment to a cellular transition precedes genome-wide transcriptional change. *Mol Cell* **43**: 515-527
- Espinoza FH, Farrell A, Erdjument-Bromage H, Tempst P, Morgan DO (1996) A cyclin-dependent kinase-activating kinase (CAK) in budding yeast unrelated to vertebrate CAK. *Science* **273**: 1714-1717
- Evans T, Rosenthal ET, Youngblom J, Distel D, Hunt T (1983) Cyclin: a protein specified by maternal mRNA in sea urchin eggs that is destroyed at each cleavage division. *Cell* **33**: 389-396
- Fadri M, Daquinag A, Wang S, Xue T, Kunz J (2005) The pleckstrin homology domain proteins Slm1 and Slm2 are required for actin cytoskeleton organization in yeast and bind phosphatidylinositol-4,5-bisphosphate and TORC2. *Mol Biol Cell* **16**: 1883-1900
- Fang G, Yu H, Kirschner MW (1998) Direct binding of CDC20 protein family members activates the anaphase-promoting complex in mitosis and G1. *Mol Cell* **2**: 163-171
- Feldman RM, Correll CC, Kaplan KB, Deshaies RJ (1997) A complex of Cdc4p, Skp1p, and Cdc53p/cullin catalyzes ubiquitination of the phosphorylated CDK inhibitor Sic1p. *Cell* **91**: 221-230
- Fero ML, Rivkin M, Tasch M, Porter P, Carow CE, Firpo E, Polyak K, Tsai LH, Broudy V, Perlmutter RM, Kaushansky K, Roberts JM (1996) A syndrome of multiorgan

- hyperplasia with features of gigantism, tumorigenesis, and female sterility in p27(Kip1)-deficient mice. *Cell* **85**: 733-744
- Fingar DC, Richardson CJ, Tee AR, Cheatham L, Tsou C, Blenis J (2004) mTOR controls cell cycle progression through its cell growth effectors S6K1 and 4E-BP1/eukaryotic translation initiation factor 4E. *Mol Cell Biol* **24**: 200-216
- Fitch I, Dahmann C, Surana U, Amon A, Nasmyth K, Goetsch L, Byers B, Futcher B (1992) Characterization of four B-type cyclin genes of the budding yeast *Saccharomyces cerevisiae*. *Mol Biol Cell* **3**: 805-818
- Fleischer TC, Weaver CM, McAfee KJ, Jennings JL, Link AJ (2006) Systematic identification and functional screens of uncharacterized proteins associated with eukaryotic ribosomal complexes. *Genes Dev* **20**: 1294-1307
- Forsburg SL, Nurse P (1991) Cell cycle regulation in the yeasts *Saccharomyces cerevisiae* and *Schizosaccharomyces pombe*. *Annu Rev Cell Biol* **7**: 227-256
- Fry AM, Yamano H (2006) APC/C-mediated degradation in early mitosis: how to avoid spindle assembly checkpoint inhibition. *Cell Cycle* **5**: 1487-1491
- Fu X, Ng C, Feng D, Liang C (2003) Cdc48p is required for the cell cycle commitment point at Start via degradation of the G1-CDK inhibitor Far1p. *J Cell Biol* **163**: 21-26
- Funabiki H, Yamano H, Kumada K, Nagao K, Hunt T, Yanagida M (1996) Cut2 proteolysis required for sister-chromatid separation in fission yeast. *Nature* **381**: 438-441
- Galdieri L, Mehrotra S, Yu S, Vancura A (2010) Transcriptional regulation in yeast during diauxic shift and stationary phase. *OMICS* **14**: 629-638
- Gander S, Bonenfant D, Altermatt P, Martin DE, Hauri S, Moes S, Hall MN, Jenoe P (2008) Identification of the rapamycin-sensitive phosphorylation sites within the Ser/Thr-rich domain of the yeast Npr1 protein kinase. *Rapid Commun Mass Spectrom* **22**: 3743-3753
- Ganoth D, Bornstein G, Ko TK, Larsen B, Tyers M, Pagano M, Hershko A (2001) The cell-cycle regulatory protein Cks1 is required for SCF(Skp2)-mediated ubiquitinylation of p27. *Nat Cell Biol* **3**: 321-324
- Gao M, Kaiser CA (2006) A conserved GTPase-containing complex is required for intracellular sorting of the general amino-acid permease in yeast. *Nat Cell Biol* **8**: 657-667
- Gari E, Volpe T, Wang H, Gallego C, Futcher B, Aldea M (2001) Whi3 binds the mRNA of the G1 cyclin CLN3 to modulate cell fate in budding yeast. *Genes Dev* **15**: 2803-2808
- Gaubitz C, Oliveira TM, Prouteau M, Leitner A, Karuppasamy M, Konstantinidou G, Rispal D, Eltschinger S, Robinson GC, Thore S, Aebersold R, Schaffitzel C, Loewith R

(2015) Molecular Basis of the Rapamycin Insensitivity of Target Of Rapamycin Complex 2. *Mol Cell* **58**: 977-988

Gharbi-Ayachi A, Labbe JC, Burgess A, Vigneron S, Strub JM, Brioude E, Van-Dorselaer A, Castro A, Lorca T (2010) The substrate of Greatwall kinase, Arpp19, controls mitosis by inhibiting protein phosphatase 2A. *Science* **330**: 1673-1677

Ghiara JB, Richardson HE, Sugimoto K, Henze M, Lew DJ, Wittenberg C, Reed SI (1991) A cyclin B homolog in *S. cerevisiae*: chronic activation of the Cdc28 protein kinase by cyclin prevents exit from mitosis. *Cell* **65**: 163-174

Glotzer M, Murray AW, Kirschner MW (1991) Cyclin is degraded by the ubiquitin pathway. *Nature* **349**: 132-138

Goffeau A, Barrell BG, Bussey H, Davis RW, Dujon B, Feldmann H, Galibert F, Hoheisel JD, Jacq C, Johnston M, Louis EJ, Mewes HW, Murakami Y, Philippsen P, Tettelin H, Oliver SG (1996) Life with 6000 genes. *Science* **274**: 546, 563-547

Gonzalez-Novo A, Jimenez J, Clotet J, Nadal-Ribelles M, Caverio S, de Nadal E, Posas F (2015) Hog1 targets Whi5 and Msa1 transcription factors to downregulate cyclin expression upon stress. *Mol Cell Biol* **35**: 1606-1618

Gould KL, Nurse P (1989) Tyrosine phosphorylation of the fission yeast cdc2+ protein kinase regulates entry into mitosis. *Nature* **342**: 39-45

Gray JV, Petsko GA, Johnston GC, Ringe D, Singer RA, Werner-Washburne M (2004) "Sleeping beauty": quiescence in *Saccharomyces cerevisiae*. *Microbiol Mol Biol Rev* **68**: 187-206

Hadwiger JA, Wittenberg C, Mendenhall MD, Reed SI (1989a) The *Saccharomyces cerevisiae* CKS1 gene, a homolog of the *Schizosaccharomyces pombe* suc1+ gene, encodes a subunit of the Cdc28 protein kinase complex. *Mol Cell Biol* **9**: 2034-2041

Hadwiger JA, Wittenberg C, Richardson HE, de Barros Lopes M, Reed SI (1989b) A family of cyclin homologs that control the G1 phase in yeast. *Proc Natl Acad Sci U S A* **86**: 6255-6259

Hao B, Oehlmann S, Sowa ME, Harper JW, Pavletich NP (2007) Structure of a Fbw7-Skp1-cyclin E complex: multisite-phosphorylated substrate recognition by SCF ubiquitin ligases. *Mol Cell* **26**: 131-143

Hara K, Maruki Y, Long X, Yoshino K, Oshiro N, Hidayat S, Tokunaga C, Avruch J, Yonezawa K (2002) Raptor, a binding partner of target of rapamycin (TOR), mediates TOR action. *Cell* **110**: 177-189

Harper JW, Elledge SJ, Keyomarsi K, Dynlacht B, Tsai LH, Zhang P, Dobrowolski S, Bai C, Connell-Crowley L, Swindell E, et al. (1995) Inhibition of cyclin-dependent kinases by p21. *Mol Biol Cell* **6**: 387-400

- Hartmuth S, Petersen J (2009) Fission yeast Tor1 functions as part of TORC1 to control mitotic entry through the stress MAPK pathway following nutrient stress. *J Cell Sci* **122**: 1737-1746
- Hartwell LH, Culotti J, Pringle JR, Reid BJ (1974) Genetic control of the cell division cycle in yeast. *Science* **183**: 46-51
- Hartwell LH, Unger MW (1977) Unequal division in *Saccharomyces cerevisiae* and its implications for the control of cell division. *J Cell Biol* **75**: 422-435
- Hashemolhosseini S, Nagamine Y, Morley SJ, Desrivieres S, Mercep L, Ferrari S (1998) Rapamycin inhibition of the G1 to S transition is mediated by effects on cyclin D1 mRNA and protein stability. *J Biol Chem* **273**: 14424-14429
- Hayles J, Beach D, Durkacz B, Nurse P (1986) The fission yeast cell cycle control gene *cdc2*: isolation of a sequence *suc1* that suppresses *cdc2* mutant function. *Mol Gen Genet* **202**: 291-293
- Heim A, Konietzny A, Mayer TU (2015) Protein phosphatase 1 is essential for Greatwall inactivation at mitotic exit. *EMBO Rep* **16**: 1501-1510
- Heitman J, Movva NR, Hall MN (1991) Targets for cell cycle arrest by the immunosuppressant rapamycin in yeast. *Science* **253**: 905-909
- Henchoz S, Chi Y, Catarin B, Herskowitz I, Deshaies RJ, Peter M (1997) Phosphorylation- and ubiquitin-dependent degradation of the cyclin-dependent kinase inhibitor Far1p in budding yeast. *Genes Dev* **11**: 3046-3060
- Hershko A, Ciechanover A (1998) The ubiquitin system. *Annu Rev Biochem* **67**: 425-479
- Hershko DD, Shapira M (2006) Prognostic role of p27Kip1 deregulation in colorectal cancer. *Cancer* **107**: 668-675
- Herskowitz I (1988) Life cycle of the budding yeast *Saccharomyces cerevisiae*. *Microbiol Rev* **52**: 536-553
- Hleb M, Murphy S, Wagner EF, Hanna NN, Sharma N, Park J, Li XC, Strom TB, Padbury JF, Tseng YT, Sharma S (2004) Evidence for cyclin D3 as a novel target of rapamycin in human T lymphocytes. *J Biol Chem* **279**: 31948-31955
- Ho Y, Costanzo M, Moore L, Kobayashi R, Andrews BJ (1999) Regulation of transcription at the *Saccharomyces cerevisiae* start transition by Stb1, a Swi6-binding protein. *Mol Cell Biol* **19**: 5267-5278
- Hodge A, Mendenhall M (1999) The cyclin-dependent kinase inhibitory domain of the yeast Sic1 protein is contained within the C-terminal 70 amino acids. *Mol Gen Genet* **262**: 55-64

- Holic R, Kukalev A, Lane S, Andress EJ, Lau I, Yu CW, Edelman MJ, Kessler BM, Yu VP (2010) Cks1 activates transcription by binding to the ubiquitylated proteasome. *Mol Cell Biol* **30**: 3894-3901
- Holloway SL, Glotzer M, King RW, Murray AW (1993) Anaphase is initiated by proteolysis rather than by the inactivation of maturation-promoting factor. *Cell* **73**: 1393-1402
- Hood JK, Hwang WW, Silver PA (2001) The *Saccharomyces cerevisiae* cyclin Clb2p is targeted to multiple subcellular locations by cis- and trans-acting determinants. *J Cell Sci* **114**: 589-597
- Horak CE, Snyder M (2002) Global analysis of gene expression in yeast. *Funct Integr Genomics* **2**: 171-180
- Huang D, Friesen H, Andrews B (2007) Pho85, a multifunctional cyclin-dependent protein kinase in budding yeast. *Mol Microbiol* **66**: 303-314
- Huebert DJ, Kuan PF, Keles S, Gasch AP (2012) Dynamic changes in nucleosome occupancy are not predictive of gene expression dynamics but are linked to transcription and chromatin regulators. *Mol Cell Biol* **32**: 1645-1653
- Inui N, Kitagawa K, Miwa S, Hattori T, Chida K, Nakamura H, Kitagawa M (2003) High expression of Cks1 in human non-small cell lung carcinomas. *Biochem Biophys Res Commun* **303**: 978-984
- Irniger S, Piatti S, Michaelis C, Nasmyth K (1995) Genes involved in sister chromatid separation are needed for B-type cyclin proteolysis in budding yeast. *Cell* **81**: 269-278
- Irwin N, Chao S, Goritchenko L, Horiuchi A, Greengard P, Nairn AC, Benowitz LI (2002) Nerve growth factor controls GAP-43 mRNA stability via the phosphoprotein ARPP-19. *Proc Natl Acad Sci U S A* **99**: 12427-12431
- Jackson LP, Reed SI, Haase SB (2006) Distinct mechanisms control the stability of the related S-phase cyclins Clb5 and Clb6. *Mol Cell Biol* **26**: 2456-2466
- Jeffrey PD, Russo AA, Polyak K, Gibbs E, Hurwitz J, Massague J, Pavletich NP (1995) Mechanism of CDK activation revealed by the structure of a cyclinA-CDK2 complex. *Nature* **376**: 313-320
- Jeoung DI, Oehlen LJ, Cross FR (1998) Cln3-associated kinase activity in *Saccharomyces cerevisiae* is regulated by the mating factor pathway. *Mol Cell Biol* **18**: 433-441
- Jiang Y, Broach JR (1999) Tor proteins and protein phosphatase 2A reciprocally regulate Tap42 in controlling cell growth in yeast. *EMBO J* **18**: 2782-2792

- Jong A, Young M, Chen GC, Zhang SQ, Chan C (1996) Intracellular location of the *Saccharomyces cerevisiae* CDC6 gene product. *DNA Cell Biol* **15**: 883-895
- Jorgensen P, Tyers M (1999) Altered states: programmed proteolysis and the budding yeast cell cycle. *Curr Opin Microbiol* **2**: 610-617
- Juanes MA, Khoueir R, Kupka T, Castro A, Mudrak I, Ogris E, Lorca T, Piatti S (2013) Budding yeast greatwall and endosulfines control activity and spatial regulation of PP2A(Cdc55) for timely mitotic progression. *PLoS Genet* **9**: e1003575
- Juang YL, Huang J, Peters JM, McLaughlin ME, Tai CY, Pellman D (1997) APC-mediated proteolysis of Ase1 and the morphogenesis of the mitotic spindle. *Science* **275**: 1311-1314
- Kaiser P, Moncollin V, Clarke DJ, Watson MH, Bertolaet BL, Reed SI, Bailly E (1999) Cyclin-dependent kinase and Cks/Suc1 interact with the proteasome in yeast to control proteolysis of M-phase targets. *Genes Dev* **13**: 1190-1202
- Kaiser P, Sia RA, Bardes EG, Lew DJ, Reed SI (1998) Cdc34 and the F-box protein Met30 are required for degradation of the Cdk-inhibitory kinase Swe1. *Genes Dev* **12**: 2587-2597
- Kaldis P, Sutton A, Solomon MJ (1996) The Cdk-activating kinase (CAK) from budding yeast. *Cell* **86**: 553-564
- Keaton MA, Lew DJ (2006) Eavesdropping on the cytoskeleton: progress and controversy in the yeast morphogenesis checkpoint. *Curr Opin Microbiol* **9**: 540-546
- Keith CT, Schreiber SL (1995) PIK-related kinases: DNA repair, recombination, and cell cycle checkpoints. *Science* **270**: 50-51
- Kellogg DR (2003) Wee1-dependent mechanisms required for coordination of cell growth and cell division. *J Cell Sci* **116**: 4883-4890
- Khazanovich N, Bateman K, Chernaia M, Michalak M, James M (1996) Crystal structure of the yeast cell-cycle control protein, p13suc1, in a strand-exchanged dimer. *Structure* **4**: 299-309
- Kim DH, Sarbassov DD, Ali SM, King JE, Latek RR, Erdjument-Bromage H, Tempst P, Sabatini DM (2002) mTOR interacts with raptor to form a nutrient-sensitive complex that signals to the cell growth machinery. *Cell* **110**: 163-175
- Kim S, Yu H (2011) Mutual regulation between the spindle checkpoint and APC/C. *Semin Cell Dev Biol* **22**: 551-558
- Kishi T, Ikeda A, Koyama N, Fukada J, Nagao R (2008) A refined two-hybrid system reveals that SCF(Cdc4)-dependent degradation of Swi5 contributes to the regulatory mechanism of S-phase entry. *Proc Natl Acad Sci U S A* **105**: 14497-14502

- Kitajima S, Kudo Y, Ogawa I, Bashir T, Kitagawa M, Miyauchi M, Pagano M, Takata T (2004) Role of Cks1 overexpression in oral squamous cell carcinomas: cooperation with Skp2 in promoting p27 degradation. *Am J Pathol* **165**: 2147-2155
- Kitamura K, Maekawa H, Shimoda C (1998) Fission yeast Ste9, a homolog of Hct1/Cdh1 and Fizzy-related, is a novel negative regulator of cell cycle progression during G1-phase. *Mol Biol Cell* **9**: 1065-1080
- Klosinska MM, Crutchfield CA, Bradley PH, Rabinowitz JD, Broach JR (2011) Yeast cells can access distinct quiescent states. *Genes Dev* **25**: 336-349
- Knapp D, Bhoite L, Stillman DJ, Nasmyth K (1996) The transcription factor Swi5 regulates expression of the cyclin kinase inhibitor p40SIC1. *Mol Cell Biol* **16**: 5701-5707
- Kobayashi H, Stewart E, Poon R, Adamczewski JP, Gannon J, Hunt T (1992) Identification of the domains in cyclin A required for binding to, and activation of, p34cdc2 and p32cdk2 protein kinase subunits. *Mol Biol Cell* **3**: 1279-1294
- Kobayashi H, Stewart E, Poon RY, Hunt T (1994) Cyclin A and cyclin B dissociate from p34cdc2 with half-times of 4 and 15 h, respectively, regardless of the phase of the cell cycle. *J Biol Chem* **269**: 29153-29160
- Kogan K, Spear ED, Kaiser CA, Fass D (2010) Structural conservation of components in the amino acid sensing branch of the TOR pathway in yeast and mammals. *J Mol Biol* **402**: 388-398
- Koivomagi M, Valk E, Venta R, Iofik A, Lepiku M, Balog ER, Rubin SM, Morgan DO, Loog M (2011a) Cascades of multisite phosphorylation control Sic1 destruction at the onset of S phase. *Nature* **480**: 128-131
- Koivomagi M, Valk E, Venta R, Iofik A, Lepiku M, Morgan DO, Loog M (2011b) Dynamics of Cdk1 substrate specificity during the cell cycle. *Mol Cell* **42**: 610-623
- Kossatz U, Malek NP (2007) p27: tumor suppressor and oncogene ...? *Cell Res* **17**: 832-833
- Kosugi S, Hasebe M, Tomita M, Yanagawa H (2009) Systematic identification of cell cycle-dependent yeast nucleocytoplasmic shuttling proteins by prediction of composite motifs. *Proc Natl Acad Sci U S A* **106**: 10171-10176
- Krek W, Nigg EA (1991) Differential phosphorylation of vertebrate p34cdc2 kinase at the G1/S and G2/M transitions of the cell cycle: identification of major phosphorylation sites. *EMBO J* **10**: 305-316
- Kunz J, Schneider U, Howald I, Schmidt A, Hall MN (2000) HEAT repeats mediate plasma membrane localization of Tor2p in yeast. *J Biol Chem* **275**: 37011-37020

- Kuranda K, Leberre V, Sokol S, Palamarczyk G, Francois J (2006) Investigating the caffeine effects in the yeast *Saccharomyces cerevisiae* brings new insights into the connection between TOR, PKC and Ras/cAMP signalling pathways. *Mol Microbiol* **61**: 1147-1166
- LaBaer J, Garrett MD, Stevenson LF, Slingerland JM, Sandhu C, Chou HS, Fattaey A, Harlow E (1997) New functional activities for the p21 family of CDK inhibitors. *Genes Dev* **11**: 847-862
- Lambrugh M, Papaleo E, Testa L, Brocca S, De Gioia L, Grandori R (2012) Intramolecular interactions stabilizing compact conformations of the intrinsically disordered kinase-inhibitor domain of Sic1: a molecular dynamics investigation. *Front Physiol* **3**: 435
- Landry BD, Doyle JP, Toczyski DP, Benanti JA (2012) F-box protein specificity for g1 cyclins is dictated by subcellular localization. *PLoS Genet* **8**: e1002851
- Lanker S, Valdivieso MH, Wittenberg C (1996) Rapid degradation of the G1 cyclin Cln2 induced by CDK-dependent phosphorylation. *Science* **271**: 1597-1601
- Laporte D, Lebaudy A, Sahin A, Pinson B, Ceschin J, Daignan-Fornier B, Sagot I (2011) Metabolic status rather than cell cycle signals control quiescence entry and exit. *J Cell Biol* **192**: 949-957
- Lee M, O'Regan S, Moreau JL, Johnson AL, Johnston LH, Goding CR (2000) Regulation of the Pcl7-Pho85 cyclin-cdk complex by Pho81. *Mol Microbiol* **38**: 411-422
- Lee P, Kim MS, Paik SM, Choi SH, Cho BR, Hahn JS (2013) Rim15-dependent activation of Hsf1 and Msn2/4 transcription factors by direct phosphorylation in *Saccharomyces cerevisiae*. *FEBS Lett* **587**: 3648-3655
- Lengronne A, Schwob E (2002) The yeast CDK inhibitor Sic1 prevents genomic instability by promoting replication origin licensing in late G(1). *Mol Cell* **9**: 1067-1078
- Leung-Pineda V, Pan Y, Chen H, Kilberg MS (2004) Induction of p21 and p27 expression by amino acid deprivation of HepG2 human hepatoma cells involves mRNA stabilization. *Biochem J* **379**: 79-88
- Lew DJ (2003) The morphogenesis checkpoint: how yeast cells watch their figures. *Curr Opin Cell Biol* **15**: 648-653
- Lew DJ, Reed SI (1993) Morphogenesis in the yeast cell cycle: regulation by Cdc28 and cyclins. *J Cell Biol* **120**: 1305-1320
- Li JM, Tetzlaff MT, Elledge SJ (2008) Identification of MSA1, a cell cycle-regulated, dosage suppressor of *drc1/sld2* and *dpb11* mutants. *Cell Cycle* **7**: 3388-3398

- Li X, Cai M (1997) Inactivation of the cyclin-dependent kinase Cdc28 abrogates cell cycle arrest induced by DNA damage and disassembly of mitotic spindles in *Saccharomyces cerevisiae*. *Mol Cell Biol* **17**: 2723-2734
- Liakopoulos D, Kusch J, Grava S, Vogel J, Barral Y (2003) Asymmetric loading of Kar9 onto spindle poles and microtubules ensures proper spindle alignment. *Cell* **112**: 561-574
- Lillie SH, Pringle JR (1980) Reserve carbohydrate metabolism in *Saccharomyces cerevisiae*: responses to nutrient limitation. *J Bacteriol* **143**: 1384-1394
- Lim HH, Surana U (1996) Cdc20, a beta-transducin homologue, links RAD9-mediated G2/M checkpoint control to mitosis in *Saccharomyces cerevisiae*. *Mol Gen Genet* **253**: 138-148
- Lin J, Reichner C, Wu X, Levine AJ (1996) Analysis of wild-type and mutant p21WAF-1 gene activities. *Mol Cell Biol* **16**: 1786-1793
- Lloyd RV, Erickson LA, Jin L, Kulig E, Qian X, Cheville JC, Scheithauer BW (1999) p27kip1: a multifunctional cyclin-dependent kinase inhibitor with prognostic significance in human cancers. *Am J Pathol* **154**: 313-323
- Loewith R, Jacinto E, Wullschleger S, Lorberg A, Crespo JL, Bonenfant D, Oppliger W, Jenoe P, Hall MN (2002) Two TOR complexes, only one of which is rapamycin sensitive, have distinct roles in cell growth control. *Mol Cell* **10**: 457-468
- Lopez-Aviles S, Kapuy O, Novak B, Uhlmann F (2009) Irreversibility of mitotic exit is the consequence of systems-level feedback. *Nature* **459**: 592-595
- Lorca T, Castro A, Martinez AM, Vigneron S, Morin N, Sigrist S, Lehner C, Doree M, Labbe JC (1998) Fizzy is required for activation of the APC/cyclosome in *Xenopus* egg extracts. *EMBO J* **17**: 3565-3575
- Lord PG, Wheals AE (1980) Asymmetrical division of *Saccharomyces cerevisiae*. *J Bacteriol* **142**: 808-818
- Luo KQ, Elsasser S, Chang DC, Campbell JL (2003) Regulation of the localization and stability of Cdc6 in living yeast cells. *Biochem Biophys Res Commun* **306**: 851-859
- Luo X, Talarek N, De Virgilio C (2011) Initiation of the yeast G0 program requires Igo1 and Igo2, which antagonize activation of decapping of specific nutrient-regulated mRNAs. *RNA Biol* **8**: 14-17
- Luo Y, Marx SO, Kiyokawa H, Koff A, Massague J, Marks AR (1996) Rapamycin resistance tied to defective regulation of p27Kip1. *Mol Cell Biol* **16**: 6744-6751
- MacGurn JA, Hsu PC, Smolka MB, Emr SD (2011) TORC1 regulates endocytosis via Npr1-mediated phosphoinhibition of a ubiquitin ligase adaptor. *Cell* **147**: 1104-1117

- Maekawa H, Schiebel E (2004) Cdk1-Clb4 controls the interaction of astral microtubule plus ends with subdomains of the daughter cell cortex. *Genes Dev* **18**: 1709-1724
- Magasanik B, Kaiser CA (2002) Nitrogen regulation in *Saccharomyces cerevisiae*. *Gene* **290**: 1-18
- Mai B, Breeden L (1997) Xbp1, a stress-induced transcriptional repressor of the *Saccharomyces cerevisiae* Swi4/Mbp1 family. *Mol Cell Biol* **17**: 6491-6501
- Mai B, Miles S, Breeden LL (2002) Characterization of the ECB binding complex responsible for the M/G(1)-specific transcription of CLN3 and SWI4. *Mol Cell Biol* **22**: 430-441
- Malumbres M (2014) Cyclin-dependent kinases. *Genome Biol* **15**: 122
- Malumbres M, Pevarello P, Barbacid M, Bischoff JR (2008) CDK inhibitors in cancer therapy: what is next? *Trends Pharmacol Sci* **29**: 16-21
- Mangus DA, Amrani N, Jacobson A (1998) Pbp1p, a factor interacting with *Saccharomyces cerevisiae* poly(A)-binding protein, regulates polyadenylation. *Mol Cell Biol* **18**: 7383-7396
- Mangus DA, Evans MC, Agrin NS, Smith M, Gongidi P, Jacobson A (2004a) Positive and negative regulation of poly(A) nuclease. *Mol Cell Biol* **24**: 5521-5533
- Mangus DA, Smith MM, McSweeney JM, Jacobson A (2004b) Identification of factors regulating poly(A) tail synthesis and maturation. *Mol Cell Biol* **24**: 4196-4206
- Masumoto H, Muramatsu S, Kamimura Y, Araki H (2002) S-Cdk-dependent phosphorylation of Sld2 essential for chromosomal DNA replication in budding yeast. *Nature* **415**: 651-655
- McGrath DA, Balog ER, Koivomagi M, Lucena R, Mai MV, Hirschi A, Kellogg DR, Loog M, Rubin SM (2013) Cks confers specificity to phosphorylation-dependent CDK signaling pathways. *Nat Struct Mol Biol* **20**: 1407-1414
- McInerney CJ, Partridge JF, Mikesell GE, Creemer DP, Breeden LL (1997) A novel Mcm1-dependent element in the SWI4, CLN3, CDC6, and CDC47 promoters activates M/G1-specific transcription. *Genes Dev* **11**: 1277-1288
- McKinney JD, Chang F, Heintz N, Cross FR (1993) Negative regulation of FAR1 at the Start of the yeast cell cycle. *Genes Dev* **7**: 833-843
- McKinney JD, Cross FR (1995) FAR1 and the G1 phase specificity of cell cycle arrest by mating factor in *Saccharomyces cerevisiae*. *Mol Cell Biol* **15**: 2509-2516

- McMillan JN, Theesfeld CL, Harrison JC, Bardes ES, Lew DJ (2002) Determinants of Swe1p degradation in *Saccharomyces cerevisiae*. *Mol Biol Cell* **13**: 3560-3575
- Measday V, McBride H, Moffat J, Stillman D, Andrews B (2000) Interactions between Pho85 cyclin-dependent kinase complexes and the Swi5 transcription factor in budding yeast. *Mol Microbiol* **35**: 825-834
- Medema RH, Kops GJ, Bos JL, Burgering BM (2000) AFX-like Forkhead transcription factors mediate cell-cycle regulation by Ras and PKB through p27kip1. *Nature* **404**: 782-787
- Meggio F, Pinna LA (2003) One-thousand-and-one substrates of protein kinase CK2? *FASEB J* **17**: 349-368
- Mendenhall MD (1993) An inhibitor of p34CDC28 protein kinase activity from *Saccharomyces cerevisiae*. *Science* **259**: 216-219
- Mendenhall MD, Hodge AE (1998) Regulation of Cdc28 cyclin-dependent protein kinase activity during the cell cycle of the yeast *Saccharomyces cerevisiae*. *Microbiol Mol Biol Rev* **62**: 1191-1243
- Menoyo S, Ricco N, Bru S, Hernandez-Ortega S, Escote X, Aldea M, Clotet J (2013) Phosphate-activated cyclin-dependent kinase stabilizes G1 cyclin to trigger cell cycle entry. *Mol Cell Biol* **33**: 1273-1284
- Messier V, Zenklusen D, Michnick SW (2013) A nutrient-responsive pathway that determines M phase timing through control of B-cyclin mRNA stability. *Cell* **153**: 1080-1093
- Miled C, Mann C, Faye G (2001) Xbp1-mediated repression of CLB gene expression contributes to the modifications of yeast cell morphology and cell cycle seen during nitrogen-limited growth. *Mol Cell Biol* **21**: 3714-3724
- Miles S, Li L, Davison J, Breeden LL (2013) Xbp1 directs global repression of budding yeast transcription during the transition to quiescence and is important for the longevity and reversibility of the quiescent state. *PLoS Genet* **9**: e1003854
- Miller ME, Cross FR (2000) Distinct subcellular localization patterns contribute to functional specificity of the Cln2 and Cln3 cyclins of *Saccharomyces cerevisiae*. *Mol Cell Biol* **20**: 542-555
- Miller ME, Cross FR (2001) Mechanisms controlling subcellular localization of the G(1) cyclins Cln2p and Cln3p in budding yeast. *Mol Cell Biol* **21**: 6292-6311
- Mittag T, Marsh J, Grishaev A, Orlicky S, Lin H, Sicheri F, Tyers M, Forman-Kay JD (2010) Structure/function implications in a dynamic complex of the intrinsically disordered Sic1 with the Cdc4 subunit of an SCF ubiquitin ligase. *Structure* **18**: 494-506

- Mizunuma M, Tsubakiyama R, Ogawa T, Shitamukai A, Kobayashi Y, Inai T, Kume K, Hirata D (2013) Ras/cAMP-dependent protein kinase (PKA) regulates multiple aspects of cellular events by phosphorylating the Whi3 cell cycle regulator in budding yeast. *J Biol Chem* **288**: 10558-10566
- Mochida S (2014) Regulation of alpha-endosulfine, an inhibitor of protein phosphatase 2A, by multisite phosphorylation. *FEBS J* **281**: 1159-1169
- Mochida S, Ikeo S, Gannon J, Hunt T (2009) Regulated activity of PP2A-B55 delta is crucial for controlling entry into and exit from mitosis in *Xenopus* egg extracts. *EMBO J* **28**: 2777-2785
- Mochida S, Maslen SL, Skehel M, Hunt T (2010) Greatwall phosphorylates an inhibitor of protein phosphatase 2A that is essential for mitosis. *Science* **330**: 1670-1673
- Moffat J, Andrews B (2004) Late-G1 cyclin-CDK activity is essential for control of cell morphogenesis in budding yeast. *Nat Cell Biol* **6**: 59-66
- Moreno S, Hayles J, Nurse P (1989) Regulation of p34cdc2 protein kinase during mitosis. *Cell* **58**: 361-372
- Moreno-Torres M, Jaquenoud M, De Virgilio C (2015) TORC1 controls G1-S cell cycle transition in yeast via Mpk1 and the greatwall kinase pathway. *Nat Commun* **6**: 8256
- Morgan DO (1995) Principles of CDK regulation. *Nature* **374**: 131-134
- Morgan DO (1997) Cyclin-dependent kinases: engines, clocks, and microprocessors. *Annu Rev Cell Dev Biol* **13**: 261-291
- Morgan DO (2007) *The Cell Cycle Principles of Control* (Primers in Biology)
- Morris MC, Kaiser P, Rudyak S, Baskerville C, Watson MH, Reed SI (2003) Cks1-dependent proteasome recruitment and activation of CDC20 transcription in budding yeast. *Nature* **423**: 1009-1013
- Mumberg D, Müller R, Funk M (1995) Yeast Vectors for the Controlled Expression of Heterologous Proteins in Different Genetic Backgrounds. *Gene* **156**: 119-122
- Murray A (1995) Cyclin ubiquitination: the destructive end of mitosis. *Cell* **81**: 149-152
- Murray AW (2004) Recycling the cell cycle: cyclins revisited. *Cell* **116**: 221-234
- Nakashima A, Maruki Y, Imamura Y, Kondo C, Kawamata T, Kawanishi I, Takata H, Matsuura A, Lee KS, Kikkawa U, Ohsumi Y, Yonezawa K, Kamada Y (2008) The yeast Tor signaling pathway is involved in G2/M transition via polo-kinase. *PLoS One* **3**: e2223

Nash P, Tang X, Orlicky S, Chen Q, Gertler FB, Mendenhall MD, Sicheri F, Pawson T, Tyers M (2001) Multisite phosphorylation of a CDK inhibitor sets a threshold for the onset of DNA replication. *Nature* **414**: 514-521

Nash R, Tokiwa G, Anand S, Erickson K, Futcher AB (1988) The WHI1+ gene of *Saccharomyces cerevisiae* tethers cell division to cell size and is a cyclin homolog. *EMBO J* **7**: 4335-4346

Nasmyth K (1993) Control of the yeast cell cycle by the Cdc28 protein kinase. *Curr Opin Cell Biol* **5**: 166-179

Nern A, Arkowitz RA (1999) A Cdc24p-Far1p-Gbetagamma protein complex required for yeast orientation during mating. *J Cell Biol* **144**: 1187-1202

Nishizawa M, Kawasumi M, Fujino M, Toh-e A (1998) Phosphorylation of sic1, a cyclin-dependent kinase (Cdk) inhibitor, by Cdk including Pho85 kinase is required for its prompt degradation. *Mol Biol Cell* **9**: 2393-2405

Noble ME, Endicott JA, Brown NR, Johnson LN (1997) The cyclin box fold: protein recognition in cell-cycle and transcription control. *Trends Biochem Sci* **22**: 482-487

Noguchi E, Gadaleta M.C. (2014) *Cell Cycle Control Mechanisms and Protocols* (Springer Protocols, Humana Press)

Norbury C, Blow J, Nurse P (1991) Regulatory phosphorylation of the p34cdc2 protein kinase in vertebrates. *EMBO J* **10**: 3321-3329

Nugroho TT, Mendenhall MD (1994) An inhibitor of yeast cyclin-dependent protein kinase plays an important role in ensuring the genomic integrity of daughter cells. *Mol Cell Biol* **14**: 3320-3328

O'Donnell AF, Apffel A, Gardner RG, Cyert MS (2010) Alpha-arrestins Aly1 and Aly2 regulate intracellular trafficking in response to nutrient signaling. *Mol Biol Cell* **21**: 3552-3566

O'Neill EM, Kaffman A, Jolly ER, O'Shea EK (1996) Regulation of PHO4 nuclear localization by the PHO80-PHO85 cyclin-CDK complex. *Science* **271**: 209-212

Ogawa N, Noguchi K, Sawai H, Yamashita Y, Yompakdee C, Oshima Y (1995) Functional domains of Pho81p, an inhibitor of Pho85p protein kinase, in the transduction pathway of Pi signals in *Saccharomyces cerevisiae*. *Mol Cell Biol* **15**: 997-1004

Ostapenko D, Solomon MJ (2005) Phosphorylation by Cak1 regulates the C-terminal domain kinase Ctk1 in *Saccharomyces cerevisiae*. *Mol Cell Biol* **25**: 3906-3913

Parge HE, Arvai AS, Murtari DJ, Reed SI, Tainer JA (1993) Human CksHs2 atomic structure: a role for its hexameric assembly in cell cycle control. *Science* **262**: 387-395

- Pathak R, Blank HM, Guo J, Ellis S, Polymenis M (2007) The Dcr2p phosphatase destabilizes Sic1p in *Saccharomyces cerevisiae*. *Biochem Biophys Res Commun* **361**: 700-704
- Patra D, Dunphy WG (1996) Xe-p9, a *Xenopus* Suc1/Cks homolog, has multiple essential roles in cell cycle control. *Genes Dev* **10**: 1503-1515
- Patra D, Wang SX, Kumagai A, Dunphy WG (1999) The *xenopus* Suc1/Cks protein promotes the phosphorylation of G(2)/M regulators. *J Biol Chem* **274**: 36839-36842
- Pearce LR, Komander D, Alessi DR (2010) The nuts and bolts of AGC protein kinases. *Nat Rev Mol Cell Biol* **11**: 9-22
- Pedruzzi I, Burckert N, Egger P, De Virgilio C (2000) *Saccharomyces cerevisiae* Ras/cAMP pathway controls post-diauxic shift element-dependent transcription through the zinc finger protein Gis1. *EMBO J* **19**: 2569-2579
- Pedruzzi I, Dubouloz F, Cameroni E, Wanke V, Roosen J, Winderickx J, De Virgilio C (2003a) TOR and PKA signaling pathways converge on the protein kinase Rim15 to control entry into G₀. *Mol Cell* **12**: 1607-1613
- Pedruzzi I, Dubouloz F, Cameroni E, Wanke V, Roosen J, Winderickx J, De Virgilio C (2003b) TOR and PKA signaling pathways converge on the protein kinase Rim15 to control entry into G₀. *Mol Cell* **12**: 1607-1613
- Peli-Gulli MP, Sardu A, Panchaud N, Raucci S, De Virgilio C (2015) Amino Acids Stimulate TORC1 through Lst4-Lst7, a GTPase-Activating Protein Complex for the Rag Family GTPase Gtr2. *Cell Rep* **13**: 1-7
- Perkins G, Drury LS, Diffley JF (2001) Separate SCF(CDC4) recognition elements target Cdc6 for proteolysis in S phase and mitosis. *EMBO J* **20**: 4836-4845
- Peter M, Gartner A, Horecka J, Ammerer G, Herskowitz I (1993) FAR1 links the signal transduction pathway to the cell cycle machinery in yeast. *Cell* **73**: 747-760
- Peter M, Herskowitz I (1994) Direct inhibition of the yeast cyclin-dependent kinase Cdc28-Cln by Far1. *Science* **265**: 1228-1231
- Piatti S, Lengauer C, Nasmyth K (1995) Cdc6 is an unstable protein whose de novo synthesis in G₁ is important for the onset of S phase and for preventing a 'reductional' anaphase in the budding yeast *Saccharomyces cerevisiae*. *EMBO J* **14**: 3788-3799
- Pines J (1996) Cell cycle: reaching for a role for the Cks proteins. *Curr Biol* **6**: 1399-1402
- Pines J (1999) Cell cycle. Checkpoint on the nuclear frontier. *Nature* **397**: 104-105
- Polymenis M, Schmidt EV (1997) Coupling of cell division to cell growth by translational control of the G₁ cyclin CLN3 in yeast. *Genes Dev* **11**: 2522-2531

- Polymenis M, Schmidt EV (1999) Coordination of cell growth with cell division. *Curr Opin Genet Dev* **9**: 76-80
- Powers RW, 3rd, Kaeberlein M, Caldwell SD, Kennedy BK, Fields S (2006) Extension of chronological life span in yeast by decreased TOR pathway signaling. *Genes Dev* **20**: 174-184
- Powis K, Zhang T, Panchaud N, Wang R, De Virgilio C, Ding J (2015) Crystal structure of the Ego1-Ego2-Ego3 complex and its role in promoting Rag GTPase-dependent TORC1 signaling. *Cell Res* **25**: 1043-1059
- Pramila T, Miles S, GuhaThakurta D, Jemiolo D, Breeden LL (2002) Conserved homeodomain proteins interact with MADS box protein Mcm1 to restrict ECB-dependent transcription to the M/G1 phase of the cell cycle. *Genes Dev* **16**: 3034-3045
- Pramila T, Wu W, Miles S, Noble WS, Breeden LL (2006) The Forkhead transcription factor Hcm1 regulates chromosome segregation genes and fills the S-phase gap in the transcriptional circuitry of the cell cycle. *Genes Dev* **20**: 2266-2278
- Prinz S, Hwang ES, Visintin R, Amon A (1998) The regulation of Cdc20 proteolysis reveals a role for APC components Cdc23 and Cdc27 during S phase and early mitosis. *Curr Biol* **8**: 750-760
- Ptacek J, Devgan G, Michaud G, Zhu H, Zhu X, Fasolo J, Guo H, Jona G, Breitkreutz A, Sopko R, McCartney RR, Schmidt MC, Rachidi N, Lee SJ, Mah AS, Meng L, Stark MJ, Stern DF, De Virgilio C, Tyers M, Andrews B, Gerstein M, Schweitzer B, Predki PF, Snyder M (2005) Global analysis of protein phosphorylation in yeast. *Nature* **438**: 679-684
- Queralt E, Lehane C, Novak B, Uhlmann F (2006) Downregulation of PP2A(Cdc55) phosphatase by separase initiates mitotic exit in budding yeast. *Cell* **125**: 719-732
- Queralt E, Uhlmann F (2008) Separase cooperates with Zds1 and Zds2 to activate Cdc14 phosphatase in early anaphase. *J Cell Biol* **182**: 873-883
- Quilis I, Igual JC (2012) Molecular basis of the functional distinction between Cln1 and Cln2 cyclins. *Cell Cycle* **11**: 3117-3131
- Rangone H, Wegel E, Gatt MK, Yeung E, Flowers A, Debski J, Dadlez M, Janssens V, Carpenter AT, Glover DM (2011) Suppression of scant identifies Endos as a substrate of greatwall kinase and a negative regulator of protein phosphatase 2A in mitosis. *PLoS Genet* **7**: e1002225
- Reed SI, Hadwiger JA, Lorincz AT (1985) Protein kinase activity associated with the product of the yeast cell division cycle gene CDC28. *Proc Natl Acad Sci U S A* **82**: 4055-4059

- Reinders A, Burckert N, Boller T, Wiemken A, De Virgilio C (1998) Saccharomyces cerevisiae cAMP-dependent protein kinase controls entry into stationary phase through the Rim15p protein kinase. *Genes Dev* **12**: 2943-2955
- Reinders A, Burckert N, Hohmann S, Thevelein JM, Boller T, Wiemken A, De Virgilio C (1997) Structural analysis of the subunits of the trehalose-6-phosphate synthase/phosphatase complex in Saccharomyces cerevisiae and their function during heat shock. *Mol Microbiol* **24**: 687-695
- Reinke A, Anderson S, McCaffery JM, Yates J, 3rd, Aronova S, Chu S, Fairclough S, Iverson C, Wedaman KP, Powers T (2004) TOR complex 1 includes a novel component, Tco89p (YPL180w), and cooperates with Ssd1p to maintain cellular integrity in Saccharomyces cerevisiae. *J Biol Chem* **279**: 14752-14762
- Reinke A, Chen JC, Aronova S, Powers T (2006) Caffeine targets TOR complex I and provides evidence for a regulatory link between the FRB and kinase domains of Tor1p. *J Biol Chem* **281**: 31616-31626
- Richardson H, Lew DJ, Henze M, Sugimoto K, Reed SI (1992) Cyclin-B homologs in Saccharomyces cerevisiae function in S phase and in G2. *Genes Dev* **6**: 2021-2034
- Richardson HE, Stueland CS, Thomas J, Russell P, Reed SI (1990) Human cDNAs encoding homologs of the small p34Cdc28/Cdc2-associated protein of Saccharomyces cerevisiae and Schizosaccharomyces pombe. *Genes Dev* **4**: 1332-1344
- Robertson LS, Fink GR (1998) The three yeast A kinases have specific signaling functions in pseudohyphal growth. *Proc Natl Acad Sci U S A* **95**: 13783-13787
- Ross KE, Kaldis P, Solomon MJ (2000) Activating phosphorylation of the Saccharomyces cerevisiae cyclin-dependent kinase, cdc28p, precedes cyclin binding. *Mol Biol Cell* **11**: 1597-1609
- Rossi RL, Zinzalla V, Mastriani A, Vanoni M, Alberghina L (2005) Subcellular localization of the cyclin dependent kinase inhibitor Sic1 is modulated by the carbon source in budding yeast. *Cell Cycle* **4**: 1798-1807
- Rossio V, Yoshida S (2011) Spatial regulation of Cdc55-PP2A by Zds1/Zds2 controls mitotic entry and mitotic exit in budding yeast. *J Cell Biol* **193**: 445-454
- Rudner AD, Murray AW (2000) Phosphorylation by Cdc28 activates the Cdc20-dependent activity of the anaphase-promoting complex. *J Cell Biol* **149**: 1377-1390
- Rudolph HK, Antebi A, Fink GR, Buckley CM, Dorman TE, LeVitre J, Davidow LS, Mao JI, Moir DT (1989) The yeast secretory pathway is perturbed by mutations in PMR1, a member of a Ca²⁺ ATPase family. *Cell* **58**: 133-145
- Rupes I (2002) Checking cell size in yeast. *Trends Genet* **18**: 479-485

- Russell P, Moreno S, Reed SI (1989) Conservation of mitotic controls in fission and budding yeasts. *Cell* **57**: 295-303
- Russo AA, Jeffrey PD, Pavletich NP (1996) Structural basis of cyclin-dependent kinase activation by phosphorylation. *Nat Struct Biol* **3**: 696-700
- Sadowski M, Mawson A, Baker R, Sarcevic B (2007) Cdc34 C-terminal tail phosphorylation regulates Skp1/cullin/F-box (SCF)-mediated ubiquitination and cell cycle progression. *Biochem J* **405**: 569-581
- Saldanha AJ, Brauer MJ, Botstein D (2004) Nutritional homeostasis in batch and steady-state culture of yeast. *Mol Biol Cell* **15**: 4089-4104
- Sambrook, J., and Russell, D.W. (2001) *Molecular cloning: a laboratory manual* (Cold Spring Harbor, Cold Spring Harbor Laboratory Press)
- Sancak Y, Peterson TR, Shaul YD, Lindquist RA, Thoreen CC, Bar-Peled L, Sabatini DM (2008) The Rag GTPases bind raptor and mediate amino acid signaling to mTORC1. *Science* **320**: 1496-1501
- Sanchez-Diaz A, Gonzalez I, Arellano M, Moreno S (1998) The Cdk inhibitors p25rum1 and p40SIC1 are functional homologues that play similar roles in the regulation of the cell cycle in fission and budding yeast. *J Cell Sci* **111 (Pt 6)**: 843-851
- Santangelo GM (2006) Glucose signaling in *Saccharomyces cerevisiae*. *Microbiol Mol Biol Rev* **70**: 253-282
- Schmidt A, Beck T, Koller A, Kunz J, Hall MN (1998) The TOR nutrient signalling pathway phosphorylates NPR1 and inhibits turnover of the tryptophan permease. *EMBO J* **17**: 6924-6931
- Schneider KR, Smith RL, O'Shea EK (1994) Phosphate-regulated inactivation of the kinase PHO80-PHO85 by the CDK inhibitor PHO81. *Science* **266**: 122-126
- Schulman BA, Lindstrom DL, Harlow E (1998) Substrate recruitment to cyclin-dependent kinase 2 by a multipurpose docking site on cyclin A. *Proc Natl Acad Sci U S A* **95**: 10453-10458
- Schwab M, Lutum AS, Seufert W (1997) Yeast Hct1 is a regulator of Clb2 cyclin proteolysis. *Cell* **90**: 683-693
- Schwob E, Bohm T, Mendenhall MD, Nasmyth K (1994) The B-type cyclin kinase inhibitor p40SIC1 controls the G1 to S transition in *S. cerevisiae*. *Cell* **79**: 233-244
- Schwob E, Nasmyth K (1993) CLB5 and CLB6, a new pair of B cyclins involved in DNA replication in *Saccharomyces cerevisiae*. *Genes Dev* **7**: 1160-1175

- Shapira M, Ben-Izhak O, Linn S, Futerman B, Minkov I, Hershko DD (2005) The prognostic impact of the ubiquitin ligase subunits Skp2 and Cks1 in colorectal carcinoma. *Cancer* **103**: 1336-1346
- Shen C, Lancaster CS, Shi B, Guo H, Thimmaiah P, Bjornsti MA (2007) TOR signaling is a determinant of cell survival in response to DNA damage. *Mol Cell Biol* **27**: 7007-7017
- Sherr CJ, Roberts JM (1995) Inhibitors of mammalian G1 cyclin-dependent kinases. *Genes Dev* **9**: 1149-1163
- Shirayama M, Toth A, Galova M, Nasmyth K (1999) APC(Cdc20) promotes exit from mitosis by destroying the anaphase inhibitor Pds1 and cyclin Clb5. *Nature* **402**: 203-207
- Shirayama M, Zachariae W, Ciosk R, Nasmyth K (1998) The Polo-like kinase Cdc5p and the WD-repeat protein Cdc20p/fizzy are regulators and substrates of the anaphase promoting complex in *Saccharomyces cerevisiae*. *EMBO J* **17**: 1336-1349
- Simon KE, Cha HH, Firestone GL (1995) Transforming growth factor beta down-regulation of CKShs1 transcripts in growth-inhibited epithelial cells. *Cell Growth Differ* **6**: 1261-1269
- Skotheim JM, Di Talia S, Siggia ED, Cross FR (2008) Positive feedback of G1 cyclins ensures coherent cell cycle entry. *Nature* **454**: 291-296
- Skowyra D, Craig KL, Tyers M, Elledge SJ, Harper JW (1997) F-box proteins are receptors that recruit phosphorylated substrates to the SCF ubiquitin-ligase complex. *Cell* **91**: 209-219
- Smets B, Ghillebert R, De Snijder P, Binda M, Swinnen E, De Virgilio C, Winderickx J (2010) Life in the midst of scarcity: adaptations to nutrient availability in *Saccharomyces cerevisiae*. *Curr Genet* **56**: 1-32
- Song L, Rape M (2010) Regulated degradation of spindle assembly factors by the anaphase-promoting complex. *Mol Cell* **38**: 369-382
- Soulard A, Cohen A, Hall MN (2009) TOR signaling in invertebrates. *Curr Opin Cell Biol* **21**: 825-836
- Spellman PT, Sherlock G, Zhang MQ, Iyer VR, Anders K, Eisen MB, Brown PO, Botstein D, Futcher B (1998) Comprehensive identification of cell cycle-regulated genes of the yeast *Saccharomyces cerevisiae* by microarray hybridization. *Mol Biol Cell* **9**: 3273-3297
- Stuart D, Wittenberg C (1995) CLN3, not positive feedback, determines the timing of CLN2 transcription in cycling cells. *Genes Dev* **9**: 2780-2794
- Sturgill TW, Cohen A, Diefenbacher M, Trautwein M, Martin DE, Hall MN (2008) TOR1 and TOR2 have distinct locations in live cells. *Eukaryot Cell* **7**: 1819-1830

- Suzuki S, Fukasawa H, Misaki T, Togawa A, Ohashi N, Kitagawa K, Kotake Y, Niida H, Hishida A, Yamamoto T, Kitagawa M (2011) Up-regulation of Cks1 and Skp2 with TNF α /NF- κ B signaling in chronic progressive nephropathy. *Genes Cells* **16**: 1110-1120
- Swinnen E, Wanke V, Roosen J, Smets B, Dubouloz F, Pedruzzi I, Cameroni E, De Virgilio C, Winderickx J (2006) Rim15 and the crossroads of nutrient signalling pathways in *Saccharomyces cerevisiae*. *Cell Div* **1**: 3
- Takeo K, Tanaka R, Miyaji M, Nishimura K (1995) Unbudded G2 as well as G1 arrest in the stationary phase of the basidiomycetous yeast *Cryptococcus neoformans*. *FEMS Microbiol Lett* **129**: 231-235
- Talarek N, Cameroni E, Jaquenoud M, Luo X, Bontron S, Lippman S, Devgan G, Snyder M, Broach JR, De Virgilio C (2010) Initiation of the TORC1-regulated G0 program requires Igo1/2, which license specific mRNAs to evade degradation via the 5'-3' mRNA decay pathway. *Mol Cell* **38**: 345-355
- Tamaskovic R, Bichsel SJ, Hemmings BA (2003) NDR family of AGC kinases--essential regulators of the cell cycle and morphogenesis. *FEBS Lett* **546**: 73-80
- Tang Y, Reed SI (1993) The Cdk-associated protein Cks1 functions both in G1 and G2 in *Saccharomyces cerevisiae*. *Genes Dev* **7**: 822-832
- Tatchell K, Makrantonis V, Stark MJ, Robinson LC (2011) Temperature-sensitive *ipl1-2/Aurora B* mutation is suppressed by mutations in TOR complex 1 via the Glc7/PP1 phosphatase. *Proc Natl Acad Sci U S A* **108**: 3994-3999
- Thornton BR, Toczyski DP (2003) Securin and B-cyclin/CDK are the only essential targets of the APC. *Nat Cell Biol* **5**: 1090-1094
- Thuret JY, Valay JG, Faye G, Mann C (1996) Civ1 (CAK in vivo), a novel Cdk-activating kinase. *Cell* **86**: 565-576
- Toda T, Uno I, Ishikawa T, Powers S, Kataoka T, Broek D, Cameron S, Broach J, Matsumoto K, Wigler M (1985) In yeast, RAS proteins are controlling elements of adenylate cyclase. *Cell* **40**: 27-36
- Toh-e A, Tanaka K, Uesono Y, Wickner RB (1988) PHO85, a negative regulator of the PHO system, is a homolog of the protein kinase gene, CDC28, of *Saccharomyces cerevisiae*. *Mol Gen Genet* **214**: 162-164
- Toyn JH, Johnson AL, Donovan JD, Toone WM, Johnston LH (1997) The Swi5 transcription factor of *Saccharomyces cerevisiae* has a role in exit from mitosis through induction of the cdk-inhibitor Sic1 in telophase. *Genetics* **145**: 85-96

- Toyoshima H, Hunter T (1994) p27, a novel inhibitor of G1 cyclin-Cdk protein kinase activity, is related to p21. *Cell* **78**: 67-74
- Tripodi F, Zinzalla V, Vanoni M, Alberghina L, Coccetti P (2007) In CK2 inactivated cells the cyclin dependent kinase inhibitor Sic1 is involved in cell-cycle arrest before the onset of S phase. *Biochem Biophys Res Commun* **359**: 921-927
- Tyers M, Jorgensen P (2000) Proteolysis and the cell cycle: with this RING I do thee destroy. *Curr Opin Genet Dev* **10**: 54-64
- Tyers M, Tokiwa G, Futcher B (1993) Comparison of the *Saccharomyces cerevisiae* G1 cyclins: Cln3 may be an upstream activator of Cln1, Cln2 and other cyclins. *EMBO J* **12**: 1955-1968
- Ubersax JA, Woodbury EL, Quang PN, Paraz M, Blethrow JD, Shah K, Shokat KM, Morgan DO (2003) Targets of the cyclin-dependent kinase Cdk1. *Nature* **425**: 859-864
- Urban J, Soulard A, Huber A, Lippman S, Mukhopadhyay D, Deloche O, Wanke V, Anrather D, Ammerer G, Riezman H, Broach JR, De Virgilio C, Hall MN, Loewith R (2007) Sch9 is a major target of TORC1 in *Saccharomyces cerevisiae*. *Mol Cell* **26**: 663-674
- Urbanowicz-Kachnowicz I, Baghdassarian N, Nakache C, Gracia D, Mekki Y, Bryon PA, Ffrench M (1999) cks1 expression is linked to cell proliferation in normal and malignant human lymphoid cells. *Int J Cancer* **82**: 98-104
- van der Felden J, Weisser S, Bruckner S, Lenz P, Mosch HU (2014) The transcription factors Tec1 and Ste12 interact with coregulators Msa1 and Msa2 to activate adhesion and multicellular development. *Mol Cell Biol* **34**: 2283-2293
- Vandenbol M, Jauniaux JC, Vissers S, Grenson M (1987) Isolation of the NPR1 gene responsible for the reactivation of ammonia-sensitive amino-acid permeases in *Saccharomyces cerevisiae*. RNA analysis and gene dosage effects. *Eur J Biochem* **164**: 607-612
- Verges E, Colomina N, Gari E, Gallego C, Aldea M (2007) Cyclin Cln3 is retained at the ER and released by the J chaperone Ydj1 in late G1 to trigger cell cycle entry. *Mol Cell* **26**: 649-662
- Verma R, Annan RS, Huddleston MJ, Carr SA, Reynard G, Deshaies RJ (1997a) Phosphorylation of Sic1p by G1 Cdk required for its degradation and entry into S phase. *Science* **278**: 455-460
- Verma R, Feldman RM, Deshaies RJ (1997b) SIC1 is ubiquitinated in vitro by a pathway that requires CDC4, CDC34, and cyclin/CDK activities. *Mol Biol Cell* **8**: 1427-1437
- Verma R, McDonald H, Yates JR, 3rd, Deshaies RJ (2001) Selective degradation of ubiquitinated Sic1 by purified 26S proteasome yields active S phase cyclin-Cdk. *Mol Cell* **8**: 439-448

- Verma R, Oania R, Graumann J, Deshaies RJ (2004) Multiubiquitin chain receptors define a layer of substrate selectivity in the ubiquitin-proteasome system. *Cell* **118**: 99-110
- Vigneron S, Brioudes E, Burgess A, Labbe JC, Lorca T, Castro A (2009) Greatwall maintains mitosis through regulation of PP2A. *EMBO J* **28**: 2786-2793
- Vigneron S, Gharbi-Ayachi A, Raymond AA, Burgess A, Labbe JC, Labesse G, Monsarrat B, Lorca T, Castro A (2011) Characterization of the mechanisms controlling Greatwall activity. *Mol Cell Biol* **31**: 2262-2275
- Visintin R, Craig K, Hwang ES, Prinz S, Tyers M, Amon A (1998) The phosphatase Cdc14 triggers mitotic exit by reversal of Cdk-dependent phosphorylation. *Mol Cell* **2**: 709-718
- Visintin R, Prinz S, Amon A (1997) CDC20 and CDH1: a family of substrate-specific activators of APC-dependent proteolysis. *Science* **278**: 460-463
- Voets E, Wolthuis RM (2010) MASTL is the human orthologue of Greatwall kinase that facilitates mitotic entry, anaphase and cytokinesis. *Cell Cycle* **9**: 3591-3601
- Wang H, Gari E, Verges E, Gallego C, Aldea M (2004) Recruitment of Cdc28 by Whi3 restricts nuclear accumulation of the G1 cyclin-Cdk complex to late G1. *EMBO J* **23**: 180-190
- Wang P, Galan JA, Normandin K, Bonneil E, Hickson GR, Roux PP, Thibault P, Archambault V (2013) Cell cycle regulation of Greatwall kinase nuclear localization facilitates mitotic progression. *J Cell Biol* **202**: 277-293
- Wanke V, Cameroni E, Uotila A, Piccolis M, Urban J, Loewith R, De Virgilio C (2008) Caffeine extends yeast lifespan by targeting TORC1. *Mol Microbiol* **69**: 277-285
- Wanke V, Pedruzzi I, Cameroni E, Dubouloz F, De Virgilio C (2005) Regulation of G0 entry by the Pho80-Pho85 cyclin-CDK complex. *EMBO J* **24**: 4271-4278
- Wasch R, Cross FR (2002) APC-dependent proteolysis of the mitotic cyclin Clb2 is essential for mitotic exit. *Nature* **418**: 556-562
- Wasch R, Engelbert D (2005) Anaphase-promoting complex-dependent proteolysis of cell cycle regulators and genomic instability of cancer cells. *Oncogene* **24**: 1-10
- Wei W, Nurse P, Broek D (1993) Yeast cells can enter a quiescent state through G1, S, G2, or M phase of the cell cycle. *Cancer Res* **53**: 1867-1870
- Welburn JP, Tucker JA, Johnson T, Lindert L, Morgan M, Willis A, Noble ME, Endicott JA (2007) How tyrosine 15 phosphorylation inhibits the activity of cyclin-dependent kinase 2-cyclin A. *J Biol Chem* **282**: 3173-3181

- Werner-Washburne M, Braun E, Johnston GC, Singer RA (1993) Stationary phase in the yeast *Saccharomyces cerevisiae*. *Microbiol Rev* **57**: 383-401
- Willems AR, Lanker S, Patton EE, Craig KL, Nason TF, Mathias N, Kobayashi R, Wittenberg C, Tyers M (1996) Cdc53 targets phosphorylated G1 cyclins for degradation by the ubiquitin proteolytic pathway. *Cell* **86**: 453-463
- Wittenberg C, Reed SI (2005) Cell cycle-dependent transcription in yeast: promoters, transcription factors, and transcriptomes. *Oncogene* **24**: 2746-2755
- Wullschleger S, Loewith R, Hall MN (2006) TOR signaling in growth and metabolism. *Cell* **124**: 471-484
- Wysocki R, Javaheri A, Kristjansdottir K, Sha F, Kron SJ (2006) CDK Pho85 targets CDK inhibitor Sic1 to relieve yeast G1 checkpoint arrest after DNA damage. *Nat Struct Mol Biol* **13**: 908-914
- Yaffe MB, Elia AE (2001) Phosphoserine/threonine-binding domains. *Curr Opin Cell Biol* **13**: 131-138
- Yaglom J, Linskens MH, Sadis S, Rubin DM, Futcher B, Finley D (1995) p34Cdc28-mediated control of Cln3 cyclin degradation. *Mol Cell Biol* **15**: 731-741
- Yahya G, Parisi E, Flores A, Gallego C, Aldea M (2014) A Whi7-anchored loop controls the G1 Cdk-cyclin complex at start. *Mol Cell* **53**: 115-126
- Yamamoto A, Guacci V, Koshland D (1996) Pds1p, an inhibitor of anaphase in budding yeast, plays a critical role in the APC and checkpoint pathway(s). *J Cell Biol* **133**: 99-110
- Yamamoto TM, Wang L, Fisher LA, Eckerdt FD, Peng A (2014) Regulation of Greatwall kinase by protein stabilization and nuclear localization. *Cell Cycle* **13**: 3565-3575
- Yu J, Fleming SL, Williams B, Williams EV, Li Z, Somma P, Rieder CL, Goldberg ML (2004) Greatwall kinase: a nuclear protein required for proper chromosome condensation and mitotic progression in *Drosophila*. *J Cell Biol* **164**: 487-492
- Yu J, Zhao Y, Li Z, Galas S, Goldberg ML (2006) Greatwall kinase participates in the Cdc2 autoregulatory loop in *Xenopus* egg extracts. *Mol Cell* **22**: 83-91
- Yu VP, Baskerville C, Grunenfelder B, Reed SI (2005) A kinase-independent function of Cks1 and Cdk1 in regulation of transcription. *Mol Cell* **17**: 145-151
- Zachariae W, Nasmyth K (1999) Whose end is destruction: cell division and the anaphase-promoting complex. *Genes Dev* **13**: 2039-2058
- Zachariae W, Schwab M, Nasmyth K, Seufert W (1998) Control of cyclin ubiquitination by CDK-regulated binding of Hct1 to the anaphase promoting complex. *Science* **282**: 1721-1724

References

- Zapater M, Clotet J, Escote X, Posas F (2005) Control of cell cycle progression by the stress-activated Hog1 MAPK. *Cell Cycle* **4**: 6-7
- Zaragoza D, Ghavidel A, Heitman J, Schultz MC (1998) Rapamycin induces the G0 program of transcriptional repression in yeast by interfering with the TOR signaling pathway. *Mol Cell Biol* **18**: 4463-4470
- Zhang N, Wu J, Oliver SG (2009) Gis1 is required for transcriptional reprogramming of carbon metabolism and the stress response during transition into stationary phase in yeast. *Microbiology* **155**: 1690-1698
- Zhang Y, Lin Y, Bowles C, Wang F (2004) Direct cell cycle regulation by the fibroblast growth factor receptor (FGFR) kinase through phosphorylation-dependent release of Cks1 from FGFR substrate 2. *J Biol Chem* **279**: 55348-55354
- Zhou C, Jong A (1990) CDC6 mRNA fluctuates periodically in the yeast cell cycle. *J Biol Chem* **265**: 19904-19909
- Zinzalla V, Graziola M, Mastroiani A, Vanoni M, Alberghina L (2007) Rapamycin-mediated G1 arrest involves regulation of the Cdk inhibitor Sic1 in *Saccharomyces cerevisiae*. *Mol Microbiol* **63**: 1482-1494

Appendix

Acknowledgements

I would like to thank to...

Claudio De Virgilio, for giving me the opportunity to work in your laboratory. It has been a privilege to enjoy from your hard work, enthusiasm and motivation. I will always be grateful to you for all what I have learnt.

Prof. Sergio Moreno and Prof. Jürg Bähler for reviewing this manuscript and being members of my thesis jury board.

Malika, for being the way you are. For all your incalculable help and support. Your kindness, serenity and your exceptional abilities in the bench always made me feel part of a great team. Working with you has been a present to me.

Serena, my friend. Nothing would have been the same without you. Because you were my family in Switzerland. For being the most precious treasure I have found here, a treasure that I will keep by my side forever.

Alessandro, for making me smile every single day. Shirish, an example of positive attitude in life. Emma and Séverine, for the warm welcome you gave me when everything was foreign and new. You are my teachers and my friends.

Floriane and Marie-Pierre for your professionalism and your efficient way of working. Riko, for your contagious enthusiasm for this profession.

Nico T, Nico P, Gregory, Judith, Yvan and all the colleagues that formed part of my life during these years. It has been a pleasure to share bench, happiness, tears, hugs and laughs with each one of you. In me, you will always find a friend.

A mis amigas, por sentirnos tan cerca a pesar de la distancia que nos separa. Por demostrarme que aunque el tiempo pase, nuestra amistad durará siempre.

A mis padres y a mi hermano por ser el pilar fundamental en mi vida. Por habérmelo dado todo. Porque yo sólo soy, si es con vosotros.

A ti Fer. Por quererme incondicionalmente y haber estado a mi lado desde el primer día que te conocí. Por haber compartido esta experiencia en la vida juntos y haberla llenado de amor y felicidad. Pero sobre todo... por querer que haya muchas más.

EUROPEAN
CURRICULUM VITAE
FORMAT



PERSONAL INFORMATION

Name **MARTA MORENO TORRES**
Address Route de la Veveyse 4, 1700 Fribourg (Switzerland)
Telephone **0034639027577**
E-mail **marta.moreno7@gmail.com; marta.morenotorres@unifr.ch**
Nationality Spanish
Date of birth 15/12/1987

**RESEARCH WORK
EXPERIENCE**

- Dates **FEBRUARY 2012- ONGOING**
- Name and address of employer *Prof. Claudio de Virgilio*. Department of Biology. University of Fribourg (UniFr).
Chemin du Musée 10, 1700 Fribourg (Switzerland).
Department of Biology. Unit of Biochemistry.
PhD student.
Study of coordination of growth and cell division by nutrient signaling pathways in yeast.
- Type of business or sector
- Occupation or position held
- Main activities and responsibilities
- Dates **SEPTEMBER 2009- JANUARY 2011**
- Name and address of employer *Prof. José Ramón Murguía Ibáñez*. Laboratory of nutrient control and genome stability. IBMCP (Technological University of Valencia,UPV).
C/ Ingeniero Fausto Elio s/n, 46022 Valencia (Spain).
Department of Biotechnology.
Master Student.
Characterization of Gcn2 new molecular functions in maintaining genomic stability and longevity in yeast. Final Grade Master Thesis: (9.5/10).
- Type of business or sector
- Occupation or position held
- Main activities and responsibilities
- Dates **SEPTEMBER 2010- OCTOBER 2010**
- Name and address of employer *Prof. Noel Lowndes*. Department of Biochemistry.
Arts/Science Building. National University of Ireland, Galway,
University Road, Galway (Ireland).
Center for Chromosome Biology National University of Ireland.
Internship.
Characterization of Gcn2 in cell cycle arrest and DNA damage response upon nutrient depletion conditions in yeast.
- Type of business or sector
- Occupation or position held
- Main activities and responsibilities
- Dates **SEPTEMBER 2009-MARCH 2010**
- Name and address of employer *Prof. José Ramón Murguía Ibáñez*. Department of Nutrient control and genome stability. IBMCP (Technological University of Valencia,UPV).

- Type of business or sector Ingeniero Fausto Elio s/n, 46022 Valencia (Spain).
- Occupation or position held Department of Biotechnology.
- Main activities and responsibilities Internship (Final Degree Research Project).
The protein kinase Gcn2 and iron homeostasis in *Saccharomyces cerevisiae*: molecular mechanisms. Final Grade: Honors (10/10).
- Dates **JULY 2008**
- Name and address of employer *D. José Antonio López Guerrero*. Valencian Institute of Oncology (IVO).
C/ Beltrán Bágüena 8, 46009 Valencia (Spain).
- Type of business or sector Laboratory of Molecular Biology (IVO).
- Occupation or position held Internship.
- Main activities and responsibilities Performance of basic procedures in molecular biology and applied genetic analysis in translational research. The basic clinical assays were molecular diagnostic of T and B lymphomas, molecular study of T translocation, detection of circulating cancer cells, and the study of *BRCA1* and *BRCA2* genes involved in breast cancer.

OTHER WORK EXPERIENCE

- Dates **FEBRUARY 2010-MARCH 2010**
- Name and address of employer *MT Educación y Formación*.
Paseo Pamplona 15, 50004 Zaragoza (Spain).
- Type of business or sector Nuestra Señora del Rosario School.
- Occupation or position held Teacher.
- Main activities and responsibilities Coordination of activities and lectures for children held in English.

EDUCATION AND TRAINING

- Dates **FEBRUARY 2012 -ONGOING**
- Organisation Department of Biology. University of Fribourg, Fribourg (Switzerland).
- Title of qualification awarded PhD student in Biochemistry and Molecular Biology.
- Dates **2010-2011**
- Organisation Technological University of Valencia (UPV), Valencia (Spain).
- Title of qualification awarded Master in Biomedical Biotechnology.
- Dates **2005-2010**
- Organisation Technological University of Valencia (UPV), Valencia (Spain).
- Title of qualification awarded Biotechnology Degree (UPV).

PERSONAL SKILLS AND COMPETENCES

MOTHER TONGUE SPANISH.

OTHER LANGUAGES ENGLISH (ADVANCED LEVEL FROM OFFICIAL LANGUAGES SCHOOL OF VALENCIA).
GERMAN (A1).
FRENCH (A1/A2).

SOCIAL SKILLS AND COMPETENCES Perseverant, independent and hard working. Excellent communication skills in English, both oral and written. Outgoing and open to share experiences with new cultures and customs. Ability to keep good relationships at work.

ORGANISATIONAL SKILLS - Supervisor of the final degree project in Biology of the bachelor student Chloé

AND COMPETENCES	<p>Sieber (UniFr, 2015).</p> <ul style="list-style-type: none"> - Member of the Biomedical Biotechnology Master academic committee (UPV, 2010-2011). - Member of INTEGRA program (which main goal is to help new students to integrate at the academic life of the university) (UPV, 2007-2008). - Collaborative actions in European convergence program (UPV, 2006-2007/2007-2008). - Member of Center Board of Higher Technical School of Agronomic Engineer (UPV, 2005-2006/2006-2007).
TECHNICAL SKILLS AND COMPETENCES	<ul style="list-style-type: none"> - Molecular Biology and Biochemistry: Technical procedures on PCR, site directed mutagenesis, DNA sequencing, cloning and molecular genetics, Phos-tag SDS-PAGE, Western Blot and Northern Blot analysis, yeast cell culture and growth, yeast two-hybrid analysis, protein and DNA extraction, mitochondria and cytosol fraction isolation, fluorescent microscopy, biochemical analysis (<i>in vitro</i> kinase and phosphatase assays), FACS analysis, co-immunoprecipitation, quantitative real time PCR, and other yeast common techniques. - Computing: FlowJo software, Serial Cloner software, MS Office, Adobe Photoshop.
TEACHING EXPERIENCE	<p>FEBRUARY 2012-ONGOING</p> <ul style="list-style-type: none"> - Teaching assistant: Advanced Practical course in Biochemistry for bachelor students (Yeast two hybrid, microscopy and pull down techniques) at UniFr. Duration: 75 hours (3 weeks/ year 2012-2014). - Teaching assistant: Laboratory practical courses in Biochemistry for Medicine and Biology students at UniFr. Duration: 194 hours.
OTHER COURSES	<ul style="list-style-type: none"> - Flow cytometer course. Place: University of Fribourg, Switzerland. Date: 27th of January 2016. - Yeast system biology workshop (StarOmics). Place: University of Fribourg, Switzerland. Date: 25th of June 2012.
PUBLICATIONS	<ol style="list-style-type: none"> 1. Authors: Rodríguez-Hernández C, Menacho-Márquez M, Moreno-Torres M, Hornillos V, Acuña AU, Rivas L, Murguía JR. Title: The antimicrobial and antitumoral drug Miltefosine activates the General Control of Nutrients pathway through Tryptophan deprivation. Publication: In preparation. 2. Authors: Moreno-Torres M, Jaquenoud M, De Virgilio C. Title: TORC1 controls G1-S cell cycle transition in yeast via Mpk1 and the greatwall kinase pathway. Publication: Nat Commun. 2015 Sep 10; 6:8256. doi: 10.1038/ncomms9256. 3. Authors: Agostini A, Mondragón L, Bernardos A, Martínez-Máñez R, Marcos MD, Sancenón F, Soto J, Costero A, Manguán-García C, Perona R, Moreno-Torres M, Aparicio-Sanchís R, Murguía JR. Title: Targeted cargo delivery in senescent cells using capped mesoporous silica nanoparticles. Publication: Angew Chem Int Ed Engl. 2012 Oct 15; 51 (42): 10556-60. 4. Authors: Moreno-Torres M, Murguía JR. Title: Between Scylla and Charibdis: eIF2α kinases as targets for cancer

chemotherapy.

Publication: **Clin Transl Oncol.** 2011 Jul; 13 (7): 442-5.

FELLOWSHIP AND HONOURS

- Novartis Foundation for Medical-Biological Research fellowship (2012).
- Collaboration fellowship at the Institute of Molecular and Cellular Biology of Plants (IBMCP). From 01/04/2010 to 30/09/2010.
- Honours in the final degree project with title: The protein kinase Gcn2 and iron homeostasis in *Saccharomyces cerevisiae* (2009-2010).
- Erasmus Fellowship in the Technische Universität München, Germany (2008-2009).
- Honours in Natural and Health Sciences High School (2004-2005).

CONFERENCES AND PRESENTATIONS

- Yeast Genetics Meeting. From 29th of July to 3th of August 2014, Seattle-Washington (USA).
Authors: Dubots E, Cottier S, Péli-Gulli MP, Jaquenoud M, Bontron S, **Moreno-Torres M**, Schneider R, De Virgilio C.
Poster Title: TORC1 regulates the yeast lipin Pah1 via the Nem1/Spo7 protein phosphatase complex.
- Targeting the kinome III. From 26th to 28th of September 2014, Basel (Switzerland).
- 26th International Conference on Yeast Genetics and Molecular Biology. From 29th of August to 3th of September 2013, Frankfurt (Germany).
Authors: Panchaud N, Péli-Gulli MP, **Moreno-Torres Marta**, De Virgilio C.
Poster Title: The Iml1/Npr2/Npr3 GAP complex regulates Gtr1 that couples amino acid signals to TORC1.
- Jornadas del Centro de Investigación Biomédica en Red Bioingeniería, Biomateriales y Biomedicina. 2012, Valencia (Spain).
Authors: C. Coll, E. Aznar, E. Climent, A. Agostini, L.Mondragón, A. Bernardos, R. Martínez-Máñez, **M. Moreno-Torres**, J. Murguía, C. Manguan-García, R. Perona.
Poster Title: Gated silica nanoparticles for diagnosis and drug delivery applications.
- 3rd Cell cycle and cancer meeting. From 2nd to 5th of April 2012. Montpellier, France.
- IV Biotechnology interuniversity congress by UPV. 2009, Valencia (Spain).

PATENTS

Release of substances in senescent cells. Spanish Patent application number 201231370. Currently patenting in USA and Japan.

REFERENCES

Prof. Claudio De Virgilio. Department of Biology. Unit of Biochemistry. University of Fribourg.
Tel: +41 026 300 8656; email: claudio.devirgilio@unifr.ch

Prof. José Ramón Murguía Ibañez. Department of Biotechnology. Technological University of Valencia.
Tel: +34 96 387 70 00/+34 96 387 94 16; email: muribajo@upvnet.upv.es

END OF DOCUMENT

Last update: 10th of April 2016

